POWER CONTROL AND INSTABILITY MITIGATION IN KIGALI NATIONAL GRID

A

THESIS

Submitted by

DARIUS MUYIZERE

In Partial Fulfillment of the Requirements for the Degree of

DOCTOR OF PHILOSOPHY IN ELECTRICAL POWER SYSTEMS

AFRICAN CENTER OF EXCELLENCE IN ENERGY FOR SUSTAINABLE DEVELOPMENT (ACE-ESD),
COLLEGE OF SCIENCE AND TECHNOLOGY,
UNIVERSITY OF RWANDA, KIGALI,
RWANDA

APRIL 2024

DECLARATION

This is to certify that this thesis has passed through the anti-plagiarism system and has been found compliant, and this is the approved final version of the thesis:
Power Control and Instability Mitigation in Kigali National Grid

Student Name: Darius Muyizere
(Reg No. 218014544)

Signature: 

Date: 22/05/2024

The Dissertation Committee for Darius Muyizere

Name of Supervisor: Lawrence K. LETTING (PhD)

Signature: 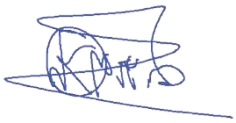

Date: 24/05/2024

Name of Co-supervisor: Bernard B. MUNYAZIKWIYE (PhD)

Signature: 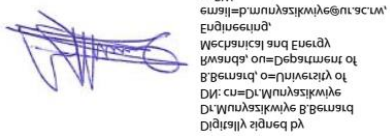

Date: 27/05/2024

DEDICATION

I dedicate this thesis to the Almighty God, my creator and protector, and to my lovely family and parents for their encouragement to complete this research.

I dedicate this work to my brother, my sister, my workmates, and all my friends for their unconditional support during this academic journey.

Special thanks go to the African Center of Excellence in Energy and Sustainable Development (ACE-ESD) management, for providing all I needed to study this Doctor of Philosophy program.

ACKNOWLEDGEMENT

I wish to thank the Lord Jesus Christ who has given me the privilege, wisdom, and strength to pursue this study.

It would not have been possible to write this doctoral thesis without the help and support of the kind people around me, only some of whom it is possible to mention in a particular here.

This thesis would not have been possible without the help, support, and patience of my principal supervisor, **Dr. Laurence K. Letting**. He has greatly helped me by providing his insight, knowledge, and perspective when required while giving me the space and time to grow on my own. His wide knowledge, his logical way of thinking, and his attitude toward science have been of great value to me over the years.

I would like to acknowledge and thank the African Center of Excellence in Energy for Sustainable Development, University of Rwanda for granting me a scholarship to carry out this research. I also wish to express my sincere gratitude to all African Center of Excellence in Energy for Sustainable Development, University of Rwanda for their invaluable guidance and advice throughout this research.

The good advice, support, and friendship of **Dr. Bernard B. Munyazikwiye** has been invaluable on both an academic and a personal level, for which I am extremely grateful for their constructive discussion and comments. My thanks have been extended to **Assoc. Prof. Charles Kabiri** for his suggestions and advice. My special thanks are expressed to **Dr. Jean De Dieu Hakizimana** for his help and support.

I praise and glorify the name of God, the Almighty, the Creator who creates all these nice people and these pleasant opportunities.

THESIS DETAILS

Thesis Title: Power Control and Instability Mitigation in Kigali National Grid

PhD Research Fellow: Darius Muyizere

Supervisors:

Main supervisor, Dr. Lawrence K. Letting, Lecturer at the Department of Electrical & Communications Engineering, Moi University, Kenya; Co-supervisor: Dr. Bernard B. Munyazikwiye, Lecturer at the Department of Mechanical and Energy Engineering, College of Science and Technology, University of Rwanda, Rwanda.

The publications mentioned below have appeared in peer-reviewed journals and conference proceedings. The version offered in this thesis differs just in formatting and minor errata.

Paper A: Darius Muyizere, Lawrence K. Letting and Bernard B. Munyazikwiye, "*Effects of Communication Signal Delay on the Power Grid: A Review*," Electronics (Switzerland), vol. 11, no. 6. 2022. doi: 10.3390/electronics11060874.

Paper B: Darius Muyizere, Lawrence K. Letting and Bernard B. Munyazikwiye, "*Under-frequency Load Shedding on the Performance Time Delay Relays of Transmission lines with difference Controllers*," 2021. doi: 10.1109/SPEC52827.2021.9709464.

Paper C: Darius Muyizere, Lawrence K. Letting and Bernard B. Munyazikwiye, "*Decreasing the negative impact of time delays on electricity due to performance improvement in the Rwanda National Grid*," Electronics (Switzerland), vol. 11, no. 3114. 2022. doi: 10.3390/electronics11193114.

Paper D: Darius Muyizere, Lawrence K. Letting and Bernard B. Munyazikwiye, "*Effect on transient stability and analyses resulting from a cyber-attack on frequency relay device*," International Journal of Performability Engineering, vol. 19, no. 1, January 2023, pp. 20-32. Doi: 10.23940/ijpe.23*.01.p3.2032.*

LIST OF ABREVIATIONS

AC	Alternative Current
ACE-ESD	The African Center of Excellence in Energy for Sustainable Development
AS-index	Angle Stability Index
AVR	Automated Voltage Regulator
BR	Breaking Resistor
CST	College of Science and Technology
DC	Direct Current
DoS	Denial of Service
DTKE index	Deviation of total kinetic energy index
EDCL	Energy Development Corporation Limited
EMT	Electromagnetic Transient
ERA	Eigen system Realization Algorithm
ETDC	Enhanced Time-Delay Compensation
EUCL	Energy Utility Corporation Limited
FACTS	Flexible Alternating Current Transmission System
FEM	Finite Element Method
FLC	Fuzzy Logic Control
FR	Frequency Responses
FRF	Frequency Response Function
GPS	Global Positioning System
GOA	Grasshopper Optimization Algorithm
GOV	Governor
GTO	Gate Turn off
IEC	International Electrotechnical Commission
KNG	Kigali's National Grid
LPM	Local polynomial Modelling
MFAC	Model-Free Adaptive Control
MP	Modified Predictor
NCS	Networked Control Systems
NL	Non-Linear
OBE/SSE	Operating Basis Earthquake and Safe Shutdown Earthquake
OKID	Observer Kalman Filter Identification
PCC	Point of Common Coupling
PhD	Doctor of Philosophy
PI	Proportional-Integral
PSO	Particle Swarm Optimization
PSS®E	Power System Simulator for Engineering
PV	Photovoltaic

REG	Rwanda Energy Group
RLS	Recursive Least Squares
RMS	Root Mean Squared
SCADA	Supervisory Control and Data Acquisition System
SIA	System Identification Algorithms
SR	Step Responses
SS	State Space
SSM	State-Space Matrices
STATCOM	Static Synchronous Compensator
SVC	Static Var Compensator
TCR	Thyristor Controlled Reactor
TCSC	Thyristor Controlled Series Capacitor
THD	Total Harmonic Distortion
TSC	Thyristor Switched Capacitor
UFLS	Under Frequency Load Shedding
UR	University of Rwanda
V-index	Voltage Index
VR	Voltage Regulator

LIST OF SYMBOLS

ΔV_{pcc}	Controller's input
$B_{C(TSC})$	Capacitive susceptance
$B_{L(TSC)}$	Inductive susceptance
C_{ij}	Capacity
C_{ijw}	Simplicity
E_f	Equivalent voltage in the excitation coil of the generator
E_{fd}	Field voltage
E_{fdo}	Reference voltage in the generator's excitation coil
E'_q	Quadrature-axis transient voltage
F_s	Safety factor
H_t	Slanted surface
K_1 and K_2	Constant values
K_{p1}, K_{p2} and K_{i1}, K_{i2}	Proportional and Integral gains
P_{PV}	Output power
P_e	Active electrical power
P_m	Damping constant of the generator
P_m	Mechanical power
P_o	Reference mechanical power
P_{ok}	Nominal active power
P_{sd} and Q_{sd}	Real and reactive load leaving the bus s
P_{si} and Q_{si}	Real and reactive flows injecting into the bus s
Q_{TSC}	Quantity of capacitive reactive power
Q_c	Reactive power
Q_{max}	Maximum reactive power demand
Q_{ok}	Nominal reactive power
R_s	Stator resistance
T_a	Ambient temperature
T_c	Hourly solar cell temperature
T_{cr}	Temperature at solar radiation flu of $1000W/m2$
T_{do}	Direct-axis open-circuit transient time constant
T_e	Electromagnetic torques
T_m	Mechanically torques
V_F	Factor of variability
V_{bus}	Operating bus voltage
V_{dc}	dc voltage across the converter
V_{index}	Voltage index

V_{max}	Maximum voltage limit
V_{min}	Minimum voltage limit
V_s	Voltage vector of ac system bus s
V_t	Synchronous generator's terminal voltage
V_{to}	Reference voltage
$V_{vref}(STATCOM)$	STATCOM output variables
$V_{vref}(SVC)$	SVC output variables
W_C	Deviation of total kinetic energy
W_i	Single fuzzy command
W_i	Kinetic energy
W_{total}	Sum of all kinetic energies
a_1,a_2,b_0, $b_1 and\ a_2, b_1$	Constant impedance load model
k_s	Converter's dc to ac gain
k_t	Coupling transformer ratio
t_d	Time delay
β_t	Temperature coefficient
δ_{max}	Greatest angle separation
μ_c	Generating efficiency of the PV system
μ_{cr}	Theoretical solar cell efficiency
ω_0	Synchronous generator
ω_m	Synchronous generator rotor speed
ω_{mo}	Reference rotor speed
ΔV	Rapidity at which the controller's signal changes
ω	Speed of the generator
H	Inertia constant
Hz and N_R	Frequency and rotor speed
J	Moment of inertia of the connected turbine and generator rotor mas
PVA	Total solar cells area
V	Voltage level deviation
VSC	Control angle
c	Steady value
i	Rule number
k	Observed location position
m	Modulation ratio of PWM control
p	Predicted position
α	Fuzzy instruction table
δ	Rotor angle of the generator
θ	Angular position of the rotor
λ and μA	Ross coefficient and least possible score for members

LIST OF TABLES

LIST OF FIGURES

ABSTRACT

The transmission grid is the backbone of the power system, and its stability and reliability are essential for the proper functioning of the entire electrical grid. The increased demand for electricity, coupled with the integration of renewable energy sources, has led to the reinforcement of the transmission grid. The newly reinforced transmission grid is characterized by longer transmission lines, higher capacities, and a more complex network, which pose new challenges to the protection coordination system. In particular, communication delays and cyber-attacks are becoming increasingly relevant issues that must be taken into account when designing the protection coordination system.

The problem of communication delays and cyber-attacks persists in the recently strengthened transmission system. The grid's strength lies in its ability to impact the protection coordination system's ability to operate correctly. Cyber-attacks may disrupt the protection coordination system by compromising its communication network or by disrupting the operation of protective devices. The impact of communication delays and cyber-attacks on protection coordination in the newly reinforced transmission grid is a critical issue that requires immediate attention. The consequences of incorrect protection coordination can be severe, including the failure of transmission equipment, blackouts, and even the collapse of the entire electrical grid. To prevent these events, it is essential to understand the impact of communication delays and cyber-attacks on protection coordination and to develop new methods to mitigate their effects.

The IEEJ West 10-machine model system, IEEE 14-bus system, and Kigali national grid that serves the city of Kigali in Rwanda are widely used in power systems research. In this research, we aim to use these systems to address several objectives: For the first objective, it aims to develop new techniques and algorithms to reduce the communication delay of electric power, which impacts control system performance and also can create energy losses. This study also examined the implications and causes of network latency while maintaining model reliability simulation using the IEEJ West 10-machine electric grid. For the second objective, which aims to develop new techniques and algorithms to reduce the impact of the delay time for under-frequency load-shedding on protection coordination in the comparison of algorithms, in this study it is focused on a test case used to evaluate the performance of different energy control strategies and to develop new methods to improve the protection of IEEE 14 bus system. The third objective aims to develop new techniques to negatively impact decision interaction on grid access control. This case study concentrates on communication signal latencies as well as how to detect them but also addresses communications network performance concerns inside the context of energy control and surveillance, including a particular on characteristics of the technology delays. An implementation to resolve this difficulty using SVC (TSC-TCR) thyristor switch capacitors (TSC) and thyristor-controlled reactors (TCR) to enhance the

system reliability of the Kigali national grid. Finally, the last objective aims to formulate methods that utilize smart systems, the much more prevalent type of cyber-physical network that provides a strong association between cyber communications and physical networks. For that reason, it is really critical to investigate how cyber-attacks affect frequency relay equipment and a circuit breaker as a control system of the automatic generator, located in the Kigali national grid. The impact of cyber-attacks that cause information network latency and their effects on transient stability are covered in this research. Utilizing measurement result devices, such as an SVC or STATCOM connected to such a grid, cyber-attacks have been conducted.

These case studies can be used to address various interventions related to the analysis and evaluation of various control techniques for improving power quality in the transmission grid system. In the first case, the IEEJ West 10-machine model system can be used to evaluate the performance of different power system stabilizers. In the second case, the IEEE 14 bus system can be used to test the performance of different control strategies. In the third case, the Kigali national grid can be used as a case study to address challenges such as grid integration of renewable energy sources, demand-side management, and grid reliability. For instance, the study of the use of non-linear control strategies to reduce the negative consequences of significant delays in electricity performance improvement. In the final case study, KNG focused on addressing the challenges of detecting and reducing these effects based on the different cases of limited-frequency relay devices. In summary, the use of these case studies can provide valuable insights into the challenges and opportunities associated with power system operations and management. They can help identify the most effective solutions to these challenges and develop new methods and strategies for enhancing stability, reliability, and sustainability of power systems.

The results showed that the suggested approaches outperformed the conventional approach, providing a solution to the challenges faced in the IEEJ West 10-machine model system. The simulation results confirmed the effectiveness of the grasshopper optimization algorithm (GOA) and particle swarm optimization (PSO) methods for reducing the negative consequences of under-frequency load-shedding (UFLS) in the IEEE 14-bus system. Moreover, the results indicated that non-linear control strategies, such as fuzzy logic control (FLC) and other modified predictor (MD) controlled SVC effectively reduced the negative consequences of significant delays in electricity performance improvement. SVC and STATCOM simulations also showed promising results that the two new methods for reducing the adverse effects of cyber-attacks on a frequency relay and circuit breaker control system for the nonlinear (NL) controller and the proportional-integral (PI) controller were effective in reducing the consequences of cyber-attacks in the KNG. In conclusion, the MATLAB/Simulink simulation results confirm the effectiveness of proposed new control

methods and their superiority over traditional approaches for contributing to power quality improvements and suggest potential for further research in the field.

Contents

PART I

INTRODUCTORY CHAPTERS

CHAPTER ONE: INTRODUCTION

1.1 Background

Modern power systems are becoming increasingly complex in detecting and making decisions, as well as handling a wide range of duties across areas like electrical generation, transmission, distribution, and consumption. However, in place of technological improvements to modern energy, poor power quality can cause greater power losses, unfavorable device behavior, and interference with surrounding communication networks for control and protection. Power electronics' extensive application increases the stress on the electrical network through causing oscillations in electrical currents and voltages, as well as an increase in reactive current [1]–[5].

System performance must be improved and then sustained at the correct scale in order to provide users with continuous voltage and frequency. Power electronics have become among the most reliable methods for decreasing power quality issues [5][6]. Static VAR compensator (SVC), static synchronous compensator (STATCOM), thyristor switched capacitor (TSC), thyristor controlled series capacitor (TCSC), and other flexible AC transmission system (FACTS) devices are examples. Reactive power supervision, improved grid stability, regulation of both reactive and active electrical power flows just on the network, damage mitigation, and improved grid effectiveness are some of its advantages [7].

Power electronic controllers are trustworthy for distribution systems, much as FACTS devices increase the reliability and quality of power transmission by concurrently increasing both power transfer volume and stability [8][9]. Voltage regulators, static potential restorers, line reactors, surge protectors, voltage conditioners, isolating transformers, continuous control supplies, correct wiring, grounding, filters, and other features are included in some of these devices [10]. TSC is a device used in electrical systems to recover power flow, is an essential way for improving power quality [1]–[4]. TSC is employed because it responds instantly to changes in system settings. TSC can additionally boost the power quality in order to eliminate oscillations, control reactive power, and maintain voltage stable [11][12]. However, all of these solutions utilized traditional proportional-integral (PI) control strategies [13]. However, because traditional power networks are now being converted to distributed generation via the integration of renewable energy integration [14] and advanced electronic power control logic, electricity performance improvement equipment must be outfitted to intelligence-based control systems, like fuzzy logic controllers (FLC) [15][16]. Furthermore, electricity networks are highly nonlinear. As a result, dynamical intelligence methods of control for intelligent energy grids are applicable [17].

The integration of renewable sources such as solar systems [18], energy storage systems, and traditional synchronous generators in the current grid creates the other two grid vulnerabilities [19].

The system incorporates many types of measuring, supervising, and connecting tools, such as phasor measurement units (PMUs) and open network technology, all of which have been widely used during measurements and tracking platforms [20]. This causes unnecessary latency and reduces the controller's damping efficiency, resulting into system instability [21]–[24]. Large-time delays not only create system instability, but also have an impact on network power quality [25]. Although PV systems are linked to the power network and the entire cyber-physical infrastructure is supervised and controlled at several layers by the supervisory control and data acquisition system (SCADA), cyber-attacks can take place at any level during supervision. This should cause a power shortage inside the network, and thus the operators will struggle to regulate the network, affecting customers [26]. Communications between the command unit and the control unit or controller are easily compromised, interrupted, or interfered with. As a result, the overall power quality of the grid degrades.

Based on these premises, the thesis outline begins with nonlinearity caused by both unbalanced and balanced fault conditions at various locations throughout the system. Due to nonlinear system concerns, the performance of the modified predictor controller (MPC) and fuzzy logic controller (FLC) based SVC (TCR and TSC) was originally developed and compared to that of the system without control. The significant delay produced inside this network as a result of its intricacies and numerous computations required is the next issue. This study addresses the reduction of the negative impacts of delay time on reliability and performance using two methods: the two-input-based fuzzy logic controller (FLC) and the modified predictor controller (MPC). The final and perhaps most important concern is the hybrid power grid's cyber-security. This study examines the impacts of Denial of Service (DoS) and switching assaults on various components of the hybrid power system, such as the frequency relay, and investigates innovative strategies to prevent the negative consequences of cyber-attacks. Two control strategies, a Nonlinear (NL) controller and a PI controller, have been developed to mitigate the negative effects of cyber-attacks upon this relay, as well as a new identification and mitigation strategy based just on voltage threshold for the voltage regulator (VR).

1.2 Significance of the research / Expected impact of research project

The main aim of Rwanda's energy sector is to develop the requisite institutional, organizational, and human capacity, which will lead to an increase in accountability, transparency, and national ownership, and to decentralize capacity for sustainable energy service delivery [27]–[29]. With efforts to access system generation, reliability, adequacy, and security systems are therefore treated independently. System adequacy is the ability of a

system to supply cumulative energy requirements to customers within its component ratings and voltage limits in the event of an outage.

A more thorough overview of security includes two fundamental elements: robustness and resilience. The capacity of the system to resist or repel attacks and interruptions is referred to as robustness. Resilience, on the other side, indicates how quickly a system responds once an incident has created an outage. This is especially important in the setting of security. Moreover, there is another element to consider prior to transmission, which is the generation's security. These criteria include the reliability of hydroelectric rains, the constancy of coal or fuel supply for thermal power plants, and the corresponding reliability of meteorological resources for renewable power plants. This idea is encapsulated by the phrase "vulnerability." Vulnerability must also be addressed to ensure a holistic strategy to power system security.

Consider the outage hours for the year caused by the grid disturbance and the total outage hours caused by the sum of internal and external factors. Internal factors are failures that originate from power generation plants; for example, poor ventilation in gas turbine compressors, fire detector alarms, low gas inlet pressure, etc. While external factors are perturbations at the grid, for example, high frequencies and supply line failure [30]. Thus, this dissertation deals with the importance of influence quality enhancement to mitigate any instability in the transmission grid by analyzing the impacts caused by communication delay, nonlinearity, and cyber-attack on modern power grids. This promotes robust power system protection and effective power control with not much loss in energy damage.

1.3 Research motivation

Electricity performance problems occur at several different levels within the system that provides electric generators or the entire region's power unit, including power lines, main power stations, distribution power stations, both main and secondary electrical lines, distribution lines, maintenance, and electrical connection construction. Power quality concerns must be addressed. There are several technologies available to minimize network power quality concerns, such as FACTS devices. There has been a lot of research done on these devices and the use of controllers, although none of it has focused on improving electric grid performance using a nonlinear controlled SVC (TCR and TSC) and STATCOM.

Because electricity grids have dynamic and unexpected characteristics in their operations, resulting in their inherent nonlinearity. In this instance, "nonlinearity" refers to the fact that the actions and reactions of energy networks are not proportionate or directly related with shifts in their inputs or conditions. Electricity networks are complicated systems that are continually affected by variable demands and unpredictable circumstances such as swings in energy consumption, power generation from various sources, and environmental influences

such as weather patterns. These components interact in complex ways, which leads to nonlinear behaviors and reactions across the grid.

In particular, during peak hours, power demand may spike dramatically, forcing generators to operate at full capacity and potentially producing bottlenecks and voltage fluctuations. Similarly, unexpected fluctuations in renewable energy inputs (e.g., solar and wind power) owing to weather changes can have an impact on the grid's stability and supply-demand balance. Understanding and regulating the nonlinearity of energy networks has become crucial for guaranteeing the grid's stability, dependability, and efficiency. This complexity needs sophisticated control and management systems to respond to the dynamic and unpredictable character of electrical networks.

This has led to the statement that there are many strong suggestions that there are issues with the quality of electricity. The network has been experiencing additional issues, such as delays and cyber-attacks, due to the consolidation of electricity generation, FACTS devices, and communication with the control center. New, cutting-edge control systems are used to measure and manage the production of electricity and FACTS devices, increasing signal time delays. While much effort has just been made to address the negative effects of delay time, nothing has been done to address the problems with time delay and cyber-attacks in order to enhance power quality.

The controllers and control parameters are observed by the SCADA, which serves as a control center. The grid is made vulnerable and susceptible to cyber-attacks by the transmission of information between controllers and control centers. Despite the fact that there has been a lot of research on cyber-attack detection and mitigation, nobody has focused on power quality. The three main challenges facing modern power grids—nonlinearity, time delay, and cyber-attack—are thus taken into consideration in this dissertation's discussion of power quality enhancement. It also offers creative solutions to enhance system efficiency.

1.4 Aim and objectives of the study

The main objectives of this research were to carry out a detailed analysis of the impact of communication delay on protection co-ordination in the newly reinforced Rwanda transmission grid, and to determine the best measures to reduce the severity of disruptions caused by delays or cyber- attack as part of the performance of power system protection.

The objectives of this research are:

- To identify the causes of communication delays in the electric grid communication system.

- To investigate instability caused by communication delays in the power grid's protection coordination.

- To design the mitigation measures in the simulation of a nonlinear network for the dissolved time delay as part of optimizing the performance of power system stability in the newly reinforced grid.

- To formulate methods to mitigate the impacts of communication delays in power system control/protection. Kigali national grid case study.

1.5 State of the art

Modern networks include a variety of operational strategies that permit tracking, coordinating, and controlling the generation, transmission, and distribution of electricity. A series of studies have come back to the main characteristics of modern electricity: dependability, adaptability in system architecture, effectiveness, task scheduling, surge reduction requirements, response support, market enablement, and durability examples. However, regarding a modern grid-like Kigali Nation's grid as a case study, there are three main challenges: lack of connectivity, latency, and cyber-attacks. These challenges have a significant impact on power quality improvement, resulting in power outages and equipment malfunctions. These limitations are described in the following subsections.

1.5.1 Time Delay

The incorporation of nonlinear control systems into hybrid electricity grids for large-area grid measurements, power performance enhancement, power stability, and other purposes causes an increase in signal delay [31]. As the system becomes more complicated, the latest technology, like PMUs [32], has been implemented in order to measure data in real-time from an electrical network, which includes volts, flow, load angle, maximum power, and frequencies. PMUs synchronize all the data they collect with GPS satellites. All signals are collected and delivered to the central controller. Since the PMUs must send signals to the central controller, they use existing channels and face delays.

Latency is measured as the time spent between the occurrence of a state and its action through an application. Based on the type of dynamic response, each application had unique delay requirements. From among the different delays [4], communication signal delay contributes to latency and must be reduced. Transmission delays, dispersion delays, operation delays, and waiting are all components of network communication delays [31]. All of these latencies must always be taken into account in order to completely comprehend network data transfer behavior. Depending on the distance, transmission protocol, and various other parameters, the

delay between the time of measurement and the time the data is accessible to the microcontroller is typically between milliseconds and microseconds [33]. The introduction of delay into the system has an impact on the system's instability and dampens its effectiveness [34][35]. According to the research, a wide-area electrical network can have temporal delays that are between tens and hundreds of milliseconds [31]. Power quality should be maintained and enhanced to preserve the performance and affordability of every electrical system.

In comparing the response times between a traditional network and a modern network, significant differences become evident. In the past, traditional networks were constrained by slower data transfer rates and older technologies, resulting in response times that often ranged from tens to hundreds of milliseconds. On the other hand, modern networks have undergone remarkable advancements, incorporating high-speed data transfer protocols, content delivery networks (CDNs), and optimized server infrastructure. As a result, modern networks now achieve substantially faster and more reliable response times, typically in the range of a few milliseconds to tens of milliseconds. This enhanced efficiency and reduced latency in modern networks have played a pivotal role in delivering smoother user experiences and supporting real-time communication and critical applications.

There are several considerable disparities in reaction times between a traditional network and a modern network. Historically, traditional networks depended on outdated technology and slower data transport techniques, resulting in response times ranging from tens to hundreds of milliseconds. Modern networks, on the other hand, use advanced technology such as fiber-optic cables, high-speed data protocols, and content delivery networks, resulting in greatly better reaction times ranging from a few milliseconds to tens of milliseconds. Modern network development has transformed how we engage with digital services, providing consumers with a quicker and more seamless experience across several apps and platforms.

In hybrid electrical grids, interaction delay occurs at several points, including signal transfer from PMUs through control centers, control units to control systems, analog-to-digital (A/D) conversions, continuous computation for globe input variables, and signal synchronization with satellite tracking time [36]. This kind of latency had a major impact on the control systems and the entire platform's functionality [37]. Data is exchanged in packets over large instrumentation and control links, like wide-area control system (WACS) links. Some other sort of delay time is called a series delay, characterized by the length of interval that passes between two sequential bits of delivered data [38]. The duration difference between two consecutive data packets is another type of delay known as "among both frame serial delay."

In addition, techniques for calculating various types of time delays were presented [23]. Unlike in local control, the time delay of a wide-area electrical network can range from tens to hundreds of milliseconds or more [4][30][37]. The latencies of optical fiber communications

technology in the Bonneville Power Administration (BPA) systems have been estimated to be roughly 38 ms one way, although the latency of modems through the microwave is above 80 ms [40]. Systems that rely on satellites for communication may experience greater delays. In some kinds of wide-area power systems, the delay of the signal response has been commonly assumed to be in the region of 100 ms [40]. Extended wait times plus unpredictability within those delays are plausible if a routing delay is included and multiple indications must be transmitted. Numerous other papers [31][39], claim that communication delay values between 50 and 300 milliseconds are taken into account when designing some real-world transient stability management systems. The impact of time delays on power systems and regulating mechanisms have been studied in the past [41][42].

Furthermore, research has been conducted to lessen the detrimental effects of time delays on response time [30]–[35], [37], [38]. Every method for reducing the impact of time delays takes into account either constant, fleeting, or randomized delays. Despite several studies on the subject of signal delay and approaches for reducing them, the consequences of significant delay and tactics for mitigating its negative effects on improving power quality remain poorly understood.

Although several strategies for enhancing the electrical performance of conventional grid systems have been developed, the SVC-TSC primarily uses conventional PI and PID control methods. For quite a while, since present power grids are already being transformed into distributed generation, power quality enhancement solutions should incorporate intelligent-based controllers. Premised on just this context, this study undertook nonlinear controllers that can improve hybrid electrical grid performance, such as fuzzy logic regulated SVC-(TSC & TCR) and statically non-linear regulated SVC-(TSC & TCR).

A lot of research has been done on how communication delays affect electric utility technologies, but less on how to minimize the negative effects that latencies pose for the effectiveness of hybrid electric grids. The FLC-based technique and the modified predictor method are two controllers that have been used to improve the performance of a hybrid electricity network with synchronized machines and constant parameters (PV) and lessen the potential negative effects of significant delay on that electricity. The FLC was selected due to its ability to handle nonlinear, unstable, and inaccurate input parameters, in addition to the option of embedding technical information into the control set of rules [4] [41] [42]. The aforementioned controller type functions effectively with moment variables and under variable operational conditions. In terms of mitigating the negative impacts of time delays, an FLC-based strategy surpassed the modified predictor method.

1.5.2 Cyber-attacks

The cyber or communication infrastructure [44], which is largely utilized directly to link up with various electrical power distribution [45], serves as the cornerstone of a contemporary power system. To manage, regulate, and coordinate power transmission and measurements, this system design employs a range of communication channels, including core networks, coaxial wires, Wi-Fi, and broadcast. Substation automation, advanced metering infrastructure (AMI), and other cutting-edge techniques for interconnection both within and between grids have all been incorporated into modern power grids [46]. Additionally, the SCADA system is utilized to monitor and manage the electrical grid [47]. The control center receives all measurements via the PMU. Many communication connections are insecure and easily penetrated, exposing networks to interruptions and various sorts of computer hackers [45]. Disclosure of information and packet forwarding espionage could send signals into the SCADA that cause it to malfunction [46]. Cyber-attacks had already gotten increasingly complex throughout the period and are currently effective in influencing utility power control systems [47]. Since SCADA regulates the processors of many devices in the hybrid power system, it increases the risk of cyber-attacks on diverse electrical power distribution. As a result, the entire utility's quality assurance may suffer.

Despite extensive prior research on cyber security issues, no one has yet looked into cyber security issues related to the reliability of hybrid grid power. Various methods of cyber-attacks on power grids are mentioned in this chapter. The research study focuses on two major types of attacks: DoS attacks and faulty switching attacks. According to recent research, Netscout Arbour's 13th Annual World-Wide Infrastructure Security Report [48] asserts that attacks account for 87% of immediate problems reported by providers, whereas the Netscout Threat Intelligence Report 2H 2020 [52] asserts that it is 95%! According to The State of the Internet, as per Akamai, DoS assaults hit 77% of electricity operations [49] in 132 countries, making them one of the most devastating attacks. Moreover, the study in [50] argues that incorrect data infiltration is really a dangerous assault that could result in power outages from consumers, incorrect dispatching just in the distribution process, and equipment failures in the electricity production process.

Many methods have been presented in recent years to protect and avoid computer hackers on electric networks. Examine various cyber-physical attacks on distributed generation and their defense strategies in [23] [51] [45]. An approach for locating cyber-physical risks in power networks is described in [42] as being distributed detection. The solutions for object detection and fault diagnosis in microgrids have been discussed [52]. Throughout [53], a strategy for detecting false numbers in software vulnerabilities is devised by looking at a collection of samples and conducting computations using them to prevent suspicious information.

This work presents two controllers, the non-linear controller and the PI controller, to limit the negative impacts of cyber-attacks on hybrid electric utility elements and then to enhance system reliability. Moreover, despite the fact that much research has already been published on cyber-attack difficulties, no one has examined cyber incidents related to the energy reliability of a hybrid electrical system. However, that study examined the effects of cyber-attacks on frequency relay circuits using the Kigali National Grid as a case study network. In order to lessen the negative effects of cyber-attacks and then identify and fix frequency relay issues, two control strategies—an NL and PI controller—as well as a special identification and reduction methodology—which depends on the frequency threshold for the relay—have now been introduced.

1.5.3 Optimization of power electronics switching devices

Some research on reducing the harmful impacts of grid faults on double-fed induction generator (DFIG)-based renewable [54]–[57] has been published in the journal, as are concerns of improving electricity network stability using FACTS devices. Renewable electricity integrating the current network required the implementation of Facts controllers, stabilizing electronic system converters, as well as rapid response control algorithms [58]. Novel FACTS designs are being developed to provide decoupling ac-dc interaction, increased voltage stability, reactive mitigation, electrical energy and power quality enhancement, and power losses [59]. These significantly improve the safety of distributed generation and standalone ac-dc DG systems that use Photovoltaic and wind, battery bank, and Gasoline GEN-sets as backup generators [60]–[62].

FACTS devices are among the most dependable technologies for enhancing power quality [63][64]. SVC [5], STATCOM [65], TCSC [58], TSC & TCR [66], UPFC with M-PSO [67], and SMES [68] are a few of the Facts controllers used to address problems with electricity quality in distribution and transmission lines, reactive current regulation, improved grid reliability, control of reactive and active electricity flows upon that network, failure reductions, and work efficacy. Although, apart from the FACTS devices discussed above, there are numerous other techniques for reducing power quality issues, including voltage regulators [69], line reactors [70], isolation equipment [71], uninterrupted energy demand [31], appropriate electrical connections and conditioning [3][4][9]. They significantly improve the reliability of renewable power with isolated ac-dc DG systems that use solar, wind, battery banks, and gasoline GEN-sets as backup generators [64][74][75].

Most studies came to the conclusion that STATCOM performed better than SVC. However, tests on the Chinese grid and on the EAF show that a VSC branch in tandem with the TSR/TSC branch is required for better reactive power adjustment and voltage support. In [74], Noroozian et al. demonstrate the advantages of STATCOM and SVC for utility applications. The authors

compared the performance of the STATCOM and SVC models. In under voltage and overvoltage situations, physical footprint, harmonics, cost, and losses were the primary themes compared. In general, STATCOM is more compact than SVC and generates fewer low-order harmonics. Additionally, STATCOM performs better under low-voltage conditions. In contrast, SVC operates more effectively when there is an overvoltage condition. The overall cost and loss can be decreased with SVC. These comparisons depend on STATCOM and SVC's deployment and architectural design, claim the authors of [74].

The main focus of this research is to improve the electrical performance of the Kigali grid as a case study. The issues with system reliability on the conventional grid, as well as power quality standards and evaluation processes, as well as solutions to power quality issues, are all covered in the state-of-the-art. In this subsection, the issues with the modern power grid are also discussed. The literature review emphasizes the significance of studying power quality because of its detrimental effects on system performance.

1.6 Contributions

The major contribution of this study is the development of novel methods for dealing with communication delays and attacks in the security management of power systems. According to the results of our numerous investigations, low-latency communications for WAC in a modern grid aim to increase power system stability. The main contributions of this thesis can be summed up as follows:

- Analysis of the various reasons for delay inside this configuration of various networks and communication systems in use, comparative analysis of various delay reduction techniques, and comparison of the effectiveness of the compensation algorithm were measured in the example of Non-Braking Resistors with Fuzzy Controlled and Braking Resistors in the IEEJ West 10-machine model system.

- Numerous studies have examined the usage of GA and PSO algorithms, two of the most recent optimizers, for load-shedding analysis. None of the studies, however, addressed the application of the GOA method, which minimizes the amount of load shed and offers excellent proof of the effects of communication delays in networks. The proposed methodology has been tested using IEEE's 14-bus system.

- The uniqueness of this work is also found in the proposal of two additional controllers, the fuzzy logic controller and the modified predictor technique, to reduce the negative consequences of the time delay introduced in the Kigali national grid system, which comprises five coupling zones and a PV system.

- This work presents an experimental transient stability analysis utilizing the results of different cyber-attack analyses of frequency relay devices on the Kigali National Grid as a case study. The PI controller and the Non-Linear controller are two additional controllers that have been suggested to help identify and neutralize cyber-attacks.

1.7 Thesis outline

This dissertation is broken down into four chapters, organized as described below: The first chapter is a broad introduction that includes the research objectives, motivations, state-of-the-art, and professional contributions, as well as the thesis's organization. After that, Chapter Two discusses the method and a step-by-step approach used to address the questions of the study provided in the first chapter. The third chapter presents extensive analyses of the results as well as key outcome research. Lastly, the fourth chapter includes the final conclusions and future work.

CHAPTER TWO: RESEARCH METHODOLOGY

This chapter presents the methodology adopted in this comprehensive thesis, based on a pragmatic research philosophy that incorporates both realism and constructivism. The study philosophy acknowledges the intricacies of power systems, examining the subjective views of various parties while emphasizing empirical evidence to efficiently address power control and instability difficulties. Ontologically, the research takes a realist approach, acknowledging that the power system in the power network has fundamental physical properties and operates according to well-defined physical standards. The study acknowledges the existence of power control challenges and instability issues as objective phenomena that may be addressed empirically through observation and measurement. Epistemologically, the research follows a positivist approach, using empirical data and quantitative analysis to examine how communication delays contribute to grid instability. Simulation studies and statistical analysis are utilized to establish causal relationships. Integrating both perspectives, the research aims to comprehensively understand the issues and formulate effective mitigation measures to optimize the performance of power system stability in the newly reinforced grid. This section focuses on the methods used in this topic to achieve the objectives of the research, so this topic is divided into four phases or stages, as revealed in Figure 2.1.

The first task (Phase 0) entails data gathering and model creation using the parameters gathered. The data of importance are the measurements recorded from measurements in different grids, especially the Kigali national grid, as collected by supervisory control and data acquisition (SCADA). Faults and attacks that have been repeated indicate the extent of the parameters and the presence of different effects when it is necessary to take measures before analysis. After the inspection, the various parameters are combined with the inspector's label to obtain a quick decision for safety management. A key factor in controlling the impact of communication delays is identifying the potential for breakdowns. After determining the impact of the short-term or large-scale error, a numerical reconstruction of the dynamic mitigation of the network's stability is considered, and all of these are reviewed in detail in Phase I, Phase II, and Phase III, as well as in Phase IV.

In phase I, a numerical method was developed to observe the behavior when the grid was subjected to a disturbance with a delay. The internal structure of the smart grid is compared to the way it behaves in relation to the distribution, which is expressed as a function of setting up electricity management. Then fuzzy logic (FL), under frequency load shedding (UFLS), and conventional methods are used to estimate and optimize the parameters of the model.

Phase II shows the control of LPM. The TSC-TCR (SVC) design employs two approaches with different impact time delays: the fuzzy logic controller (FLC) method and the modified

predictor method (MPM). This test is only done in the three separate areas where the fault occurred.

Phase III shows the LPM verification control of PI and NL for the various impacts of the disturbance model in special situations with the help of the grid with SVC and STATCOM. This validation through simulation was conducted in response to a cyber-attack on the relay frequency.

Towards the end of these phases, Phase IV required a conclusion to be drawn, recommendations to be made, and a direction gap to be found in the next research.

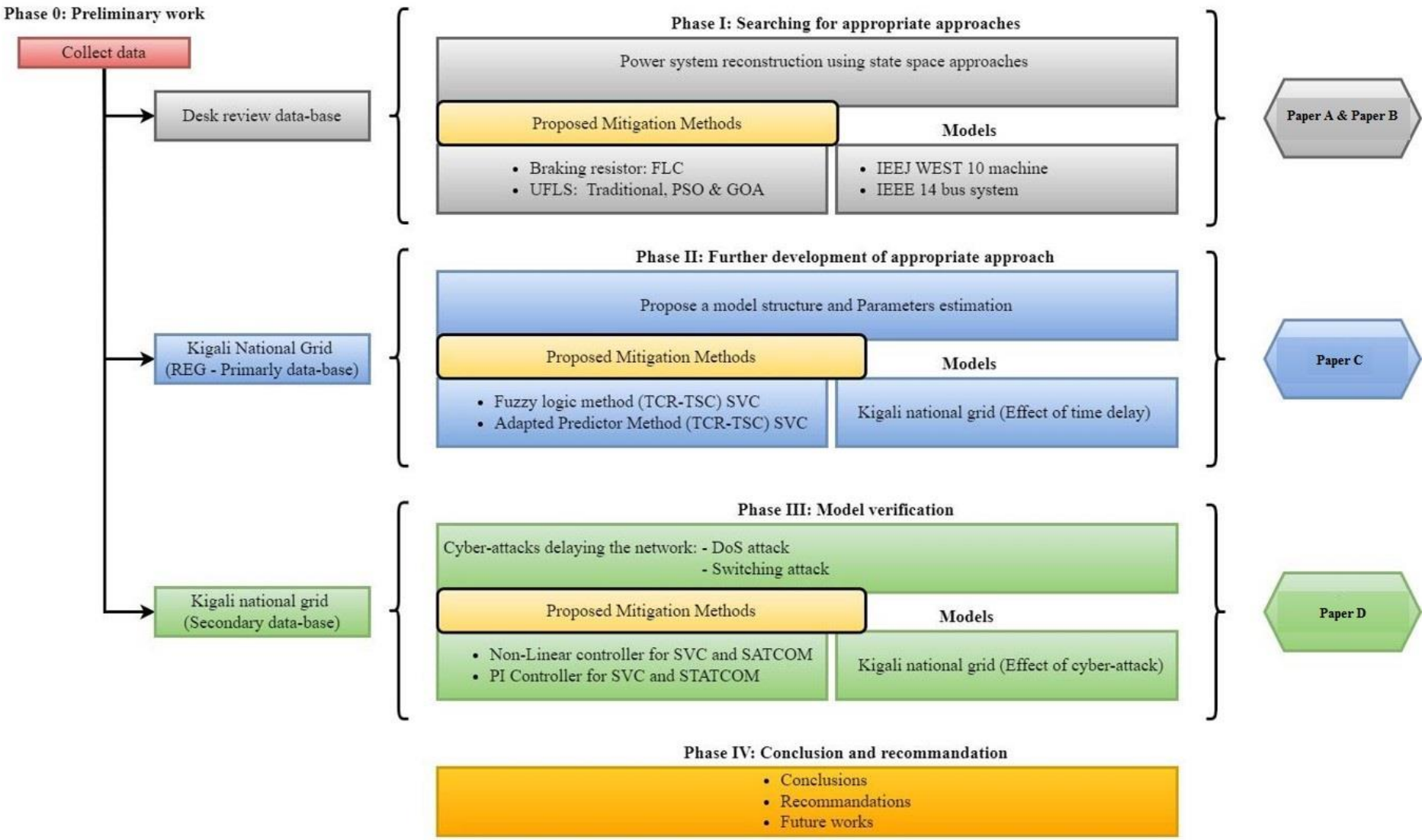

Figure 2.1: A diagram summarizing the thesis framework.

2.1 Data collection and pre-processing tests for power quality management

The complete study is depicted in Figure 2.2 and 2.3, which includes nonlinear approaches with experimental methodologies, theoretical analysis, and simulations to provide a universal system-level methodology and tools for analyzing and predicting grid control and instability mitigation in Kigali's national grid of AC power systems. In this proposed research, we utilized information obtained out of Energy Utility Corporation Limited (EUCL) Company's dispatching center to analyze the operational status of Rwanda's high voltage (110 kV) power system. These power stations have been simulated as synchronous machines containing salient pole rotors, including nominal power, line-to-line voltage, frequency, reactance, stator impedance (R_s), plus time constants. For each case study, important informants were used as primary data sources. Secondary data sources mostly included government papers, technical documents, and company annual reports, were implemented to validate the mathematical models outlined in this thesis. The theoretical test case was numerically resolved utilizing orthogonal collocation approach and simulated, culminating in a Matlab/Simulink evaluation of alternative controls, Electrical Transient Analyzer Program (ETAP) and SCADA Data collection of renewable energy resources that enables the design, modification, and analysis of the control model to fit the specific common aspects for protection grid requirements by using Rwanda Standards IEC 6211 - IEC 61140: 2009.

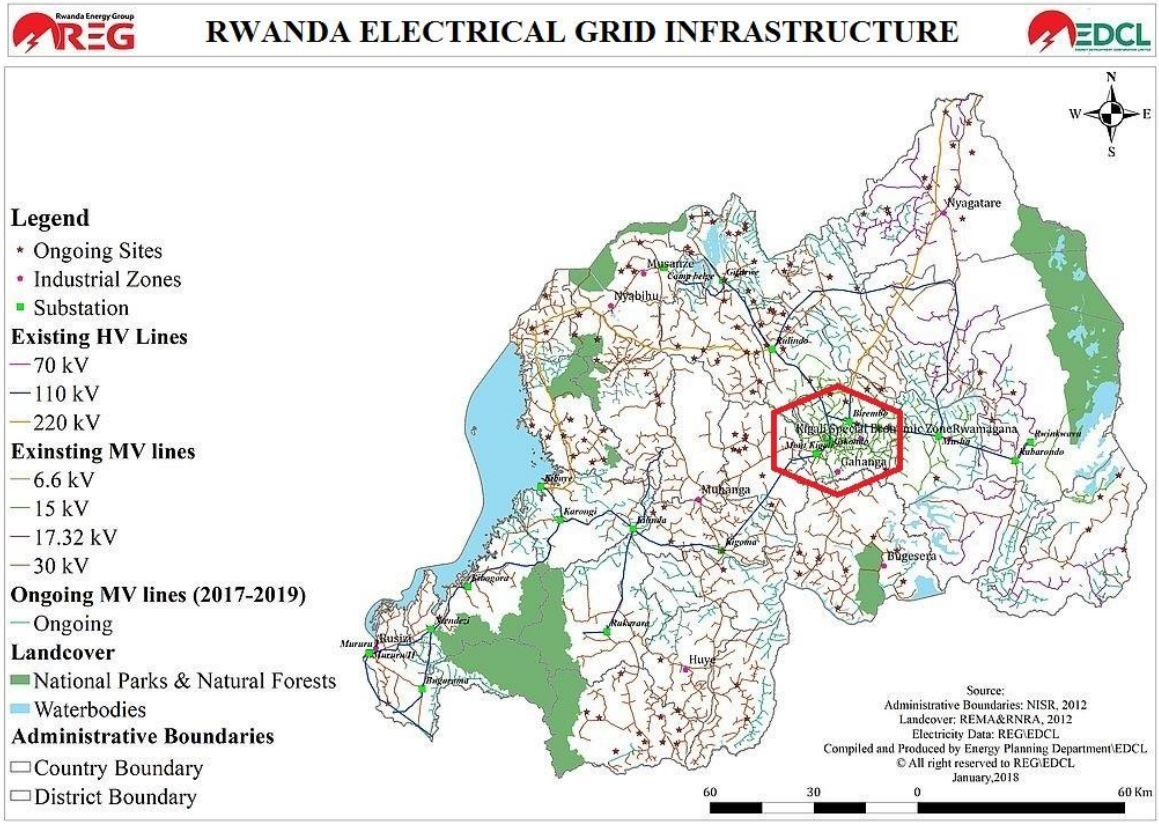

Figure 2.2: Rwanda national grid system [27].

2.2 Future development of existing power grid models

In this research, a Kigali national grid comprised of both the Substation 11 power system [4] and a Jali PV generator was used to assess power quality, as illustrated in Figure 2.3. A 15 kV/110 kV step-up transformer connects the PV generator to the Mount Kigali SS9. The system is comprised of six synchronous generators with three bank capacities of 4.5 MVA, as indicated in Figure 2.3. Resistivity, capacitive coupling, as well as susceptibility for each phase of each line, are transmission line parameters. A, B, and C are the fault sites under consideration. For synchronous machines, an automated voltage regulator (AVR) & governor (GOV) controller systems were used in this study. The cyber-attack targeted two frequency relay components. The synchronous generator parameters are shown in the Papers A to D.

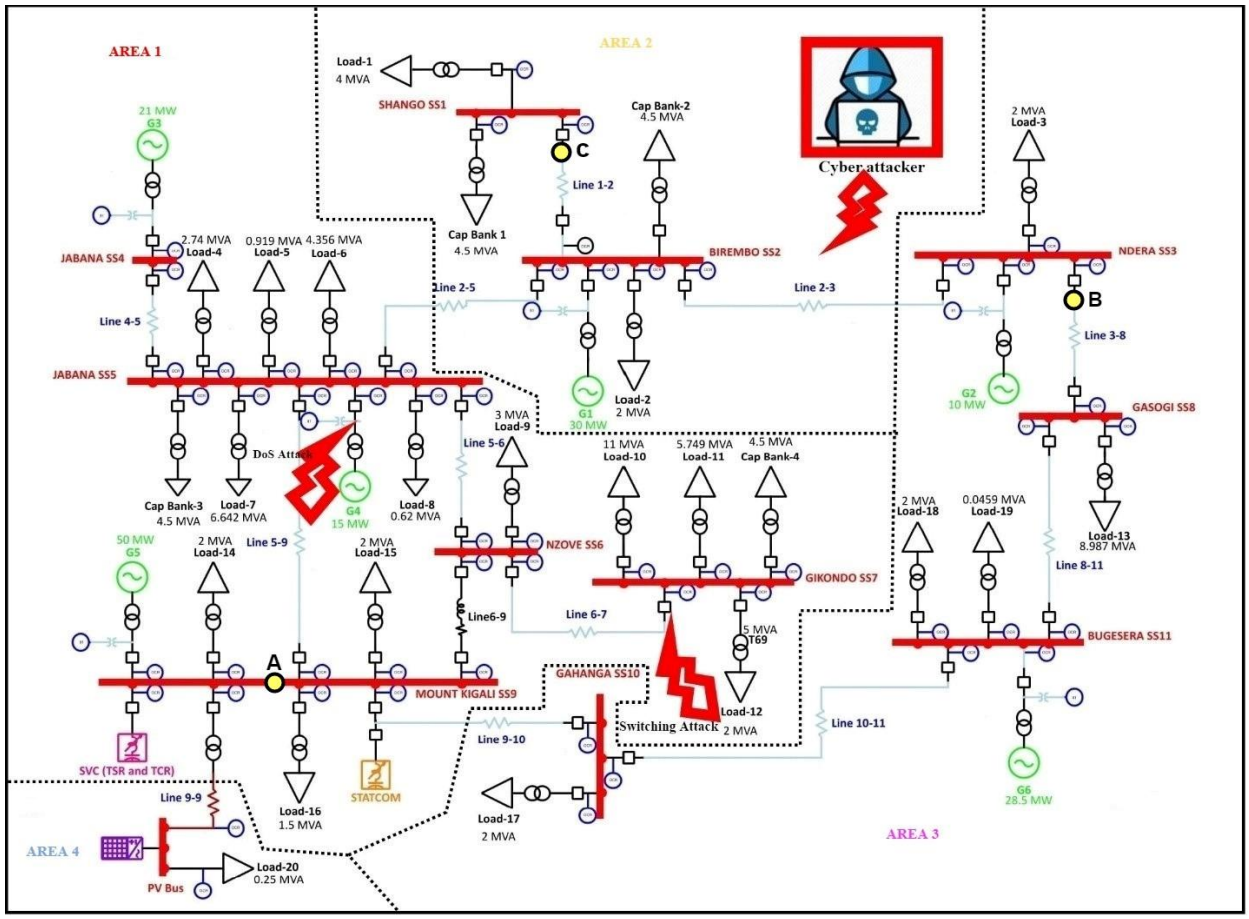

Figure 2.3: Kigali national grid system.

2.3 Modeling Systems

Models are developed using precise information about the electrical characteristics of the grid assets that comprise the power grid, such as line impedance, PV parameters, load, etc., as well as information about how the assets are interconnected. They also comprise a modest number of measurements from sensors positioned at transmission line terminals, distribution circuit head-ends, and other critical points, which are covered in particular in papers A–D.

2.3.1 Photovoltaic model

The solar radiation on a slanted surface $H_t(t)$ may be computed using solar insolation, ambient temperature, PV panel manufacturer's data, PV panel slope, and site latitude and longitude [74] [75]. The PV system's output power, P_{PV} is computed using the following equation: (2.1) [76].

$$P_{PV}(t) = H_t(t) \times PVA \times \mu_c(t) \tag{2.1}$$

Where $\mu_c(t)$ is the hourly generating efficiency of the PV system and can be obtained in terms of the cell temperature as shown in the following equation (2.2).

Where $\mu_c(t)$ is the photovoltaic system's daily production effectiveness, which may be calculated regarding the cell temperatures using equation (2.2) [77].

$$\mu_c(t) = \mu_{cr}[1 - \beta_t \times (T_c(t) - T_{cr})] \tag{2.2}$$

Where, β_t is the heat capacity, which in silicon cells ranges from 0.004 to 0.006 per °C [77]. The hypothetical photovoltaic cells' efficiencies and temperatures at $1000W/m^2$ radiation from the sun flu are denoted by μ_{cr} and T_{cr}, respectively. Throughout this thesis, β_t was set to 0.004 per °C. Photovoltaic modules manufacturers often provide μ_{cr} and β_t. The research estimated that the value of silicon cells' theoretical effectiveness is $\mu_{cr} = 0.12$. for the normal experimental temperature $T_{cr} = 25℃$. $T_c(t)$ is really the hourly photovoltaic solar temperature at ambient temperature (T_a) and may be calculated using the equation (2.3) [77].

$$T_c(t) = T_a + \lambda H_t(t) \tag{2.3}$$

Where, λ is the Ross factor, which represents the increase in temperature over ambient with increasing solar flux. Previously published values λ for varied between 0.02-0.04 Cm^2/Wrange [77]. In this study, the quantity has been set to 0.03 Cm^2/W.

PVA can be calculated using equation (2.4) and is simply the total area of photovoltaic modules required to satisfy the load requirement.

$$PVA = \frac{1}{8760} \sum_{t=1}^{8760} \frac{P_{Lav}(t) F_s}{H_t \eta_c(t) V_F} \tag{2.4}$$

Whereas F_s is still the safety factor, which covers the possibility of solar irradiance standard deviation, V_F is just the variability factor, which takes into account the influence of annual irradiation variance, and their levels are about 1.1 and 0.95, respectively.

2.3.2 Synchronous generator model

The most basic form of a power distribution diagram has been the connecting of a synchronous machine to just an infinite bus via transmission lines and transformers. The physical dynamics of a synchronous machine in only one unbounded bus network are described by the following equations:

$$\delta = \omega - \omega_0 \tag{2.5}$$

$$\omega = -\frac{D}{2H}(\omega - \omega_0) + \frac{\omega_0}{2H}(P_m - P_e) \tag{2.6}$$

Wherein δ indicates the generator's rotors angles, ω is the generator's operating rate, ω_0 is the synchronous generator which is additionally the required speed, H is the inertial steady, P_m is the generator's damping constant, and P_e is the active or effective electricity generated by the engine.

The preceding equations describe the electricity dynamic behavior of a synchronous generator in a separate unbounded bus network [78]:

$$E'_q = \frac{1}{T_{do}}\left(E_f - E_q\right) \tag{2.7}$$

where E'_q is the particular during summer transitory voltages, E_q is the quadrature-axis electrical energy, T_{do} is the direct-axis open-circuit transitory constant value, and E_f is the corresponding voltage in the generator's excited coils. Each synchronous motor is outfitted with two principal process controls, the automated voltage regulator (AVR) and governor (GOV), which are discussed more below.

Automatic voltage regulator

The automated charge controller, commonly known as the excitation current, controls the output voltages of the synchronous generator. Field currents for a large synchronous generator may be needed by the exciter [33][83][84]. It is also used in conjunction with the stabilizer of the electricity system to maintain the electric grid's voltage. The generator's output voltage is compared with a reference voltage, and any discrepancy is magnified and fed into the fields of an elevated DC machine. The basic AVR controller block is borrowed from [81] and is depicted in Figure 2.5, where V_t is the node voltage of the synchronous generator, V_{to} is the reference voltage, E_{fdo} is the position voltage index in the generator's excitation coil, and E_{fd} is the fielding potential difference.

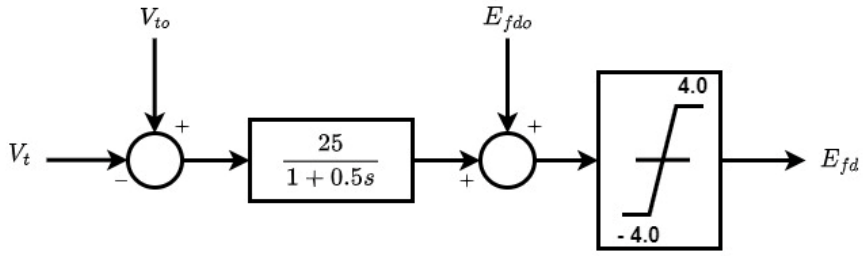

Figure 2.4: Voltage regulator's automatic control block.

Governor

A governor is a mechanism that regulates the performance of a primary motion. Another governor prevents and preserves the primary motor velocity during or around the required number of rotations per minute [82]. The GOV control structure is depicted in Figure 2.5, where ω_m is the observed synchronous generator rotor speed, ω_{mo} denotes the standard rotation speed, P_o denotes the referenced mechanical energy, and P_m denotes the mechanical energy.

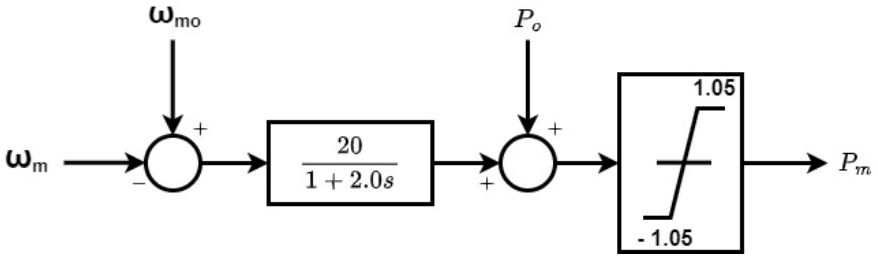

Figure 2.5: The governor's model's control block.

2.3.3 Load model

Nonlinear voltage-dependent loads are examined, namely the polynomial ZIP (constant impedance, constant current, and constant power) load models [1][2]. Active and reactive load power components are expressed as at bus k, where $k = 1, \dots, n$.

$$P_{Lk}(V_k) = (a_{ok} + a_{1k}V_k + a_{2k}V_k^2)P_{ok} \quad (2.8)$$

$$Q_{Lk}(V_k) = (a_{ok} + a_{1k}V_k + a_{2k}V_k^2)Q_{ok} \quad (2.9)$$

Where a $a_{0k} + a_{1k} + a_{2k} = 1$, $b_{0k} + b_{1k} + b_{2k} = 1$, P_{0k} and Q_{0k} denote the nominal active and reactive power components. Table A1.2 in Appendix A1 shows the active and reactive load components. For dynamic simulation in this thesis, the constant impedance load model is utilized, with a $a_0 = a_1 = b_0 = b_1 = 0$ and $a_2 = b_2 = 1$.

2.3.4 Transmission line model

π- Circuit and series resistance value indicate the transmission line or cable connecting the two buses (Figure) *i* and *j*:

$$\bar{z}_{IJ} = z_{ij}e^{j\delta_{ij}} = r_{ij} + jx_{ij} \quad (2.10)$$

Aside from that, there's a shunt admittance on the *i* side.

$$\bar{y}_{IJ} = g_{ij} + jb_{ij} \quad (2.11)$$

Because the π-circuit is symmetrical, we may write:

$$g_{ij} = g_{ji} = 0 \quad (2.12)$$

and

$$b_{ij} = b_{ji} = \frac{c_{ij\omega}}{2}0 \quad (2.13)$$

Where;
$C_{ij}\omega$ shows simplicity

ω is the same angle as the base frequency
C_{ij} is capacity

2.3.5 Combined TSC and TCR (SVC) model

TCR and TSC are the two components of the SVC FACTS device. The TCR device is used to control the maximum voltage. A TSC device is used to control the minimum voltage. The simulation software Matlab is used to calculate the size of SVC. After determining the quantity of capacitive reactive power $[Q_{TSC}]$ for the system by capacitor bank using optimal capacitor placement, the slope for SVC characteristics in percent and the slope of the operating terminal voltage in the inductive and capacitive region can be calculated using the following equation [74] and more details can be found in papers C and D.

The rated inductive and capacitive currents of SVC are determined at the rated line to line voltage V_{rated} as follows:

$$Q_{TCR} = 2Q_{TSC} \tag{2.14}$$

$$Q_{Lrated} = \sqrt{3}V_{rated}I_{Lrated} \tag{2.15}$$

$$I_{Lrated} = \frac{Q_{Lrated}}{\sqrt{3}V_{rated}} \tag{2.16}$$

$$Q_{Crated} = \sqrt{3}V_{rated}I_{Crated} \tag{2.17}$$

$$I_{Crated} = \frac{Q_{Crated}}{\sqrt{3}V_{rated}} \tag{2.18}$$

The maximum inductive voltage, inductive susceptance, and minimum inductive current of SVC may be computed at the minimum line to line voltage as follows:

$$V_{indmax} = V_{ref} + (X_{capacitive}\, I_{max}) \tag{2.19}$$

$$B_{L(TCR)} = \frac{Q_{TCR}}{V_{indmax}^2} \rightarrow (\alpha = 90°) \tag{2.20}$$

$$I_{indmax} = \frac{Q_{SVC}}{\sqrt{3}V_{indmax}} = \frac{Q_{TCR}}{\sqrt{3}V_{indmax}} \tag{2.21}$$

The capacitance voltage, capacitive susceptance, and maximum capacitive current may be computed at the minimum line to line voltage as follows:

$$V_{capmax} = V_{ref} + (X_{inductive}\, I_{max}) \tag{2.22}$$

$$B_{C(TSC)} = \frac{Q_{SVC}}{V_{capmax}^2} \rightarrow (\alpha = 180°) \tag{2.23}$$

$$I_{capmax} = \frac{Q_{SVC}}{\sqrt{3}V_{capmax}} = \frac{-Q_{TSC}}{\sqrt{3}V_{capmax}} \tag{2.24}$$

The value of the inductive reactance, capacitive reactance, capacitive and reactive suscepatance of SVC at the given frequency may be computed using inductive susceptance $B_{L(TCR)}$ in Siemens and capacitive susceptance $B_{C(TSC)}$ in Siemens as follows:

$$X_{L(TCR)} = \frac{1}{B_{L(TCR)}} = 2\pi fL \tag{2.25}$$

$$L = \frac{1}{2\pi fLB_{L(TCR)}} \tag{2.26}$$

$$X_{C(TSC)} = \frac{1}{B_{C(TSC)}} = \frac{1}{2\pi fC} \tag{2.27}$$

$$C = \frac{B_{C(TSC)}}{2\pi f} \tag{2.30}$$

A constant capacitance (CC) quantity of the SVC may be calculated as $Q_c = Q_{max} - Q_{ref}$, in which Q_c is just the electrical energy of the (CC) and Q_{max} is the highest reactive current demand. Equation 2.31 shows the TCR-TSC type SVC with control circuit.

$$Q_{SVC} = \frac{V^2(X_c[2\pi - \alpha + \sin 2\alpha] - \pi X_L)}{(\pi X_C X_L)} \tag{2.31}$$

i. Power loss constraints

After compensation, the system power loss must be less than or equal to the loss before compensation. i.e.

P_L with SVC $\leq P_L$ without SVC
Q_L with SVC $\leq Q_L$ without SVC

ii. Voltage constraints

This restriction is used to ensure that the voltage of any bus remains within set limits. That is, 10% of the bus voltage.

$$V_{bus-min} \leq V_{bus} \leq V_{bus-max} \tag{2.31}$$

Where; V_{min} = minimum voltage limit
V_{bus} = operating bus voltage
V_{max} = maximum voltage limit

2.3.6 STATCOM model

The STATCOM equivalent circuit is shown in Figure 2.6. In this circuit, the inductance x_s reflects the leaking inductance of the transformer; the resistor r_s indicates the total of the conduction and switching inefficiencies; and the shunt resistance r_p indicates the energy loss in the dc capacitor. As illustrated in Figure 2.6, the VSC acts as an alternate voltage; the current source has a variable magnitude behind the equivalent impedance, and the phase angle [85]–[87] represents the voltage vector.

$$V_c = k_s k_t m V_{dc} \angle \alpha \tag{2.32}$$

Where V_{dc} is the direct current voltage from across inverters, k_s is the converter's direct current (DC) to alternating current (AC) gain, m is the modulating rate of PWM control, VSC is the regulator angle, and k_t is still the coupling transformer rate. The injection current into the AC system via the STATCOM shunt is represented as:

$$I_S = \frac{V_s - V_c}{Z_s} \tag{2.33}$$

Where $V_s = |V_s|\angle\theta_s$ denotes the voltage vector of AC power bus s, and where $Z_s = Z_s\angle\beta = r_s + jx_s$. STATCOM's active and reactive power injections into the AC system via STATCOM are presented as follows

$$P_s = Re(V_s I_s^*) = \frac{k_c k_t m\, V_{dc} V_s\, cos(\theta_s - \alpha + \beta) - V_s^2 \cos\beta}{Z_s} \tag{2.34}$$

$$Q_s = Im(V_s I_s^*) = \frac{V_s^2 \sin\beta - k_c k_t m\, V_{dc} V_s\, sin(\theta_s - \alpha + \beta)}{Z_s} \tag{2.35}$$

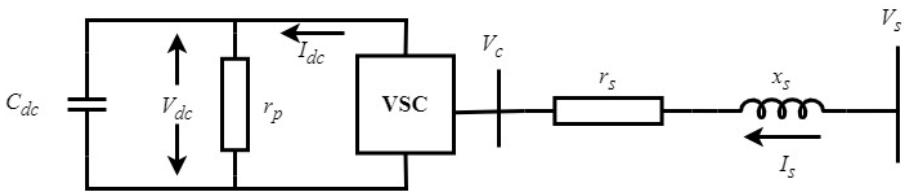

Figure 2.6: Equivalent circuit of STATCOM.

The power balancing equations at the AC system bus s are therefore written as

$$\Delta P_s = P_s + P_{si} - P_{sd} = 0 \tag{2.36}$$

$$\Delta Q_s = Q_s + Q_{si} - Q_{sd} = 0 \tag{2.37}$$

Where P_{sd} and Q_{sd} represent the real and reactive load exiting the bus s, while P_{si} and Q_{si} represent the real and reactive fluxes injecting into the bus s, respectively. The reactive power of VSC's ac side is provided as

$$P_{ac} = Re(V_c I_s^*) = \frac{V_c V_s\, cos(\theta_s - \alpha + \beta) - V_c^2 \cos\beta}{Z_s} \tag{2.38}$$

The real power of the VSC's dc side is stated as

$$P_{dc} = V_{dc} I_{dc} = V_{dc}\left(C_{dc}\frac{\mathrm{d}V_{dc}}{d_t} + \frac{V_{dc}}{r_p}\right) \tag{2.39}$$

The power balance between the ac and dc side of the STATCOM is given as

$$P_{ac} = P_{dc} + losses \tag{2.40}$$

Losses can be important, but in this study they were neglected in the analysis of the system ($losses = 0$). This is because the losses are usually small compared to the required power and generation. In steady-state operating condition, the active power exchange equation is given as

$$P_{ex} = r_p(k_s k_t m)^2 V_{dc} \cos\beta + V_{dc} I_{dc} - r_p k_t m V_s \cos(\alpha - \theta_s + \beta) = 0 \tag{2.41}$$

2.4 Proposed mitigation methods

In this research, we first demonstrated the influence of time delay signals on anti-brake (BR) behavior utilizing a suggested fuzzy logic control implementation as well as the important quantities linked to the PSO and GOA implementation flowcharts in UFLS development. The efficacy of the newly suggested TSC and TCR (SVC)-based mitigation FLC and Adapted Predictor Technique is evaluated in the second step. We then offer a unique mitigation methodology that effectively decreases the impact of a cyber-attack, allowing PI and non-linear controller implementation of SVC and STATACOM mitigation methods to be investigated.

The mitigation measures proposed here provide the results of the procedure when the effect of communication delay is found in the process design. Based on the delayed results achieved in different ways, delay reduction measures based on the faults that had occurred in the attacks had occurred in the electrical design in order to avoid the occurrence of grid-damaging disturbances during the monitoring of the grid performance, as discussed below and also in research papers A, B, C, and D.

2.4.1 Fuzzy logic controller implementation for anti-brake (BR)

The intended control technique comprises only three control rules for each unit, according to Table 2.1, at which variables represent the fuzzy output of such a controller as the language evolves. FLC is returned to the detailed rule table, where it is determined by the minimum score of all members of the performance control BR.

Table 2.1 Fuzzy rule table.

$\mathbf{TKED'\ (pu/s)}$	$\boldsymbol{\alpha}$ **(Firing angle)**
N	Big
Z	Medium
P	Small

Fuzzy interference

Mandani's [92] approach is utilized to determine, based on a fuzzy analysis. Regarding Mandani's degrees of fitting together, W_i is associated with each fuzzy command as follows:

$$W_i = \mu_A(TKED') \tag{2.42}$$

Where $\mu_A(TKED')$ is the member's lowest potential score and i is the step number. The center area has become an established and readily reduced strategy for controlling the output level (i.e., GHF). The following sentence provides it [88]:

$$\alpha = \frac{\sum W_i C_i}{\sum W_i} \tag{2.43}$$

Where C_i represents the cost of α in the fuzzified instruction set.

2.4.2 PSO and GOA implementation flowchart in UFLS development

The optimal UFLS software is provided to minimize load shed and enhance the system's bottom swing times. PSO and GOA set the highest standards. The diagram used with the GOA algorithms to produce UFLS is shown in Figures 2.7 and 2.8.

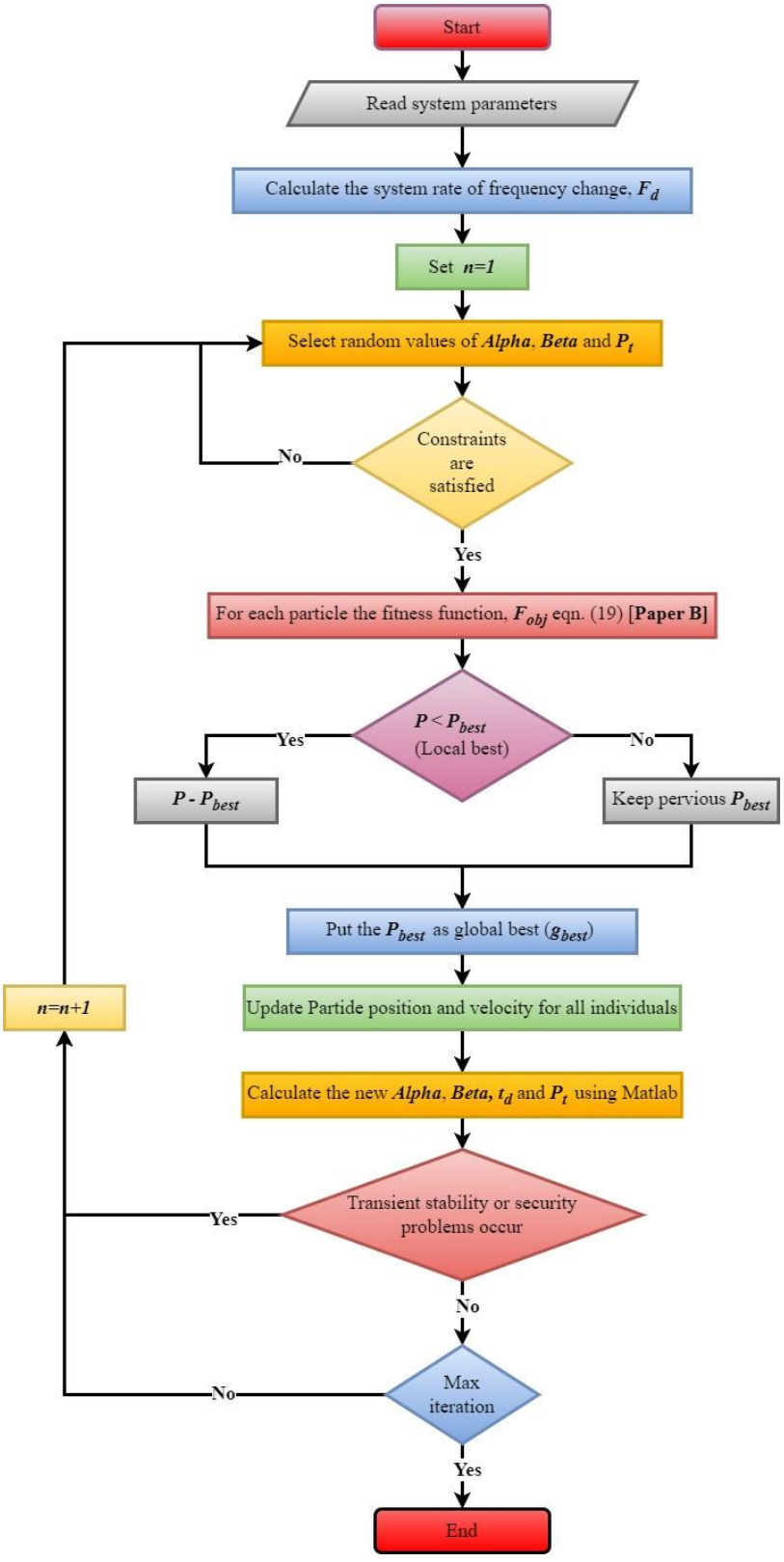

Figure 2.7: GOA Flowchart in UFLS Development.

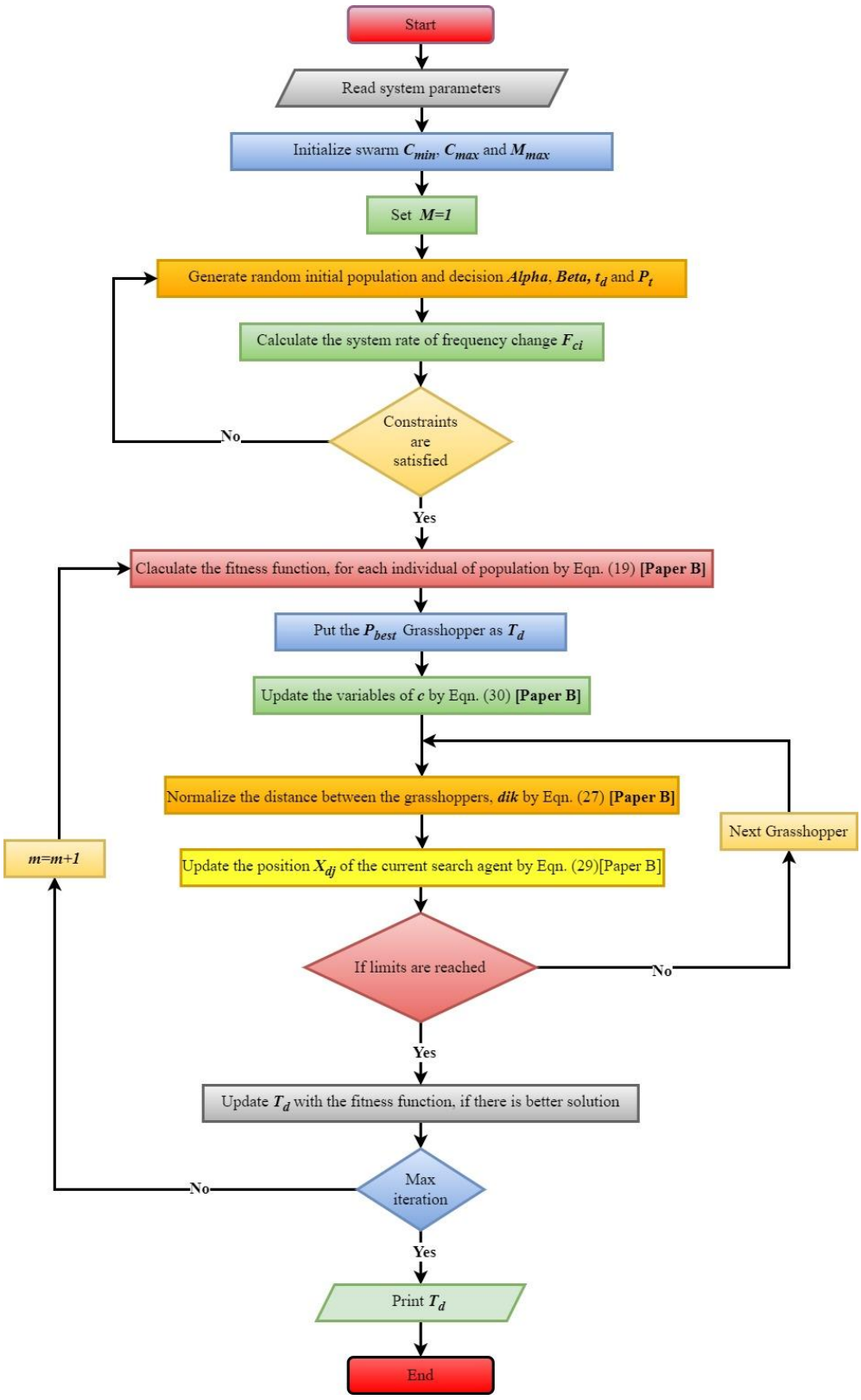

Figure 2.8: PSO Flowchart in UFLS Development.

2.4.3 FLC and adapted predictor method implementation for TSC and TCR (SVC)

In this study, the two-input FLC is employed to mitigate the adverse effects of temporary latencies for TSC performances. For FLC, inputs are really ac voltage variations in PCC and V, in addition to the control input response time (D). Each operator's outcome is alpha (α), which corresponds to the firing angles of the thyristor. As during the controller's concept stage, the signal delay ranges from 100 to 900 ms, covering all practical scenarios [38][42]. The following is an outline of the proposed FLC.

Characters NB indicating negative big, NM meaning a negative medium, Z meaning zero, PM meaning a positive medium, PB for positive big, N meaning negative, and P meaning positive are shown in Figure 2.9. Figure 2.10 and Table 2.2 illustrate the membership functions of the thyristors' firing angle, alpha (α). These are as follows: NB, NM, Z, PM, and PB. To evaluate the degree of crispness, a single continuity equation (2.44) [94] has been used throughout this investigation:

$$\mu_{Ai}(x) = \frac{1}{b}(b - 2|x - a|) \tag{2.44}$$

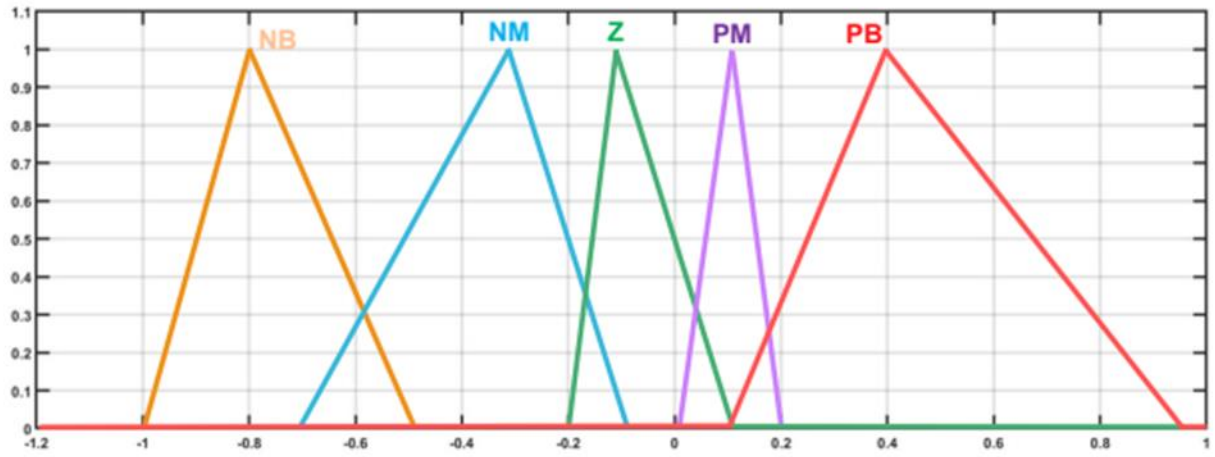

(a)

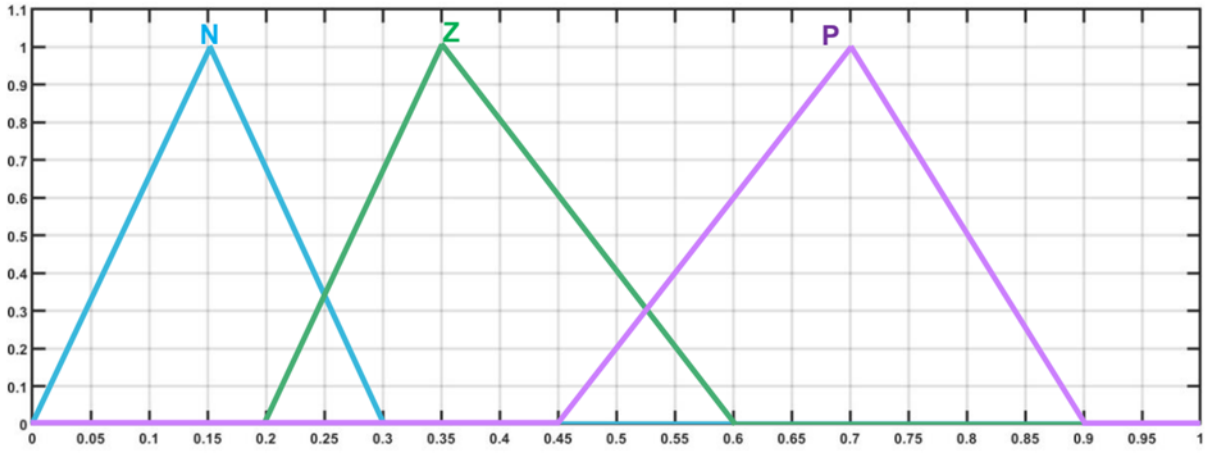

(b)

Figure 2.9: Fuzzy logic control function applies functions (a) ΔV. (b) Delay.

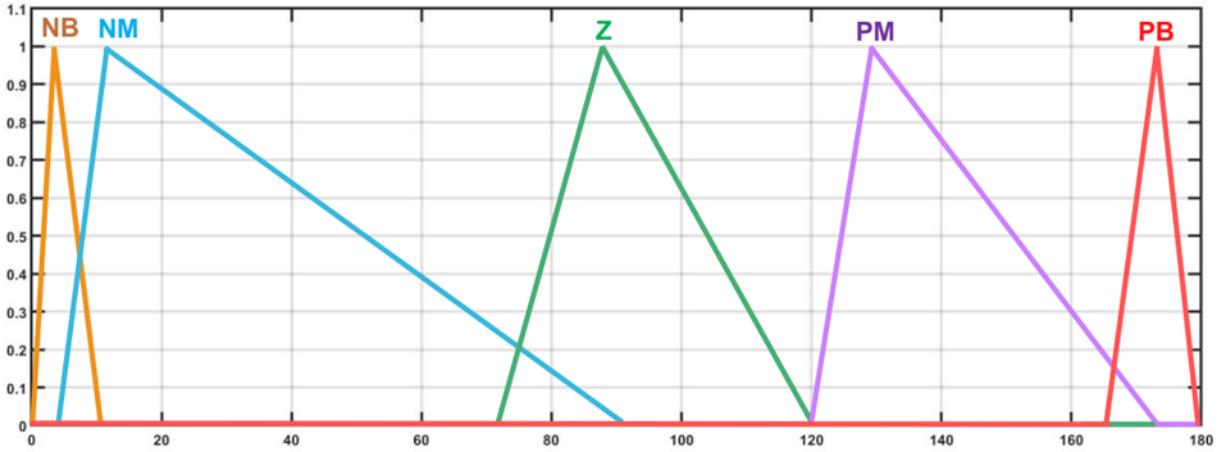

Figure 2.10: Membership purposes of fuzzy controller output Linear.

Table 2.2 Corresponding membership input and output

ΔV / D	NB	NM	Z	PM	PB
N	PB	PM	Z	NM	NB
Z	PB	PM	Z	NM	NB
P	PB	PM	Z	NM	NB

Equation (2.45) depicts the degree of conformance Wi of each fuzzy rule based on Mamdani's technique.

$$W_i = \mu_{Ai}(\Delta V) \times \mu_{Bi}(D) \tag{2.45}$$

Where $\mu_{Ai}(\Delta V)$ and $\mu_{Bi}(D)$ are the membership grade values and i represents the rule number.

Defuzzification is a procedure used to fix the crisp output (i.e., the firing angle of the thyristor, α) for the controller using the center-of-area approach.

$$\Delta V_p = \Delta V_{previous} + t_d . \Delta V . c \tag{2.46}$$

$$\Delta V = \frac{\Delta V_k - \Delta V_{(k-1)}}{\Delta t} \tag{2.47}$$

Figures 2.11 and 2.12 demonstrate the predictive technique, which is adaptable to any controller. The anticipated ΔV can be calculated using the value in relation to previously recorded values and estimates, even though there is a significant delay in t_d.

k indicates the actual placement, whereas p indicates the projected position. c denotes a constant value, whereas ΔV denotes the rate at which the operator's signal changes. Through trial and error, the c was found to be 0.25.

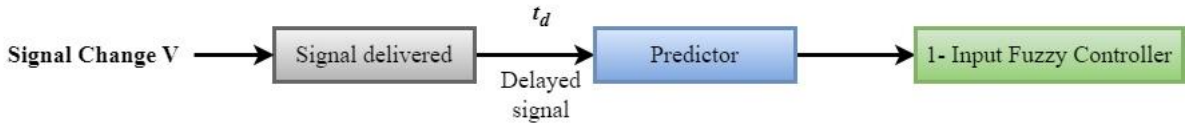

Figure 2.11: Model predictor.

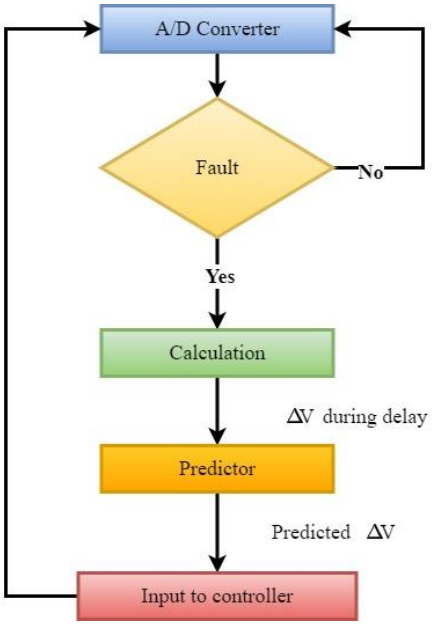

Figure 2.12: Diagram structure of the improved prediction method.

2.4.4 Non-linear controller implementation for SVC and STATACOM

Figures 2.13 and 2.14 depict the SVC and STATCOM control blocks, respectively. The Mount Kigali SSB-9 bus voltage is linked to the situation value, and the difference is communicated via a PI or NL controller to calculate the shunted capacitor. In two case studies, the frequency relay's failure due to a cyber-attack was used.

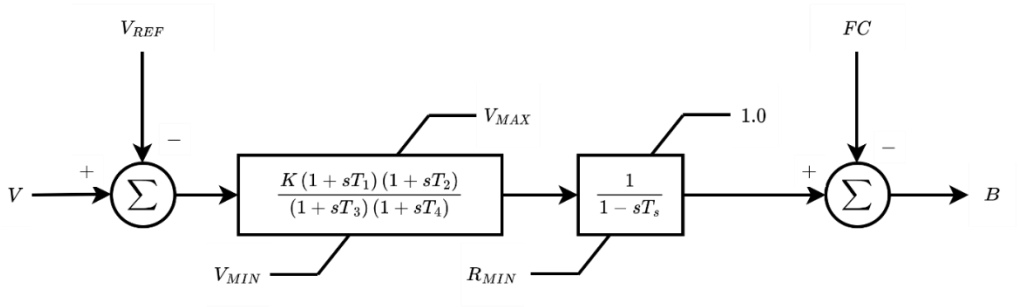

Figure 2.13: Block diagram of the SVC control system.

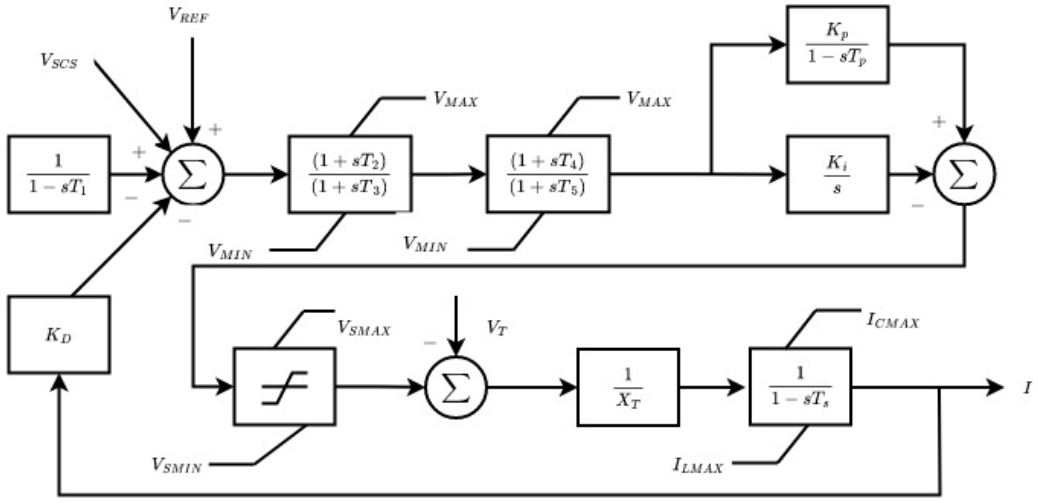

Figure 2.14: STATCOM control system block diagram.

$$V_{vr_{ref(SVC)}} = K_1 \left|\Delta V_{pcc}\right| \tag{2.48}$$

$$V_{vr_{ref(STATCOM)}} = K_2 \left|\Delta V_{pcc}\right| \tag{2.49}$$

Where ΔV_{pcc} is the controller's input and K_1 and K_2 are constant values. The necessary values of the $V_{vr_{ref(SVC)}}$ and $V_{vr_{ref(STATCOM)}}$ are achieved by adjusting the values of K_1 and K_2. The

parameters were chosen such that the controller could tolerate any voltage fluctuation, from extremely high to extremely low.

2.4.5 PI Controller for SVC and STATCOM

$$V_{vr_{ref(SVC)}} = \left|\Delta V_{pcc}\right| \left[K_{p1} + \frac{1}{s} K_{i1}\right] \tag{2.50}$$

$$V_{vr_{ref(STATCOM)}} = \left|\Delta V_{pcc}\right| \left[K_{p2} + \frac{1}{s} K_{i2}\right] \tag{2.51}$$

Where K_{p1}, K_{p2}, and K_{i1}, K_{i2} represent the proportional and integral gains of the PI controller. From Figure 2.15, the controller's input is ΔV_{pcc}, and its output variables are $V_{vr_{ref(SVC)}}$, $V_{vr_{ref(STATCOM)}}$ respectively. These parameters were discovered by using trial and error, and they are capable of mitigating any sudden change in the input.

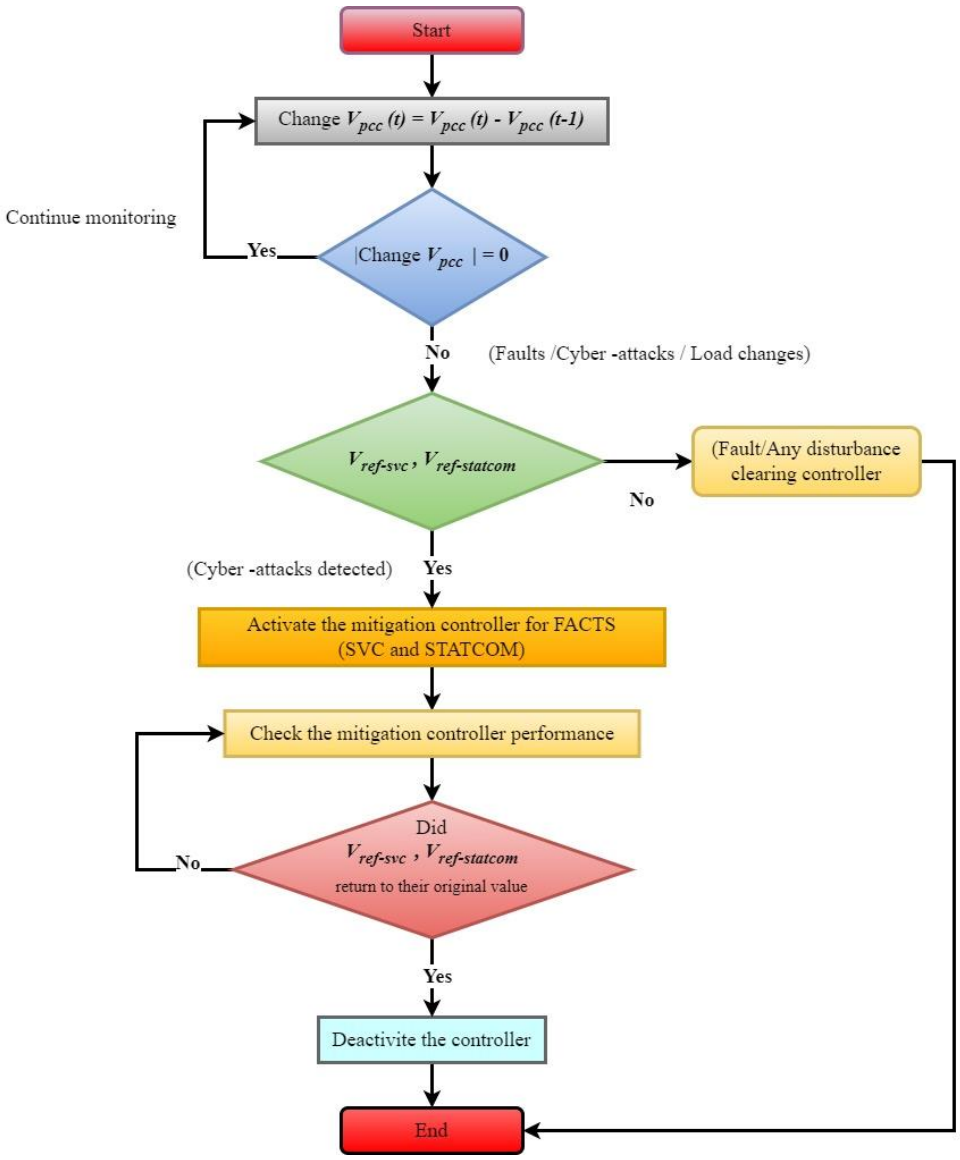

Figure 2.15: Proposed control algorithm for SVC and STATCOM.

2.5 Model accuracy indicators

An index that could be used to gauge the suggested model's effectiveness must be defined to assess its performance. The Total Harmonic Distortion (THD), Voltage Index (V index), and angle stability index are the most often utilized performance indicators in monitoring power quality disturbances [89]. Furthermore, papers A–D define the restrictions in full.

2.5.1 Total kinetic energy deviation (TKED)

Fuzzy-controlled BRs are useful in enhancing short-term stability by addressing various issues, as shown in Table 11, which is readily apparent. The number of fuzzy controller lines in the BR input controller, which alter the short-term impact of grid faults, turns out to be a significant factor in communication delays. To investigate the impact of communication delays on power system integration, we initially performed a study with no communication delays. Moreover, we proceed to investigate the short-term system in terms of fitting deviation of total kinetic energy (W_c) values as supplied by

$$W_c(sec) = \int_0^T \left| \frac{d}{dt} W_{total} \right| dt / system\ base\ power \tag{2.52}$$

The system's structure is discovered during the process of determining it, and working hours are under control. According to equation (2.51), T is the imitation time, which is 0.7 seconds, and W_{total} is the total kinetic energy. Additionally, the use of W_c was necessary to evaluate the effectiveness of the system's downtime.

$$W_{total} = \sum_{i=1}^{N} W_i \tag{2.53}$$

Where

$$W_i = \frac{1}{2} J_I {\omega_{mi}}^2 (J) \tag{2.54}$$

Since the system is designed to govern power generating behavior, W_i represents the generator's kinetic energy (in joules), i represent the number of generators, and N represents the overall number of generators.

$$J_i = \frac{H \times MVA\ rating}{5.48 \times 10^{-9} N_s^2} \tag{2.55}$$

Where

$$\omega_{mi} = \frac{2\pi N_R}{60} \tag{2.56}$$

In addition, equation (2.50) indicates the inertia moment in $Kg.m^2$, where N_s^2 are synchronized advancing at constant rpm and inertia is fixed; moreover, ω_mi is the rotor's highest speed in electromechanical rad/sec) and N_R is the rotor speed in rpm (rpm).

2.5.2 Total harmonic distortion (THD)

THD has been defined as the actual value of the harmonic components of a distorted fundamental waveform. In other terms, the THD has been the sum of all harmonic content of the current or voltage waveform relative to the foundational element of the voltage or current waveform, as proven in [79] [80]. THDu was determined via an equation (2.51).

$$THDu = \frac{\sqrt{(V_2^2 + V_3^2 + \cdots + V_n^2)}}{V_1} * 100\% \tag{2.57}$$

When V_1 represents the fundamental potential (typically the 1st harmonic) and $V_2, V_3 \ldots V_n$ n represent the magnitudes of the individual harmonic potentials (2nd, 3rd, ..., nth harmonics) of something like the PCC voltage, the higher the THDu, the worse the distortion of the basic signal. The THDu restrictions are around 5%.

2.5.3 Analysis of power quality in terms of voltage index

Through (2.58), the voltage index (V_{index}) is utilized to investigate the effectiveness of the recommended TSC techniques in further detail.

$$V_{index} = \int_0^T \left| \frac{d}{dt} \Delta V \right| dt \tag{2.58}$$

Where V signifies the different voltage variations just at the PCC and T denotes a 30-second computation time. Usually, the smaller the indicator overall, the better the functionalization.

2.5.4 Angle stability and index of angle stability

Angle stability is the capacity of an electricity system to sustain synchronization in the face of a disturbance by maintaining or restoring the balance between mechanical and electromagnetic torque [90]. To investigate the motion of a single synchronous generator, are using the condensed swing equation (2.58).

$$J \frac{d^2\theta}{dt^2} = T_m - T_e \tag{2.59}$$

Where θ is the angular position of the rotor, J is the combined moment of inertia of the connected turbine and generator rotor masses, and T_m and T_e are the mechanically and electromagnetic torques, respectively. An angle stability index [90] is developed to measure the impact of cyber-attacks on angle stability (2.59).

$$\eta = \frac{360^0 - \delta_{max}}{360^0 + \delta_{max}} \times 100\%, -100 < \eta < 100 \tag{2.60}$$

In the post-contingency system, δ_{max} specifies the greatest angle separation between two generators. Understand as $\eta > 0$ and $\eta \leq 0$ represent stable and unstable situations, respectively.

2.6 Several power quality issues in the modern power grid

Unfortunately, there are three primary difficulties to modern electricity: nonlinearity (Non-Linear Controllers), signal delay, and cyber-attacks, all of which have a significant influence on improving the quality of electricity. Finally, the constraints are described in detail in sections papers 1 to 4.

2.7 Software used for modeling

Data is collected and analyzed for the chosen system. For simulation, Matlab R2021a Simulink software is utilized. Simulations are performed both with and without FACTs. The FACTs are placed in Mount Kigali substations, and simulations are run to assess how they affect the system. The existence of reactors on the system is also simulated, and their impact is examined. Finally, the constraints are described in detail in papers A to D.

CHAPTER THREE: RESULTS AND DISCUSSION

This section presents and discusses the most important aspects of the resurgence in communication delays and cyber-attacks. The correctness of the created model is assessed using the total harmonic distortion (THD), Voltage Index (V-index), Deviation of total kinetic energy index (DTKE-index) and Angle Stability Index (AS-index), based on the results from simulation. Detailed Notes on the trends are shown below, and in the attachment, there is a sequence of steps that will be used in the table.

3.1 Power grid implications of communication signal delay

Table 3.1 summarizes some results from comparing this delay control strategy to the delay compensation that is related to the power management unit described in the preceding sections, with further information available in review papers A–D. A comparison of the thirteen validated adaptation strategies explained mostly in the table has already revealed the best results in various latencies that affect the frequency and amplitude of something like the entire network, in addition to the significance of mathematical ability, reliability, numeracy's continued growth, validation of dependence on wireless transmission methods, security mechanisms, and various other practical research results as evidenced by the integrity of the use of the ETDC method and the MFAC method.

Figures 3.1 and 3.2 illustrate fixes for points A and C, which makes it essential to comprehend well how to rectify the short fault throughout to operate as intended and preserve the electric grid. To restrict the current harmonics before the initial peak, the malfunction must always be detected at least 5 different milliseconds after it occurs (assuming the apparatus used to clear the fault has zero operating time). In fact, the overall operational duration of the switch utilized for the present diversions would be approximately 3-5 ms, including around one millisecond available for fault detection, assuming a threshold of 1-3 ms is adequate to ensure that the fault was lowered prior to the initial highest peak.

Figures 3.1 and 3.2 depict the associated location's active power and fault behavior, as well as the BR fuzzy control, throughout the delay period. Figure 9 shows that the short-term performance is poorer than in Figure 3.2. This demonstrates that the communication delay affects the fault's short-term performance, implying that perhaps the peaks of G2 & G3 become different in 300 ms owing to the fault. Paper A contains further results, including those obtained without and with a fuzzy-controlled BR index, for the influence of critical defects on different communication delays.

Table 3.1 comparison of various algorithms.

Techniques	**Application Size**	**Threshold Parameters Applied**	**Compared with**	**Results**
[91] BA and BESS (2019)	Java 500 kV Indonesian grid (WAMC)	$T_d = 100\ ms\ to\ 700\ ms$, $f = 0.6567\ Hz,\ \rho = 0.0569$	POD and BESS	Higher accuracy and faster than BESS, highly competitive with POD and BESS
[92] DOFC (2021)	Four Machine Two-Area Power System (WADC)	$T_d = 100\ ms, f = 0.6567\ Hz,$ $\rho = 0.0823$	PID	Better performance than PID, Execution time is less.
[93] ETDC + MPC (2021)	Kundur's 2-area test system (WAMS)	$T_d = 100\ ms\ to\ 500\ ms,$ $f = 0.598\ Hz, \rho = 0.0205$	SPB + MPC	More accurate, scalable and efficient reduction of overshoot (about 39%) implies less stress over the thermal limits and less impact of isolation due to protective actions.
[31] FLC (2021)	IEEJ WEST 10-machine system	$T_d = 50\ ms\ to\ 300\ ms,$ $f = 0.1\ Hz\ to\ 2.0\ Hz,$ $\rho = 0.0315, 0.0246,$ $0.016, 0.0077$	Fuzzy controlled BR	More time efficient and faster than without SDC
[38] UFLS Traditional (2020)	IEEE 14 bus system	$T_d = 2.043\ s\ to\ 2.214\ s, f =$ $0.1\ Hz\ to\ 2.0\ Hz, \rho =$ $0.0315, 0.0246,\ 0.016\ \ 0.0077$	PSO and GOA	GOA method can best work within a given local area to avoid the spread to other regions within the grid network.
[4] FLC (2021)	Kigali National Grid system	$T_d = 100\ ms\ to\ 900\ ms, f =$ $0.1\ Hz\ to\ 2.0\ Hz, \rho =$ $0.0315, 0.0246,\ 0.016, 0.0077$	MPM	More consistent and highly effective at classification and has minimize the impact of delay in positioning on the power structure of the Hybrid system.
NL (2021)	Kigali National Grid system	$T_d = 100\ ms\ to\ 900\ ms$ $f = 0.1\ Hz\ to\ 2.0\ Hz$ $\rho = 0.0315, 0.0246,$	PI	NL is more effective during various attacks and is employed for STATCOM than SVC.

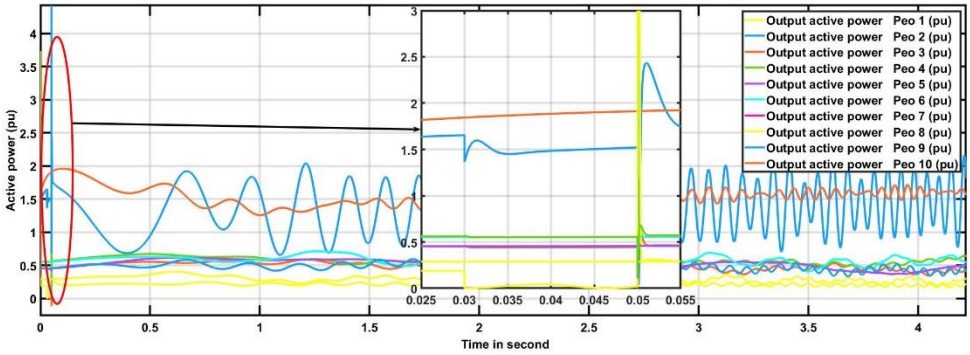

Figure 3.1: Active power response at point A for 3 LG faults.

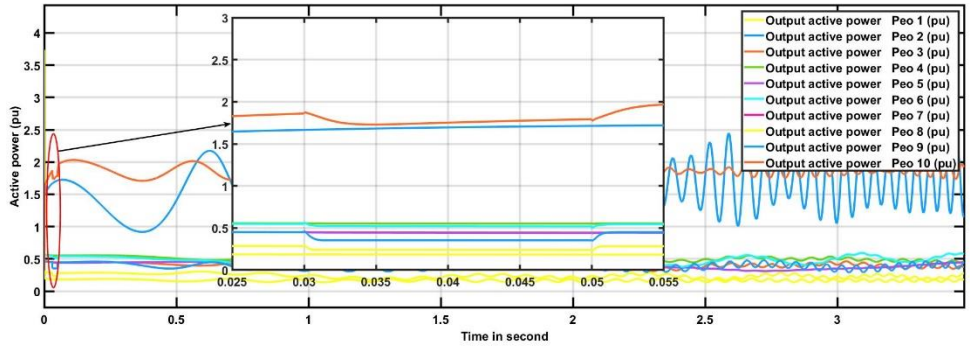

Figure 3.2: Active power response at point C for 3 LG faults.

3.2 UFLS techniques for the effects of communication delay

The findings are depicted in Figure 3.3. The experiment revealed that, while the load shedding scheme's activities had little effect on the number of loads shed, and also the period of the shedding operations, the micro-grid frequency limitation was very well-preserved at the necessary 47 Hz. Variations in dumping activities are to be expected because communication delays during the load sequence caused the functionality to fluctuate. As demonstrated in Figure 3.4, a signaling latency of 150 ms has been found to affect load shedding, resulting in a lengthy delay with the highest benefit of 0.448 MW load shedding compared to certain other delays of around 50 ms with a peak value of 0.25 MW.

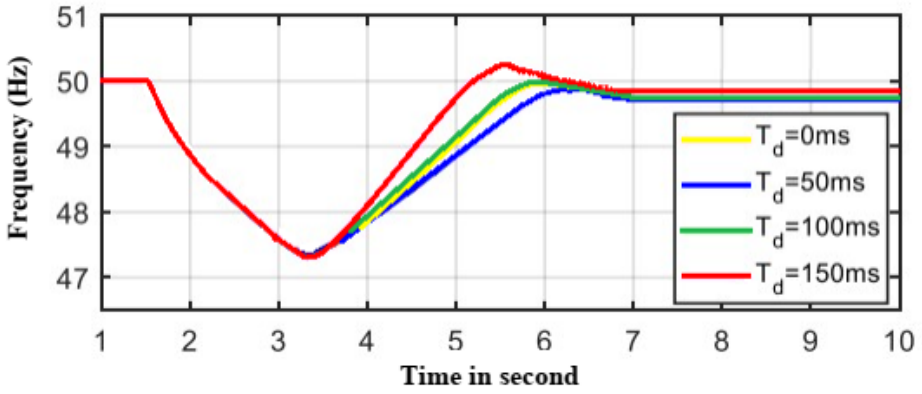

Figure 3.3: Effect of communication delays on the performance of the suggested load-shedding scheme.

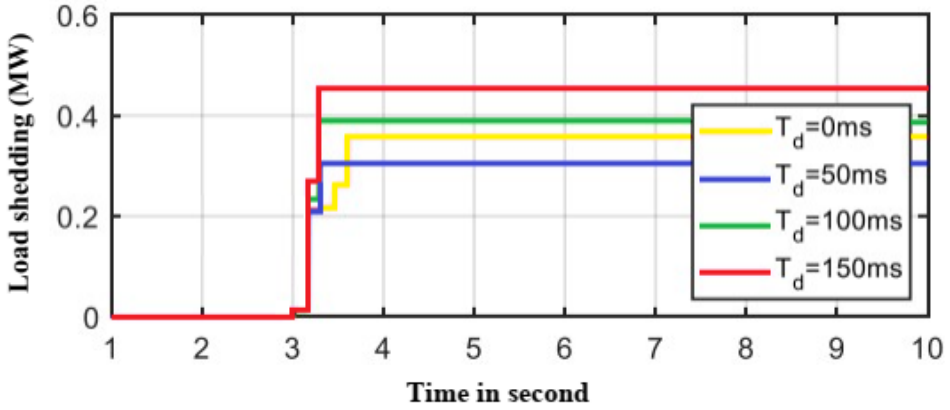

Figure 3.4: The effect of communication delays the functioning of the suggested load-shedding scheme.

During this case, Table 3.2 also provides numerical data from traditional, PSO, and GOA techniques. The GOA criteria has a low swing frequency value and a restricted number of loads, as shown in Table 3.2. GOA provides great overall functionality since it improves the number of oscillations while decreasing loads. The objective of reinstating the permanent line system and lowering the amount of load in a short period of time has led to a rise in the number of GOA categories. GOA additionally contains a tiny communication delay between phases, which decreases the automatic strain on the producing parts. Further results include the severity of the bus voltages for different losses in a 72 MW generation. Additional outcomes, including the bus voltage and power at different buses, can be found in Paper B.

Table 3.2 Traditional, PSO, and GOA IEEE 14 bus system performance comparison.

Disturbance	Method	Traditional	PSO	GOA
Line 2-4	Percentage of load shedding, α [%]	44.24	40.875	40.872
	Lowest frequency, [Hz]	48.42862	48.67239	48.8675
	Delay time, t_d [sec]	0.184	0.01	0.0112
	Number of load shedding stages, β	3	6	6
Line 2-4 & Line 2-3	Percentage of load shedding, α [%]	72.3294	69.0536	69.0233
	Lowest frequency, [Hz]	47.62531	48.59842	48.61582
	Delay time, t_d [sec]	1.22	0.08	0.08
	Number of load shedding stages, β	4	9	9

3.3 TSC-TCR (SVC) electric improvements in the Kigali national grid

Hybrid grid includes a Jali PV plant - based diet on Substation (SS9) Mount Kigali, as shown in Figure 3.5, and more details can be found in Paper C. Its functioning is dependent on temperature and irradiance conduction inputs. As a result, the temperature ranges from 25 to 45 °C, and the irradiance ranges from 200-1000 W/m^2. Figure 13 illustrates how V_{dc} and P_{dc} fluctuate with irradiance and temperature, and data points at 10 seconds (on-grid) reveal that Load 20 and Filter C require active and reactive power before functioning with the power network at Substation (SS9) Mount Kigali. Being on the power network appears to cause a power decrease, but it is capable of maintaining Load 20, and when it is fully off, there is a disruption in the readings acquired from all the G1-G6 machines.

The modeled power flow results for a solar module linked to the power grid at various levels of solar irradiation and demand are shown in Table 3.3. As shown in Table 3.3, the power generated by a solar panel is proportional to its solar irradiation. There are several kinds of testing. The first option is that when the output power of the PV system components reaches the load, the extra electricity is consumed by the utility grid. The second alternative is that no electricity is given to the grid if the power generated by the PV system equals the power demand. In the third case, the load will be split between the solar panels and the grid to make up the difference when the PV plant's energy output is insufficient to support self-sufficiency. As demonstrated, using about 30 °C with 400 $400\ W/m^2$ is the best choice for serving our electric system centered on Mount Kigali SS9.

Table 3.3 Results of the planned system's power flow simulations for various levels of solar irradiation.

N_0	Temperature (℃)	Irradiation (W/m^2)	V_{dc} (V)	P_{dc} (kW)	Active Power (kW)		Load capacity (kW)
					PV	Grid	
4	45	1000	481.2	241.5	117.5	-132.5	250.8
3	35	600	493.4	148.6	730.6	-50.9	780.9
2	30	400	497.2	99.75	489.6	356	133.6
1	25	200	495.9	49.67	245.9	-245.9	300.4

The grid's behavior is depicted in Figures C.11 and C.12. For example, in Figure C.11, when there was a single example r separated by the grid and running at 45 degrees and 1000 degrees of irradiance, the PV was deleted. Active power, reactive power,P_{dc}, and V_{dc} grids were all affected by these variations, which occurred between 0 and 18 seconds.

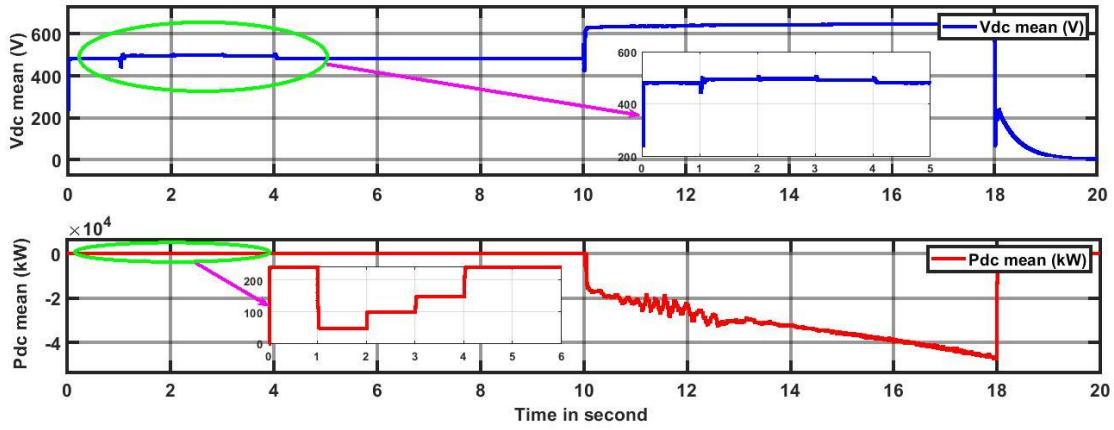

Figure 3.6: Grid-connected PV inverter power converter signals with four-step irradiance P_{dc} and V_{dc} .

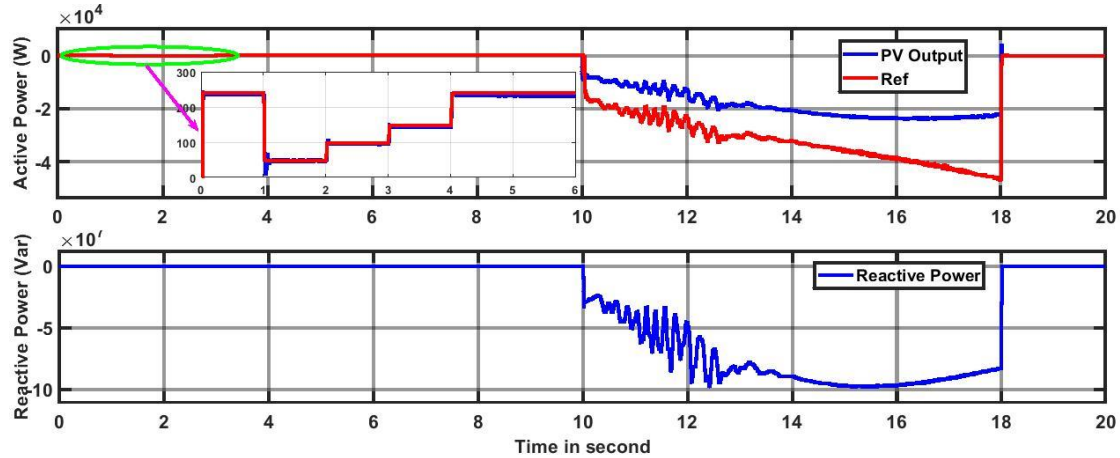

Figure 3.7: PV active and reactive electrical outputs.

3.3.1 Impact of time delay considering minimization techniques

The results of simulation experiments showed that regardless of the amount of signal delay the system was willing to accept for stable operation, the influence of significant delay has been assessed from three aspects: without communication delay, with both the smallest and greatest network latency that the process could tolerate while also maintaining acceptable performance, and using the smallest and greatest latency issues that the system could tolerate while maintaining acceptable performance. The performance significantly contributed to the failure scenarios (G1-G6) when the generators had a 900-ms delay. As shown in the graph, the delay made it harder for the control system to find and address the problem. By adjusting for the delay, the control system may indeed provide effective damping.

The controller took a bit longer to respond to the situation because the power stations (G1-G6) had a 900 ms delay. Despite this, the controller provided appropriate damping performance. Nevertheless, the entire Kigali national grid (KNG) system became unreliable. The simulation results of the study showed that for the system to be more dependable, low-latency communication was necessary. The slower the control operations, which could lead to oscillation and instability of the electric grid, the higher the network latency. The control scheme experienced greater system maximum overshoot and longer settle times as network delays rose from 100 ms to 900 ms.

Figure 3.8 of active and reactive power illustrates how the grid changed whenever the shunted reactors and the two capacitor banks started working 10 seconds after the PV system was flooded for 7 seconds. There was a slight impact when the Jali PV facility was unplugged after 18 seconds.

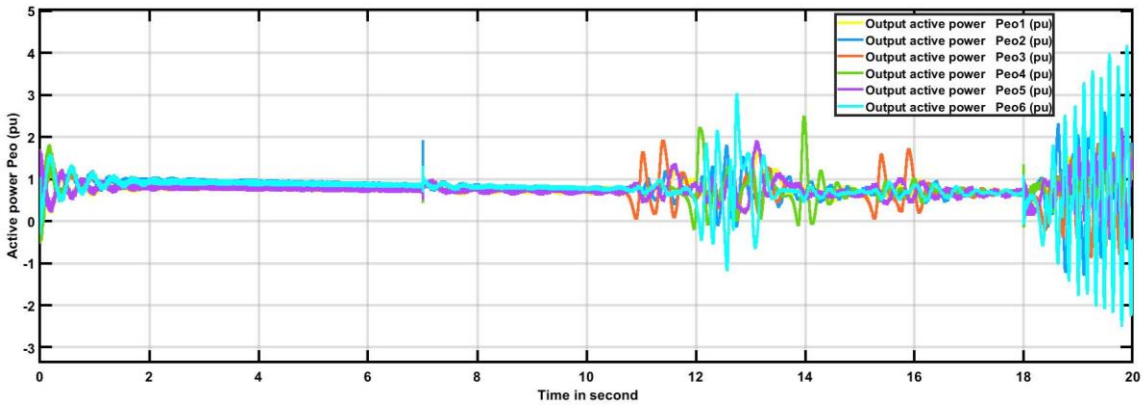

(a)

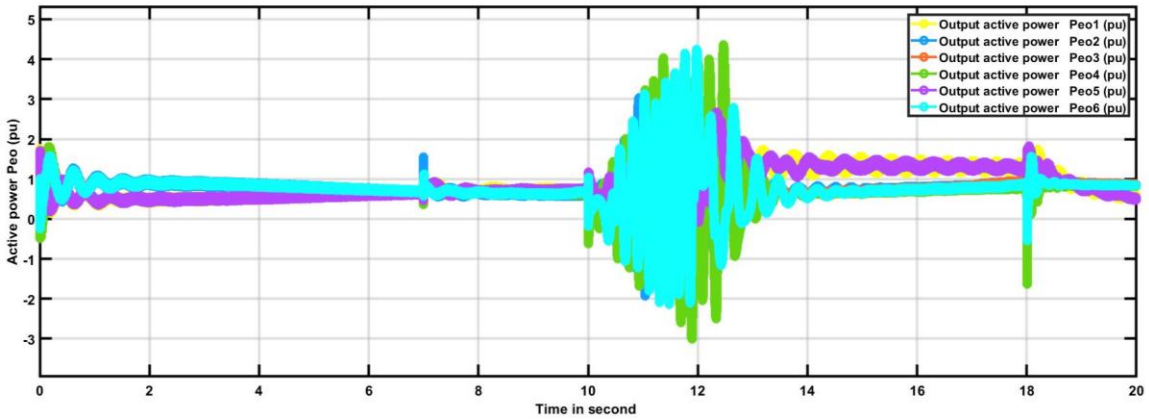

(b)

Figure 3.8: System responses to the fault scenario with constant time delays of 900 ms (a) and 100 ms (b).

According to the modified predictor-delayed elimination method and the fuzzy-regulated delaying reductions methodology, respectively, the voltage index at the PCC for permanent and temporary 3LG faults at electric grid sites A, B, and C with delays of 900, 700, 500, 300, and 100 ms are shown in Table 3.4. The indicator results show how fuzzy-controlled methods with modernized estimation techniques were successful in reducing latency issues while enhancing system voltage stability. Furthermore, the fuzzy-regulated system outperformed the improved prediction technique.

Table 3.5 displays the photovoltaic array voltage index values for both transient and persistent 3LG faults at grid points A, B, and C with 900, 700, 500, 300, and 100 ms of delay for the fuzzy-controlled delay reduction strategy and the improved predictor delayed optimization methodology. According to the indicators, fuzzy-controlled strategies combined with predictive techniques may reduce delay and enhance the voltage profile in the hybrid power system. In contrast, the enhanced predictor technique beat the more-fuzzified, controlled strategy. Paper C has further results, including the overall harmonic distortion at the PCC severity index.

Table 3.4 Indices of voltage at the PCC.

Delay Value	Fault Type	Fault Point	Voltage Indices at PCC		
			No compensation	Predictor method	Fuzzy method
900 ms	3LG Temp	A	0.2201	0.1967	0.1797
		B	0.2035	0.1942	0.1772
		C	0.2201	0.1968	0.1798
	3LG Perm	A	0.1973	0.1897	0.1727
		B	0.0521	0.0189	0.0172
		C	0.2088	0.1897	0.1727
700 ms	3LG Temp	A	0.2265	0.1990	0.1823
		B	0.2079	0.1943	0.1773
		C	0.2265	0.1991	0.1741
	3LG Perm	A	0.1975	0.1911	0.1741
		B	0.0660	0.0169	0.0132
		C	0.1975	0.1911	0.1741
500 ms	3LG Temp	A	0.2085	0.1975	0.1805
		B	0.2072	0.1932	0.1762
		C	0.2213	0.1961	0.1791
	3LG Perm	A	0.1885	0.1881	0.1711
		B	0.0848	0.0218	0.0048
		C	0.1885	0.1463	0.1293
300 ms	3LG Temp	A	0.2105	0.1984	0.1804
		B	0.2060	0.1927	0.1747
		C	0.2168	0.1948	0.1768
	3LG Perm	A	0.1960	0.1897	0.1717
		B	0.0715	0.0482	0.3213
		C	0.1995	0.1866	0.1656
100 ms	3LG Temp	A	0.2030	0.1947	0.1767
		B	0.2019	0.1889	0.1720
		C	0.2140	0.1920	0.1742
	3LG Perm	A	0.1857	0.1766	0.1596
		B	0.1117	0.0566	0.0405
		C	0.1664	0.1489	0.1472

Table 3.5 Indices of voltage for PV plants.

Delay Value	Fault Type	Fault Point	Voltage Indices at PCC		
			No compensation	Predictor method	Fuzzy method
900 ms	3LG Temp	A	0.2128	0.1898	0.1698
		B	0.2055	0.1966	0.1776
		C	0.2128	0.1976	0.1776
	3LG Perm	A	0.1090	0.1060	0.0789
		B	0.1651	0.1551	0.1351
		C	0.1828	0.1091	0.0891
700 ms	3LG Temp	A	0.2126	0.2084	0.1894
		B	0.2043	0.1978	0.1778
		C	0.2265	0.1992	0.1802
	3LG Perm	A	0.1059	0.1093	0,0893
		B	0.1659	0.1560	0.1352
		C	0.1827	0.1093	0,0893
500 ms	3LG Temp	A	0.2128	0.2097	0.1897
		B	0.2044	0.2004	0.1814
		C	0.2128	0.2035	0.1845
	3LG Perm	A	0.1061	0.1095	0.0895
		B	0.1669	0.1406	0.1216
		C	0.1819	0.1095	0.0895
300 ms	3LG Temp	A	0.2032	0.2059	0.1876
		B	0.2042	0.2053	0.1844
		C	0.2085	0.2056	0.1846
	3LG Perm	A	0.1059	0.1091	0.0891
		B	0.1655	0.1594	0.1384
		C	0.1678	0.1095	0.0895
100 ms	3LG Temp	A	0.2089	0.2090	0.1872
		B	0.2110	0.2066	0.1756
		C	0.2135	0.2080	0.1915
	3LG Perm	A	0.1062	0.1094	0.0894
		B	0.1664	0.1597	0.1297
		C	0.0111	0.0109	0.0074

3.3.2 Harmonic spectrum of nonlinear loads

The study's harmonic power flow patterns were employed, enabling network distribution in three-phase balanced and unbalanced categories. The selected temporal domain employed the coordinating factor. Additional harmonic modes were linked as well. The investigation used the first harmonic list's seven harmonics. Figure 3.10 displays the harmonic spectra of the voltage, current, and nonlinear properties of the PCC used in this investigation.

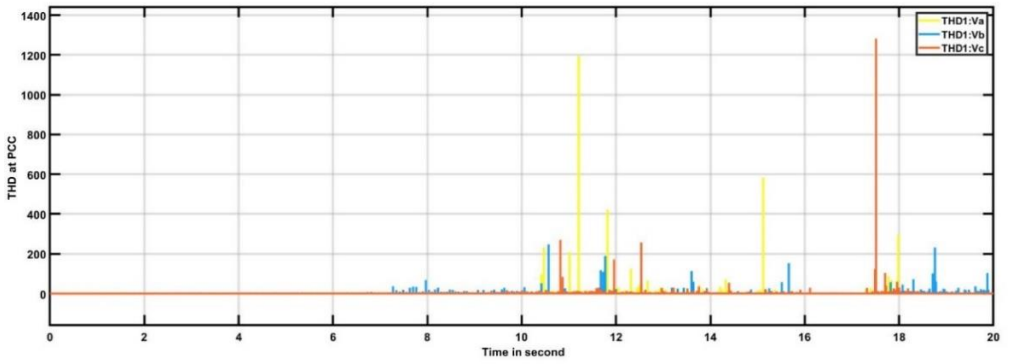

(a)

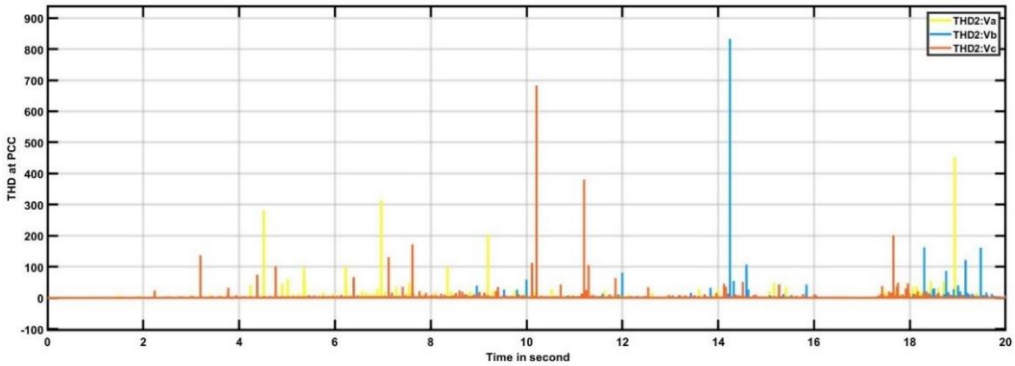

(b)

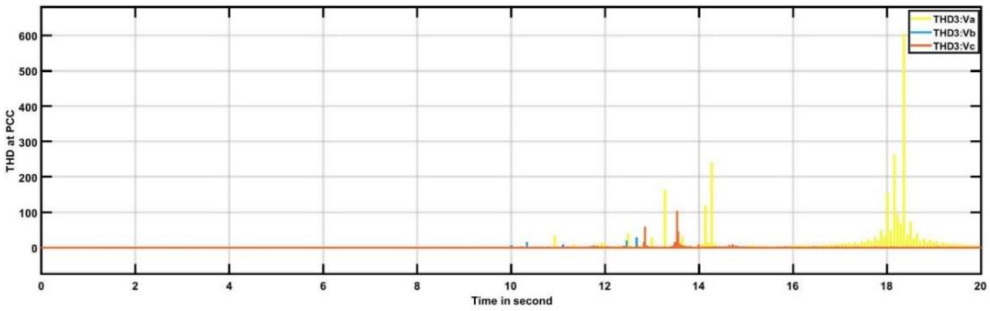

(c)

Figure 3.10: Harmonic spectrum of voltage in PCC for (a) no control, (b) predictor controller, and (c) fuzzy controller methods.

3.4 Network communication cyber-attacks

The outcomes of 11 TSAT case studies are described in this part. As a result of cyber-attacks, a network with an SVC faced constant latency in cases 1–6. For instance, in Case 1, no network latency has been deemed relevant for purposes of comparison. In cases 2-6, fixed delays varied from 100 ms to 900 ms, with a 200 milliseconds increase. The lookup table's fixed latency was set to between 100 and 900 milliseconds for each scenario. In all six cases, the time difference between the two cyber-attacks on the frequency relay of Generator 4 and Gikondo SS7, which resulted in a 3-phase connected failure on Generator Bus 6, was compared at 10.0 s for the DoS attack and 6.0 s for the switching assault.

At 10.0 s, a three-phase on ground fault is spread on line generator 4 to the Jabana SS5 bus to show a DoS attack scenario. Despite the fact that the over frequency protection relay RG4 detects the over frequency immediately, the implementation command is delayed by 0.4 s due to the DoS assault, and the CB GR4 trips after 0.6 s. Such a delay violates the norm of the power system and has a substantial influence on its dynamic response. A 0.2 s delay in power systems reflects the processing and communication time required to execute the tripping command. As the failure persists substantially longer than the normal performance time, the system becomes increasingly unstable (0.2 s). Each of these factors reduced the simulation time under load to roughly 5 seconds. After three steps to break the load, about 18 seconds, system. The frequency begins to recover since generator 5 is equipped to handle load shedding and is a swing type machine, whereas the others are PV system plants.

All of this made it feel under the load break down to about 5s of simulation. After three steps to break the load, about 18 s, system. The frequency starts to recover because generator 5 is ready because it has to deal with load shedding, and it is a swing type machine while the others are PV type machines.

3.4.1 Effects of SVC's fixed network latency

Table 3.6 shows the angle, frequency, and voltage profile indices for cases 1–6. The added facts' controller in Case 1 was zero. In other words, no fixed delay network was simulated on the SVC controller system in this situation. In comparison to case 1 (no delay), most instances 2–6 (with Dos constant latencies) displayed poorer angle stability, frequency stability, and voltage stability indexes [4][64]. Continuous increases in delay duration (100 ms - 900 ms) reduced both indices in examples 2–6, but the system remained unstable ($\eta > 0$). In examples 1–6, the disturbance was generated by a switching assault, yet the system remained stable ($\eta > 0$) and even showed a greater reduction in NL findings than PI. In accordance with the results of SVC Table 3.6, when the controller, like PI, uses 300 ms and 500 ms, it causes a problem so that P_{vcc} appears to be unstable, whereas the results of STATCOM Table 3.6 show that

when the controller PI uses 700 ms and 800 ms, it causes a problem so that P_{vcc} appears to be unstable.

Table 3.6 Angle and voltage stability indexes for SVC cases 1-6.

Case No.	Fixed Delay/ β	Cyber attack	Transient Stability Indices					
			SVC					
			PI			NL		
			Angle (%)	Freq (%)	Voltage (s)	Angle (%)	Freq (%)	Voltage (s)
1	0	DoS	27.93	0.823	0.5400	24.00	1.623	0.1594
2	100 ms	DoS	27.63	6.567	0.4900	24.00	1.623	0.1468
3	300 ms	DoS	27.38	4.838	1.9310	24.00	1.620	0.1172
4	500 ms	DoS	27.37	1.278	1.1430	24.00	1.624	0.1756
5	700 ms	DoS	28.59	12.81	0.4040	24.00	1.614	0.0864
6	900 ms	DoS	25.06	39.50	0.4180	24.00	1.622	0.1441
1	0	Switching	29.13	01.65	0.0004	5.594	0.202	0.0123
2	100 ms	Switching	28.87	01.74	0.1078	5.679	0.212	0.0979
3	300 ms	Switching	28.48	02.51	0.0881	6.338	0.531	0.0726
4	500 ms	Switching	27.97	03.55	0.0449	6.848	0.099	0.0334
5	700 ms	Switching	27.52	04.02	0.0211	6.825	0.171	0.0024
6	900 ms	Switching	27.21	04.20	0.0187	7.328	0.195	0.0008

3.4.2 STATCOM's constant network delay effects

Table 3.6 shows the angle, frequency, and voltage stability indexes from cases 1–6. Each example used fixed delay periods and separate collections of randomized relays that had identical β values. Due to the fixed latency ($\eta > 0$), the system remained stable under any scenario.

Figures 3.11 and 3.12 show the generator frequency, angles, and electrical energy between regions. The STATCOM controller received measurement readings with a 900-ms delay in those numbers. STATCOM output was delayed as a result of this. As a consequence, the voltage on the PCC bus varied more, taking longer to stabilize the relative generator frequency and angles. STATCOM output in instance 6 (Dos attack) boosted P_{vcc} to 1.2 p.u. at 8 seconds while dropping P_{vcc} to 0.4 p.u. at 10 seconds, as shown in Figure 7. In comparison to sample 1, STATCOM in condition 6 consumed reactive power when the P_{cc} bus demanded the most. This reflects the worst-case situation. The system became unstable when the generator angles diverged. According to the results in figures 3.11, 3.12, and Table 3.6, our controller works so effectively that the NL method outperforms the PI method in the case of switching assaults,

while the PI method outperforms the NL method in the case of a sudden attack such as DoS, as indicated in Table 3.7.

In consequence, cyber-attack-caused communication latencies may reduce that system's transient reliability and efficiency or cause it to become unstable. Excessive fixed delays may cause the grid to become unstable, as in a DoS. Fixed delay, on the other hand, has a smaller effect on transient stability during switching attacks. After that, as shown in Tables 3.6 and 3.7, there is a critical value at which the voltage values exceed 1, causing our system to operate poorly and indicating that the system is unstable. Additional results are included in Paper D, including forecasts of the angle and voltage severity index for various facts.

Table 3.7 Angle and Voltage stability indices for STATCOM cases 1 to 6.

Case No.	**Delay/ β**	**Fixed Cyber attack**	**Transient Stability Indices**					
			STATCOM					
			PI			NL		
			Angle (%)	Freq (%)	Voltage (s)	Angle (%)	Freq (%)	Voltage (%)
1	0	DoS	26.96	1.1280	0.6961	22.93	6.612	0.1318
2	100 ms	DoS	26.63	4.4470	0.6795	22.93	6.612	0.1315
3	300 ms	DoS	26.32	2.3630	0.1220	22.93	6.611	0.1384
4	500 ms	DoS	26.66	16.260	0.0566	22.93	6.611	0.1320
5	700 ms	DoS	23.95	18.320	3.6300	22.93	6.612	0.1311
6	900 ms	DoS	23.38	29.560	4.4782	22.93	6.612	0.1291
1	0	Switching	40.65	24.970	0.00150	6.204	0.141	0.00065
2	100 ms	Switching	40.56	24.590	0.00278	5.879	0.012	0.00214
3	300 ms	Switching	39.66	22.090	0.00239	5.766	0.048	0.00166
4	500 ms	Switching	38.49	19.090	0.00242	5.438	0.074	0.00060
5	700 ms	Switching	37.49	16.700	0.00095	5.324	0.147	0.00062
6	900 ms	Switching	36.84	15.120	0.00096	5.976	0.073	0.00273

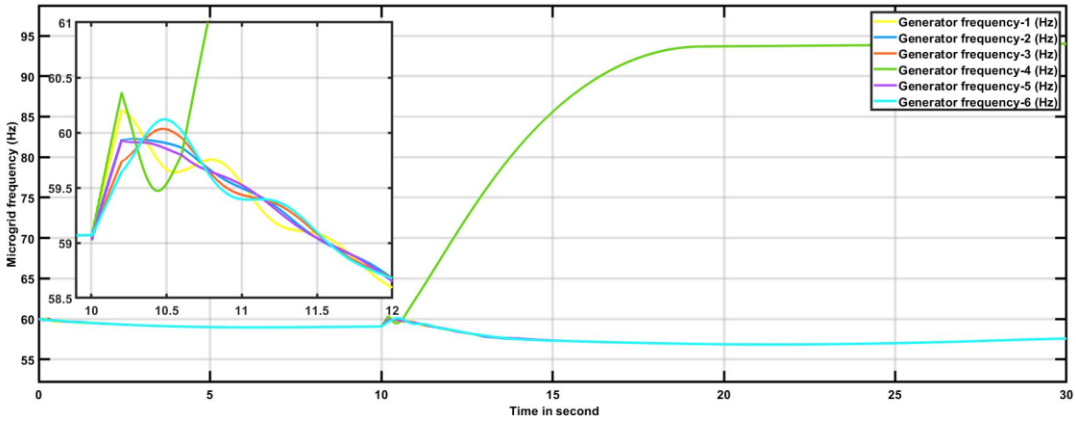

(a)

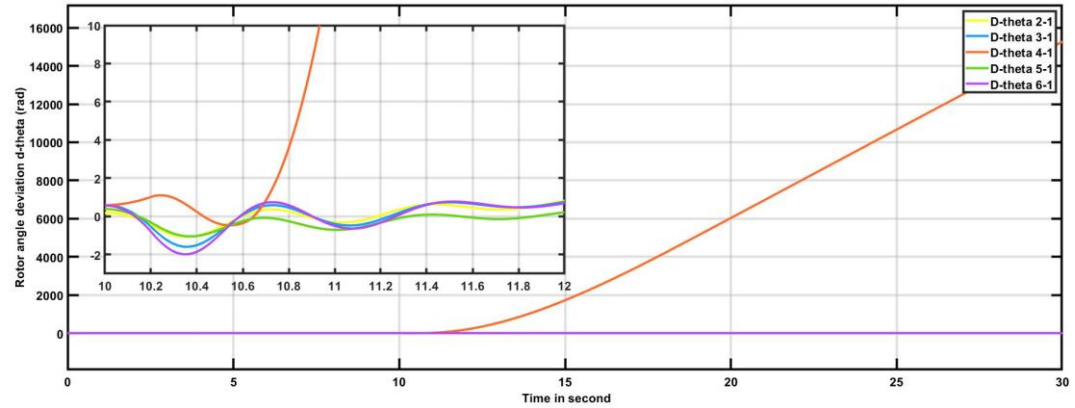

(b)

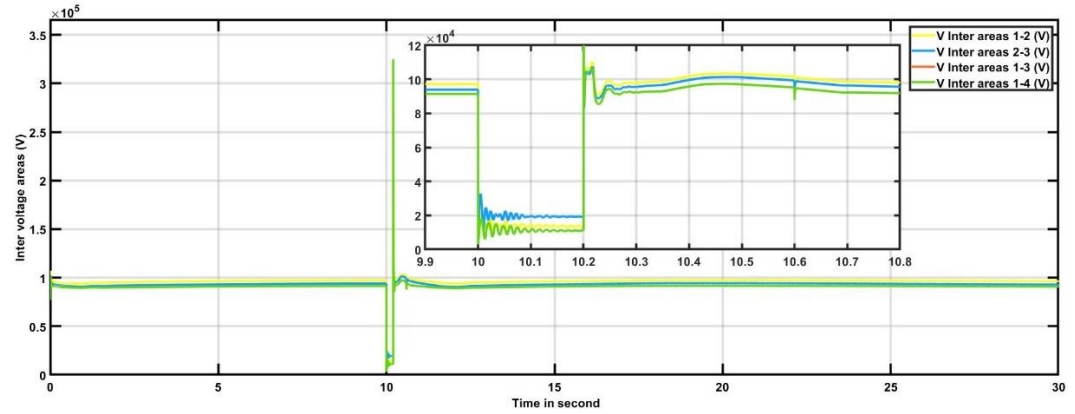

(c)

Figure 3.11: Microgrid frequency, angles and voltages STATCOM output in event of DoS attack.

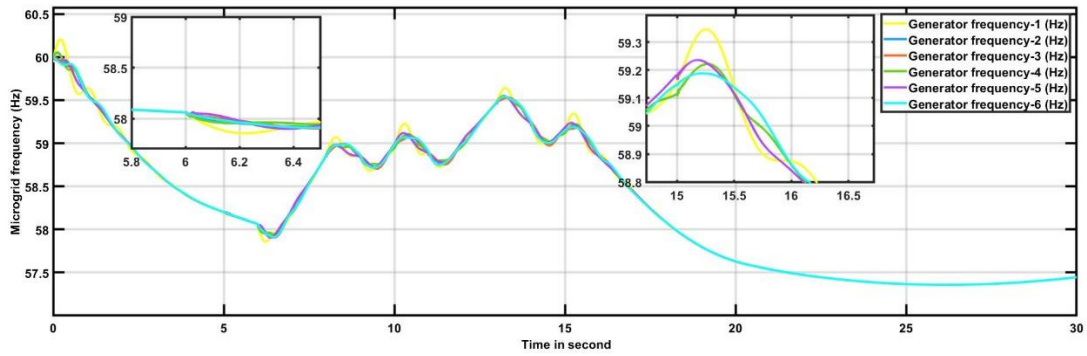

(a)

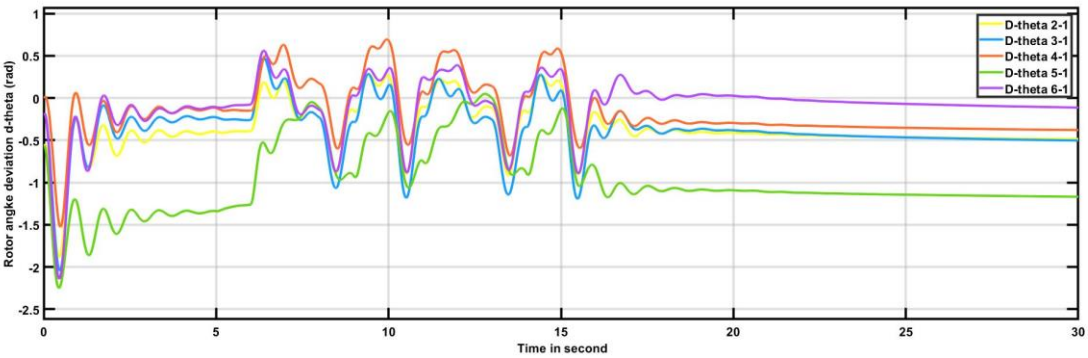

(b)

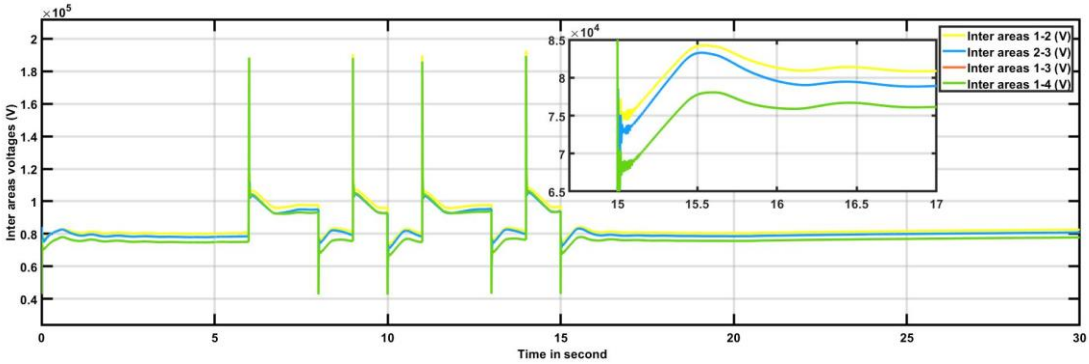

(c)

Figure 3.12: Microgrid frequency, angles and voltages for STATCOM output in event of switching attack.

3.5 Comparisons of facts controller

According to the results of Figure 3.13, the performance of STATCOM is significantly superior compared to employing SVC and STATCOM during the assault through frequency relay. Going to the current or new function demonstrates that STATCOM solves a much even if it is an impediment to fraud, as demonstrated in Paper C. The prospective cost of FACTS

controllers must be addressed in these cases. FACTS controllers are quite expensive as compared to standard devices. The anticipated cost is also impacted by the amount of set and adjustable FACTS controller pieces [94].

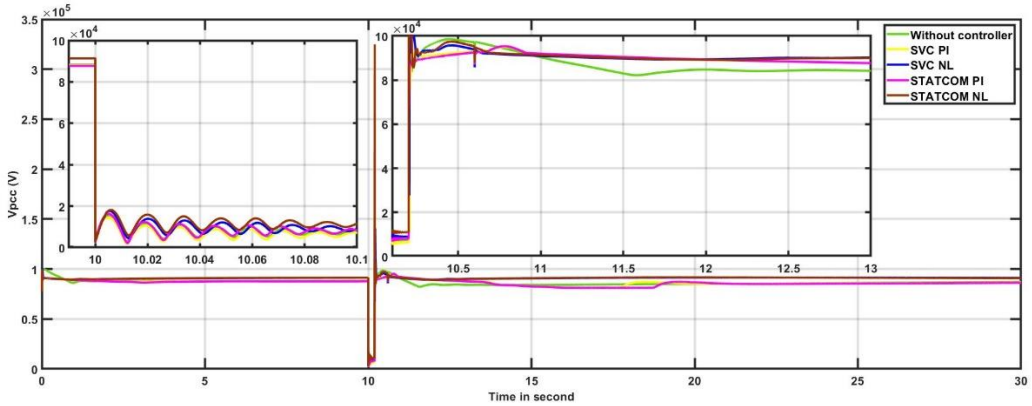

(a)

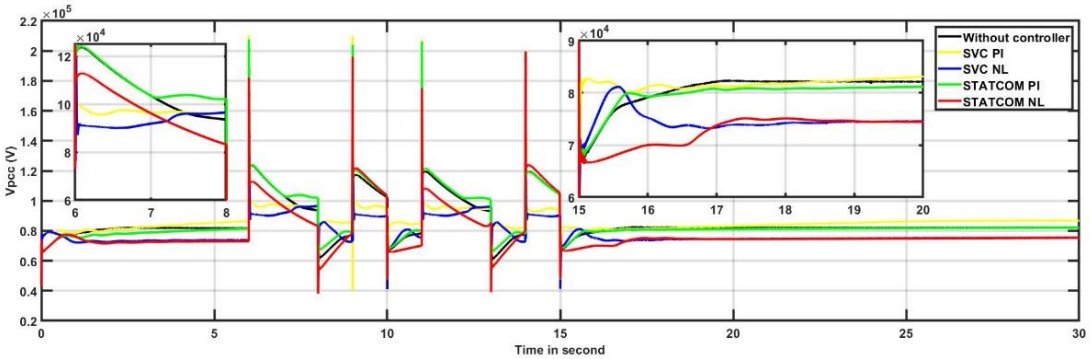

(b)

Figure 3.13: Comparison of various controllers for the simulation results.

CHAPTER FOUR: CONCLUSIONS AND FUTURE WORK

The primary purpose of this dissertation is really to contribute significantly here to the improvement of power quality in the face of multiple challenges including failures, communication delays, and cyber-attacks. Findings related to the objectives of the thesis are listed below.

4.1 Summary of the research

1. The primary objective of this study was to investigate the reasons for communication delays in the electric grid communication system. To accomplish this purpose, the researchers undertook a detailed examination of the many elements that lead to transmission delays of crucial information throughout the power network. The research aims to shed light on the issues that impede efficient communication and may have an influence on the overall operation and quality of the electrical system by identifying these core causes. This goal is significant because it has the potential to pave the way for targeted solutions and improvements, therefore improving the reliability and efficacy of the electric grid communication system.

   Finally, the study delivers a comprehensive overview of the impact of propagation delays on monitoring the operation and maintaining the quality of the power system. Through this analysis, the study presents valuable insights into the effects of network delays on different interaction strategies within the electric network communication system. By evaluating different control methods, it is possible to better understand their strengths and limitations in mitigating the negative effects of delays. Moreover, the research highlights the importance of considering continual or permanent delays, as they can significantly affect the responsiveness of the power network. In addition, the study points out that addressing sudden delays can be more challenging compared to dealing with permanent delays when the braking resistors are switched, utilizing fuzzy design logic controllers for the IEEJ WEST 10-machine model. This research's findings contribute to a broader understanding of communication delays in the electric network and offer potential directions for implementing effective measures to improve communication competence and maintain the stability of the power network.

2. The second goal of this research was focused on investigating the instability caused by communication delays specifically in the protection coordination of the IEEE 14-bus system grid. It was critical since communication delays can have significant consequences for the electrical grid's reliability, particularly in terms of protection coordination. The study sought to investigate the underlying reasons of these delays inside the IEEE 14-bus system, as well as how they can impair the efficiency of

preventive mechanisms in response to various operating scenarios and disruptions. The study sought to gain insights into the vulnerabilities of the grid's communication systems, identify potential areas for improvement, and propose viable solutions to improve the overall stability and reliability of the IEEE 14-bus system's protection coordination by conducting this investigation.

Finally, the research thesis successfully investigated and evaluated the performance of the grasshopper optimization algorithm (GOA) proposal in mitigating the impact of communication delays on the IEEE 14-bus system's protection coordination, particularly in the context of under-frequency load shedding (UFLS). The researchers compared the efficiency of GOA to conventional and particle swarm optimization (PSO) strategies in a variety of operational scenarios, including those featuring UFLS caused by disturbances. The results showed that GOA was a very efficient strategy, resulting in a reduction in load-shedding size and greatly improved communication system performance. Additionally, in tests with the IEEE 14-bus system, GOA offers the fastest performance. These findings have significant implications for power system operators and grid protection coordination researchers, as they provide valuable insights into how GOA can be used as an effective tool to address communication delays and improve the stability and reliability of the IEEE 14-bus system grid's protection coordination.

3. The third goal of this research was focused on designing mitigation events in the simulation of a nonlinear network to address dissipated time delays in the newly reinforced Kigali national grid. The significance of this goal resides in optimizing the performance of power system stability. The study sought to comprehend the impact of time delays on power system stability in the grid and proposed specific controllers, namely the Fuzzy Logic Controller (FLC)-based technique and the Modified Predictor technique, to mitigate the negative effects of these delays on power quality in a hybrid network. By considering a range of time delays from 100 to 900 ms, the investigation sought to comprehensively assess the network's efficiency and the efficacy of the suggested controllers. These mitigating measures were critical for improving power quality and maintaining the dependable and stable functioning of Kigali's newly strengthened national grid, eventually benefiting consumers and industries that rely on a reliable and resilient power supply.

   Ultimately, the study successfully addressed communication delays in the context of power system stability in the hybrid network of the newly reinforced Kigali national grid. The study recommended two controllers, the FLC-based approach and the Modified Predictor technique, as useful techniques of mitigating the negative impact of time delays on power quality. Through quantitative analysis, evaluating voltage

index at the Point of Common Coupling (PCC) and Total Harmonic Distortion (THD), the investigation demonstrated the success of the fuzzy logic-controlled TSC-TCR (Thyristor-Switched Capacitor-Thyristor-Controlled Reactor) in improving power quality in the hybrid system. Furthermore, it presented that the proposed fuzzy logic-controlled TSC-TCR outperformed the modified predictor method-controlled TSC-TCR in terms of performance. Moreover, both the FLC and Modified Predictor Method (MPM) control-based TSC methods were effective in improving power quality in the hybrid grid system. While the fuzzy-controlled approach generally outperformed the modified predictor method, certain cases, such as the 3LG (three-line-to-ground) temporary or permanent fault points at locations A, B, and C, favoured the Modified Predictor technique over the 2-Input Fuzzy controller method. These research findings provide valuable insights into optimizing power system stability and power quality in the newly reinforced Kigali national grid, providing practical guidance for power system operators and researchers in implementing appropriate control techniques to mitigate communication delays and ensure a reliable and high-quality power supply to consumers.

4. The final objective of this research was to devise ways for mitigating the effects of communication delays in power system control and protection, using a case study focusing on the Kigali national grid as a model. This goal was critical since communication delays can cause severe interruptions in power system control and protection, thus jeopardizing electricity system reliability and stability. The study aims to develop appropriate ways and strategies for dealing with these delays and improving the performance of the electricity system in the context of the Kigali national grid. The study's goal was to contribute to the creation of more robust and efficient power systems, particularly in the face of communication issues that might emerge in real-world scenarios, by investigating mitigating approaches.

   Finally, the research dissertation extended the possible repercussions of cyber-attacks on hybrid power grid frequency relay controllers, such as SVC (Static Var Compensator) and STATCOM (Static Synchronous Compensator) systems, outside communication delays. The study looked at two forms of cyber-attacks, Denial-of-Service (DoS) attacks and switching assaults, and how they affected power system performance. Furthermore, the dissertation presented two controllers, the Non-Linear (NL) controller and the Proportional-Integral (PI) controller, to efficiently identify and mitigate cyber-attacks. The simulation findings demonstrated that cyber-attacks had a negative impact on system performance and the power quality of the hybrid grid. However, the proposed NL and PI controllers proved their capacity to mitigate the detrimental implications of these attacks while also improving the system's overall power quality. Specifically, the mitigation strategies effectively returned the signals to

their former condition, limiting assaults and improving the power quality of the system through the injection. The research findings emphasize the need of protecting power systems from cyber threats and show the potential of the suggested controllers to enhance the resilience and stability of power grids against such attacks.

4.2 Limitations and future directions

The major weakness of this study is that the proposed technique requires further, extensive testing. This implies that the system should be tested in a real-time power system simulation. However, due to time constraints, we were unable to test our system in a real-time digital simulator. In the future, we will put our suggested method to the test in a real-time digital simulator under various power system circumstances.

In the future, a comparative stability analysis will be performed for the proposed nonlinear control. For the stability analysis of the controller, the Lyapunov method will be used. This method provides a system with dynamic (boundary) uncertainties in the system dynamics and adds some (weak) terms to control the stability of the system for many uncertainties. Compensation schemes, such as ETDC and MFAC updates, show research progress in reducing various delays. According to the questions described in this section in of review paper, there are quick ways to reduce various unexpected delays that should be taken into account.

Other novel approaches to reducing the detrimental impact of random delays will be investigated. Furthermore, cyber-attack delays will be evaluated, and relevant reduction approaches will be examined. New approaches for detecting and mitigating cyber-attacks in smart hybrid grids will be investigated. Appropriate control algorithms for microgrid functioning will be explored and developed. To ensure secure electricity distribution to customers, data-driven algorithms will be created.

REFERENCES

[1] B. Zhou *et al.*, "Multi-microgrid Energy Management Systems: Architecture, Communication, and Scheduling Strategies," *J. Mod. Power Syst. Clean Energy*, vol. 9, no. 3, pp. 463–476, 2021, doi: 10.35833/MPCE.2019.000237.

[2] D. Vinay, "Improvement of Power Quality using a Robust Hybrid Series Active Power Filter," *Int. J. Res. Appl. Sci. Eng. Technol.*, vol. 9, no. VI, pp. 2311–2316, 2021, doi: 10.22214/ijraset.2021.35494.

[3] C. K. Manikanta, I. Manoj Kumar, D. Seshi Reddy, G. Lakshmi Narayana, and P. Dharani, "Power quality improvement in grid connected solar system," *Journal of Critical Reviews*, vol. 7, no. 6. pp. 904–908, 2020. doi: 10.31838/jcr.07.06.155.

[4] D. Muyizere, L. K. Letting, and B. B. Munyazikwiye, "Decreasing the Negative Impact of Time Delays on Electricity Due to Performance Improvement in the Rwanda National Grid," *Electron.*, vol. 11, no. 19, p. 3114, Sep. 2022, doi: 10.3390/electronics11193114.

[5] G. A. Salman, H. G. Abood, and M. S. Ibrahim, "Improvement the voltage stability margin of Iraqi power system using the optimal values of FACTS devices," *Int. J. Electr. Comput. Eng.*, vol. 11, no. 2, 2021, doi: 10.11591/ijece.v11i2.pp984-992.

[6] M. Hoseynpoor, M. Najafi, R. Ebrahimi, and M. Davoodi, "Power system stability improvement using comprehensive FACTS devices," *Int. Rev. Model. Simulations*, vol. 4, no. 4, 2011.

[7] Z. Čonka, M. Kolcun, M. Kolcun Jr., J. Dudiak, M. Mikita, and M. Vojtek, "Improvement of Power System Stability Using FACTS Device," *Power Electr. Eng.*, vol. 33, pp. 12–15, 2016, doi: 10.7250/pee.2016.002.

[8] A. Ghosh and G. Ledwich, *Power Quality Enhancement Using Custom Power Devices*. 2002. doi: 10.1007/978-1-4615-1153-3.

[9] S. Ghosh and M. H. Ali, "Minimization of Adverse Effects of Time Delay on Power Quality Enhancement in Hybrid Grid," *IEEE Syst. J.*, vol. 13, no. 3, pp. 3091–3101, 2019, doi: 10.1109/JSYST.2019.2891425.

[10] S. D. Swain, P. K. Ray, and K. B. Mohanty, "Improvement of Power Quality Using a Robust Hybrid Series Active Power Filter," *IEEE Trans. Power Electron.*, vol. 32, no. 5, pp. 3490–3498, 2017, doi: 10.1109/TPEL.2016.2586525.

[11] J. A. Ghaeb, M. Alkayyali, and T. A. Tutunji, "Wide Range Reactive Power Compensation for Voltage Unbalance Mitigation in Electrical Power Systems," *Electr. Power Components Syst.*, vol. 49, no. 6–7, 2022, doi: 10.1080/15325008.2021.2002474.

[12] W. Jing, F. Chang, G. Wang, and J. Chen, "Research on TSC control strategy based on the average of TCR threephase trigger angles," *Zhongshan Daxue Xuebao/Acta Sci. Natralium Univ. Sunyatseni*, vol. 60, no. 6, pp. 54–61, Nov. 2021, doi: 10.13471/j.cnki.acta.snus.2020.01.15.2020B005.

[13] R. Sharma, A. Singh, and A. N. Jha, "Performance evaluation of tuned PI controller for power quality enhancement for linear and non linear loads," Sep. 2014. doi: 10.1109/ICRAIE.2014.6909134.

[14] N. Safitri, A. M. S. Yunus, F. Fauzi, and N. Naziruddin, "Integrated arrangement of advanced power electronics through hybrid smart grid system," *TELKOMNIKA (Telecommunication Comput. Electron. Control.*, vol. 18, no. 6, p. 3202, 2020, doi: 10.12928/telkomnika.v18i6.13433.

[15] P. K. Ray, S. R. Das, and A. Mohanty, "Fuzzy-controller-designed-pv-based custom power device for power quality enhancement," *IEEE Trans. Energy Convers.*, vol. 34, no. 1, pp. 405–414, 2019, doi: 10.1109/TEC.2018.2880593.

[16] S. A. Mohamed, "Enhancement of power quality for load compensation using three different FACTS devices based on optimized technique," *Int. Trans. Electr. Energy Syst.*, vol. 30, no. 3, 2020, doi: 10.1002/2050-7038.12196.

[17] J. Park, G. Jang, and K. M. Son, "Modeling and control of VSI type FACTS controllers for power system dynamic stability using the current injection method," *Int. J. Control. Autom. Syst.*, vol. 6, no. 4, pp. 495–505, 2008.

[18] R. G. Wandhare and V. Agarwal, "Novel stability enhancing control strategy for centralized PV-grid systems for smart grid applications," *IEEE Trans. Smart Grid*, vol. 5, no. 3, pp. 1389–1396, 2014, doi: 10.1109/TSG.2013.2279605.

[19] A. S. Leger, J. James, and D. Frederick, "Smart grid modeling approach for wide area control applications," 2012. doi: 10.1109/PESGM.2012.6345511.

[20] B. A. Ahmad, H. H. Elsheikh, and A. Fadoun, "Review of power quality monitoring systems," 2015. doi: 10.1109/IEOM.2015.7093825.

[21] B. Naduvathuparambil, M. C. Valenti, and A. Feliachi, "Communication delays in wide area measurement systems," in *Proceedings of the Annual Southeastern Symposium on System Theory*, 2002, vol. 2002-Janua, pp. 118–122. doi: 10.1109/SSST.2002.1027017.

[22] X. Shi, Y. Cao, M. Shahidehpour, Y. Li, X. Wu, and Z. Li, "Data-Driven Wide-Area Model-Free Adaptive Damping Control with Communication Delays for Wind Farm," *IEEE Trans. Smart Grid*, vol. 11, no. 6, 2020, doi: 10.1109/TSG.2020.3001640.

[23] M. E. C. Bento, R. Kuiava, and R. A. Ramos, "Design of Wide-Area Damping Controllers Incorporating Resiliency to Permanent Failure of Remote Communication Links," *J. Control. Autom. Electr. Syst.*, vol. 29, no. 5, 2018, doi: 10.1007/s40313-018-0398-3.

[24] W. Yao, L. Jiang, J. Wen, Q. H. Wu, and S. Cheng, "Wide-area damping controller of Facts devices for inter-area oscillations considering communication time delays," *IEEE Trans. Power Syst.*, vol. 29, no. 1, 2014, doi: 10.1109/TPWRS.2013.2280216.

[25] G. Cai, D. Yang, and C. Liu, "Adaptive wide-area damping control scheme for smart grids with consideration of signal time delay," *Energies*, vol. 6, no. 9, pp. 4841–4858, 2013, doi: 10.3390/en6094841.

[26] R. V. Yohanandhan, R. M. Elavarasan, P. Manoharan, and L. Mihet-Popa, "Cyber-Physical Power System (CPPS): A Review on Modeling, Simulation, and Analysis with Cyber Security Applications," *IEEE Access*, vol. 8. pp. 151019–151064, 2020. doi: 10.1109/ACCESS.2020.3016826.

[27] Rwanda Energy Group Limited, "Annual Report For Rwanda Energy Group , of the Year 2019-2020," District, Nyarugenge City, Kigali-Rwanda, 2020. [Online]. Available: https://www.reg.rw/fileadmin/REG_ANNUAL_REPORT_2020-2021_V3.pdf

[28] Rwanda Energy Group Ltd, "Annual Report For Rwanda Energy Group 2020-2021," no. Septembre. Kigali, p. 29, Sep. 2021. Accessed: Aug. 09, 2022. [Online]. Available: https://www.reg.rw/fileadmin/REG_ANNUAL_REPORT_2020-2021_V3.pdf

[29] Ministry of Infrastructure, "Energy Sector Strategic Plan 2018/19 - 2023/24," *Repub. Rwanda*, no. September, 2018.

[30] L. Zhao, X. Li, M. Ni, T. Li, and Y. Cheng, "Review and prospect of hidden failure: protection system and security and stability control system," *J. Mod. Power Syst. Clean Energy*, vol. 7, no. 6, pp. 1735–1743, 2019, doi: 10.1007/s40565-015-0128-9.

[31] D. Muyizere, L. K. Letting, and B. B. Munyazikwiye, "Effects of Communication Signal Delay on the Power Grid: A Review," *Electronics (Switzerland)*, vol. 11, no. 6. 2022. doi: 10.3390/electronics11060874.

[32] M. A. A. Sufyan, M. Zuhaib, and M. Rihan, "An investigation on the application and challenges for wide area monitoring and control in smart grid," *Bull. Electr. Eng. Informatics*, vol. 10, no. 2, 2021, doi: 10.11591/eei.v10i2.2767.

[33] "Power System Stability Controls," in *Power System Stability and Control*, 2020, pp. 169–188. doi: 10.1201/9781420009248-18.

[34] H. Yang, S. Ju, Y. Xia, and J. Zhang, "Predictive Cloud Control for Networked Multiagent Systems with Quantized Signals under DoS Attacks," *IEEE Trans. Syst. Man, Cybern. Syst.*, vol. 51, no. 2, pp. 1345–1353, Feb. 2021, doi: 10.1109/TSMC.2019.2896087.

[35] A. Khalil and A. Swee Peng, "A new method for computing the delay margin for the stability of load frequency control systems," *Energies*, vol. 11, no. 12, 2018, doi: 10.3390/en11123460.

[36] M. H. Ali and D. Dasgupta, "Effects of communication delays in electric grid," in *2011 Future of Instrumentation International Workshop, FIIW 2011 - Proceedings*, 2011, pp. 38–41. doi: 10.1109/FIIW.2011.6476816.

[37] M. Gamal, N. Sadek, M. R. M. Rizk, and A. K. Abou-Elsaoud, "Delay compensation using Smith predictor for wireless network control system," *Alexandria Eng. J.*, vol. 55, no. 2, 2016, doi: 10.1016/j.aej.2016.04.005.

[38] D. Muyizere, L. K. Letting, and B. B. Munyazikwiye, "Under-frequency Load Shedding on the Performance Time Delay Relays of Transmission lines with difference

Controllers," 2021. doi: 10.1109/SPEC52827.2021.9709464.

[39] H. Wu, K. S. Tsakalis, and G. T. Heydt, "Evaluation of time delay effects to wide area power system stabilizer design," *IEEE Trans. Power Syst.*, vol. 19, no. 4, pp. 1935–1941, 2004, doi: 10.1109/TPWRS.2004.836272.

[40] K. S. Ko and D. K. Sung, "The effect of EV aggregators with time-varying delays on the stability of a load frequency control system," *IEEE Trans. Power Syst.*, vol. 33, no. 1, pp. 669–680, 2018, doi: 10.1109/TPWRS.2017.2690915.

[41] X. Lou *et al.*, "Assessing and mitigating impact of time delay attack: Case studies for power grid controls," *IEEE J. Sel. Areas Commun.*, vol. 38, no. 1, 2020, doi: 10.1109/JSAC.2019.2951982.

[42] D. K. Tiep, K. Lee, D. Y. Im, B. Kwak, and Y. J. Ryoo, "Design of fuzzy-PID controller for path tracking of mobile robot with differential drive," *Int. J. Fuzzy Log. Intell. Syst.*, vol. 18, no. 3, 2018, doi: 10.5391/IJFIS.2018.18.3.220.

[43] S. Raja and N. P. Ananthamoorthy, "Evaluation of Newly Developed Liquid Level Process with PD and PID Controller without Altering Material Characteristics," *J. New Mater. Electrochem. Syst.*, vol. 24, no. 3, pp. 218–223, 2021, doi: 10.14447/jnmes.v24i3.a10.

[44] B. M. R. Amin, S. Taghizadeh, M. S. Rahman, M. J. Hossain, V. Varadharajan, and Z. Chen, "Cyber attacks in smart grid - Dynamic impacts, analyses and recommendations," *IET Cyber-Physical Syst. Theory Appl.*, vol. 5, no. 4, 2020, doi: 10.1049/iet-cps.2019.0103.

[45] P. S. Sarker, V. Venkataramanan, D. S. Cardenas, A. Srivastava, A. Hahn, and B. Miller, "Cyber-physical security and resiliency analysis testbed for critical microgrids with IEEE 2030.5," Apr. 2020. doi: 10.1109/MSCPES49613.2020.9133689.

[46] G. N. Ericsson, "Cyber security and power system communicationessential parts of a smart grid infrastructure," *IEEE Trans. Power Deliv.*, vol. 25, no. 3, 2010, doi: 10.1109/TPWRD.2010.2046654.

[47] Netscout, "13th Worldwide Infrastructure Security Report," 2021. Accessed: Dec. 16, 2022. [Online]. Available: https://www.netscout.com/resources/threat-report-archives/13th-worldwide-infrastructure-security-report

[48] O. KUPREEV, A. GUTNIKOV, and Y. SHMELEV, "Report on DDoS attacks in Q3 2022 | Securelist," 2022. Accessed: Dec. 13, 2022. [Online]. Available: https://securelist.com/ddos-report-q3-2022/107860/

[49] M. A. Rahman and G. K. Venayagamoorthy, "A Survey on the Effects of False Data Injection Attack on Energy Market," 2019. doi: 10.1109/PSC.2018.8664017.

[50] V. S. Rajkumar, M. Tealane, A. Stefanov, and P. Palensky, "Cyber attacks on protective relays in digital substations and impact analysis," Apr. 2020. doi: 10.1109/MSCPES49613.2020.9133698.

[51] E. M. Ferragut, J. Laska, A. Melin, and B. Czejdo, "Addressing the challenges of

anomaly detection for cyber physical energy grid systems," 2013. doi: 10.1145/2459976.2459980.

[52] M. Dehghani *et al.*, "Cyber Attack Detection Based on Wavelet Singular Entropy in AC Smart Islands: False Data Injection Attack," *IEEE Access*, vol. 9, pp. 16488–16507, 2021, doi: 10.1109/ACCESS.2021.3051300.

[53] H. M. Fekry, A. A. Eldesouky, A. M. Kassem, and A. Y. Abdelaziz, "Power management strategy based on adaptive neuro fuzzy inference system for AC microgrid," *IEEE Access*, vol. 8, pp. 192087–192100, 2020, doi: 10.1109/ACCESS.2020.3032705.

[54] M. S. Nazir, N. Ali, T. Yongfeng, A. N. Abdalla, and H. M. J. Nazir, "Renewable energy based experimental study of doubly fed induction generator: Fault case analysis," *J. Electr. Syst.*, vol. 16, no. 2, pp. 235–245, 2020.

[55] A. R. Solat, A. M. Ranjbar, and B. Mozafari, "Coordinated control of doubley fed induction generator virtual inertia and power system oscillation damping using fuzzy logic," *Int. J. Eng. Trans. A Basics*, vol. 32, no. 4, 2019, doi: 10.5829/ije.2019.32.04a.11.

[56] J. Nan *et al.*, "Wide-area power oscillation damper for DFIG-based wind farm with communication delay and packet dropout compensation," *Int. J. Electr. Power Energy Syst.*, vol. 124, 2021, doi: 10.1016/j.ijepes.2020.106306.

[57] *Power System Small Signal Stability Analysis and Control*. Elsevier, 2020. doi: 10.1016/c2018-0-02439-1.

[58] H. Liao, S. Abdelrahman, and J. V. Milanović, "Zonal mitigation of power quality using FACTS devices for provision of differentiated quality of electricity supply in networks with renewable generation," *IEEE Trans. Power Deliv.*, vol. 32, no. 4, pp. 1975–1985, 2017, doi: 10.1109/TPWRD.2016.2585882.

[59] A. K. Goswami, C. P. Gupta, and G. K. Singh, "Minimization of voltage sag induced financial losses in distribution systems using FACTS devices," *Electr. Power Syst. Res.*, vol. 81, no. 3, pp. 767–774, 2011, doi: 10.1016/j.epsr.2010.11.003.

[60] W. U. Tareen, S. Mekhilef, M. Seyedmahmoudian, and B. Horan, "Active power filter (APF) for mitigation of power quality issues in grid integration of wind and photovoltaic energy conversion system," *Renewable and Sustainable Energy Reviews*, vol. 70. pp. 635–655, 2017. doi: 10.1016/j.rser.2016.11.091.

[61] K. L. Shenoy, C. G. Nayak, and R. P. Mandi, "Fuzzy controller based grid integration of hybrid solar photovoltaic and DFIG wind energy system to improve power quality," *Appl. Math. Inf. Sci.*, vol. 13, no. Special Issue 1, pp. 447–469, 2019, doi: 10.18576/amis/13S148.

[62] L. Langer, P. Smith, M. Hutle, and A. Schaeffer-Filho, "Analysing cyber-physical attacks to a Smart Grid: A voltage control use case," 2016. doi: 10.1109/PSCC.2016.7540819.

[63] B. Tavassoli, A. Fereidunian, and S. Mehdi, “Communication system effects on the secondary control performance in microgrids,” *IET Renew. Power Gener.*, vol. 14, no. 12, 2020, doi: 10.1049/iet-rpg.2019.1170.

[64] B. Chen, S. Mashayekh, K. L. Butler-Purry, and D. Kundur, “Impact of cyber attacks on transient stability of smart grids with voltage support devices,” 2013. doi: 10.1109/PESMG.2013.6672740.

[65] B. Bimali, S. Uprety, and R. P. Pandey, “VAR Compensation on Load Side using Thyristor Switched Capacitor and Thyristor Controlled Reactor,” *J. Inst. Eng.*, vol. 16, no. 1, pp. 111–119, 2021, doi: 10.3126/jie.v16i1.36568.

[66] R. H. AL-Rubayi and L. G. Ibrahim, “Enhancement transient stability of power system using UPFC with M-PSO,” *Indonesian Journal of Electrical Engineering and Computer Science*, vol. 17, no. 1. pp. 61–69, 2019. doi: 10.11591/ijeecs.v17.i1.pp61-69.

[67] M. H. Ali, B. Wu, J. Tamura, and R. A. Dougal, “Minimization of shaft oscillations by fuzzy controlled SMES considering time delay,” *Electr. Power Syst. Res.*, vol. 80, no. 7, pp. 770–777, 2010, doi: 10.1016/j.epsr.2009.12.001.

[68] Ashfaque Ahmed Hashmani, “Damping of Electromechanical Oscillations in Power Systems using Wide Area Control Ashfaque Ahmed Hashmani,” 2010.

[69] J. Gutiérrez, J. C. Montaño, M. Castilla, and A. López, “Power-quality improvement in reactive power control using FC-TCR circuits,” in *IECON Proceedings (Industrial Electronics Conference)*, 2002, vol. 2, pp. 880–885. doi: 10.1109/iecon.2002.1185388.

[70] X. Lou, C. Tran, R. Tan, D. K. Y. Yau, and Z. T. Kalbarczyk, “Assessing and mitigating impact of time delay attack: A case study for power grid frequency control,” 2019. doi: 10.1145/3302509.3311042.

[71] P. B. Prasad, K. H. Reddy, and V. N. Murthy, “Notice of Removal: Distributed Static Series compensators in mitigating sub-synchronous resonance improved with ANFIS controller,” *International Conference on Electrical, Electronics, Signals, Communication and Optimization, EESCO 2015*. 2015. doi: 10.1109/EESCO.2015.7253937.

[72] A. Mohanty, M. Viswavandya, D. K. Mishra, P. K. Ray, and S. Pragyan, “Modelling & Simulation of a PV Based Micro Grid for Enhanced Stability,” in *Energy Procedia*, 2017, vol. 109, pp. 94–101. doi: 10.1016/j.egypro.2017.03.060.

[73] D. Gaur and L. Mathew, “Optimal placement of FACTS devices using optimization techniques: A review,” in *IOP Conference Series: Materials Science and Engineering*, 2018, vol. 331, no. 1. doi: 10.1088/1757-899X/331/1/012023.

[74] A. Ghorbani, B. Mozafari, S. Soleymani, and A. M. Ranjbar, “Operation of synchronous generator LOE protection in the presence of shunt-FACTS,” *Electr. Power Syst. Res.*, vol. 119, pp. 178–186, 2015, doi: 10.1016/j.epsr.2014.09.019.

[75] A. M. Eltamaly and M. A. Mohamed, “A novel software for design and optimization

of hybrid power systems," *J. Brazilian Soc. Mech. Sci. Eng.*, vol. 38, no. 4, pp. 1299–1315, 2016, doi: 10.1007/s40430-015-0363-z.

[76] M. A. Habib, S. A. M. Said, M. A. El-Hadidy, and I. Al-Zaharna, "Optimization procedure of a hybrid photovoltaic wind energy system," *Energy*, vol. 24, no. 11, pp. 919–929, 1999, doi: 10.1016/S0360-5442(99)00042-0.

[77] E. Skoplaki, A. G. Boudouvis, and J. A. Palyvos, "A simple correlation for the operating temperature of photovoltaic modules of arbitrary mounting," *Sol. Energy Mater. Sol. Cells*, vol. 92, no. 11, pp. 1393–1402, 2008, doi: 10.1016/j.solmat.2008.05.016.

[78] R. Angu and R. K. Mehta, "A single machine infinite bus power system damping control design with extended state observer," *Cogent Eng.*, vol. 4, no. 1, 2017, doi: 10.1080/23311916.2017.1369923.

[79] A. R. Bergen and V. Vittal, "Power systems analysis 2nd ed. – National Library," *Upper Saddle River, N.J. : Pearson/Prentice Hall, c2000.*, 2000. https://www.nlb.gov.sg/biblio/9441928 (accessed Nov. 07, 2022).

[80] R. C. Dorf, "Power System Analysis Software," in *Systems, Controls, Embedded Systems, Energy, and Machines*, 2020. doi: 10.1201/9781420037043-15.

[81] M. H. Ali, T. Murata, and J. Tamura, "Effect of coordination of optimal reclosing and fuzzy controlled braking resistor on transient stability during unsuccessful reclosing," *IEEE Trans. Power Syst.*, vol. 21, no. 3, pp. 1321–1330, 2006, doi: 10.1109/TPWRS.2006.876670.

[82] G. Fusco and M. Russo, "Adaptive voltage regulator design for synchronous generator," *IEEE Trans. Energy Convers.*, vol. 23, no. 3, pp. 946–956, 2008, doi: 10.1109/TEC.2008.921463.

[83] K. R. Padiyar and H. S. Y. Sastry, "Topological energy-function analysis of stability of power systems," *Int. J. Electr. Power Energy Syst.*, vol. 9, no. 1, 1987, doi: 10.1016/0142-0615(87)90020-2.

[84] W. W. Price *et al.*, "Standard Load Models for Power Flow and Dynamic Performance Simulation," *IEEE Trans. Power Syst.*, vol. 10, no. 3, 1995, doi: 10.1109/59.466523.

[85] Z. Yang, C. Shen, M. L. Crow, and L. Zhang, "An improved StatCom model for power flow analysis," in *Proceedings of the IEEE Power Engineering Society Transmission and Distribution Conference*, 2000, vol. 2, pp. 1121–1126. doi: 10.1109/pess.2000.867536.

[86] P. Rao, M. L. Crow, and Z. Yang, "STATCOM control for power system voltage control applications," *IEEE Trans. Power Deliv.*, vol. 15, no. 4, pp. 1311–1317, 2000, doi: 10.1109/61.891520.

[87] D. N. Kosterev, "Modeling synchronous voltage source converters in transmission system planning studies," *IEEE Trans. Power Deliv.*, vol. 12, no. 2, pp. 947–952, 1997, doi: 10.1109/61.584418.

[88] K. Mentesidi, R. Garde, M. Aguado, and E. Rikos, "Implementation of a fuzzy logic

controller for virtual inertia emulation," in *Proceedings - 2015 International Symposium on Smart Electric Distribution Systems and Technologies, EDST 2015*, 2015, pp. 606–611. doi: 10.1109/SEDST.2015.7315279.

[89] H. León, C. Montez, O. Valle, and F. Vasques, "Real-time analysis of time-critical messages in IEC 61850 electrical substation communication systems," *Energies*, vol. 12, no. 12, 2019, doi: 10.3390/en12122272.

[90] M. H. Ali, T. Murata, and J. Tamura, "Influence of communication delay on the performance of fuzzy logic-controlled braking resistor against transient stability," *IEEE Trans. Control Syst. Technol.*, vol. 16, no. 6, pp. 1232–1241, 2008, doi: 10.1109/TCST.2008.919443.

[91] H. Setiadi, N. Mithulananthan, R. Shah, K. Y. Lee, and A. U. Krismanto, "Resilient wide-area multi-mode controller design based on Bat algorithm for power systems with renewable power generation and battery energy storage systems," *IET Gener. Transm. Distrib.*, vol. 13, no. 10, pp. 1884–1894, 2019, doi: 10.1049/iet-gtd.2018.6384.

[92] M. Sun, Y. Guo, and S. Song, "The delay-dependent dofc for damping inter-area low-frequency oscillations in an interconnected power system considering packet loss of wide-area signals," *Energies*, vol. 14, no. 18, 2021, doi: 10.3390/en14185892.

[93] A. Molina-Cabrera, M. A. Ríos, Y. Besanger, N. Hadjsaid, and O. D. Montoya, "Latencies in power systems: A database-based time-delay compensation for memory controllers," *Electron.*, vol. 10, no. 2, 2021, doi: 10.3390/electronics10020208.

[94] A. Jamali and I. Z. M. Darus, "Intelligent Evolutionary Controller for Flexible Robotic Arm," in *Journal of Physics: Conference Series*, May 2020, vol. 1500, no. 1. doi: 10.1088/1742-6596/1500/1/012020.

PART II

PUBLICATIONS

Paper A

Title:	Effects of Communication Signal Delay on the Power Grid: A Review
Authors:	Darius Muyizere[1*], Lawrence K. Letting [1,2] and Bernard B. Munyazikwiye[1,3]
Affiliation:	[1] African Centre of Excellence in Energy and Sustainable Development, College of Science and Technology, University of Rwanda, KN 67 Street Nyarugenge, Kigali P.O. Box 3900, Rwanda [2] Department of Electrical & Communications Engineering, Moi University, Eldoret 30100, Kenya [3] Department of Mechanical and Energy Engineering, College of Science and Technology, University of Rwanda, KN 67 Street Nyarugenge, Kigali P.O. Box 3900, Rwanda
Article:	MDPI Electronics, 2022, 11, 874. https://doi.org/10.3390/electronics11060874
Layout:	The format of the paper has already been altered to match that of the thesis.

Paper A: Effects of Communication Signal Delay on the Power Grid: A Review

***Abstract* — Communication plays a huge role in the operation of modern power systems. It permits a real-time monitoring coordination and control of the transmission, generation and distribution of electrical energy. As the modern grid grows towards an increased reliance on communication systems for the protection, metering and monitoring for as well as data acquisition for planning; there is a need to understand the challenge in the powers' system communication and their impact on the uninterrupted supply of electrical energy. Communication delays are one of the challenges that might affect the performance of the power system and lead to power losses and equipment damage, it is important to investigate the causes and the mitigation options available. Thus, this paper the state of arts on the cause, the effect and mitigation of communication delays in the power system. Furthermore, in this paper an analysis of different causes of the delays for different network configurations and communication systems used; a comparative analysis of different latency mitigation methods and system performance simulations of a given compensation algorithm is tested against the existing methods. The pros and cons of these control strategies are illustrated in this paper. The summary and assessment of those methods of control in this review offer scholars and utilities valuable direction-finding to design superior communication energy control systems in the future.**

***Keywords*:** smart grid; communication system; controller; operations; communication delay; mitigations; power control system.

A.1 Introduction

In today's world, modern power systems are becoming more and more sophisticated in identifying and making decisions and controlling various tasks that are going to be solved in different sectors such as power generation, transmission, distribution, and consumers as we find below in Figure A.1. However, with the rise of technology in modern electricity, there is a growing trend in a structure that is changing and consists of efficient monitoring and regulation of each area of the electricity network. The functioning of the intelligent system has been shown to be reliable in combining efforts to improve the quality of information exchange.

In an electricity grid, communication delays arise at a number of stages, which include the signal transmission from phasor measurement unit (PMUs) to the manage centers, from the manage centers to the controllers, analog-to-digital conversion, computing on overall enter adjustable, and the phase synchronization of alerts through Global Positioning System (GPS) [1]. Such delay will have an effect on the controllers and device performance [1]. Wide control system communication networks, information sent in the shape of a package. For the most part in controlling the

communication system, there are many time delays that come in the form of a packet such as latency, which is the time delay between the two sequential bits dispatched to its destination, although it also happens to be done in different communication modes [2].

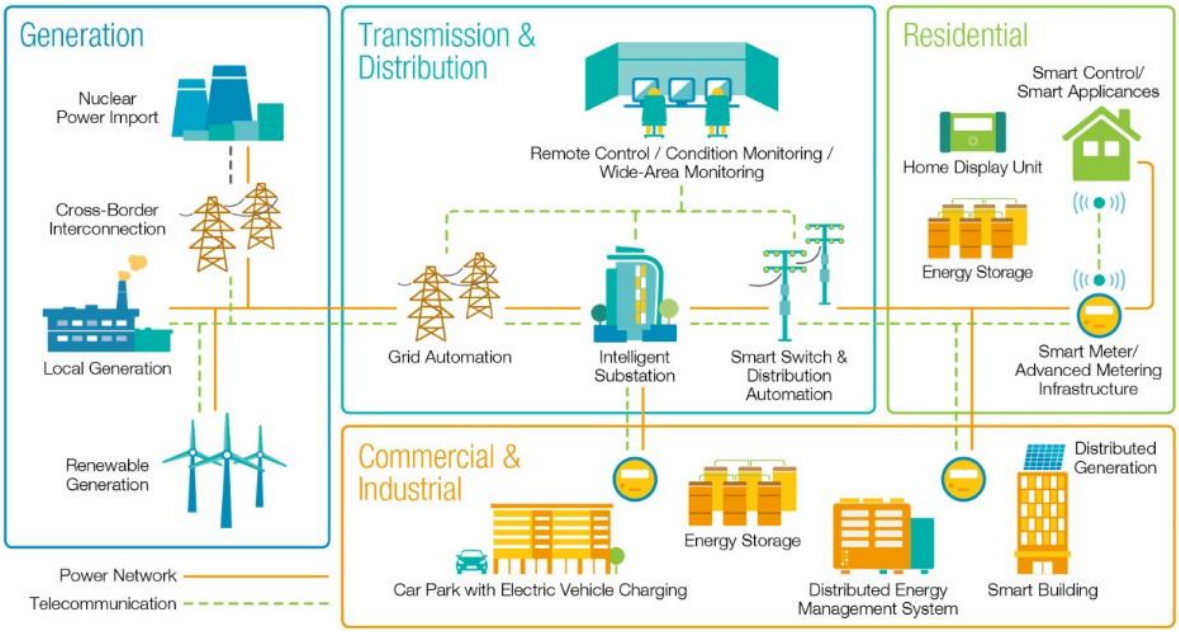

Figure A.1: A comprehensive smart grid infrastructure with its components [3].

In this connection, a request is made in support of this initiative and the development of reliable telecommunications infrastructure by establishing a strong network of broad-band (WAN) to feeding and customer service. WAN-based electrical equipment is based on the interconnectedness of technology in communication technology such as fiber optics, power line communication (PLC), copper-wire line, and various technologies (i.e., media communication in mobile networks such as GSM/GPRS/WiMAX/WLAN and Smart Radio). They are set up to support some monitoring/control programs such as control and information control (SCADA)/Energy Management System (EMS), Distribution System (DMS), Equipment Development System (ERP), and physical safety of equipment in large areas and broadband and capacity in closed networks.

The act of the intelligent system has been shown to be reliable in combining efforts to improve the quality of information leading to the idea of control such as relay in closing through the actual line depending on the performance of actuators, sensors, and controllers are some components of real time communication. The other is that it is repeated in different research papers in the form of feedback. Signals are generated through a communication line to avoid costs and easy access to control, easy maintenance, and special attention is now given to the use of information technology in the control the control [4].

Therefore, facilitate the supervision and regulator of electricity systems and will increase the ability to know the situation [5,6]. That is why it has been identified as one of the most important

achievements of the grid, including the fact that there are many measurements and there are to communicate for control assembly as the backbone of the system. It has also been found that various measurement information, instructional signals, appeals, and up-to-date information are used among many intelligent electronic devices. Some of the papers also go back to describing the structure and size of a high-speed communication network. The amount of information from the actuators, sensors, controllers, and processes is going to focus on intelligent electronic devices (IEDs), customer advanced metering infrastructure (AMI), and distributed energy resources (DER) [7]. And it turns out that depending on the different types of components such as fiber optic communication, power line communications, and wireless technologies are the other determinants of performance as has been the case in many studies that have been revisited in the practical use of supervisory control and data acquisition (SCADA) [8–11].

The intelligent and powerful network of systems and communications continues to be taken into account, as some differences in performance depend on the architecture, at the current level, the power grid is characterized by a cyber-physical system (CPS), which includes the physical process, sensor/actuator, network, control centers, and information that indicates the disturbance information depending on the position or function [3,8] The use of each category is possible, and information flows between all levels, as they only work together [12]. As there are delays in communication and cyber-attacks appear in many and varied ways, for example, there is a basic description of it is to use power lines and direct/indirect electricity where no network user is installed. As the various interactions of the intelligent grid include the physical, functional, and commercial complementarity through the communication network to exchange information, the attacks are larger than those listed in Table A.1. However, in this table, we show the latency and the normal surface area that has the potential to be affected by modern power systems that are reviewed as a baseline to determine the domain and the type of normal attack and as we will see later in order to take precautionary measures against the grid [8]. According to Wei L. et al. [9], the main attacks are most likely due to the technology being used, and the communication delay shows that it has a part to be counted as shown in Table A.2. As exposed in Table A.2, the SCADA, control system, and State estimator there is a communication delay, but you see in the attacks there are other major loopholes such as service denial of service (DoS), false data injection attack (FDIA) [8,13] robbery [14], the introduction of destructive programs or worms, and damage to the electrical system such as attacking 14 destructive devices [15].

Table A.1 The difference between communication delays and cyber-attack in power systems [8].

	Transmission System	**Distribution System**	**Device**	**System**	**Cyber Attack**	**Delay**
Data concentrator (DC)	√	√		√	FDIA	√
SCADA	√	√		√	FDIA/DOS	
Control system	√		√	√	FDIA/DOS	
State estimator	√			√	FDIA	
Communication channel	√	√		√	DOS	√
Power market	√			√	FDIA/DOS	√
Remote Terminal Unit (RTU)	√	√			FDIA/DOS	√
Phasor Measurement Unit (PMU)	√	√			FDIA	√
Programmable Logic Controller (PLC)	√	√			FDIA	√
Advanced Meter Infrastructure (AMI)		√			FDIA	
Intelligent Electronic Device (IED)		√			FDIA	

Recently, the suggestion that follow-up assessments are due to delays in some effects of power system levels as described in these papers [16,17]. There are also different ways to control, to evaluate the communication delay in the AGC system discussed in [18]. Security-related delayed system measurements between equipment and controller [14,18]. Heydari et al. have shown that communication in delays affects microgrid island and continue with the second inspection that took place the survey was conducted with a small sample [19,20]. Some researchers showed one of the ways in which literature only assessed its power delayed check for the second check (e.g., [21]) and others (e.g., [22]) on the full line of the power of the system, both are small-scale signals. There are also indications of the effects of testing delays on the distribution system state estimation (DSSE) were investigated using Monte Carlo (MC) analysis in [23,24] are evaluated, using a well-defined weighted least squares (WLS) the weight of the matrix, in [25], however, to the knowledge of the authors, it has never been established as an undoubted source for growth the analytical expression for calculating the final state estimation (SE) is undoubtedly related to the shock from the communication. As Hasan Ali has highlighted in the lines of analysis in various power system activities, namely in view of the delay in communication, it has been shown to be necessary to dramatically reduce delays to secure the line to be firm. However, the practical experiences of the rope you have calm in many cases ignoring the effects of communication delays as they are categorized [26–29]. The stable security system has been restored to the role of telecommunications delays, while telecommunications delays are calculated in the diagrams [8,18,30].

The results of this study show that ignoring the effects of communication can not only undermine control performance, but also can disrupt the entire system in some cases. The time it takes to send data from a dimension position to a switching center or data concentrator, as well as the period it takes to relay this information to command devices, exists referred to as communication delay or latency in a wide-area control system [31]. This can give insight into communication on methods and technology for analyzing and overcoming delay-based problems in the smart grid. Interval delays may want to stand up in energy systems for not the same motives, and their magnitudes depend on the communique link form, for example, cellular phone strains, fiber-optics, and satellites. Delays in communication can take place at any point in a control system. The addition of a time delay to a response circle destabilizes the system and decreases the damping efficiency or quality of the control actions [14,32,33].

This paper summarizes the state of affairs in the research and summarizes the findings in the event of a delay in communication in the management of security in the power system. Based on the results of our various studies, we make new contributions in the following ways:

- Indicate the causes and effects of communication delays in the power system and research activities in these specific areas.
- Develop a plan to reduce or compensate strategies for the impact of communication delays in the power system.

- To test the simulation of the performance of a given algorithm, its performance is compared to other development methods tested on the widely used system in the literature.
- Examines how the system can be delayed in dealing with cyber-attacks that can cause delays.
- Therefore, this review aims to demonstrate the status of the problem and to show a new research direction provided can be a guideline for different researchers.

The rest of the review paper is prepared as follows: Section A.2 discusses previous and ongoing related works. Section A.3 deals with contracts and robust telecommunications analytics based on the power control system with Network-Induced Delay and Packet Dropout. Section A.4 outlines the different types of mitigation techniques. Section A.5, which is devoted to the main results and discussion of the results of the literature review. In Section A.6, Barriers to communication latency over unstable smart grids and network control are briefed. Lastly, in Section A.7, conclusions and remarks are finished for this paper.

A.2 Previous and Current Related Works

Nowadays, it has been pointed out that the proposed method of strengthening the system for monitoring the flow of information and external disturbances has continued to be demonstrated in a variety of ways to address delays and loss of information. The current user interface is based on a modified switch that is checked to stop the system from connecting in an early manner. It has been shown that the suggested method strengthens the network monitoring system related to information flow and external disturbance. In reference [34], a T-S fuzzy network-based investigation was conducted using a delayed fuzzy control and was not performed by a well-positioned controller. In reference [35], a major innovation in the change in control time has been introduced based on time delays and loss in radio packages. In [36], the decentralization process—is driven by the control over the research done on a system with a different structure. In [37], the reduced NCS program is provided in view of communication delays. The solutions were used to reduce the integration of multiple regions into the power grid. A brief overview of NCSs is provided by reference [38] on system configuration, complex problems, and how they are used [39].

In reference [40], a time-varying algorithm for measuring the power equal to the sensor side has been proposed to lead to a closed-loop system. The algorithm was successfully introducing zoom measurements. Full description of the different types of control techniques provided by reference [41]. The results of the network control and the delay and loss of packet information were reviewed in Reference [42], In Reference [43] how to delay the time in a large system that connects the wiring harnesses to the wiring harnesses, the new selection and control method is provided by reference [44], a first state-space model was established, in which the error was monitored, and the state variables were combined and implemented [45]. The good comparison problem in the network control has been lost with the planning to store information in detail as shown by the researchers [24]. In [46], the Slide Mode Controller (SMC) issue for NCSs was concerned with

the stochastic partial rotation, better known as Markov, or object rotation, and with unplanned measurements [39]. In [47], for which a model for the removal of a model, it is provided for a system that is compatible with thinking about data loss and communication delays. Therefore, it is found that in [47] the communication load can be significantly reduced, and the useful energy can be greatly improved while maintaining the performance of H∞. The pendulum fluctuates with a single power line system controlled by a sensor network that does not have wires provided to indicate the performance of a given self-triggered sampling scheme (STS).

The summary of NCSs in Ref. [38] goes on to address a variety of issues. According to the modified system problem, the external system connects to the network with the errors investigated in [48]. Wei Y and colleagues [49], showed the difficulty of delay-based severity is the main reason for controlling Output Solutions (SOF) control for indefinite phase T-S fuzzy (FA). In return, the issue of unstable comparisons of the state through communication and the loss of the park has been solved in [50]. The study on reduced species and the type of filtration that was provided by reference [51] on industrial CPS, was explained by different genders. In Ref. [52], the authors addressing the concerns of many sections, which are based on information from cyber-attacks, designed to improve ICS security. He described the new Lyapunov-Krasovskii method, shown in the rapid analysis of the analysis of a large closed-loop system. Moreover, an investigation into the controlled and reduced type of filtering on CPSs was defined by the comparative data provided by the Ref. [53]. In [54], the authors were interested in the exchange of information between the integrated microgrid and the second-hand controllers in the management of the microgrid. Liu S et al. They continued to show the effects of delayed communication on the second microgrid control island and several generators were reduced. They conclude that the A gain scheduling approach (GS) is also proposed to pay late compensation by contacting the secondary frequency control. In Ref. [55] the authors suggested the control of droop to two new secondary control system (SCSs) monitoring programs were discussed to address the issue: (1) a model predictive controller (MPC); and (2) a Smith predictor-based controller [55]. However, even if they do, they are still trying to figure it out on the delay of different periods in the microgrids (MGs).

Yan H et al. showed that the method of comparing the microgrid method with the delay. They continue to make it clear that Lyapunov's method is used to analyze functional stability. Finally, the expected sliding mode control (SMC) strategies are confirmed by comparative microgrid studies and delays problems [16]. In [56], the authors investigated the robust problem of the network control system. In [57] focused on solving the problem of sliding on continuous-flow control systems without a control system line. They keep in mind the delay in importing and the lack of high-speed communication including the time of transmission and the protocol being sent. Although research papers are available, they continue to address the issue of delays and delays. There is a team of researchers consisting of Fang F et al. [58], in their achievements and in the fact that the problem of fault tolerance-measured-data H∞ controls the network control system and the delay and the fault of the actuator. In [59] have demonstrated an effective way to model-free adaptive control (MFAC), which uses pseudo-partial (PPD) materials to connect unconnected

power lines, considering WADC requirements and system disruptions are required to eliminate disruption at the inter-area oscillation for a wind farm [59,60]. In addition, to compensate for the delays of communication in the wide-area measurement system (WAMS), the compensation for delay coordination and adaptive delay compensator (ADC) is used to pay for constant and variable delay. In addition, to compensate for communication delays in a wide-area measurement system (WAMS), an adaptive delay compensator (ADC) is active to repay both continuous and adjustable delays [59–61].

In reference [16,62], the authors discussed the effects of time-delays in WAMS-based monitoring activities on the performance of the system [63]. Molina-Cabrera A et al. demonstrated the ETDC, which uses a delay method to differentiate a line delay method rather than a deadline; moreover, the ETDC uses real-time signals and how to send measurements to WAMS that builds a closed-loop database system [62]. In [64], the authors deliberated the combination of power control and communication in network control which yields interesting results in the design, and they reported that because the analytical approach is not feasible in the form of a robust system, the paper also prepares a new general method for calculating the system's eigenvalues and various delays that cannot be explained by the analysis of possible objects. In Ref. [65], the authors discussed the LMI method to better compensate for the delay caused by the delay and to provide the desired performance [39]. The authors of [66] used the NN method to accurately compare the TDS attack in real-time and to assess the delay in the NCS system to see its safety effects on two power systems. In [21], the authors provide an analysis of a one-time load control program, the main way to maintain the safety and security of the energy system. Moreover, Markov's idea is the basis on which they set up a model to better explain how to combat inaccuracies in measurement and external disturbances. Then, a new fractional-order global sliding mode control scheme containing fractional-order terms on the sliding surface is accepted to improve the robustness of load frequency control. In [67], the authors gave a new idea of calculation, and the statistics given on this structure were given to illustrate the positive effects of calculation. The above development can be grouped in table form according to the region/network/criteria as follows.

Table A.2 summarizes information on how to distribute the paper in various sections published since 2015. The main focus of the research in this section was on delay-based networks [39]. That is why it has been shown that the difference between the tasks reported in the research has been varied depending on the safety approach, the model-based approach, and the model-based approach including the initiation of the delay. In addition, some summaries have shown that there are various ways to combat delays in communication based on design or topology as they are built in three types, as has been shown in some research papers presented in Summary in Table A.3.

In the past and in the present research, it has been shown that some advantages and disadvantages of problem-solving, are also indicative of weakness. Table A.4 summarizes results based on current events and compares them to their pros and cons. Recent papers have found that it solves many problems in terms of efficiency and security.

Table A.2 Summary of discussions on control system development since 2015.

S. No.	Reference No.	Parameter/Area/Network
1	[4,14–16,18,25,30,31,33,35–38,46]	Model/Sampling Based Networks
2	[21,22,24,36,40,42,43,48,55,58,67–69]	Stability Analysis/Approach
3	[9,14–16,18,20,22,26–28,31,33–37,39, 41–63]	Time Delay/Fault/Track/Detection/Packet Loss
4	[4,11,12,17,25,26,30–32,34,39,41,42,50,52,54,56,64]	Internet/Communication Based Multi-Rate Control Networks
5	[16,17]	Distributed Networked Control Approach
6	[17,25,28,32,37,60,65]	Event Based Networks/Interactive Networks
7	[59,61,62,70–74]	Compensate network/Compensation strategies

Table A.3 Summary of different types of topological discussions.

S. No.	Reference No.	NCS Topology
1	[12,17,30,33,41,44]	Centralized Topology
2	[16,36–38,64,67,75]	Decentralized Topology
3	[37,38,53,55–58,64,66,68,70,71,76]	Distributed Topology

Table A.4 Comparison of current activities with previous activities.

	Present Work		**Previous Work**	
S. No.	**Pros**	**Cons**	**Pros**	**Cons**
1	Minimizing outages and their effects	Overhead costs	It is easy to implement	Network model is limited
2	Automatic processes and user controls	Expensive	Capacity	The method can be expensive
3	Incorporate more renewable energy resources	Time-consuming	Various network configurations can be easily analyzed	Some method limits inaccuracies
4	Communication technologies and autonomous networks	Hacks or other malware attacks	Cost effective, reliable, suitable for establishing back bone communication infrastructure	Low bandwidth
5	Corporate IT departments and Safety factor increases	Complexity and congestion	Closing the gap between periodic tests	
6	Asset management and High channel capacity, data rates	Low range of capacities for distributed generation	Introduction of LAN in substations and interactive networks	
7	Rapid installation and wide range of applications		Merging protection and SCADA networks	
8	Effective reduction of system complexity		Basic data collection and long delay	

A.3 A Robust Telecommunications Analysis Based on the Power of the Control System and the Network Caused by the Delay and the Packet Dropout

In the study, there were many delays caused by the network [74,77]. In Ref. [77], four main types of delay are discussed, namely: (a) the model of constant delay, (b) the model of extreme delay, (c) the Markov chain model, and (d) the Markov model. The reasons for this type of delay are in a low speed, network speed, and the protocol sent [19]. There are two types of delay, especially (i) sensor for delay controllers and (ii) controller delay for the actuator. Because network latency is due to network connectivity, it is sometimes fluctuating, unexpected, and the upper boundary is unknown. As a result, the delay caused by the network is usually done as a time delay between [69,78] and a Markov network with a known transitional probability, a probability of a partial transition, and an arbitrary change [77]. As declared, in reference to [79], network delays have been identified as a reason to undermine the functioning of the system or possibly as a reason for insecurity. In [39,80] authors proposed an algorithm based on a gradual push of money to address Electronic Data Processing in a way that is reduced to a communication network with different topology and communication latency. The proposed algorithm is allowed to solve Electronic Data Processing if different communication networks are connected together. There are some systems where communication delays can have a positive impact on system performance, as described in [39,81]. In Ref. [82] the authors asked for an LMI method to identify the two-way static solution provided by the gain controller to compensate for delays and a well-planned network and provide audit performance. Table 5 shows the statistical delays in the various studies conducted in the reference paper. The maximum delay to be assessed is 500 ms [62,83].

The data packet has dropped the problem and is a major issue, depending on the shipping method. Broadband and a lot of information are sent to one line responsible for this defect [39]. Numerous studies have examined losses in network control [47,84,85]. These difficulties often occur due to the exchange of information between different devices, which degrades performance and can disrupt the system. Due to numerous vehicles, the loss of parking information is also a major concern [39]. Basically, the effects of dropping out of school are also known as Bernoulli or Markov. In many communication networks, various data packets are slow to arrive, providing times when the previously sent data packet can reach its destination later [42,43]. Tables 5 and 6 show the statistical data for the loss of the pack considered in the various studies in the literature. The estimated rate of park loss is 80% in the definition [25,39].

Table A.5 Delay data measured in dissimilar studies.

Reference No.	**Type of Delay**	**Delay/Delay Range (*in ms*)**	**Merits**
[81] (2019)	Random Delay	0 to 100	Secure the system
[86] (2020)	Random Delay	30 to 300	Maintain operational stability
[87] (2018)	Network-Induced Time Delay	0 to 700	Identify the distribution of time delay
[88] (2021)	Constant Delay	300 and 500	Improving the stability of the power system
[62] (2021)	Time-Varying Delay	100 to 500	Increases the transfer capabilities in tie
[89] (2021)	Variable Delay	50 to 100	attenuate the influence

Table A.6 Packet loss degree measured in different studies.

Reference No.	**Loss Rate/Loss Rate Range (in %)**
[90] (2014)	0 to 5
[42] (2016)	20 to 70
[44] (2016)	20 to 40
[91] (2020)	0.05 to 1.5

A.4 Compensation for Electricity-Based Communication and Network Latency

Communication delays may lead to insecurity of communication-patrol frameworks. Expanding inquiries about efforts have been committed to planning progress control strategies to overcome the impacts of network-induced delays [70]. In this segment, various switch strategies have been presented to compensate for the impacts of delay caused by the network within the power control framework.

A.4.1 Evaluations between Direct and Indirect Methods

Modeling the uncertainties, in terms of time delay, packet loss probability, queue length, and throughput is greatly highlighted to confirm that communication infrastructure remains robust under malicious attack [92]. So, it is essential to build an appropriate communication infrastructure, otherwise, the system may introduce potential degradation of dynamic and static performance of power system and result in system instability [92,93]. In LFC, due to the use of open communication infrastructure and phasor measurement units (PMU) in the wide-area monitoring systems (WAMS), communication delays have become assured and raise concerns about the system's steady-state and dynamic response [61,92,94].

According to the data collected by the researchers in Table A.7 with respect to the delay initiated in the control activities carried out, there are two types of delays that coincide with the power system. The first is a direct method based on the tracking of eigenvalues. However, the direct method can only solve delays in the system [95,96] and the method cannot withstand the delay [88,92]. The second and most direct method is based on H-infinity robust synthesis, Lyapunov's unstable theory, and matrix equilibrium (LMIs) technique for controlling the delay of the controller [88,92,97]. Although limited, these skills can solve a variety of problems and delay those [68,75,81,98].

Table A.7 Assessments between direct and indirect methods.

Methods	Calculation Load	Cooperativeness	Delay Type	Application
Direct	High	Low	Constant	[80] (2019), LFC., [96] (2015) WADC
Indirect	Medium	Medium	Constant and time varying	[99] (2020), [100] (2019) LFC, [75] (2017) LFC with DDC, [98] (2014) WADC

On the one hand, in the case of the stochastic switching method, both the forces of delay due to the delay and of the power system are considered [70,101]. The ongoing interaction between the communication network and the power system is well-considered and comparable [70]. On the contrary, the expected system method shows the optimal value using the delayed data due to the network. This method is used more easily than before. Just as the delay in communication is not too late, it is serious that a quiet analysis method of communication based on an energy control system is essential. However, so far only a handful of cases has been reported. Therefore, research efforts are needed to conduct a reliable and reliable investigation of the effectiveness of the communication power control system.

A.4.2 Nonlinear Control

In addition to the adaptive self-tuning control method, there are still many important non-linear monitoring methods to address malfunctions in power systems, including the sliding mode control (SMC), fuzzy logic (FL) control method, network control (NN) methods, and hybrid system methods [70,95].

A.4.2.1 Sliding Mode Control

SMC is a variable structure control method that drives and then maintains the system trajectory within a particular neighborhood of a sliding surface [16,70,74,95]. The generally, there are two steps to designing a sliding mode controller.

- Step 1: Describes the switching work: the switching work is planned to protect the framework while sliding in a dynamic manner.
- Step 2: Define a switched control law: the switched control law is designed to move the framework state vector to the sliding mode and maintain it once it arrives.

Sliding mode control has proven to be an efficient approach to compensate for power systems [70]. To compensate for the delay in communication, SMC monitoring is based on broad areas and has been monitored to ensure that WADC does not misinterpret communication delays [52,70]. In terms of latency indefinitely, it was discovered that residing on a slippery slope due to the lower and upper slopes causes endless delay [102]. Only fuzzy control measures have been taken, except for the fuzzy-based integral sliding mode load frequency control system (FISMLFC) which is required for many parts of the integrated Wind Farming (WF) system [26,95].

A.4.2.2 Fuzzy Logic Control

Planning an FL controller incorporates three stages:

- Step 1: Fuzzily (Make membership work): this step includes mapping numerical in-put parameters to fuzzy factors for a characterized membership work.
- Step 2: Indicate the run the show table: this alludes to making a run the show table to determine all combinations of input signals and compare output signals for these input signals.

- Step 3: Defuzzily the outcomes: it includes producing numerical input values which can be utilized as control inputs of a control framework, based on the outputs of the fuzzy rules.

FL controllers have been broadly utilized to handle vulnerabilities in control frameworks. In [75], an FL wide-area damping controller with moving membership capacities is proposed to compensate for the expansive latency included within the transmission of wide-area estimation signals. In [31], both time delay and uncertainties in measurements in the fuzzy type-2 WADC [31]. In [103], a new direction was established by the T-S Fuzzy Control System (TSFC) and the delayed separation time in many parts of the system is applied for the load-frequency control of a three-area electrical interconnected power system to enhance the system stability under uncertain disturbances [70,95].

A.4.2.3 Neural Network Control

Understanding an artificial issue without a numerical demonstration of a real framework, as it were, by utilizing the interconnects between the neurons within the various layers of each framework is part of planning a NN controller. Association of neurons can be modified in its structure to clearly demonstrate the relationship between input signals and their valid fields. Learning gives NN controllers the capacity to infer subjective straight or nonlinear mapping [66]. Because of this feature, NN-based control can be used to improve the resilience of control frameworks and address communication link weaknesses. The use of NN-based wide-area damping controllers to adjust for wide range of communication delays was investigated in [104]. Wang S. et al. [71], neural network approximate-based feedback adaptive quantized control protocol based on k-filter observer is proposed to reduce the estimated error and external disturbances resulted from multi-machine excitation system.

A.4.2.4 Comparisons of Remuneration Approaches

Table A.8 summarizes a comparison of these control strategies utilized to compensate for network-induced delays in communications-based frameworks within the literature. As can be seen from the table, the nonlinear control strategy is generally autonomous of the framework shown and has high robustness to parameter vulnerability and unsettling influences, particularly ETDC, MFAC, and NN. Be that as it may, due to the plan of these controllers, preparing the LKF, FL, and NN controllers involve a huge sum of estimation information. Planning H_2/H_∞, SMC, and other model-based strong controllers are moderately direct but have constrained vigor to parameter instability compared to non-linear controllers. Luckily, most of these controllers can be utilized to compensate for both deterministic and arbitrary arranged delays. As for the structure, these recompense strategies have been connected within the interconnected electricity framework control, such as WAMS, WAC and WAMC, whilst their purposes in microgrids are right now within the infants as most of the current microgrids are still in-lab demonstration projects and have not been broadly connected within the real world. In any case, functions of these manipulation

techniques in microgrids vitality administration and manipulation have been drawing in quickly expanding consideration as the critical requirement for smart networks around the world.

Table A.9 provides a comparison of experimental analysis of various traditional and associate classification techniques. Through the analysis of the table below, it shows the indicators of the performance of the algorithm for different power systems. We have compared different techniques, and they have different criteria in the system, for example accuracy, consistent, scalable and efficient reduction of overshoot. Many research results have shown that smart building techniques are more effective and predictable than traditional techniques. In the case of strategies such as ETDC + MPC, DOF-WADC, FLC and DOFC they are being used to assess performance, in fact, and F-scale. The comparative analysis concluded that ETDC + MPC and DOFC are superior to other techniques.

Table A.8 Evaluations between direct and indirect methods.

Detail Modelling Techniques	Model Dependence	Robustness	Design Difficulty	Delay Type	Applications	Main Contribution
(2016) (MPC) and Smith predictor-based controller	Low	Medium	Low	Deterministic and random	[55] Microgrid	Stability analysis based on small-signal
(2016) $\boldsymbol{H_2/H_\infty}$ synthesis controller	High	Low	High	Deterministic and random	[61] WAMS	Considers model of time delays
(2018) LKF	High	High	High	Deterministic and random	[22] WAPS	Stability analysis
(2018) LMIs	Medium	Medium	Medium	Deterministic and random	[69] WADC	Optimization-based information sharing
(2019) Sliding mode control (SMC)	High	Medium	High	Deterministic and random	[16] Microgrid	Stability enhancement
(2020) Fuzzy logic	Low	Low	High	Deterministic and random	[94] WAMS	Calculate delay margins
(2020) T-S Fuzzy control (TSFC)	High	Medium	High	Deterministic and random	[68] LFC	High Stability system
(2016) Model-free adaptive control (MFAC)	High	Medium	High	Deterministic and random	[43] WADC	Calculate delay margins delays Scenarios.
(2021) Enhanced Time Delay Compensator (ETDC)	High	High	High	Deterministic and random	[62] WAMS, WAC, WAMC	Calculate reduction of overshoot (almost 39%)
(2021) Analytical approach and Optimal control gain	Medium	Low	High	Deterministic and random	[105] WAMSs	Design robustness of a small-signal stability
(2021) Neural network control and new Fractional-Order Global Sliding Mode Control	Medium	High	High	Deterministic and random	[71] LFC, [21] multi-area power system LFC	Compensate approximation error and The stability and stabilization

Table A.9 Comparative analysis of different algorithms.

Techniques	**Application Size**	**Threshold Parameters Applied**	**Compared with**	**Results**
[106] SDC (2013)	IEEE 50-generator test system	$T_d = 0.1\ s\ to\ 0.7\ s$ $f = 0.1\ Hz\ to\ 2.0\ Hz$ $\rho = 0.0315, 0.0246,$ 0.016 0.0077	Without SDC	More time efficient and faster than without SDC
[107] DD-WADC and DOF-WADC (2016)	IEEE benchmark system (WADC)	$T_d = 800\ ms\ to\ 250\ ms$ $f = 0.5777\ Hz$ $\rho = 0.0152$	PC-WADC	More time efficient and faster than PC-WADC. Even under the effect of the time-varying delay of the wide-area communication network, it knows how to still maintain a good damping performance.
[108] BA and BESS (2019)	Java 500 kV Indonesian grid (WAMC)	$T_d = 100\ ms\ to\ 700\ ms$ $f = 0.6567\ Hz$ $\rho = 0.0569$	POD and BESS	Higher accuracy and faster than BESS, highly competitive with POD and BESS
[1] FLC (2019)	IEEE nine bus power system (WAMS)	$T_d = 0\ ms\ to\ 700\ ms$ $f = 0.5777\ Hz$ $\rho = 0.0152$	MPM	More consistent and highly effective at classification and has minimize the impact of delay in positioning on the power structure of the Hybrid system.
[109] DOFC (2021)	Four Machine Two-Area Power System (WADC)	$T_d = 100\ ms$ $f = 0.6567\ Hz$ $\rho = 0.0823$	PID	Better performance than PID, Execution time is less.
[62] ETDC + MPC (2021)	Kundur's 2-area test system (WAMS)	$T_d = 100\ ms\ to\ 500\ ms$ $f = 0.598\ Hz$ $\rho = 0.0205$	SPB + MPC	More accurate, scalable and efficient reduction of overshoot (about 39%) implies less stress over the thermal limits and less impact of isolation due to protective actions.

A.5 Results and Discussion of the Literature Reviewed

In this section we take a look at an assessment that leads to a variety of results caused by communication delays. First, we look at the evaluation we have done in MATLAB/Simulink software, the last we look at the evaluation together and it is the results from different researchers.

A.5.1 IEEJ West 10-Machine Model System Results

To analyze the communication delay in the IEEJ West 10-machine model system (60 Hz) [91] is under review (as shown in Figure A.2). According to this system the Japanese model consists of 10 generators, G 1 to G10, Generator G 10 is considered a swing generator. In this work, five braking resistors are installed at the terminal buses of generators G1, G4–G6, and G10 for the stabilization of the overall system. Therefore, it is essential to notice that every single system has the ability to tolerate delays, depending on how it is built and the tools that help it to operate. Normally, communication delays can range from several microseconds to hundreds of milliseconds [40,75,88,89]. Moreover, according to some other reports [62,86], the normal 150 to 300 milliseconds of telecommunications are considered to be the plans to perform actual transient stability control system, stability index, fault clearance time and delay in response. In this work, a lot of simulation is done with different values of delay. Some systems can withstand a delay of 100 ms, while other systems have a delay of 200 ms. For the power system model, we tested in this process, if the delay is more than 300 ms, then the system presentation is compromised, and the system changes smoothly. Therefore, it can be said or expressed that the extreme allowable delay on this system is 300 ms.

A.5.1.1 Scheme of Fuzzy Logic Controller

The braking resistors are switched using fuzzy design logic controllers, which are defined in the section below.

Fuzzification

Figure A.3 demonstrations the anti-brake (BR) value of the GTCSBR conductor connected through the thyristor to one of the generator bus lines. Brake rotation is performed by the fuzzy logic controller. All total kinetic energy deviation (TKED) is used as input to the fuzzy switch controller. For diagrams requested by the fuzzy logic controller, the time from the TKED of the generator, TKED, and firing angle,$\propto$ was selected as input and output. In this case, the difference is between the total kinetic energy (W_{total}) of the generator in the transient state and that the constant state is defined as the total kinetic energy, $TKED$, i.e., TKED = (W_{total} for the transient state) - (W_{total} for the state stability). The performance of the TKED triangle is shown in Figure A.4 where the N, Z, and P variables are negative, zero, and positive. It is important to note that member functionality is the same for each fuzzy controller. A comparison of the performance of a triangular member is used to determine the level of member values and the following [110]:

$$\mu_A(TKED') = \frac{1}{b}(b - 2[TKED' - a]) \quad (1)$$

Where $\mu_A(TKED')$ is the value of the points of the members, 'b' is the width, 'a' is the sum of the points where the members are 1, and '$TKED'$' is the value of the input of the variables.

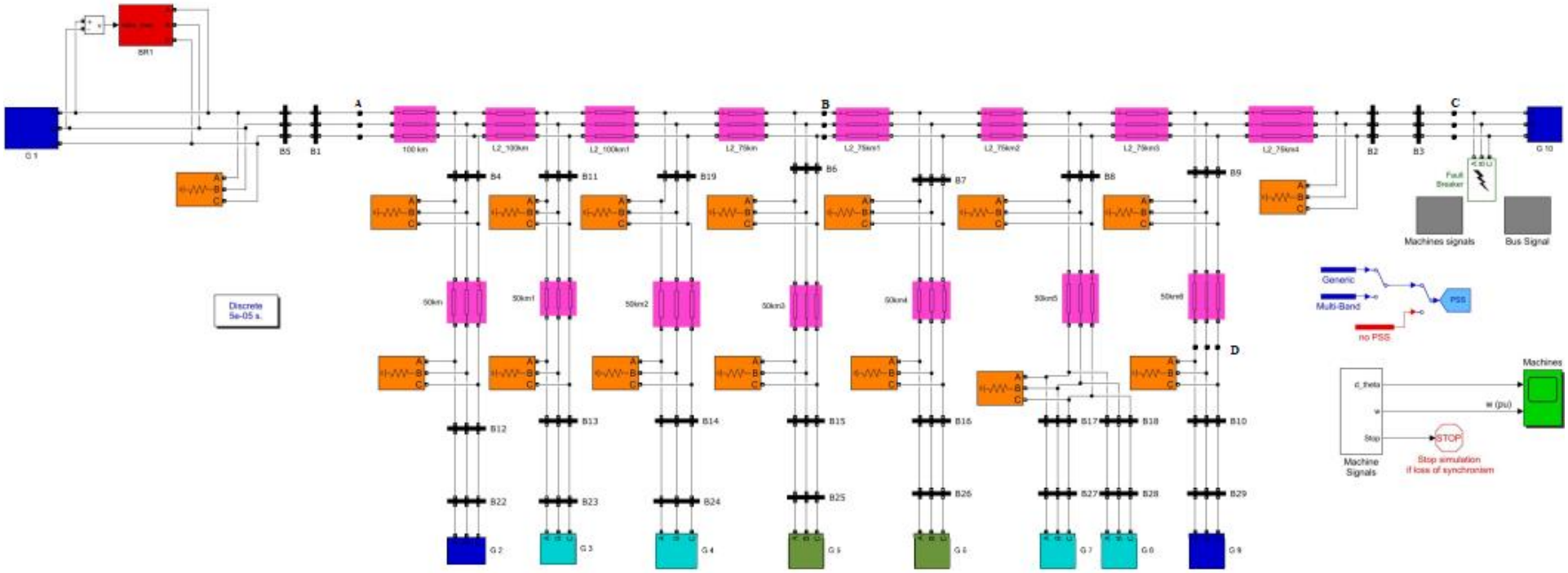

Figure A.2: IEEJ WEST 10-machine model.

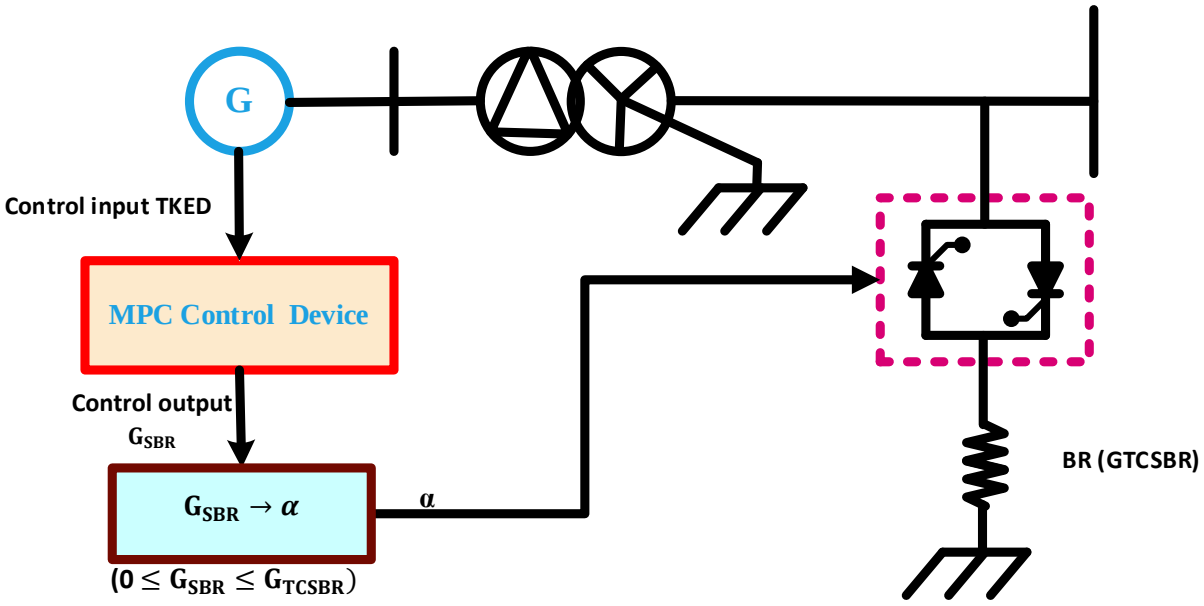

Figure A.3: BR with thyristor switching circuit.

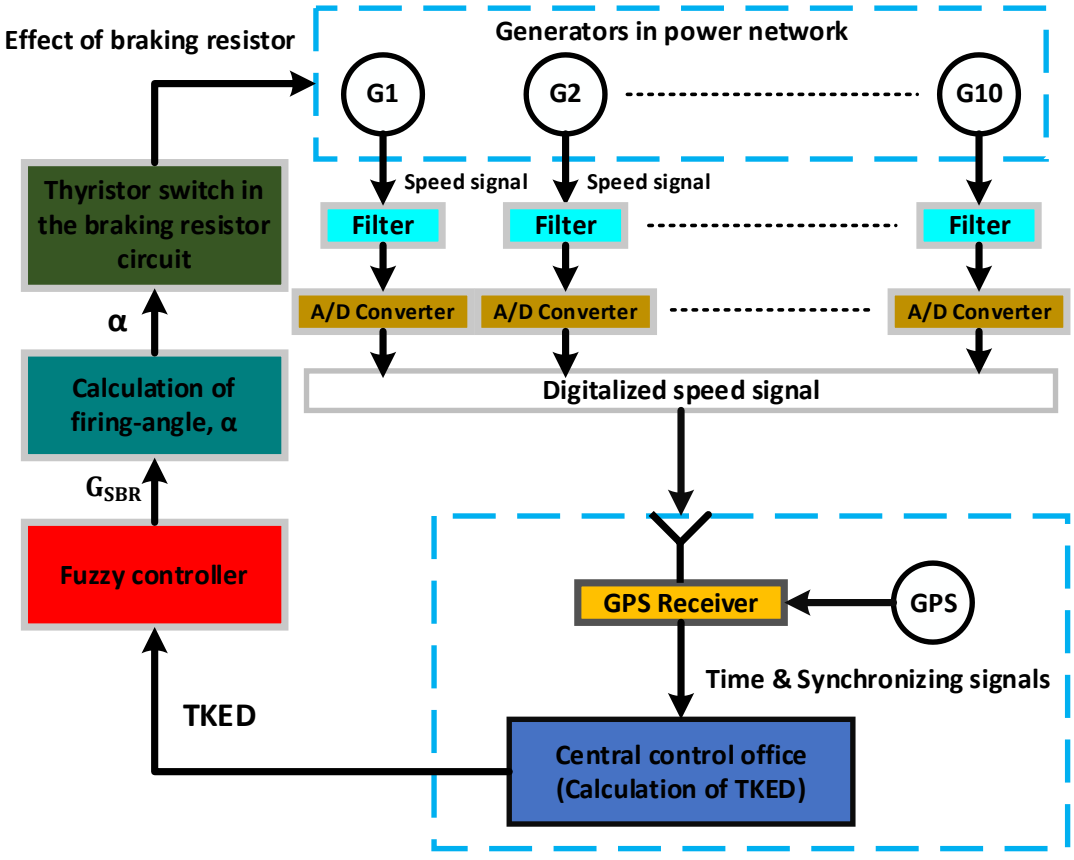

Figure A.4: Closed loop control system counting GPS occupation [111].

Fuzzy Rule Table

A unique feature of the fuzzy controller is its simple design, which has only one input and output. The use of inputs and outputs makes fuzzy control more efficient [111]. The planned control approach has only three control rules for each controller as shown in Table A.10, where the values of α according to the language changes indicate the fuzzy output of the controller.

Table A.10: Fuzzy rule table.

TKED′(pu/s)	**α (Firing Angle)**
N	Big
Z	Medium
P	Small

Fuzzy Inference

By deciding on fuzzy research, Mamdani's method [110] is used. For Mamdani, a degree of connection, W_i of each fuzzy command is as follows:

$$W_i = \mu_A(TKED') \tag{2}$$

Where $\mu_A(TKED')$ is the minimum score for members and i is the rule number.

The central region is a well-known and easily devalued method that is implemented to determine the output value (i.e., GHF) [112]. This is provided by the following statement:

$$\propto = \frac{\sum W_i C_i}{\sum W_i} \tag{3}$$

Where C_i is the price of $\propto$ in the fuzzy instruction table.

One key point to note here is that normally two input elements (error and time derivatives) are used in fuzzy logic design. In this work, the first two input elements (TKED and its derivatives) are used. On the other hand, the presentation of the two input variables was almost the same as the use of the same variable. In addition, the use of two input elements increases the number of fuzzy rules and member activities. For that reason, to make a simple controller, only one input, i.e., time the origin of TKED is used in this work.

An adaptive neuro-fuzzy inference system (ANFIS) logic expands on two-valued Boolean logic by allowing truth values in the continuous interval [0, 1], where 0 is not absolutely true, 1 is absolutely true, and all values in between are degrees of truth. This expansion is best suited for resolving problems involving uncertainty or ambiguity. Because each controller is controlled by only three IF-THEN control rules, the ANFIS method of control is very simple. It should be noted

that the control rules were developed through trial and error using system-specific functions. A brake resistor (BR), for example, can produce and use active power at high speeds (P: Positive), but not at low speeds (N: Negative). Furthermore, the brake resistor is not required to use active power consumption while the system is in steady-state (Z: Zero). As a result, the ANFIS rule table is made up entirely of positive (P) elements.

In this work, a lot of imitation has been done cheaply for a short-term analysis based on different values of communication delays, the consequences of this are discussed in more detail in the table below. Figures A.5 and A.6 show the active power responses without and with fuzzy controlled BR. Communication delays are not considered in this case. It is clear from these results that the system is in good standing when BR is used by fuzzy. Figures A.7 and A.8 show the heavy load with the fuzzy controlled BR during a delay of between 200 and 300 ms. It appears that the short-term performance in Figure 8 is worse than that in Figure A.7. This fact shows that the delay in communication affects the transient stability performance, the amplitudes of G2 and G3 reach and increase as shown in 1 s.

Table A.11 displays the (W_c) values for 3 LG in the faults shown at 4 different points from A, B, C and D as shown in Figures A.7 and A.8 with related to different communication delay values such as 50, 100, 200 and 300 msec intended for use and fuzzy controlled delay minimization technique. The simulation results from that review paper indicate that in order to maintain the stability of the system, it is necessary to have a low-latency communication. The larger communication delay causes slower control actions (fault clearance time) that can cause power system instability and oscillation. As the network delays increase from 50 msec to 300 msec, the rise in the system overshoots and longer settling time is experienced by the control system.

It seems that the BR-controlled fuzzy works fine in the improvement of evolutions, to quiet down erroneously in different places. It is also appreciated selection that the (W_c) values correspond differently, the communication delays vary according to the subjects. Here the truth is that the communication delays are related to the number of fuzzy lines in the BR controller, the change affects the line in the short term. As can be seen in the Table A.11, it is clear that fuzzy-controlled BRs are useful in improving short-term stability by correcting different points. As it turns out, communication delays are related to the number of fuzzy controller lines in the BR input controller that change the short-term effect of a grid faults. To understand the effect of communication delays on the integration of components of the power system, we first conducted research when communication delays were zero. And we continue to examine the short-term system when it comes to matching deviation of total kinetic energy (W_c) values as provided by

$$W_c(sec) = \int_0^T \left| \frac{d}{dt} W_{total} \right| dt / system\ base\ power \tag{4}$$

During the process of determining the structure of the system, it becomes known and there is a control over the working time. And T is an imitation time of 0.7 s, while W_{total} is the sum of all kinetic energies, as shown in Equation (4). And due to the desire to reflect on the efficiency of the system downtime it required the use of W_c.

$$W_{total} = \sum_{i=1}^{N} W_i \tag{5}$$

Where

$$W_i = \frac{1}{2} J_I {\omega_{mi}}^2 (J) \tag{6}$$

As the system is built to control power generation behavior, W_i shows the kinetic energy (in joules) of the generator, i shows the number of generators, and N indicates the total number of generators.

$$J_i = \frac{H \times MVA\ rating}{5.48 \times 10^{-9} N_s^2} \tag{7}$$

Where

$$\omega_{mi} = \frac{2\pi N_R}{60} \tag{8}$$

Moreover, in equation (4) shows the moment of inertia in $Kg.m^2$ where N_s^2 are synchronously accelerating at constant rpm and inertia is constant, and, also, the ω_{mi} is rotor the fastest speed in the (mechanical rad/sec) and N_R where the rotor speed in (rpm).

Table A.11: W_c Values and communication delays.

Fault point	Communication Delay	Head Value of WC (sec)	
		Without BR	With Fuzzy Controlled BR
A	50 msec	235.756	33.586
	100 msec	235.756	35.276
	200 msec	235.756	39.359
	300 msec	235.756	43.196
B	50 msec	71.895	30.314
	100 msec	71.895	32.896
	200 msec	71.895	36.945
	300 msec	71.895	37.998
C	50 msec	154.352	40.412
	100 msec	154.352	41.834
	200 msec	154.352	43.846
	300 msec	154.352	44.605
D	50 msec	69.874	34.769
	100 msec	69.874	35.934
	200 msec	69.874	39.436
	300 msec	69.874	39.768

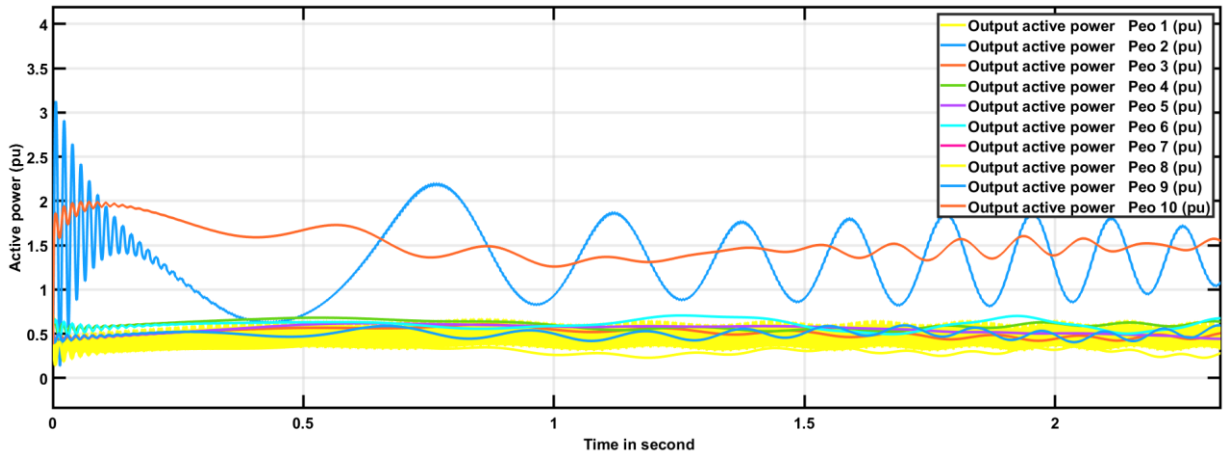

Figure A.5: Active power responses without BR and communication delay.

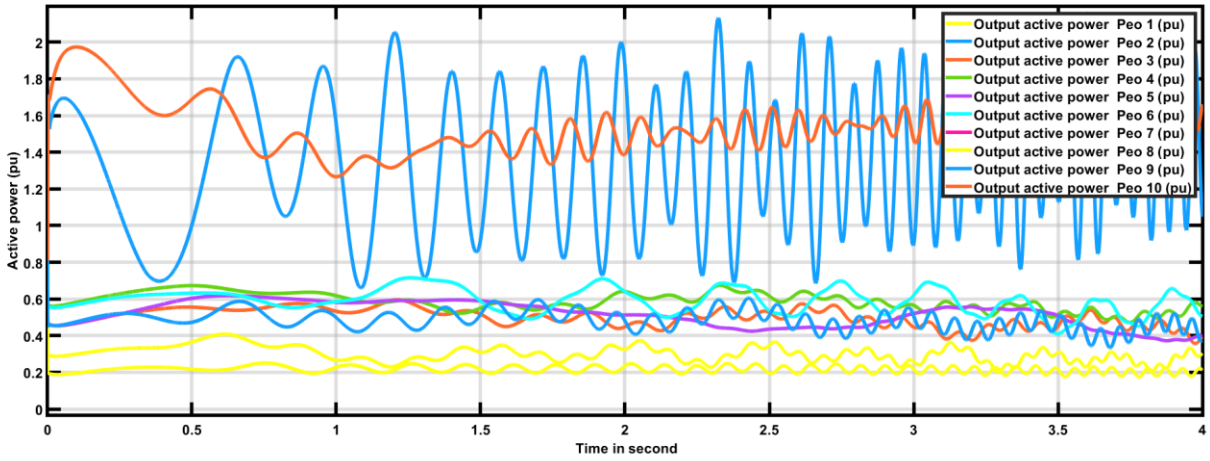

Figure A.6: Active power responses with BR and communication delay.

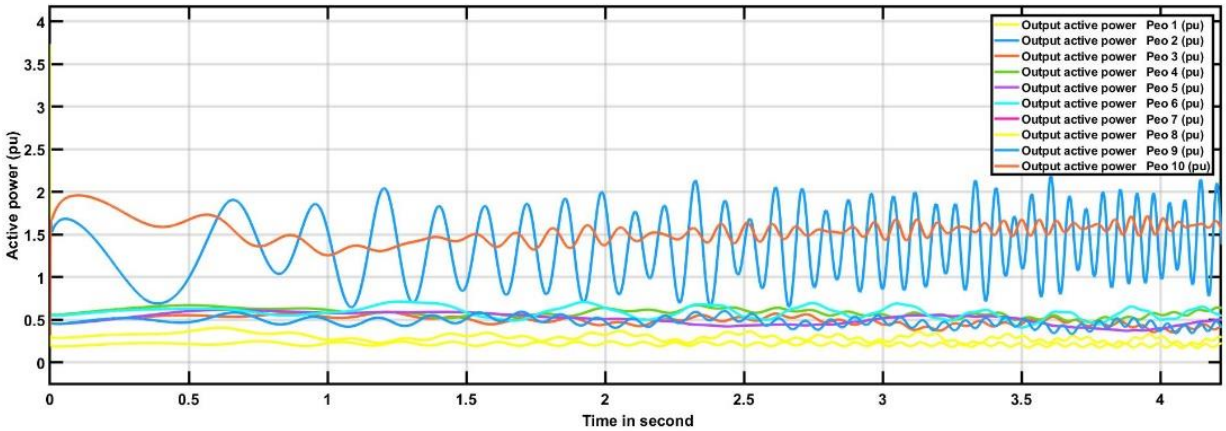

Figure A.7: Active power responses with fuzzy controlled BR and communication delay of 20 ms

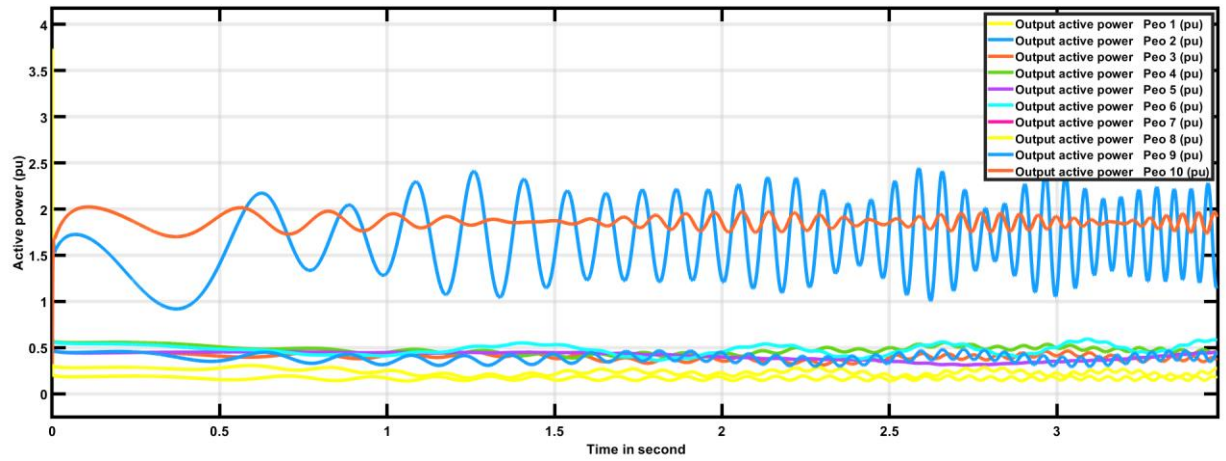

Figure A.8: Active power responses with fuzzy controlled BR and communication delay of 300 ms.

The standard IEC 61850 system is advancing in the field of alternative communication, so it is only natural that we would expand this technology in the form of grid security [113]. As shown in Figures A.9 and A.10, the corrections to points A and C are shown, it is important to understand how to correct or take action in the event of a quick error in order to perform as intended to protect the power system. To be able to limit the fault current before the first current peak, the fault must be detected at least five milliseconds after fault initiation (assuming the apparatus used to clear the fault has zero operating time). In practice, the operating time of a switch used for the current diversion is about 3–5 ms. If a safety margin of 1–3 ms is sufficient to ensure that the fault current is limited before the first current peak, approximately 1 ms is available for fault detection.

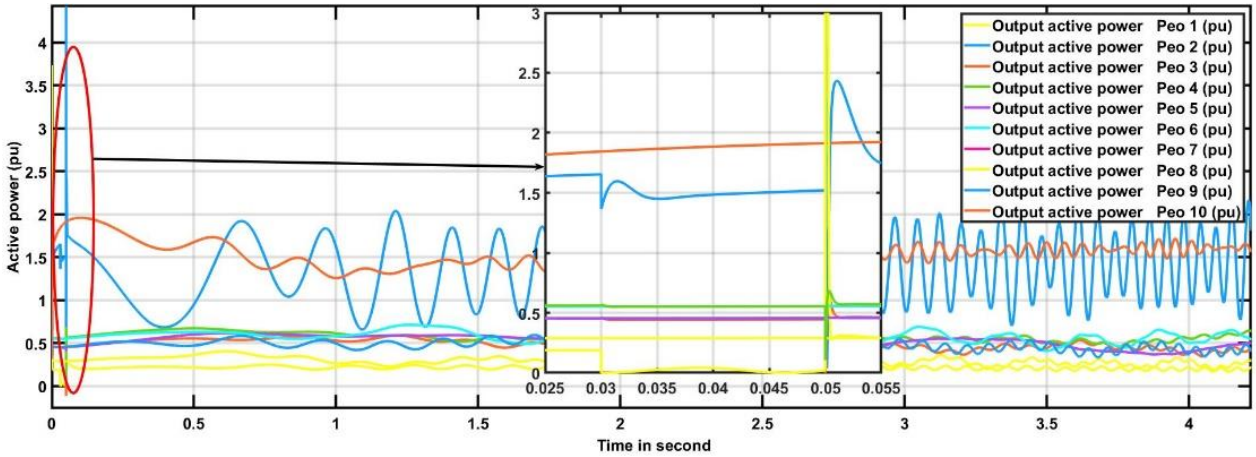

Figure A.9: Active power responses for 3 LG fault at point A.

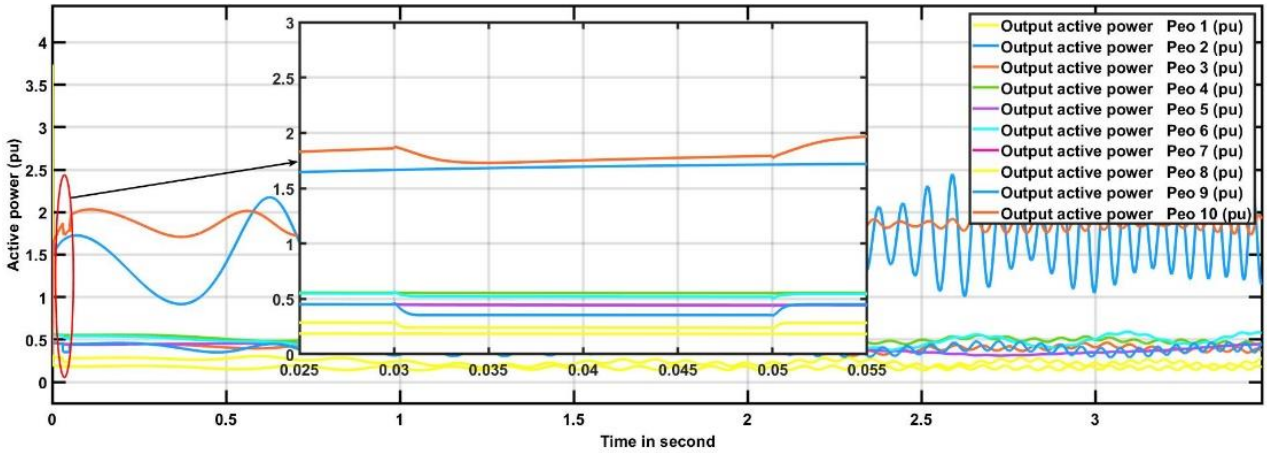

Figure A.10: Active power responses for 3 LG fault at point C.

As we have seen above in security management it is important to keep in mind that there are cyber-attacks that go hand in hand with Digital Signals that need to be closely interconnected and go

hand in hand when using GPS clocks. However, a number of telecommunications networks may be more vulnerable to service denials and central attacks. Unauthorized attacks can cause false alarms to disrupt the SCADA, resulting in a fire escape system designed by these hackers. The attack can also use a service cut-off or stop the flow of messages and control messages in communication networks. As various studies have shown some of the malware such as Stuxnet and the Botnets that are being used are now showing up in malware. There is also an Advanced Persistent Threat, and Backdoor can severely disrupt communication and connect devices in different parts of the power system. Terrorism will intensify in the smart grid, where communication latency should be low, and instead of delaying the introduction of security measures such as data storage and verification.

A.5.2 General Results Achieved

In the preceding sections, a summary of some results of comparing this delay control method is used for the compensation for delays based on communication to the power control system in the collected works is exposed in Table A.7. Comparison between the thirteen verified response strategies described in the table above, considering the importance of numeracy, robustness, numeracy obtained, demonstration of reliance on a model of a wireless system, system security and various other findings of practicality as evidenced by the integrity of the use of the ETDC method and the MFAC method have shown the best results in different latencies that affect the amplitude and frequency of the whole system.

Compared to the stability index we find in Table A.11 and others who have prioritized displaying (W_c) values such as [114,115], so our critical indexes you see are good because they are smaller compared to the others mentioned above. Because their stability index (W_c) is so large that their safety is lower than ours we have a small index in various parts that have been considered in the IEEJ WEST 10-machine model. Much of the work has been done in the past to illustrate the impact of communication delays [19–21], on the results obtained based on the impact on the feedback controller. Controllers need to be able to cope with communication delays, and how to reduce the risk of adverse effects should be addressed accordingly. Finding the optimal time to slow down the upper boundaries to determine the stability of the power system, an example of the high response to the results we found that in the 50 ms and 300 ms ranges provide a clear performance leading to a stable stability index in each case. As you can see from the other studies we have done, it has been shown that the stability index we have shown above fuzzy you find gives less results than those who have used other methods as shown in this paper [92,102]. Comparisons with [17,81] have also been made in [65] and it has been shown that their chosen method provides the best system in the event of a communication delay compared to the other two. Thus, the major controller provided in [65] seems to be a choice that should be compared to Lyapunov based indirect method.

As it turns out, a large step was taken to address the effects of delays in the system as a new solution but did not provide a directional approach. The H_∞ -based WADC demonstrated good performance in short communication delays but insufficient resilience in high communication delays, which can destabilize the system. Then, with the advent of the Hybrid control system, there is a need to take into account the delays in addressing local and PSS systems and regional and WADC systems. However, the final performance of the low communication delay is not as good as the previous one. In addition, due to the slow communication, the performance of the system and the Hybrid system is still very dramatically. In the wide area environment, time delay occurs in terms of signal transmission and processing especially in the long run. It has been presented that even a short delay can have a detrimental effect on the stable performance of the power system. Therefore, it is very important to study the stability of the power system due to the delay.

As we have seen from the above, there are some solutions that we need to know that each system has to deal with delays in order to function properly. Some systems can withstand a delay of 50 msec while others can work with a delay of up to 300 msec. However, in the case of a power system considered in these tasks, if the delay is more than 500 msec, then the device overall performance deteriorates and the device turns into marginally stable. Therefore, the most allowable put off for the device is 500 msec. As a result, those delays might also additionally differ randomly in a positive range. Therefore, it's far important to estimate the most quantity of time put off referred to as the put off margin that the device should tolerate without turning into unstable. Such know-how at the put off margin (top certain with inside the time put off) could be useful with inside the controller layout for instances in which uncertainty with inside the put off is unavoidable.

Seeking help to ensure security and not forgetting about sections 2 and 3 and not forgetting the use of Smart Grid Technology (SGT) such as development and measurement, requires media infrastructure to enable two-way communication across all levels of electricity grid-generation, transmission, distribution and consumer mechanisms/ parts of the field. These communication requirements include latency, broadband, reliability, and security in order to exchange information and reduce signal delay. The open communication substructures along with Ethernet, the Internet, worldwide interoperability for microwave access (WiMax), and wireless fidelity (WiFi) are gradually being number of applied for smart grid communications. However, delays or loss of information may occur when sent. Therefore, the way out to reducing costs and increasing latency is one of the future directions of microgrid research. And there are some ways we mentioned above that can be used in the Section A.7 that can be used to prevent communication delays that affect the operation of the control system, which can reduce power loss and damage to equipment. Another possible concern is that there is a delay in communication and communication due to cyber-attacks that need to be addressed using tracking and response equipment, as well as vehicle analysis.

A.6 Smart Grids Face Challenges in Terms of Stability and Control

Tests for in-depth analysis of communication delays and loss have been exacerbated by various aspects, including stability evaluation and control of smart grids that have been briefed as detailed below.

Modeling methodologies: Due to the uncertainties introduced by the integration of communication technology and the power system, traditional deterministic modeling strategies used in electricity system analysis are no longer adequate for modeling the smart grid. It is critical to develop new modeling strategies for smart grid staleness analysis and management, such as event-based strategies, hybrid stochastic methods, probabilistic analysis strategies, and so on.

Control methodologies: As discussed in the preceding sections, communication delays networks, renewable energy sources, and security devices such as relays that appear in the stability and control of the smart grid. Deterministic control cannot ensure the overall stability of electricity dynamics. As a result, extensive research on control methods, as well as analytical approach and optimal control gain [50], a random model predictor control, and so on, is required.

Communication construction: since it necessitates the integration of numerous interconnections consisting of generation, transmission, and distribution based on wide-area control, it necessitates large bandwidths for data transmission and data collection. Furthermore, because a smart grid communication structure includes a wide area network (WAN), a neighborhood area network (NAN), and a home area network (HAN), these various network structures require the ability to bring together communications within each subarea and between specific areas.

Stages of simulation: Interaction between the communication network and the power grid is critical for smart grid control and operation. In addition, many important renewable energy sources, such as wind and PV, are linked to the grid via electronic power converters. These changes present two new challenges to network control: broadband pulse size modulation signals, various synchrophasor communication technologies between devices, and a plethora of switching devices. Large efforts should be made to increase simulation systems for intelligent grid research in order to better identify new controls and performance strategies for intelligent grids. Recently, real-time simulation platforms for intelligent grids have been mentioned [116].

A.7: Concluding Remarks and Future Potentials

This piece of paper shows a review of the analysis that leads to the effect of communication delay by controlling the performance and quality of the electricity grid. Various control methods for analyzing the impacts of network-induced delays on these communication based strategies are briefed and compared. Strategies that have been thought out and achieved should be shown to be

delayed by a continuous or irreversible delay, and that sudden delays are more difficult to solve than permanent delays. To reduce network latency due to delays, it has to imitate appropriate compensation plans that are designed to reduce or eliminate adverse effects on the functioning of the system. As we saw above in Table A.8 and Section A.6, it can be seen that the method has different capabilities in reducing delay, while all the above methods were appropriate for the linear system, only the stress-based, robust and incident-based methods can work on non-linear systems. Compensation plans, such as the revised ETDC & MFAC show the progress of research in reducing the various delays. Based on the problems described in Section 6 there is a quick way to reduce the various sudden delays that should be taken into account in the following areas:

- Communication network is a network of choice based on latency.
- Network control system issues are limited to online delays.
- Delay is considered to be between the sensor and the controller, between the controller and the actuator, and the combination of both delays;
- Imitation is done by delaying suddenness and suddenness.

In addition, it'll be exciting to reveal the effectiveness of the proposed techniques in case of a large electricity network such as no one else has ever done that leading up to the Rwanda National Grid project, in which the total harmonic distortion (THD) values may be large than 5%.

Author Contributions: Authorship must be limited to those who have contributed substantially to the work reported. Conceptualization, D.M., L.K.L. and B.B.M.; methodology, D.M., L.K.L. and B.B.M.; investigation, D.M., L.K.L. and B.B.M.; writing—original draft preparation, D.M.; writing—review and editing, D.M., L.K.L. and B.B.M.; supervision, L.K.L. and B.B.M.; funding acquisition, L.K.L. All authors have read and agreed to the published version of the manuscript.

Funding: This research is partially funded by African Centre of Excellence in Energy for Sustainable Development, University of Rwanda (Research Core Funding No. ACE II-017).

Acknowledgments: The first author would like to thank The African Center of Excellence in Energy for Sustainable Development (ACEESD), University of Rwanda (UR) for his support in this investigation. The second author appreciates the way it is presented to do more research and learn more in Department of Electrical & Communications Engineering, Moi University. The third author thanks the Department of Mechanical and Energy Engineering), University of Rwanda (UR) thanks to their support and strength the role of the successful system of knowledge and technology in short-term analysis.

Conflicts of Interest: The authors declare no conflict of interest.

Abbreviations

SDC	Supplementary Damping Controller
DD-WADC	Delay-Dependent-Wide Area Damping Control
DOF-WADC	Dynamic Output Feedback–Wide Area Damping Control
BA	Bat Algorithm
BESS	Battery Energy Storage Systems
DOFC	Dynamic Output Feedback Controller
POD	Oscillation Damping
MPM	Modified Predictor Method
POD	Oscillation Damping

References

[1] Ghosh, S; Ali, M. H. Minimization of Adverse Effects of Time Delay on Power Quality Enhancement in Hybrid Grid. *IEEE Syst.J.* **2019**, 13, 3091-3101. [CrossRef]

[2] Naduvathuparambil, B.; Valenti, M. C.; Feliachi A. Communication delays in wide area measurement systems. In Proceedings of the Annual Southeastern Symposium on System Theory, Huntsville, AL, USA, 9 March 2002. [CrossRef]

[3] Kumar, N.M.; Chand, A.A.; Malvoni, M.; Prasad, K.A.; Mamun, K.A.; Islam, F.; Chopra, S.S. Distributed energy resources and the application of AI, IOT, and blockchain in smart grids. *Energies*, **2020**, 13, 5739. https://doi.org/ 10.3390/en13215739. [CrossRef]

[4] Villamil, S.; Hernández, C.; Tarazona, G. An overview of internet of things. *Telkomnika Telecommunication Comput. Electron. Control.* **2020**, 18, 2320-2327. [CrossRef]

[5] Mondal, D.; Chakrabarti, A.; Sengupta, A. *Power System Small Signal Stability Analysis and Control;* Elsevier: Amsterdam, The Netherlands, 2020. [CrossRef]

[6] Patrick, I.O.; Chidolue, G.C, Protection and Control of Power System-a Review. *Int. J. Adv. Res. Technol.* 2014, 3, 158–166. [CrossRef]

[7] Markushevich, N. The benefits and challenges of the integrated volt/var optimization in the smart grid environment. in Proceedings of the IEEE Power and Energy Society General Meeting, Detroit, MI, USA, 24–28 July 2011; pp. 118–122. [CrossRef]

[8] Nguyen, T.; Wang, S.; Alhazmi, M.; Nazemi, M.; Estebsari, A.; Dehghanian, P. Electric Power Grid Resilience to Cyber Adversaries: State of the Art. *IEEE Access* **2020**, 8, 87592–87608. [CrossRef]

[9] Sufyan, M.A.A.; Zuhaib, M.; Rihan, M. An investigation on the application and challenges for wide area monitoring and control in smart grid. *Bull. Electr. Eng. Inform.* **2021**, *10*, 580 587. [CrossRef]

[10] Babu, B.; Ijyas, T.; P., M.; Varghese, J. Security issues in SCADA based industrial control systems. In Proceedings of the 2nd International Conference on Anti-Cyber Crimes, ICACC

2017, Abha, Saudi Arabia, 26–27 March 2017; pp. 47–51. [CrossRef]
[11] Khanna, M. *Communication Challenges for the FREEDM System*; Ph.D. Thesis, NC State University, Raleigh, NC, USA, 2009. [CrossRef]
[12] Wei, L.; Rondon, L.P.; Moghadasi, A.; Sarwat, A.I. Review of Cyber-Physical Attacks and Counter Defense Mechanisms for Advanced Metering Infrastructure in Smart Grid. In Proceedings of the IEEE Power Engineering Society Transmission and Distribution Conference, Denver, CO, USA, 16–19 April 2018. [CrossRef]
[13] Zhang, F.; Kodituwakku, H.A.D.E.; Hines, J.W.; Coble, J.B. Multilayer Data-Driven Cyber-Attack Detection System for Industrial Control Systems Based on Network, System, and Process Data. *IEEE Trans. Ind. Inform*. **2019**, 15, 4362–4369. [CrossRef]
[14] Lou, X.; Tran, C.; Tan, R.; Yau, D.K.Y.; Kalbarczyk, Z.T.; Banerjee, A.K.; Ganesh, P. Assessing and Mitigating Impact of Time Delay Attack: Case Studies for Power Grid Controls. *IEEE J. Sel. Areas Commun.* **2019**, *38*, 141–155. [CrossRef]
[15] Gao, B.; Shi, L. Modeling an Attack-Mitigation Dynamic Game-Theoretic Scheme for Security Vulnerability Analysis in a CyberPhysical Power System. *IEEE Access* ***2020***, 8, 30322–30331. [CrossRef]
[16] Yan, H.; Zhou, X.; Zhang, H.; Yang, F.; Wu, Z.-G. A Novel Sliding Mode Estimation for Microgrid Control With Communication Time Delays. *IEEE Trans. Smart Grid* **2019**, *10*, 1509–1520. [CrossRef]
[17] Ashfaque, A.H. Damping of Electromechanical Oscillations in Power Systems Using Wide Area Control Ashfaque Ahmed Hashmani. Ph.D. Thesis, University of Duisburg-Essen, Duisburg, Germany, 2020. [CrossRef]
[18] Guo, Y.; Zhang, L.; Zhao, J.; Wen, F.; Salam, A.; Mao, J.; Li, L. Networked Control of Electric Vehicles for Power System Frequency Regulation with Random Communication Time Delay. *Energies* **2017**, *10*, 621. [CrossRef]
[19] Heydari, R.; Khayat, Y.; Amiri, A.; Dragicevic, T.; Shafiee, Q.; Popovski, P.; Blaabjerg, F. Robust High-Rate Secondary Control of Microgrids with Mitigation of Communication Impairments. *IEEE Trans. Power Electron.* **2020**, *35*, 12486–12496. [CrossRef]
[20] Dias, J.A.; Serni, P.J.A.; Bueno, A.; Godoy, E. The study of communication between distributed generation devices in a smart grid environment. In *Networked Control Systems: Research Challenges and Advances for Application*; IEEE: New York, NY, USA, 2018. [CrossRef]
[21] Lv, X.; Sun, Y.; Hu, W.; Dinavahi, V. Robust load frequency control for networked power system with renewable energy via fractional-order global sliding mode control. *IET Renew. Power Gener.* **2021**, *15*, 1046–1057. [CrossRef]
[22] Wang, C.-C.; Qian, W.; Li, B.-F.; Zhao, Y. Stability analysis of wide area power system under the influence of interval timevarying delay. *Syst. Sci. Control Eng.* **2018**, *6*, 1–9. [CrossRef]
[23] Amraee, T.; Darebaghi, M.G.; Soroudi, A.; Keane, A. Probabilistic Under Frequency Load Shedding Considering RoCoF Relays of Distributed Generators. *IEEE Trans. Power Syst.*

2018, *33*, 3587–3598. [CrossRef]
[24] Lin, H.; Su, H.; Shu, Z.; Wu, Z.-G.; Xu, Y. Optimal Estimation in UDP-Like Networked Control Systems with Intermittent Inputs: Stability Analysis and Suboptimal Filter Design. *IEEE Trans. Autom. Control* **2015**, *61*, 1794–1809. [CrossRef]
[25] Alcaide-Moreno, B.A.; Fuerte-Esquivel, C.R.; Castro, L.M.; Zamora-Cárdenas, E.A. Generalized State Estimation of Flexible AC Power Systems Considering Wind Generators and Primary Frequency Control. *Electr. Power Components Syst.* **2015**, *43*, 1534–1547. [CrossRef]
[26] Mani, P.; Joo, Y.H. Fuzzy logic-based integral sliding mode control of multi-area power systems integrated with wind farms. *Inf. Sci.* **2021**, *545*, 153–169. [CrossRef]
[27] Zheng, A.; Huang, Q.; Cai, D.; Li, J.; Jing, S.; Hu, W.; Wu, J. Quantitative Assessment of Stochastic Property of Network-Induced Time Delay in Smart Substation Cyber Communications. *IEEE Trans. Smart Grid* **2020**, *11*; 2407–2416. [CrossRef]
[28] IEEE. *IEEE Guide for Synchronous Generator Modeling Practices and Parameter Verification with Applications in Power System Stability Analyses*; IEEE: New York, NY, USA, 2019. [CrossRef]
[29] Suyono, H.; Hasanah, R.N. Analysis of power losses due to distributed generation increase on distribution system. *J. Teknol.* **2016**, *78*. https://doi.org/10.11113/jt.v78.8923. [CrossRef]
[30] Gupta, B.B.; Akhtar, T. A survey on smart power grid: frameworks, tools, security issues, and solutions. *Ann. Telecommun.* **2017**, *72*, 517–549. [CrossRef]
[31] Sharma, C.; Tyagi, B. Fuzzy Type-2 Controller Design for Small-Signal Stability Considering Time Latencies and Uncertainties in PMU Measurements. *IEEE Syst. J.* **2017**, *11*, 1149–1160. [CrossRef]
[32] Gao, W.; Ye, H.; Liu, Y.; Wang, L.; Ci, W. Comparison of three stability analysis methods for delayed cyber-physical power system. In Proceedings of the China International Conference on Electricity Distribution, CICED, Xian, China, 10–13 August 2016. [CrossRef]
[33] Isa, A.I.M.; Mohamad, H.; Naidu, K.; Dahlan, N.Y.; Musirin, I. Method of determining load priority using fuzzy logic for adaptive under frequency load shedding technique. *Pertanika J. Sci. Technol.* **2017**, *25*, 239–247. [CrossRef]
[34] Zhang, D.; Han, Q.-L.; Jia, X. Network-Based Output Tracking Control for a Class of T-S Fuzzy Systems That Can Not Be Stabilized by Nondelayed Output Feedback Controllers. *IEEE Trans. Cybern.* **2014**, *45*, 1511–1524. [CrossRef]
[35] Truong, D.Q.; Ahn, K.K. Robust Variable Sampling Period Control for Networked Control Systems. *IEEE Trans. Ind. Electron.* **2015**, *62*, 5630–5643. [CrossRef]
[36] Zhang, X.-M.; Han, Q.-L. A Decentralized Event-Triggered Dissipative Control Scheme for Systems with Multiple Sensors to Sample the System Outputs. *IEEE Trans. Cybern.* **2015**, *46*, 2745–2757. [CrossRef]
[37] Tavassoli, B.; Amraee, T.; Amanzadeh, M. Design and evaluation of distributed networked

control for a dual-machine power system. In Proceedings of the 25th Iranian Conference on Electrical Engineering, ICEE, Tehran, Iran, 2–4 May 2017. [CrossRef]
[38] Ge, X.; Yang, F.; Han, Q.-L. Distributed networked control systems: A brief overview. *Inf. Sci.* **2017**, *380*, 117–131. [CrossRef]
[39] Gautam, M.; Pati, A.; Mishra, S.; Appasani, B.; Kabalci, E.; Bizon, N.; Thounthong, P. A Comprehensive Review of the Evolution of Networked Control System Technology and Its Future Potentials. *Sustainability* **2021**, *13*, 2962. [CrossRef]
[40] Liu, K.; Fridman, E.; Johansson, K.H. Dynamic quantization of uncertain linear networked control systems. *Automatica* **2015**, *59*, 248–255. [CrossRef]
[41] Zhang, X.-M.; Han, Q.-L.; Yu, X. Survey on Recent Advances in Networked Control Systems. *IEEE Trans. Ind. Informatics* **2016**, *12*, 1740–1752. [CrossRef]
[42] Chen, H.; Gao, J.; Shi, T.; Lu, R. H ∞ control for networked control systems with time delay, data packet dropout and disorder. *Neurocomputing* **2016**, *179*, 211–218. [CrossRef]
[43] Freirich, D.; Fridman, E. Decentralized networked control of systems with local networks: A time-delay approach. *Automatica.* **2016**, *69*, 201–209. [CrossRef]
[44] Lu, R.; Xu, Y.; Zhang, R. A New Design of Model Predictive Tracking Control for Networked Control System Under Random Packet Loss and Uncertainties. *IEEE Trans. Ind. Electron.* **2016**, *63*, 6999–7007. [CrossRef]
[45] Todescato, M.; Carli, R.; Schenato, L.; Barchi, G. Smart Grid State Estimation with PMUs Time Synchronization Errors. *Energies* **2020**, *13*, 5148. [CrossRef]
[46] Liu, X.; Yu, X.; Ma, G.; Xi, H. On sliding mode control for networked control systems with semi-Markovian switching and random sensor delays. *Inf. Sci.* **2016**, *337–338*, 44–58. [CrossRef]
[47] Peng, C.; Han, Q.-L. On Designing a Novel Self-Triggered Sampling Scheme for Networked Control Systems with Data Losses and Communication Delays. *IEEE Trans. Ind. Electron.* **2015**, *63*, 1239–1248. [CrossRef]
[48] Li, M.; Chen, Y. Robust Adaptive Sliding Mode Control for Switched Networked Control Systems with Disturbance and Faults. *IEEE Trans. Ind. Inform.* **2018**, *15*, 193–204. [CrossRef]
[49] Wei, Y.; Qiu, J.; Shi, P.; Wu, L. A Piecewise-Markovian Lyapunov Approach to Reliable Output Feedback Control for FuzzyAffine Systems with Time-Delays and Actuator Faults. *IEEE Trans. Cybern.* **2017**, *48*, 2723–2735. [CrossRef]
[50] Sun, Y.C.; Yang, G.H. Event-triggered state estimation for networked control systems with lossy network communication. *Inf. Sci.* **2019**, *492*, 1–12. [CrossRef]
[51] Ding, D.; Han, Q.-L.; Wang, Z.; Ge, X. A Survey on Model-Based Distributed Control and Filtering for Industrial Cyber-Physical Systems. *IEEE Trans. Ind. Inform.* **2019**, *15*, 2483–2499. [CrossRef]
[52] Bento, M.E.C. An optimization approach for the wide-area damping control design. In Proceedings of the 13th IEEE International Conference on Industry Applications, INDUSCON, Sao Paulo, Brazil, 12–14 November 2018; pp. 269–276. [CrossRef]

[53] Yi, X.; Yang, T.; Wu, J.; Johansson, K.H. Distributed event-triggered control for global consensus of multi-agent systems with input saturation. *Automatica* **2019**, *100*, 1–9. [CrossRef]
[54] Liu, S.; Wang, X.; Liu, P.X. Impact of Communication Delays on Secondary Frequency Control in an Islanded Microgrid. *IEEE Trans. Ind. Electron.* **2015**, *62*, 2021–2031. [CrossRef]
[55] Ahumada, C.; Cardenas, R.; Saez, D.; Guerrero, J. Secondary Control Strategies for Frequency Restoration in Islanded Microgrids with Consideration of Communication Delays. *IEEE Trans. Smart Grid* **2016**, *7*, 1430–1441. [CrossRef]
[56] Liu, K.-Z.; Sun, X.-M.; Teel, A.R.; Liu, J. Stability analysis for networked control systems with sampling, transmission protocols and input delays. *Nonlinear Anal. Hybrid Syst.* **2021**, *39*, 100974. [CrossRef]
[57] Liu, Y.-A.; Tang, S.; Liu, Y.; Kong, Q.; Wang, J. Extended dissipative sliding mode control for nonlinear networked control systems via event-triggered mechanism with random uncertain measurement. *Appl. Math. Comput.* **2021**, *396*, 125901. [CrossRef]
[58] Fang, F.; Ding, H.; Liu, Y.; Park, J.H. Fault tolerant sampled-data H∞ control for networked control systems with probabilistic time-varying delay. *Inf. Sci.* **2021**, *544*, 395–414. [CrossRef]
[59] Shi, X.; Cao, Y.; Shahidehpour, M.; Li, Y.; Wu, X.; Li, Z. Data-Driven Wide-Area Model-Free Adaptive Damping Control with Communication Delays for Wind Farm. *IEEE Trans. Smart Grid* **2020**, *11*, 5062–5071. [CrossRef]
[60] Guo, Z.; Gong, S.; Wen, S.; Huang, T. Event-Based Synchronization Control for Memristive Neural Networks with Time-Varying Delay. *IEEE Trans. Cybern.* 2019, 49, 3268–3277. [CrossRef]
[61] Beiraghi, M.; Ranjbar, A.M. Adaptive Delay Compensator for the Robust Wide-Area Damping Controller Design. *IEEE Trans. Power Syst.* **2016**, *31*, 4966–4976. [CrossRef]
[62] Molina-Cabrera, A.; Ríos, M.A.; Besanger, Y.; Hadjsaid, N.; Montoya, O.D. Latencies in power systems: A database-based timedelay compensation for memory controllers. *Electronics* **2021**, *10*, 208. [CrossRef]
[63] Quanyuan, J.; Zhenyu, Z.; Yijia, C. Wide-area TCSC controller design in consideration of feedback signals' time delays. In Proceedings of the IEEE Power Engineering Society General Meeting, San Francisco, CA, USA, 16 June 2005; Volume 2. [CrossRef]
[64] Zhao, Y.B.; Sun, X.M.; Zhang, J.; Shi, P. Networked Control Systems: The Communication Basics and Control Methodologies. *Math. Probl. Eng.* **2015**, *2015*. https://doi.org/10.1155/2015/639793. [CrossRef]
[65] Haghighi, P.; Tavassoli, B. Robust H∞ output feedback design for networked control systems with partially known delay probabilities. *Optim. Control Appl. Methods* **2020**, *41*, 1052–1067. [CrossRef]
[66] Abbasspour, A.; Sargolzaei, A.; Victorio, M.; Khoshavi, N. A Neural Network-based Approach for Detection of Time Delay Switch Attack on Networked Control Systems.

Procedia Comput. Sci. **2020**, *168*, 279–288. [CrossRef]
[67] Luo, H.; Hu, Z. Stability Analysis of Sampled-Data Load Frequency Control Systems with Multiple Delays. *IEEE Trans. Control Syst. Technol.* **2021**, *30*, 434–442. [CrossRef]
[68] Islam, S.; El Saddik, A.; Sunda-Meya, A. Robust load frequency control for smart power grid over open distributed communication network with uncertainty. In Proceedings of the IEEE International Conference on Systems, Man and Cybernetics, Bari, Italy, 6–9 October 2019; pp. 4341–4346. [CrossRef]
[69] Bento, M.E.C.; Kuiava, R.; Ramos, R.A. Design of Wide-Area Damping Controllers Incorporating Resiliency to Permanent Failure of Remote Communication Links. *J. Control. Autom. Electr. Syst.* **2018**, *29*, 541–550. [CrossRef]
[70] Liu, S.; Liu, P.X.; Wang, X. Stability analysis and compensation of network-induced delays in communication-based power system control: A survey. *ISA Trans.* **2017**, *66*, 143–153. [CrossRef]
[71] Wang, S.; Ou, X.; Li, D.; Wang, H.; Zhu, G. K-Filter Observer Based Adaptive Quantized Decentralized Excitation Control for Multi-Machine Power Systems with the Line Transmission Delays. *IEEE Access* **2021**, *9*, 51355–51367. [CrossRef]
[72] Chae, S.; Huang, D.; Nguang, S.K. Robust partially mode delay-dependent H∞ output feedback control of discrete-time networked control systems. *Asian J. Control* **2014**, *16*, 1764–1773. [CrossRef]
[73] Yin, X.; Wang, W.; Lam, H.K. Fuzzy logic wide-area damping control with delay compensation for power system. *Xi Tong Gong Cheng Yu Dian Zi Ji Shu/Systems Eng. Electron.* **2019**, *41*, 2343–2351. [CrossRef]
[74] Soleymani, M.; Abolmasoumi, A.H.; Bahrami, H.; Khalatbari-S, A.; Khoshbin, E.; Sayahi, S. Modified sliding mode control of a seismic active mass damper system considering model uncertainties and input time delay. *J. Vib. Control* **2018**, *24*, 1051–1064. [CrossRef]
[75] Zhu, Q.; Jiang, L.; Yao, W.; Zhang, C.-K.; Luo, C. Robust Load Frequency Control with Dynamic Demand Response for Deregulated Power Systems Considering Communication Delays. *Electr. Power Components Syst.* **2016**, *45*, 75–87. [CrossRef]
[76] Dotoli, M.; Fay, A.; Miśkowicz, M.; Seatzu, C. An overview of current technologies and emerging trends in factory automation. *Int. J. Prod. Res.* **2019**, *57*, 1–21.
[77] Mo, H.; Sansavini, G. Hidden Markov model-based smith predictor for the mitigation of the impact of communication delays in wide-area power systems. *Appl. Math. Model.* **2021**, *89*, 19–48. [CrossRef]
[78] Bhadu, M.; Senroy, N.; Kar, I.N.; Sudha, G.N. Robust linear quadratic Gaussian-based discrete mode wide area power system damping controller. *IET Gener. Transm. Distrib.* **2016**, *10*, 1470–1478. [CrossRef]
[79] Bhattarai, B.; Marinovici, L.; Touhiduzzaman; Tuffner, F.K.; Schneider, K.P.; Xie, J.; Mana, P.T.; Du, W.; Fisher, A. Studying impacts of communication system performance on dynamic stability of networked microgrid. *IET Smart Grid* **2020**, *3*, 667–676. [CrossRef]
[80] León, H.; Montez, C.; Valle, O.; Vasques, F. Real-Time Analysis of Time-Critical

Messages in IEC 61850 Electrical Substation Communication Systems. *Energies* **2019**, *12*, 2272. [CrossRef]
[81] Jin, L.; Zhang, C.-K.; He, Y.; Jiang, L.; Wu, M. Delay-Dependent Stability Analysis of Multi-Area Load Frequency Control with Enhanced Accuracy and Computation Efficiency. *IEEE Trans. Power Syst.* **2019**, *34*, 3687–3696. [CrossRef]
[82] Zhang, L. ; Shi, Y.; Chen, T.; Huang, B. A new method for stabilization of networked control systems with random delays. *IEEE Trans. Automat. Contr.* **2005**, 50, 1177-1181. [CrossRef]
[83] Darabian, M.; Ashouri, A.; Bagheri, A. Hierarchical damping controller design in large-scale power systems including hybrid renewable energy sources for compensation of time delays. *Int. Trans. Electr. Energy Syst.* **2020**, *30*, e12362. [CrossRef]
[84] Ali, M.H.; Dasgupta, D. Effects of communication delays in electric grid. In Proceedings of the Future of Instrumentation International Workshop, FIIW, Oak Ridge, TN, USA, 7–8 November 2011; pp. 38–41. [CrossRef]
[85] Klaimi, J.; Rahim-Amoud, R.; Merghem-Boulahia, L.; Jrad, A. A novel loss-based energy management approach for smart grids using multi-agent systems and intelligent storage systems. *Sustain. Cities Soc.* **2018**, *39*, 344–357. [CrossRef]
[86] Wang, B.; Tang, Z.; Liu, W.; Zhang, Q. A Distributed Cooperative Control Strategy of Offshore Wind Turbine Groups with Input Time Delay. *Sustainability* **2020**, *12*, 3032. [CrossRef]
[87] Wang, Y.; Yu, S. An improved dynamic quantization scheme for uncertain linear networked control systems. *Automatica*, **2018**, 92, 244–248. [CrossRef]
[88] Nan, J.; Yao, W.; Wen, J.; Peng, Y.; Fang, J.; Ai, X.; Wen, J. Wide-area power oscillation damper for DFIG-based wind farm with communication delay and packet dropout compensation. *Int. J. Electr. Power Energy Syst.* **2021**, *124*, 106306. [CrossRef]
[89] Zhong, Z.; Zhu, Y.; Lin, C.-M.; Huang, T. A fuzzy control framework for interconnected nonlinear power networks under TDS attack: Estimation and compensation. *J. Frankl. Inst.* **2021**, *358*, 74–88. [CrossRef]
[90] Yilmaz, M.; Adediran, S.A.; McLauchlan, L. Hydro plant network control LPV framework. In Proceedings of the IEEE International Conference on Systems, Man and Cybernetics, San Diego, CA, USA, 5–8 October 2014.
[91] Cheng, L. Research on remote monitoring of smart power grid using wireless sensor network. *Int. J. Mechatronics Appl. Mech.* **2020**, *1*, 243–249. [CrossRef]
[92] Singh, V.P.; Kishor, N.; Samuel, P. Communication time delay estimation for load frequency control in two-area power system. *Ad Hoc Networks* **2016**, *41*, 69–85. [CrossRef]
[93] Sönmez, Ş.; Ayasun, S.; Eminoglu, U. Computation of Time Delay Margins for Stability of a Single-Area Load Frequency Control System with Communication Delays. *WSEAS Trans. Power Syst.* **2014**, *9*, 67–76. [CrossRef]
[94] Wang, S.; Wang, Z. Sliding Mode Dynamic Surface Control for Multi-Machine Power Systems with Time Delays and DeadZones. *Cybern. Syst.* **2021**, *52*, 58–72. [CrossRef]

[95] Katipoglu, D.; Sonmez, S.; Ayasun, S. Stability Delay Margin Computation of Load Frequency Control System with Demand Response. In Proceedings of the IEEE 1st Global Power, Energy and Communication Conference, GPECOM, Nevsehir, Turkey, 12–15 June 2019; pp. 473–478. [CrossRef]
[96] Liu, F.; Yan, W.; Wu, M. Wide-area signals time-delay STATCOM additional damping control for power system. In *Power and Energy, Proceedings of the International Conference on Power and Energy, CPE, Shanghai, China, 29–30 November 2014*; CRC Press: Boca Raton, FL, USA, 2015; pp. 371–374. [CrossRef]
[97] Chen, B.Y.; Shangguan, X.C.; Jin, L.; Li D.Y. An improved stability criterion for load frequency control of power systems with time-varying delays. *Energies* **2020**,13, 2101. [CrossRef]
[98] Yang, B.; Sun, Y. A Novel Approach to Calculate Damping Factor Based Delay Margin for Wide Area Damping Control. *IEEE Trans. Power Syst.* **2014**, *29*, 3116–3117. [CrossRef]
[99] Aslam, M.S.; Dai, X. H ∞ Control for Network T-S Fuzzy Systems under Time Varying Delay for Multi-area Power Systems. *Int. J. Control. Autom. Syst.* **2020**, *18*, 2774–2787. [CrossRef]
[100] Wu, Y.; Wu, Y.; Guo, L. Stochastic stabilizing control of networked control system with Markovian parameters. In *Lecture Notes in Electrical Engineering*; Springer: Cham, Switzerland, 2014; Volume 237. [CrossRef]
[101] Zheng, S.; Shi, P.; Wang, S.; Shi, Y. Adaptive Robust Control for Stochastic Systems with Unknown Interconnections. *IEEE Trans. Fuzzy Syst.* **2021**, 29, 1008–1022. [CrossRef]
[102] Zhong, Z.; Lin, C.-M.; Shao, Z.; Xu, M. Decentralized Event-Triggered Control for Large-Scale Networked Fuzzy Systems. *IEEE Trans. Fuzzy Syst.* **2018**, *26*, 29–45. [CrossRef]
[103] Zhang, R.; Zeng, D.; Park, J. H.; Lam, H. K.; Xie, X. Fuzzy Sampled-Data Control for Synchronization of T-S Fuzzy ReactionDiffusion Neural Networks with Additive Time-Varying Delays. *IEEE Trans. Cybern.* **2021**, 51, 2384–2397. [CrossRef]
[104] Dinh, T.Q.; Ahn, K.K.; Marco, J. A Novel Robust Predictive Control System Over Imperfect Networks. *IEEE Trans. Ind. Electron.* **2016**, *64*, 1751–1761. [CrossRef]
[105] Liu, M.; Dassios, I.; Tzounas, G.; Milano, F. Stability Analysis of Power Systems with Inclusion of Realistic-Modeling WAMS Delays. *IEEE Trans. Power Syst.* **2018**, *34*, 627–636. [CrossRef]
[106] Zhang, S.; Vittal, V. Design of Wide-Area Power System Damping Controllers Resilient to Communication Failures. *IEEE Trans. Power Syst.* **2013**, *28*, 4292–4300. [CrossRef]
[107] Li, Y.; Zhou, Y.; Liu, F.; Cao, Y.; Rehtanz, C. Design and Implementation of Delay-Dependent Wide-Area Damping Control for Stability Enhancement of Power Systems. *IEEE Trans. Smart Grid* **2016**, *8*, 1831–1842. [CrossRef]
[108] Setiadi, H.; Mithulananthan, N.; Shah, R.; Lee, K.Y.; Krismanto, A.U. Resilient wide-area multi-mode controller design based on Bat algorithm for power systems with renewable power generation and battery energy storage systems. *IET Gener. Transm. Distrib.* **2019**, *13*, 1884–1894. [CrossRef]

[109] Sun, M.; Guo, Y.; Song, S. The Delay-Dependent DOFC for Damping Inter-Area Low-Frequency Oscillations in an Interconnected Power System Considering Packet Loss of Wide-Area Signals. *Energies* **2021**, *14*, 5892. [CrossRef]
[110] Driankov, D. *An Introduction to Fuzzy Control*, 2nd ed.; Springer: Berlin, Germany, 1993. [CrossRef]
[111] Ali, M.H.; Wu, B.; Tamura, J.; Dougal, R.A. Minimization of shaft oscillations by fuzzy controlled SMES considering time delay. *Electr. Power Syst. Res.* **2009**, *80*, 770–777. [CrossRef]
[112] Mentesidi, K.; Garde, R.; Aguado, M.; Rikos, E. Implementation of a fuzzy logic controller for virtual inertia emulation. In Proceedings of the International Symposium on Smart Electric Distribution Systems and Technologies, EDST, Vienna, Austria, 8–11 September 2015. [CrossRef]
[113] IEC. *61850: Communication Networks and Systems in Substations*; IEC: Geneva, Switzerland, 2003; Volume 3. [CrossRef]
[114] Ali, H.; Dasgupta, D. Effects of time delays in the electric power grid. In *IFIP Advances in Information and Communication Technology*; Springer: Cham, Switzerland, 2012, Volume 390, pp. 139–154. [CrossRef]
[115] Ali, M.; Murata, T.; Tamura, J. Effect of Coordination of Optimal Reclosing and Fuzzy Controlled Braking Resistor on Transient Stability During Unsuccessful Reclosing. *IEEE Trans. Power Syst.* **2006**, *21*, 1321-1330. [CrossRef]
[116] Azeroual, M.; Lamhamdi, T.; El Moussaoui, H.; El Markhi, H. Simulation tools for a smart grid and energy management for microgrid with wind power using multi-agent system. *Wind Eng.* **2020**, *44*, 661–672. [CrossRef]

Paper B

Title:	Under-frequency Load Shedding on the Performance Time Delay Relays of Transmission lines with difference Controllers.
Authors:	Darius Muyizere[1*], Lawrence K. Letting [1,2] and Bernard B. Munyazikwiye[1,3]
Affiliation:	[1] African Centre of Excellence in Energy and Sustainable Development, College of Science and Technology, University of Rwanda, KN 67 Street Nyarugenge, Kigali P.O. Box 3900, Rwanda [2] Department of Electrical & Communications Engineering, Moi University, Eldoret 30100, Kenya [3] Department of Mechanical and Energy Engineering, College of Science and Technology, University of Rwanda, KN 67 Street Nyarugenge, Kigali P.O. Box 3900, Rwanda
Article:	2021 IEEE Southern Power Electronics Conference (SPEC) https://doi.org/10.1109/SPEC52827.2021.9709464
Copyright ©:	**IEEE**
Layout:	The format of the paper has already been altered to match that of the thesis.

Paper B: **Under-frequency Load Shedding on the Performance Time Delay Relays of Transmission lines with difference Controllers.**

***Abstract* — This paper analyses the load shedding methods for the impact of communication delays. Therefore, the research investigates the impacts and effects of communication networks in the grid systems which might cause imperfections such as delays and noise among others related to relays. The model of the power system and the design of the controllers are done using Simulink, the Matlab software. The controllers are designed to output power imbalance based on frequency deviation during various systems under frequency conditions. They also shed loads continuously until the frequency is restored within the safe operating range. Different cases of the system under frequency are used to analyze the performance of the grasshopper optimization algorithm (GOA) proposal based on under-frequency load Shedding UFLS, a comparison with Traditional and particle swarm optimization (PSO). UFLS is performed due to various disturbances. It has been found that a GOA method provides excellent communication networks and reduces the size of the load is shed. Moreover, and what's more, GOA achieves the fastest solution we've ever used in IEEE 14 Bus system.**

***Keywords*:** Load shedding, communication delays, impacts, effects, controllers.

B.1 Introduction

The smart system, which includes the use of modern computer tools in the direction of operate and control grid or load management systems in the event of a power disturbance, are considered to be the main part of the technology of the smart grids. As a consequence, the concept of a smart grid is used to combine renewable energy resources, understanding and sorting out special moments, state comparisons, load organization, commitment and efficiency.

Grid safety is reflected to be a major issue among smart grid barriers, especially for generation and load. However, certain types of disturbances cause uncertainty in the safety of load management. The most significant constraint to take into explanation for the smart grid model is the security of the electrical system. The highest objective of system security is to eliminate system disruption and to achieve the stability of the power system. The instability on the side of the load poses a serious threat to the security of the electrical system. Some of the most important methods to connect the load side with the delivery system in the event of a disturbance is load shedding (LS). The highest indication of LS is to select and stop unnecessary loads in the event of a disturbance. This activity will help the scheme restore calm with a quick response and will avoid a total failure of the power system load or needing to design a new level of power system load network which can be equipped with a generation of a power supply system after a disturbance. For this reason, LS is considered a fast and reliable solution to maintain the security and stability of the system.

LS continues in accordance with at least one of the two methods used to attain the goal of load management. The first method is used to avoid the breakdown of busbar voltage and is branded as under-voltage load shedding (UVLS). The second method is used to regulator the frequency by changing its assessment to keep the frequency close to the power system and avoid it from all of a sudden decreasing. This method is known as Under Frequency Load Shedding (UFLS) [1].

The multi-stage UFLS is reviewed to be the last step to restore energy equal to extreme frequency drip. The UFLS learning method aims to establish a UFLS relays, which is modified through the operation of non-linear dynamics simulations. Many UFLS structures are required under full load in the in electrical networks. These practice is established in a variability of ways such as traditional, adaptive and intelligence [2]. UFLS performs better than UVLS. This conclusion is based on the assumption that the voltage does not change in the power system grid. This unstable state can be achieved in normal operation without butt in the grid power supply. Therefore, this voltage fluctuation can lead to illegal activities in UVLS techniques [3].

The criteria to be considered for the relay parts shown during the online imitation are the number and magnitude of the LS step, position delay, and the frequency threshold each step [4]. The amount and step size of LS have a major impact on the reliability and safety of the electrical system. If stable and large quantities are taken into account for all predicted disturbances, then LS is no longer needed. Therefore, the amount and step size of the LS should be vary at each stage, depending on the type and severity of the disorder.

Delay time and frequency for each phase are the main criteria for the proper design of the UFLS relay. Each delay and each frequency take an important impact on relay performance, especially in large-scale disturbances that have need of a quick response. The significance of the idea is that in the event of a major disturbance, the sudden decrease in frequency will cause a lot of stress to the turbine blades, resulting in severe loss to the blades.

As inequality usually exists in a powerful and everevolving system. Inequalities in power output result in severe disruption of the grid system. The cracking system is used to reduce the problem of extreme inequalities in the system, which can result in dark or unstable systems. In this way, buses are taken to solve problems where those with high-speed accidents are given the first priority to reduce loads. Many methods have been put in place to reduce network interruptions that slow communication in a given system. Some researchers identified some strategies known as the artificial neural networks (ANN) and the provisional analysis as found in [2]. Some other researchers have shown two ways to reduce the amount of stress that can occur at different times. They testified that ANN controls all fertility, frequency of damage, and all requirements along with decay. The Particle Swarm technique (PSO) can be used to reduce UFLS problems in cases without considering time delay [5]. An intelligent UFLS gradient frequency method using fuzzy logic (FL) was investigated in [6], in which the authors concluded that the FL deviates from the optimal number of loads shed if the prior system knowledge required by the membership parameters is insufficient.

Therefore, the genetic algorithm (GA) is more effective and applicable in power systems in establishing the real cause of communication delays in power systems. Understanding the issues is an important approach to solving several issues that are related to power delays. Moreover, the advanced methods also utilize modern technologies such as GOA in establishing the causes of delays in electric power systems and proposing possible solutions.

The grasshopper optimization algorithm (GOA) is one of the newest optimization algorithms, proposed in [7], and is a more efficient algorithm than GAs and PSO for solving multiobjective optimization problems. GOA has been applied in solving many electrical power system engineering problems, such as optimal compensator allocation [8], optimal distributed generation placement, and load forecasting. These constraints include the allowable LS percentage, line flow limits, number of LS stages and time delay of each stage. The proposed approach overcomes the disadvantages of the PSO method while achieving a faster converging solution. The proposed method is tested using two standard power systems: the IEEE 14-bus systems.

The rest of this page is organized as follows. Section B.II describes the model and its construction in the event of a communication delay in the transmission area. This special Section B.III summarizes the Grasshopper Optimization Algorithm used to solve the UFLS problem. Section B.IV describes the distribution of UFLS Algorithms. System Statement is shown in Section B.V. The results indicate delays on the IEEE 14 bus and discussing some possible consequences in section B.VI. Then, the papers are completed in Section B.VII.

B.2 Model for UFLS parameters identification and formulation

UFLS relay parameters have needed the delay time and frequency threshold of each phase of the disturbance step to fix the number of loads that should be shed, and the magnitude suspended for each phase of the disturbance. And so, the most important first phase in this strategy is to get hold of a mathematical model for each frequency limit and communication delay in setting. This adaptive method for analyzing a calculated equation for each parameter of the UFLS relay has the advantage of using GOA techniques to achieve load management by optimum required LS and increasing the lowest oscillation frequency.

The overload ratio or excessive load, L_{oi} along with the rate of change over time, F_{ci} is the main items are used as indicators of volatility, where they indicate the number of categories. The extreme figure is the direction of the load and the system of equal force. This ratio is the percentage of between excess and remaining energy and can be calculated by [9].

$$L_{oi} = \frac{\sum P_{Li} - \sum P_{Gi}}{\sum P_{Gi}} \tag{1}$$

Where P_{Li} is the increase in energy efficiency and the decrease in generation efficiency. The balance F_{ci} is provided by

$$F_{ci} = \frac{F_{i+1} - F_i}{t_{1+1} - t_i} \tag{2}$$

Where F_i, F_{i+1}, t_i and t_{i+1} are the frequencies and activation times at stages i and $i + 1$.

$$F_{ci} = \frac{pf \times L_{oi}}{H_i} \frac{F_{i+1} - F_i}{1 - \frac{F_{i+1}}{F_1^2}} \tag{3}$$

Where pf and H_i are the power factor and inertia for a long time, respectively.

F_{ci} tin can be used to judge types of disturbance such as large or small disturbance, represented by from above and below of F_{ci}, respectively [7].

$$H_{sys} = \frac{H_1 S_1 + H_2 S_2 + \cdots + H_n S_n}{S_1 + S_2 + \cdots + S_n} \tag{4}$$

Where s is the apparent power in MVA for n generators.

The percentage of LS,$\propto$ is given by

$$\propto_i = -F_{ci} \times \frac{2H_{syss_i}}{F_{nt}} \tag{5}$$

Where F_{nt} is a regular occurrence of the system.
The amount of energy to be shed, P_{LS_i} in MW at each class is provided by

$$P_{LS_i} = P_{Lt_i} \times \propto_i \tag{6}$$

Where P_{Lt_i} is a full load for each stage before performing an LS. After shedding the load at the level, the remaining load can be found by subtracting the fractured amount P_{LS_i}, from the total load before shedding P_{LS_i}, now the new value of the total load Z for each phase can be designed by

$$P_{Ln_i} = P_{Lt_i} - P_{LS_i} \tag{7}$$

The frequency difference between the two consecutive LS segments is given by

$$\Delta F_i = F_i - F_{i+1} \tag{8}$$

When the frequency is identified by the UFLS transmission relay, it sends a series of warnings about breaking down the barriers. However, the delay time found in such activities is called the decay time,t_{d_i}. The decay time,t_{d_i} is given by

$$t_{d_i} = \frac{\Delta F_i}{F_{ci}} \tag{9}$$

Reducing the delay time improves the performance of the system and increases the efficiency. As has been shown in various studies such as X. Xiong and W. Li it has been shown that other delays in time result from the work of the circular mechanics. The relationship separation requires a certain period of time that may be longer than a sequence. This delay usually results from the above rot times. Delays in delays usually vary depending on the level of confusion. Travel time is provided by

$$t_t = \frac{N}{D_N} \tag{10}$$

Where N compares the number of circles to D_N indicates the number of times a circle is rotated. During round trips, the number of times it travels, F_t due to slow travel may be available from

$$F_t = t_t \times F_{ci} \tag{11}$$

The F_t frequency eventually reduces the number of times in the $(i + 1)$ level,

$$F_{i+1_{Mod.}} = F_{i+1} - F_t \tag{12}$$

Frequency variation must be adjusted to reduce deceleration over time.

$$\Delta F_{i_{Mod.}} = F_i - F_{i+1_{Mod.}} \tag{13}$$

Decay time during travel must also be updated to calculate the time delay for machines such as the following:

$$t_{d_{i_{Mod.}}} = \frac{\Delta F_{i_{Mod.}}}{F_{ci}} \tag{14}$$

The next level should now be updated as follows

$$F_{si} = F_{i+1_{Mod.}} - \delta \tag{15}$$

This is where F_{si} was established several times after the second phase of LS and δ with a safety margin, which is considered to protect the turbine from stress and efficiency [11]. Load reduction coefficient R_{co_i} according to the excessive rate and setting the possible frequency counted from

$$F_{si} = F_{i+1_{Mod.}} - \delta \tag{16}$$

Where L_{o_0} is the beginning of the overload ratio and $F_{s_0}$is the original frequency. As it turned out, the R_{co_i} can also be described as a ratio between the load power and the frequency.R_{co_i} can also be represented as the ratio of load power to frequency by the equation

$$R_{co_i} = \frac{\left(1 - \frac{P_{Li}}{P_{LO}}\right)}{\left(1 - \frac{F_{s_i}}{F_{s_O}}\right)} \tag{17}$$

Where P_{LO} is the primary load power, Knowing the R_{co_i}, the minimum allowable frequency, called swing frequency, F_{swing} can be calculated from the following equation:

$$F_{swing} = F_{s_0}\left(1 - \frac{L_{o_0}}{R_{co_i} \times \left(1 + L_{o_0}\right)}\right) \tag{18}$$

Now, the problem with UFLS is the small increase in swing frequency, F_{swing} and reduction the amount of loads shed, P_{LS_i} and the number of loads shed. Therefore, practical activities, F_{obj}, the statistical model required to solve the UFLS problem, should have two barriers to multiplication and reduction in the best way to compare. A large action can be taken as 1 / a reduction function, so that both barriers can be listed in the so-called practical activities such as the following:

$$F_{obj} = Min\left[R_1 \times U\left(P_L, P_G, P_{t,} t_{t,} t_{d,} \propto, \beta\right) + R_2 \times \frac{1}{V(P_L, P_G, P_t, t_d, \propto, \beta)}\right] \tag{19}$$

Where U represents the work of reducing LS and V shows the performance of multiplication low swing frequency. R_1 and R_2 show heavy loads for each activity. Both functions are described in terms of the load active of the P_L power, the P_G power generation, the P_t border transmission line, the flow time t_t, time delay t_d, percentage of LS $\propto$, and a valid number of LS categories β.

All pre-operative words have a finite and indefinite purpose exceeded. The main goal of the metaheuristic optimization algorithm is to achieve the goal performance and real and fast response and how you can identify the various effects in the system when there is a delay in communication delay in security management.

B.3 Optimization framework

This section is dedicated to providing a brief overview of the integration of the Grasshopper Optimization Algorithm used to solve the UFLS problem. In addition, the best way to develop is to develop calculating the best UFLS program, which consists mainly of GOA, PSO and ANN are accurate and reliable optimization techniques. It is used to reduce the size of the load is broken and reduces the number of times the swing of the power system. PSO and GA asked to improve the UFLS [12]. But the literature is about the application of the GOA of UFLS is missing.

Many parts inspired by algorithms have to go through two main tasks: research and use. In the process of research, selected candidates are treated as a sudden change of position, while in the way they are used, they move.

These two common ways of behaving are grasshopper analysed and compared to achieve a successful algorithm called "grasshopper's optimization algorithm (GOA)"in [13]. As a result, GOA has developed a code of conduct of insects. The number of locomotives can be compared to

$$X_j = FO_j + G_j + A_j \tag{20}$$

Where X_j, FO_j, G_j and A_j are located, space, the power of fellowship, Great power too j^{th} grasshopper wind. A search worker was provided voluntarily in lieu of a search warrant. To find inappropriate behavior, Reference (20) was amended as follows:

$$X_j = r_1 FO_j + r_2 G_j + r_3 A_j \tag{21}$$

Where r_1, r_2 and r_3 are chance numbers in [0, 1]. j^{th} Grasshopper interaction efforts locusts can be counted by

$$FO_j = \sum_{\substack{k=1 \\ k \neq j}}^{n} s\left(d_{jk}\right) u_{d_{jk}} \tag{22}$$

Where d_{jk} is the intermediate between the j^{th} and k^{th} grasshoppers, $u_{d_{jk}}$ is the line vector from j^{th} to k^{th} grasshopper, n is a complete number of grasshoppers, and s is a powerful interconnecting force performance and can be calculated by

$$s(r) = fe^{\frac{-r}{l}} - e^{-r} \tag{23}$$

Where l and f are the attractive distance measure and the attractive weakness, correspondingly. The suggested the values of f and l are respectively 0.5 and 1.5 [14]. The force of gravity of the j^{th} grasshopper, G_j is calculated by

$$G_j = -gu_{G_j} \tag{24}$$

Where g and u_{G_j} are respectively the gravitational constant and the unit vector towards the center of the Earth. The incoming wind, A_j can be calculated by

$$A_j = vu_{A_j} \tag{25}$$

Where KSD and ELF are the constant drift and the vector of the wind direction components. As a substitute for the values of A_j, G_j and FO_j in (21) given the equation,

$$X_j = r_1 \sum_{\substack{k=1 \\ k \neq j}}^{n} s(d_{jk})\ u_{d_{jk}} - r_2 g\ u_{g_j} + r_3 v\ u_{A_j} \tag{26}$$

The intermediate between j^{th} and k^{th} grasshoppers can be denoted by

$$d_{jk} = |x_j - x_k| \tag{27}$$

Where X_j is the site of j^{th} grasshopper and x_k is the site of k^{th}. Equation (27) now it can be changed to

$$X_j = r_1 \sum_{\substack{k=1 \\ k \neq j}}^{n} s(|x_j - x_k|) \frac{x_j - x_k}{d_{jk}} - r_2 g\ u_{g_j} + r_3 v\ u_{A_j} \tag{28}$$

The first statistical model cannot be used to solve development problems because the vast majority of grasshoppers do not match a particular location. Finding the right answer to problems, Equation estimation (28) was amended as follows:

$$X_j^d = c\left(\sum_{\substack{k=1 \\ k\neq 1}}^{n} c\frac{ub_d - lb_d}{2} s\left(\left|x_j^d - x_k^d\right|\right)\frac{x_j - x_k}{d_{jk}}\right) + T_d \tag{29}$$

Where lb_d and ub_d are the lower and upper boundaries in the d^{th} level and T_d is the d^{th} model purpose (positive answer); in the end, c is a decreasing coefficient, which needs to be reduced compared to the number of repetitions. To find out how to calculate coefficient c it would go as follows:

$$c = c_{max} - \mu\frac{c_{max} - c_{min}}{\mu_{max}} \tag{30}$$

Where c_{min} and c_{max} are the minimum and maximum values of the c coefficient, while μ and μ_{max} are normal and maximum repeatability.

B.4 Optimization algorithms for UFLS

The optimum UFLS program is available to reduce the load shed and maximize the bottom of the swing times of the system. The best standards are set through PSO and GOA. The graphs for implementing the PSO and GOA algorithms in the development of UFLS are shown in Figure B.1.

B.5 System modelling

The proposed method is implemented for IEEE 14 systems. The program for shedding purposes should be in the position of shedding the minimum number of loads within the shortest time possible and be able to meet the technical constraints for the stability of the system. In this paper, the IEEE 14 bus measurement system is reviewed and compared using MATLAB. Figure B.2. shows the information for the IEEE 14 bus system consisting of a bus and a line data as exposed in [15], [16].

The procedure for implementing the Traditional, PSO and GOA method known as breaker interlock loading shedding is done by identifying the input, generating the dataset, design the neutral network, and evaluating performance. The simulation results are implemented by considering 1000 Mw and observation of the frequency deviations of systems [13]. The values of load and frequency are also obtained. The values are also extracted from the dispatch centre and compared with neural network output values.

The procedure for implementing the Traditional, PSO and GOA method known as breaker interlock loading shedding is done by identifying the input, generating the dataset, design the neutral network, and evaluating performance. The simulation results are implemented by

considering 1000 Mw and observation of the frequency deviations of systems [10]. The values of load and frequency are also obtained. The values are also extracted from the dispatch centre and compared with neural network output values.

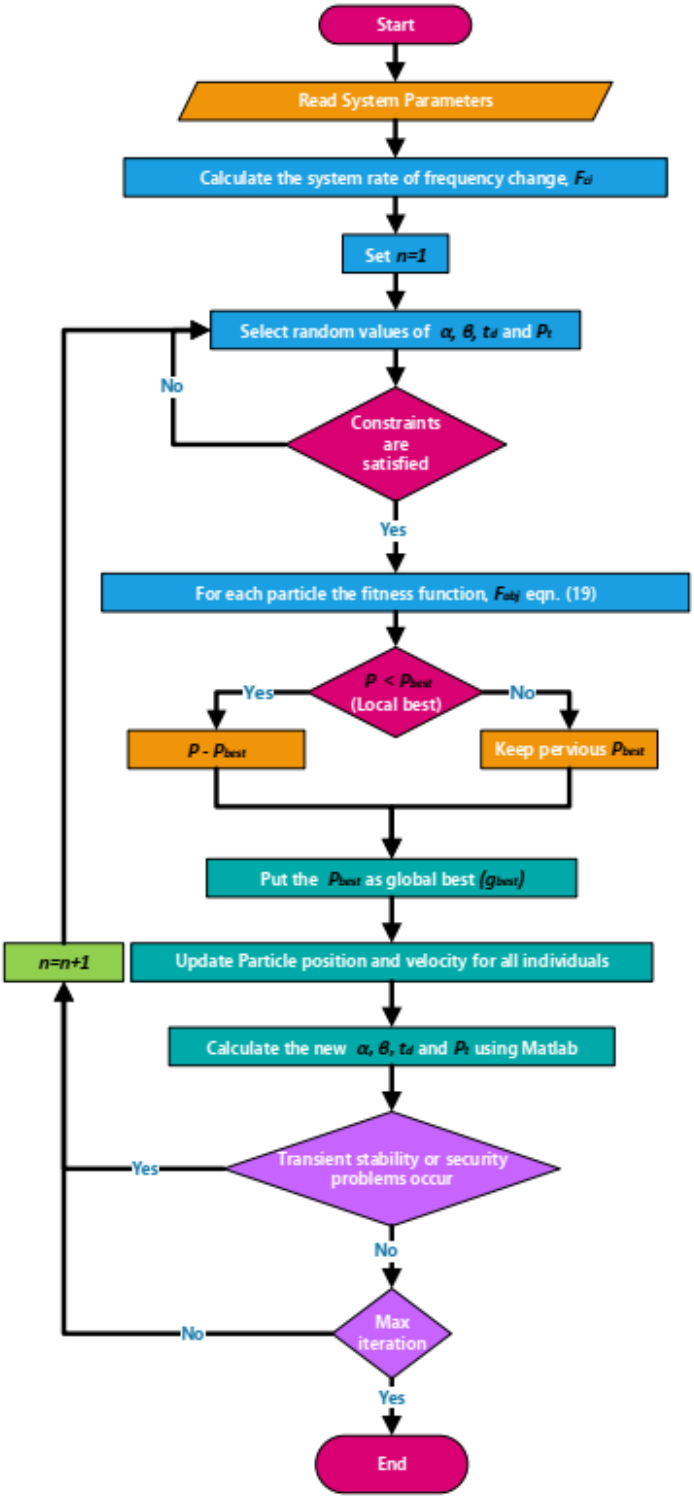

Figure B.1: Simulation of the IEEE 14 BUS System.

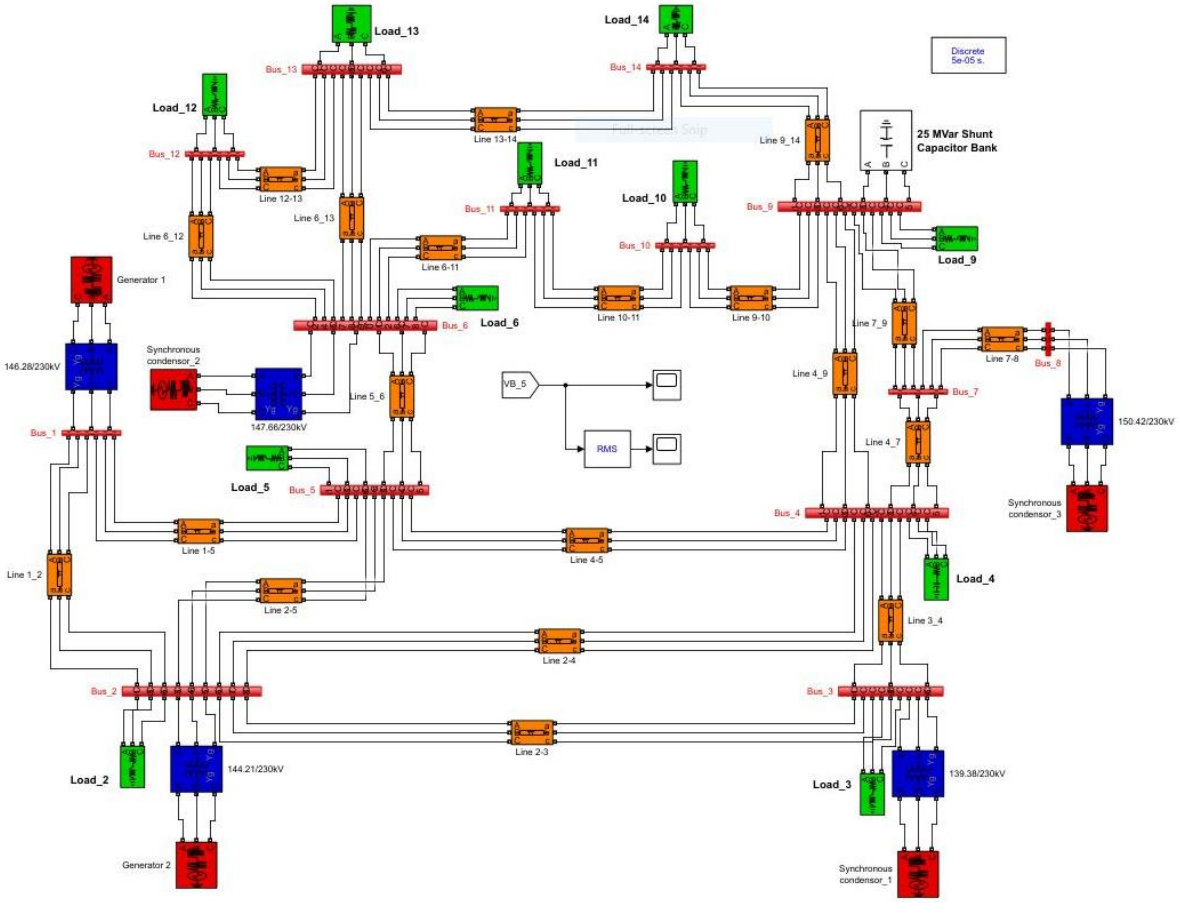

Figure B.2: Simulation of the IEEE 14 BUS System.

B.6 Results and discussions

As the planned load shedding is a centralized method, it is important to consider the performance of the proposed system and the effects of the actual delay in communication. The proposed scheme contains only two signals between the central controller and the load switches. The performance of the system in various cases is being investigated by UFLS relays measurements that have been shown using a delayed line-based communication that has been shown to be effective in microgrid protection and control. As a result, in this case study, the performance of the proposed load shedding system is assessed with communication delays of 50 ms, 100 ms and 150 ms. Case 1 is used as the basis for the comparative case, where there is delay in communication for the duration of the load shedding. The results are shown in Figure B.3. As it can be seen from the experiment, with the increase of the communication delay, while the activities of the load shedding scheme have a small impact on the amounts of loads being shed and the timing of the shedding activities, the microgrid frequency limit was well maintained at the required 47 Hz. Changes in the shedding

actions are anticipated, as delay in communication has caused the behavior to change during the sequence of the load.

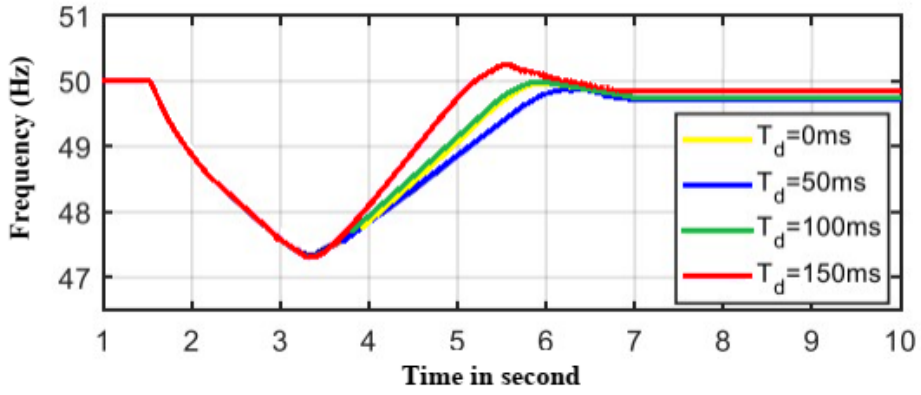

Figure B.3: Impact of communication delays on the performance of the proposed load shedding scheme

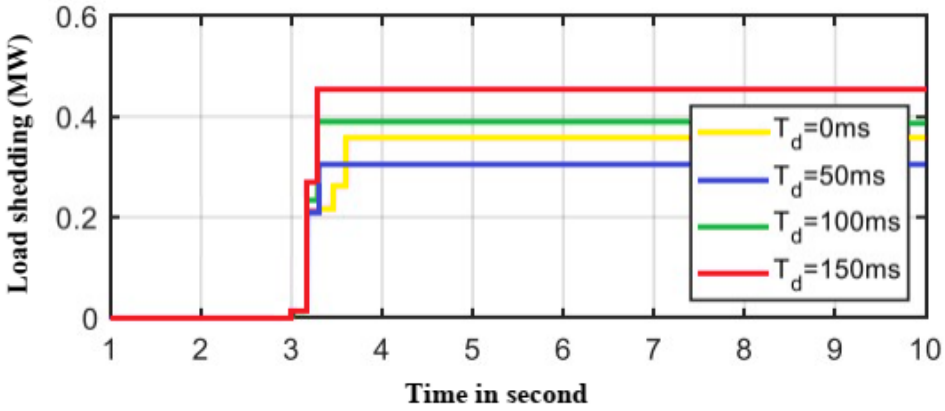

Figure B.4: The impact of communication delays the functioning of the proposed load shedding scheme.

As shown in Figure B.4, the delay has been shown to affect the load shedding in the event of a communication delay of 150 ms so that there is a long delay that gives a maximum value of 0.448 MW load shedding compared to other delays of about 50 ms delivering 0.25 MW.

The system performance under different operating situations is investigated for UFLS relay parameters tuned via the control of traditional, PSO and proposed GOA approaches. Case 2 is used as the basis for the comparative situation, where there is a uniform constant delay in communication during the breaking of the load. In this case, Line 2-4 is tripped at 1.5 sec, and the LS signals are operated at 2.043 sec. In case 3, Line 2-4 and Line 2-3 are tripped at 1.5 sec, and the LS signals are operated at 2.214 sec.

Figure B.5 shows the magnitude of the voltage of the IEEE 14 bus system after period outage lines 2-4 and lines 2-3. As shown in Table B.1 it shows the ratio between the average of disturbance period outage line 2-4 and line 2-3. From this table, the GOA request is of little value to LS. As a result, the overall performance of the GOA is superior to that of the UFLS methods.

GOA's proposal has a smallest amount of load shed and a high cost of low-speed swing for all surveys, which results in immediate impacts on the reduction in electricity to circulating electricity. Table B.1 continues to show the benefits of GOA by increasing the lower boundaries of the line frequency and preventing needless LS.

The Table B.1 shows that the various UFLS approaches successfully restore a stable system after loss Line 2-4. Comparing disturbances show that outage of line 2-4 has a greater effect on the maximum swing line than Line 2-4 and Line 2-3. Which results in continued attention to communication latency in the grid.

Numerical results from traditional, PSO and GOA methods were also note down in Table B.1 on this case. Table B.1 shows that the GOA requirement has a small number of amount loads and a very good low swing frequency value. GOA has a good overall performance, as it increases the number of swings a few times while reducing loads. The increasing number of GOA categories is due to the goal of restoring the permanent line system and reducing the amount of load shed in shot time. In addition, GOA has a short communication delay between stages, wich reduces the automatic stress on the generating sections.

Table B.1 IEEE 14 bus system performance comparison: Traditional, PSO and GOA.

Disturbance	Method	Traditional	PSO	GOA
Line 2-4	Percentage of load shedding, α [%]	44.24	40.875	40.872
	Lowest frequency, [Hz]	48.42862	48.67239	48.8675
	Delay time, t_d [sec]	0.184	0.01	0.0112
	Number of load shedding stages, β	3	6	6
Line 2-4 & Line 2-3	Percentage of load shedding, α [%]	72.3294	69.0536	69.0233
	Lowest frequency, [Hz]	47.62531	48.59842	48.61582
	Delay time, t_d [sec]	1.22	0.08	0.08
	Number of load shedding stages, β	4	9	9

The load power is calculated by the size of the bus voltage, the actual power, and the value of the load are calculated, as shown in Table B.1. The results of the 14 bus system show that the proposed GOA presented has reached excellent voltage stability and minimum load shedding values.

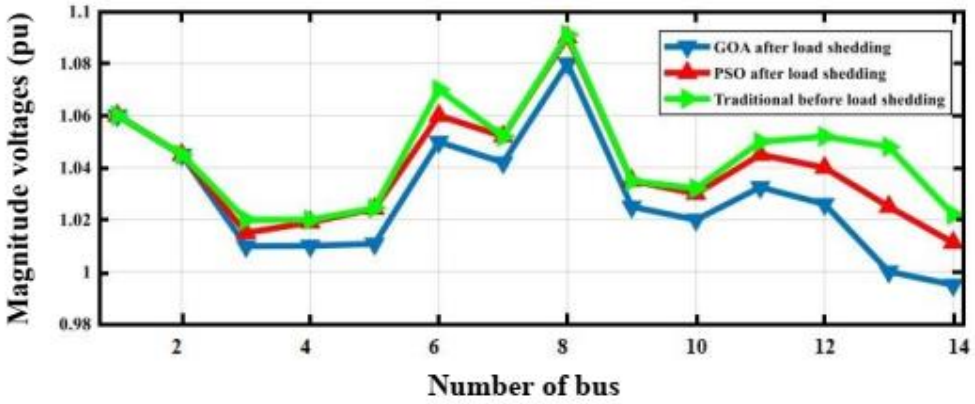

Figure B.5: Bus voltages before and after load shedding for IEEE 14-bus system under loss of generation of 72 MW.

B.7 Conclusion

Several methods and models have been proposed in solving the impact of communication delays in grid systems. The assessment and analysis of the UFLS methods for the impact of communication delay have been achieved by focusing on several models and techniques. For instance, the utilization of the UFLS method has an impact on reducing voltage instability or collapse in electric power systems. The other strategy is known as the grasshopper optimization algorithm (GOA) which has been proven and tested to help in investigating and solving the issues of power delays/imbalances. On the other hand, the traditional, PSO techniques have limitations of shedding the excess amount of load or insufficient loads. However, methods such as the adaptive are the most appropriate in this approach because they determine the amount of load by measuring the derivatives of frequencies. Additionally, GOA is considered a new metaheuristic optimization algorithm and is used with UFLS to obtain the optimum solution for load management with a fast response. GOA can successfully prevent the unnecessary shedding of loads, which boosts the power system security and proposed method has capable of minimize the frequency recovery communication delays and frequency fluctuations.GOA which involves several sets of equations for investigating the impact of communication delays which forms the best background of solving several problems facing the power grid systems that causes the delays. Therefore, GOA method can best work within a given local area to avoid the spread to other regions within the grid network. The Rwandan government should adopt and utilize the techniques in its fast-growing grid system which will increase its stability and performance.

References

[1] T. Amraee, M. G. Darebaghi, A. Soroudi, and A. Keane, “Probabilistic under Frequency Load Shedding Considering RoCoF Relays of Distributed Generators,” *IEEE Trans. Power*

Syst., vol. 33, no. 4, 2018. [CrossRef]

[2] A. A. Koosha and T. Amraee, "Under frequency load shedding against severe generation outages in low inertia power grids," in *2020 15th International Conference on Protection and Automation of Power Systems*, IPAPS 2020, 2020. [CrossRef]

[3] J. Wang, H. Zhang, and Y. Zhou, "Intelligent under Frequency and under Voltage Load Shedding Method Based on the Active Participation of Smart Appliances," *IEEE Trans. Smart Grid*, vol. 8, no. 1, 2017. [CrossRef]

[4] M. N. Acosta et al., "Optimal under-frequency load shedding setting at Altai-Uliastai regional power system, Mongolia," *Energies*, vol. 13, no. 20, 2020. [CrossRef]

[5] T. Yang and D. Wu, "Distributed load shedding over directed communication networks with time delays," in *Proceedings of the IEEE Power Engineering Society Transmission and Distribution Conference*, 2016, vol. 2016-July. [CrossRef]

[6] A. I. M. Isa, H. Mohamad, K. Naidu, N. Y. Dahlan, and I. Musirin, "Method of determining load priority using fuzzy logic for adaptive under frequency load shedding technique," *Pertanika J. Sci*. Technol., vol. 25, no. S, 2017. [CrossRef]

[7] M. Talaat, A. Y. Hatata, A. S. Alsayyari, and A. Alblawi, "A smart load management system based on the grasshopper optimization algorithm using the under-frequency load shedding approach," *Energy*, vol. 190, 2020. [CrossRef]

[8] M. Liu, G. Tzounas, and F. Milano, "A model-independent delay compensation method for power systems," in *2019 IEEE Milan PowerTech*, PowerTech 2019, 2019. [CrossRef]

[9] A. Gjukaj, G. Kabashi, G. Pula, N. Avdiu, and B. Prebreza, "Re-design of load shedding schemes of the Kosovo power system," *World Acad. Sci. Eng. Technol*., vol. 50, 2011. [CrossRef]

[10] X. Xiong and W. Li, "A new under-frequency load shedding scheme considering load frequency characteristics," in *2006 International Conference on Power System Technology*, POWERCON2006, 2006. [CrossRef]

[11] M. Talaat, M. H. Gobran, and M. Wasfi, "A hybrid model of an artificial neural network with thermodynamic model for system diagnosis of electrical power plant gas turbine," *Eng. Appl. Artif. Intell*., vol. 68, 2018. [CrossRef]

[12] Y. Y. Hong and S. F. Wei, "Multiobjective under frequency load shedding in an autonomous system using hierarchical genetic algorithms," *IEEE Trans. Power Deliv*., vol. 25, no. 3, 2010. [CrossRef]

[13] X. Xiang, X. Ma, Y. Fang, W. Wu, and G. Zhang, "A novel hyperbolic time-delayed grey model with Grasshopper Optimization Algorithm and its applications," *Ain Shams Eng. J*., vol. 12, no. 1, 2021. [CrossRef]

[14] N. E. Y. Kouba, M. Menaa, M. Hasni, and M. Boudour, “Optimal load frequency control based on artificial bee colony optimization applied to single, two and multi-area interconnected power systems,” in *3rd International Conference on Control, Engineering and Information Technology*, CEIT 2015, 2015. [CrossRef]

[15] Y. Y. Hong and P. H. Chen, “Genetic-based under frequency load shedding in a stand-alone power system considering fuzzy loads,” *IEEE Trans.* Power Deliv., vol. 27, no. 1, 2012. [CrossRef]

[16] M. Sanaye-Pasand and M. Davarpanah, “A new adaptive multidimensional load shedding scheme using genetic algorithm,” in *Canadian Conference on Electrical and Computer Engineering*, 2005, vol. 2005. [CrossRef]

Paper C

Title:	Decreasing the Negative Impact of Time Delays on Electricity Due to Performance Improvement in the Rwanda National Grid.
Authors:	Darius Muyizere[1*], Lawrence K. Letting [1,2] and Bernard B. Munyazikwiye[1,3]
Affiliation:	[1] African Centre of Excellence in Energy and Sustainable Development, College of Science and Technology, University of Rwanda, KN 67 Street Nyarugenge, Kigali P.O. Box 3900, Rwanda [2] Department of Electrical & Communications Engineering, Moi University, Eldoret 30100, Kenya [3] Department of Mechanical and Energy Engineering, College of Science and Technology, University of Rwanda, KN 67 Street Nyarugenge, Kigali P.O. Box 3900, Rwanda
Article:	MDPI Electronics 2022, 11, 3114. https://doi.org/10.3390/electronics11193114
Layout:	The format of the paper has already been altered to match that of the thesis.

Paper C: **Decreasing the Negative Impact of Time Delays on Electricity Due to Performance Improvement in the Rwanda National Grid.**

***Abstract* — One of the most common power problems today is communication and control delays. This can adversely affect decision interaction in grid security management. This paper focuses on communication signal delays and how to identify and address communication system failure issues in the context of grid monitoring and control, with emphasis on communication signal delay. An application to solve this problem uses a thyristor switch capacitor (TSC) and a thyristor-controlled reactor (TCR) to improve the power quality of the Rwandan National Grid (RNG) with synchronous and PV generators. It is to counteract the negative effects of time delays. To this end, the TSC and TCR architectures use two methods: the fuzzy logic controller (FLC) method and the modified predictor method (MPM). The experiment was performed using the Simulink MATLAB tool. The power quality of the system was assessed using two indicators: the voltage index and total harmonic distortion. The FLC-based performance was shown to outperform the MPM for temporary or permanent failures if the correct outcome was found. As a result, we are still unsure if TSC and TCR can continue to provide favorable results in the event of a network cyber-attack.**

***Keywords*:** communication and control; Rwandan National Grid (RNG); fuzzy logic controller (FLC); power quality; modified predictor method (MPM).

C.1 Introduction

The modern grid has a large number of controllers in the measurement of electricity that are widespread in different parts of the world, such as generation, transmission, and distribution, for which control and construction often lead to delays in communication [1]. As the system becomes more complicated, new technology phasor measuring units (PMUs) are created to measure dynamic data from the power system, such as voltage, flow, demand angles, frequency, and power factor. Global positioning system (GPS) satellites synchronize all the collected information with PMUs. Signals such as voltage response, speed response, rotor angle, and so on are evaluated and transmitted to the control center. Because the PMUs must send signals to the control center, they depend on various communication infrastructure [2], which introduces time delays. Delays between the moment of measurement and the signal reaching the controller are generally in the nanoseconds to seconds range, depending on location, structures, and various other parameters [3,4]. The quality of the electricity supplied to a customer is referred to as power quality [5]. In order to maintain the reliability and cost of electrical machinery, it is necessary to maintain and improve the comfortable energy of the machine. In this article, we use a combination of a thyristor switch capacitor (TSC) and a thyristor-controlled reactor (TCR) [6–8] to make an

energy-friendly improvement for a hybrid machine. The total voltage deviation (TVD) at the point of common coupling (PCC) is sent to the TSC and TCR controllers. All of these measurements are collected and delivered via the PMU. This causes a delay and delays the controller input.
Previously, several studies on the effects of time on the control mechanism and feeding system have been performed [5,9–12]. Furthermore, several studies have been performed with the aim of minimizing the negative impact of delays on system performance [13–17]. All of these available solutions to mitigate the effects of delays are considered to be ongoing delays, time-varying delays, or random delays [4].

The inter-area oscillations of a multiarea-linked power system could be successfully suppressed under the impact of time-varying delays on a wide-area communication network, according to Li et al. [18]. Bilinear transforms were used to obtain a discrete-time model of a long-range attenuation controller. Zappone et al. proposed a new approach to power control for wireless networks [19]. This approach optimized both the energy efficiency and the latency of the communication together, taking into account the quality of the service constraints associated with the maximum bit error rate or the minimum achievable bit error rate [19]. Sargolzaei et al. concentrated on time delays introduced into the control system by hackers to destabilize the system, and a time delay estimator was modified using an indirect supervisor and a modified minimum average. A squared minimization technique that tracked the time delay introduced by an attacker used model reference control [20]. Alexander et al. proposed an enhanced time delay compensator (ETDC) approach that managed varying time delays, introducing the perspective of network latency instead of dead time; also, the ETDC took advantage of real signals and measurement transmission procedures in WAMS, building a closed-loop memory control for the power system [21]. The authors of [22] addressed the time delay effect of wide-area monitoring and control systems (WAMCS) in smart power grids, which can have a significant impact on system stability. The main purpose was to perform a detailed WAMCS delay analysis in the event of a network failure.

In addition, [23] addressed the issue of delay minimization for wireless sensor network (WSN) relay-based delay minimization routing (DMR) and cooperative delay minimization routing (CoDMR) issues. This work suggested a greedy technique for finding a workable DMR and CoDMR scheme with low overall total energy cost, energy balancing, and latency when using binary fields. In [24], Hai proposed a time synchronization solution based on time division long-term evolution (TD-LTE) frame synchronization to improve the accuracy by correcting the delay caused by the radio propagation path. In this work, Padhy described a time delay compensation (ATDC) method's system, structure, features, and implementation strategy, as well as timing accuracy. In [25], a compensation technique was proposed that took into account the time-varying delay of wide-area power grid stabilizers. In this task, Zhang considered splitting a finite random delay into multiple delay intervals and designed a compensator for each interval. In addition, a

predictive-based hierarchical delay compensation method was proposed at the data-processing level to handle delays in a wide-area control system (WACS) power system [26].

Although, as mentioned earlier, much work has been conducted on time delay impact and techniques for minimizing it, most of these analyses have been performed in the steady state of the power grid. None of the studies has looked at the influence of time delay, as well as how to reduce the negative impacts of a delay by using a TSC and TCR approach in the event of a failure to enhance power quality under fault situations.

Predicated on this context, this paper presents two methods, a fuzzy logic controller (FLC)-based method and a modified predictor method, to reduce the harmful effects of time delays on power quality management with a combined thyristor switch capacitor (TSC) and a thyristor-controlled reactor (TCR) for reactive power compensation in the situation of a hybrid electric grid comprised of sequential and changeable irradiances with a temperature PV plant. The FLC method was chosen because it can manage the nonlinear behavior, instability, inaccuracy, or fluctuation of input parameters and allows for the incorporation of expert knowledge into control rules [2,16,17,27,28]. This type of controller works well under shifting system parameters and with moment signals. In terms of reducing the negative impacts of temporal delays, the FLC-based technique outperforms the modified predictor method. Two indices are utilized to evaluate the system's power quality: the voltage indication and the total harmonic distortion (THDu). At several sites in the electrical network, such as the Kigali National Grid (KNG), temporary and permanent faults, both balanced and unbalanced, are investigated.

The following is the structure of this paper: Section C.2 covers the proposed study's Kigali National Grid power system model. Section C.3 discusses communication delays with the combined TSC and TCR controllers. Section C.4 discusses ways to reduce communication delays. The simulation findings are described in Section C.5. Finally, Section C.6 gives this paper's findings.

C.2 Kigali National Grid Description

Generally, the study shows an analysis of the performance of a region (surrounded by a red marker) with one central, regional power station in central Rwanda in the Great Rift Valley of central Africa where the African Great Lakes region and east Africa converge, and the behavior in the electricity map is as shown in Figure C.1. The solution is based on the Kigali National Grid (KNG) system and includes the integration of a PV farm, as illustrated in Figure C.2, to test the suggested technique's applicability to a complex power system. The details on the network data, generators, excitation systems, and PSSs are as follows. Generators 1-6 had local PSSs installed. The PV farm is located near the SS9 Mount Kigali substation.

The automated voltage regulator and the governing control models were installed on synchronous generators. This system had eleven substations that were linked together via transmission lines. In addition, twenty loads, such as Load 1, Load 2, and Load 20, were connected at separate buses. Loads such as Load 5, Load 13, and Load 16 employed in the case study were voltage-stiff nonlinear loads [29–32]. Section C.6 demonstrates and explores the nonlinear characteristics of nonlinear loads, i.e., the harmonic spectra of these loads.

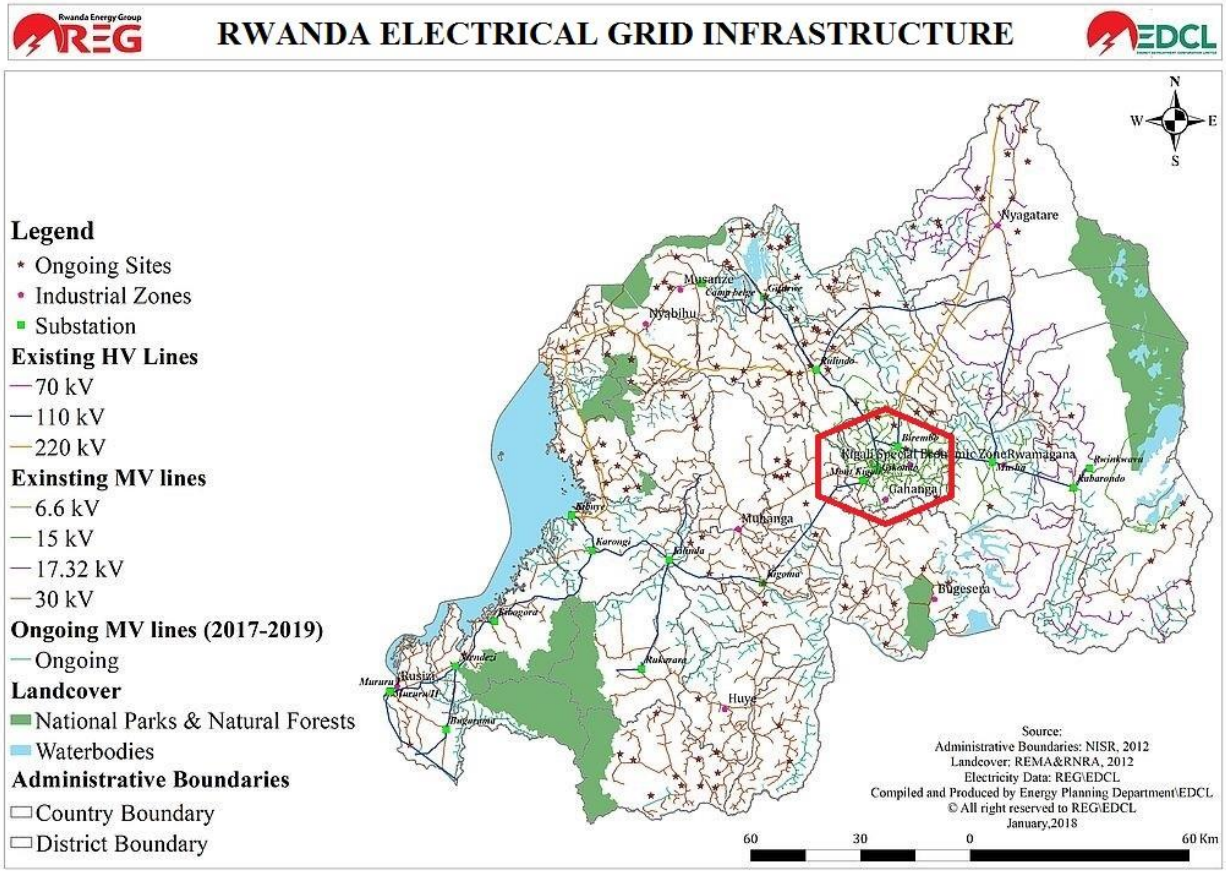

Figure C.1: Estimated location of electricity transmission and distribution network, Source: REG [32].

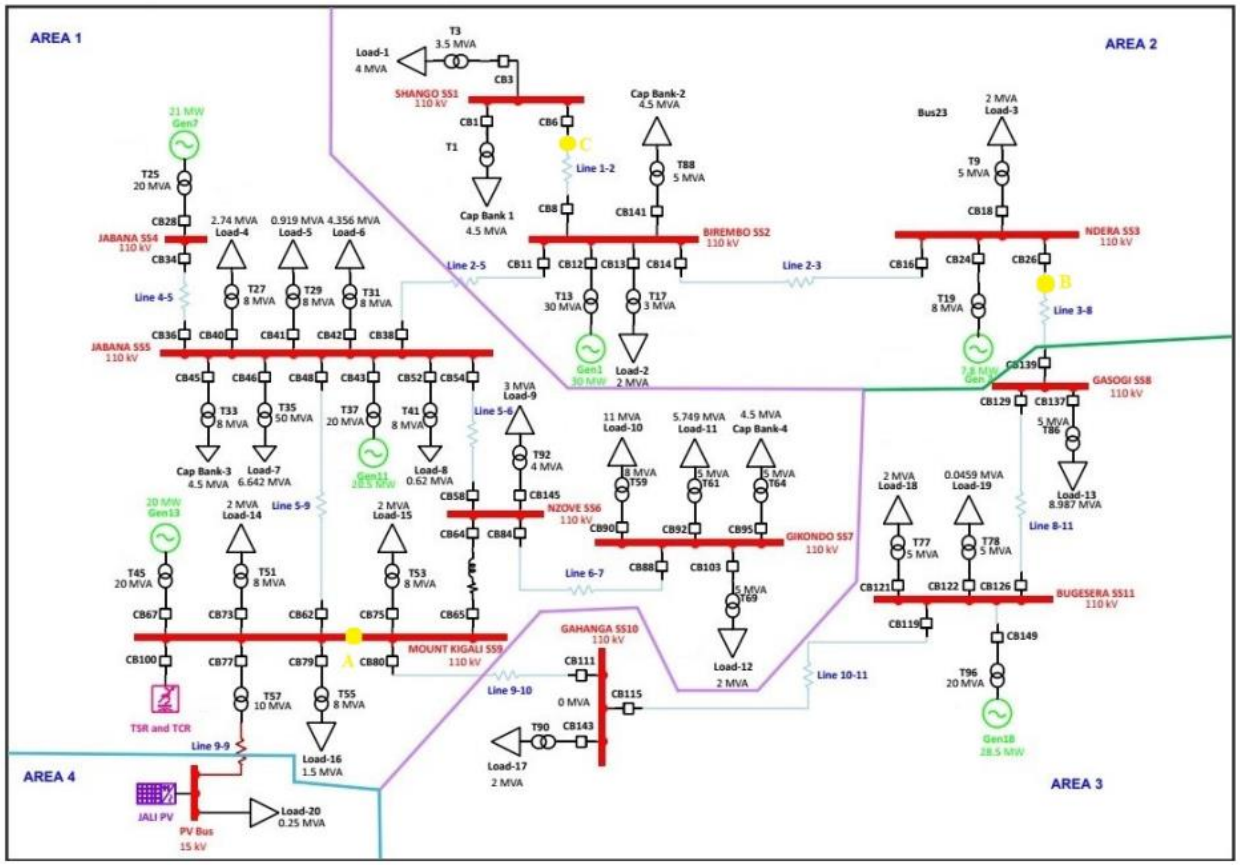

Figure C.2: Kigali national grid system with five coherence areas.

In this research, a 94-Mvar thyristor-switched capacitor bank (TSC) and a 109-Mvar thyristor controlled reactor bank (TCR) linked to the substation Mount Kigali SS9 bus through the secondary side of the transformer were employed to improve power quality. The measurements utilized in the hybrid system stated above may be found in the study's appendices, and the solar power plant has a capacity of 0.25 MW. Table 1 provides an overview of the model's many components. Transmission and distribution voltage ranges ranging from 110kV to 15 kV are included in the present model. Rwanda's highest voltage network is now 110 kV, with intentions to upgrade to 220 kV soon [33].

In this study, we used data collected from the Energy Utility Corporation Limited (EUCL) at Rwanda Electricity Group (REG). The data collected was intended to match the output of the algorithm used. With regard to freight and emergency analysis, we have collected information on the real power and causes of the bus and cargo buses, the real energy needed and the distribution. The details of the research are attached to the back pages of this report [30]–[34]. The use of the Data of Utility Data Center and the Power National Dispatching Center are recommended for full access information required for this research.

Table C.1 Number of components in system model.

Devices	Numbers
Substations	11
Shunt Reactor	1
Capacitor Bank	2
Buses	69
Machines	6
Loads	20
Branches	13
Two-winding transformers	27
PV System	1

C.3 Communication Delay Issues with Combined TSC and TCR Controller

As demonstrated in Figure C.1, TSC and TCR can be utilized in tandem to govern the reactive power flow from the source to the loads. The separate modules are connected together to provide maximum flexibility to the consumers' loads by concurrently changing the switching of the capacitor banks in discrete numbers in the TSC branch and constantly modifying the flow of the current in the inductor in the TCR branch. It is possible to obtain completely stepless control by coordinating the control between the continuous reactor and the capacitor stages (which are discrete).

Dynamic control strategies of coupled TSC and TCR methods have continuous control, almost no transients, and reduced harmonic production (due to the regulated reactor rating being tiny in comparison to the overall power flow) with control and operation flexibility [35,36]. The drawback of the TSC-TCR method compared to TCR- and TSC-type compensators is the greater installation cost; nevertheless, the cost can be repaid in a shorter period of time: in the long term, this plan is more cost-effective than paying the Electricity Authority for KVA demand charges on a regular basis. A static VAR system compensates for reactive power delivered into the line in a rapid, smooth, and stepless manner. It guarantees that bus voltages are accurately controlled throughout a wide variety of loads.

C.3.1 Combined TSC and TCR model

The TSC-TCR was linked to the general grid line, as indicated in Figure C.3. Six thyristors were linked to the capacitor, while the other six were connected to the inductor [37]. The thyristors were used to convert these capacitors. The reaction capacitor's capacitance, C, was 94 Mvar, while the inductor's capacitance was 109-Mvar. It only worked when the error rate between the voltage lines was more than 2%. The controller's output was alpha ($\propto$), which was used to modify the thyristors' pulses. The control of switching TSC and TCR for fuzzy input is shown in Figure C.4. It is worth

noting that this one-of-a-kind fuzzy controller could help assist other delay reduction approaches, such as PSS and PSS fuzzy.

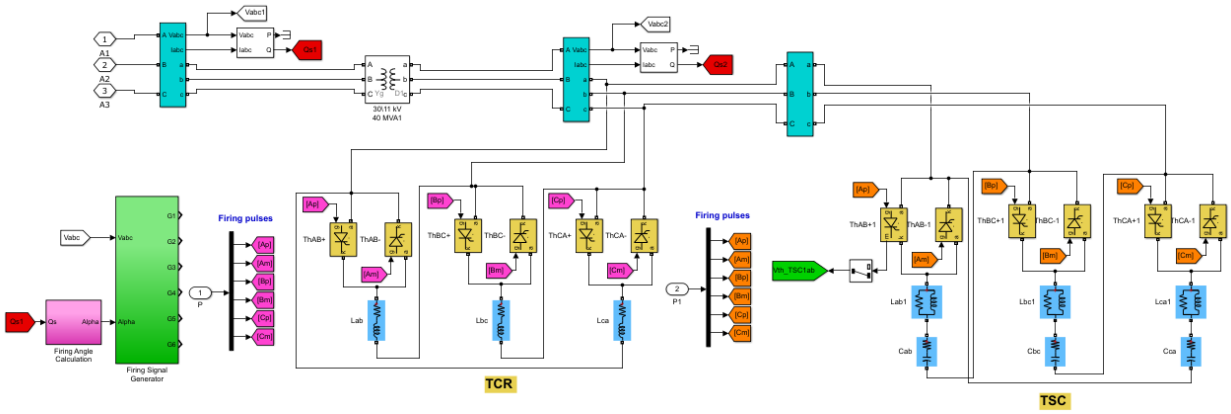

Figure C.3: TSC-TCR 3-phase circuit diagrams with grid connection concept.

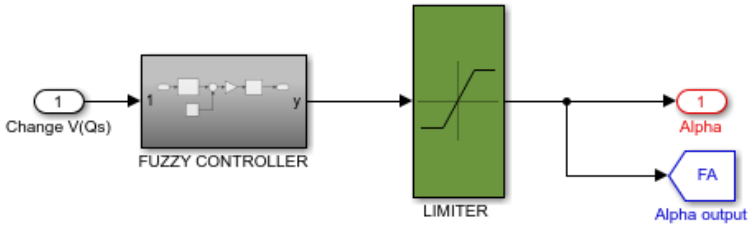

Figure C.4: Control block for switching of TSC-TCR.

C.3.2 Causes of electrical network communication delays

Connectivity delays in the hybrid power grid include signal transmission from PMUs to control centers, control centers to controllers, analog-to-digital conversion, online calculation of global input variables, and signal time synchronization utilizing GPS. As a result of this delay, controllers and system performance will suffer [1]. In wide-area control system communication networks, data is sent in packets. Serial delays, defined as the time elapsed between two consecutive bits of data supplied, are one type of temporal delay [38]. A different type of delay is between packet serial delays, which are defined as the time gap between two consecutive data packets. The time it takes for data to be transferred through a network and then resend to another location is known as routing delay. The time it takes to send data via a communications channel is known as propagation delays. As a result, the following equations may be used to express the entire time delay:

$$\mathrm{T} = T_s + T_b + T_p + T_r \quad (1)$$

$$T_s = \frac{P_s}{D_r} \quad (2)$$

$$T_p = \frac{l}{v} \tag{3}$$

Where T_s is really a sequential delay; T_b represents a difference between latency. T_p is just a phase delay. T_r is still a transportation delay; P_s is now a packet size (bits/packet). D_r is really the data transmission rate; l is the length of the network connection, and v seems to be the data transmission speed [39].

C.3.3 TSC-TCR Controller Time Delay Issue

Figure 5 displays TSC's GPS-based shut control system. The controller input is gathered from the control center, as shown in Figure C.5, and delays are created throughout signal transmission, causing a production of such controller output (alpha) to be delayed, reducing the system's power quality. Figure 5 depicts GPS-enabled feedback control. It's also important to note that such delays affect both transmission and distribution connections. As illustrated in Figure C.5, the speed equivalent signal from each generator is routed through filters and an A/D adapter. The digitalized rate equivalent signals from the generators are then routed to a central control office, where they are synced using a GPS receiver. The synchronized signals are used to calculate the total W and time derivatives of TKED. The time derivative of the TKED signal is then given as data output to the other fuzzy controller input. In this case, instructions might be transmitted and received by wireless or fiber optic.

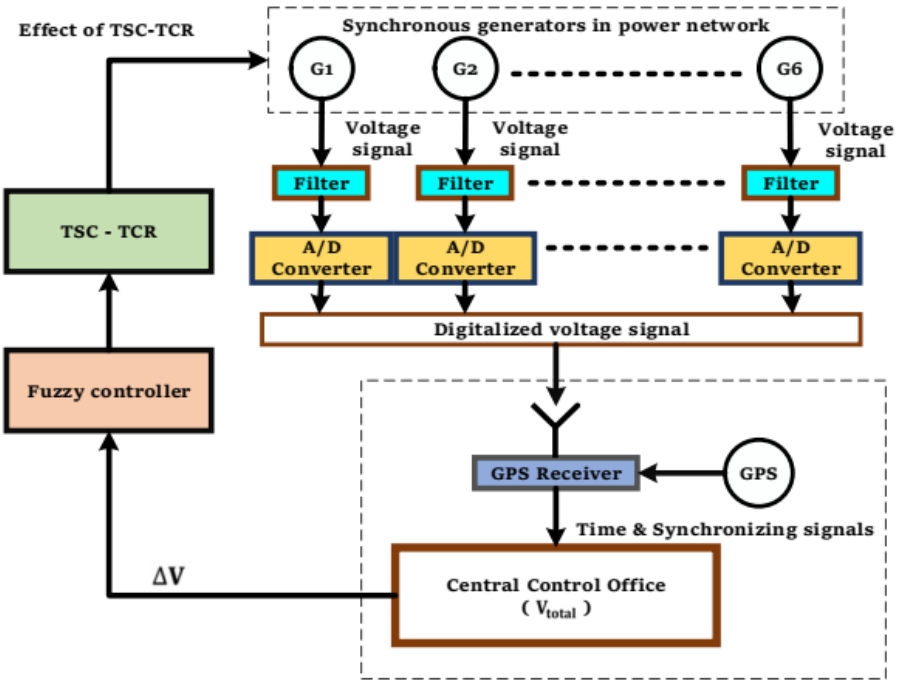

Figure C.5: GPS-enabled shuttered monitoring system.

C.3.4 Performance Expectations

Additionally, temporal delays are introduced as during continuous computation of such partial derivatives for TKED, due mostly to data propagation across optical fibers or wireless, A/D transition, determination of W cumulative, while also period derivation of TKED, and signal data communication using GPS. Time delays may have an influence just on control logic, affecting the minimization of shaft torsional oscillations. As a result, while studying a decrease in shaft torsional waves, such constraints must be considered. In most circumstances, time delays might vary from several microseconds to a few more hundred milliseconds [38]–[41]. Comprehensive simulations are done in this work utilizing a variety of common time delay settings. Section C.5.2 describes some of the simulated occurrences that correspond to a 900 ms significant delay.

C.4 Modeling the problem to suggest a solution includes developing communication delay reduction solutions.

C.4.1 Method Using FLC

A two-input-based FLC method was used in this work to reduce the negative impacts of time delays on the TSC performance. The FLC inputs were the voltage-level fluctuations at the PCC and V, as well as the latency of the control input (D). The controller's output was alpha (α), which was the thyristor's firing angle. The signal delays ranged from 100 to 900 ms during the controller design phase, which covered all the practical scenarios [40,42]. The following is a description of the planned FLC.

During the fuzzification process, the membership grade was determined. Both the inlet and outlet triangles formed control parameters, as depicted in Figures C.6 and C.7, and were obtained after a sequence of trial and error. It is worth mentioning that, when additional fuzzy measures were set, such as nonlinear regression features, and were examined and tried, the system functioned admirably. Unfortunately, in several cases, the input and output membership algorithms produced great outcomes. This is why triangle membership functions were used for this study. Figure C.6 depicts the symbols NB (negative large), NM (negative medium), Z (zero), PM (positive medium), PB (positive big), N (negative), and P (positive). In Figure C.7, the membership functions of the thyristors' firing angle (alpha), are NB, NM, Z, PM, and PB. Throughout this work, one continuity formula [41] was used to determine the degree of crisp values:

$$\mu_{Ai}(x) = \frac{1}{b}(b - 2|x - a|) \tag{4}$$

Where $\mu_{Ai}(x)$ is the value of the membership grade, "x" is the value of V and D, a is the position where the membership grade is one, and b is the length. In this work, Table C.2 shows 15 guidelines for items such as the independent variables, V, and outcome variable. The management guidelines were published with certain system functioning, as well as a defect detecting technique.

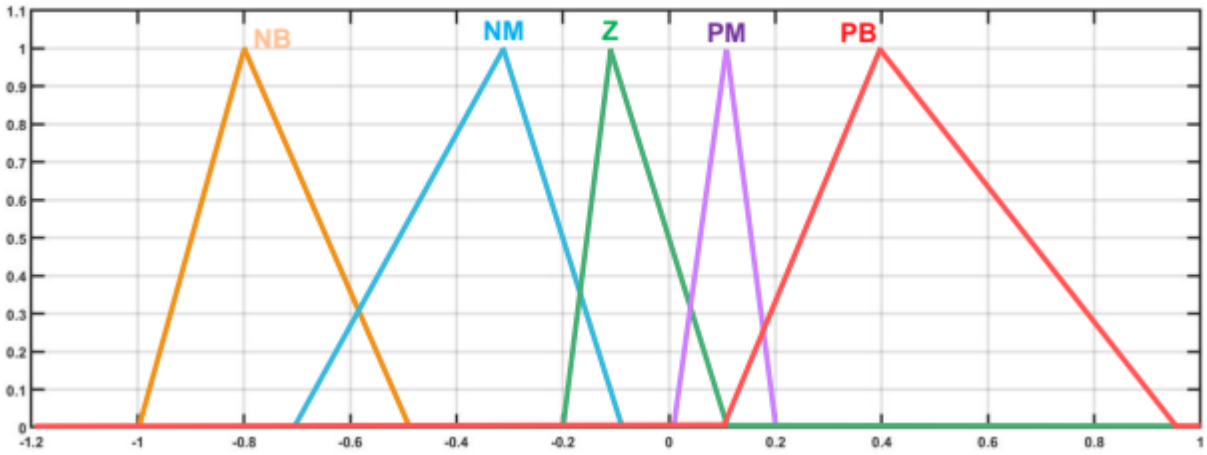

(a)

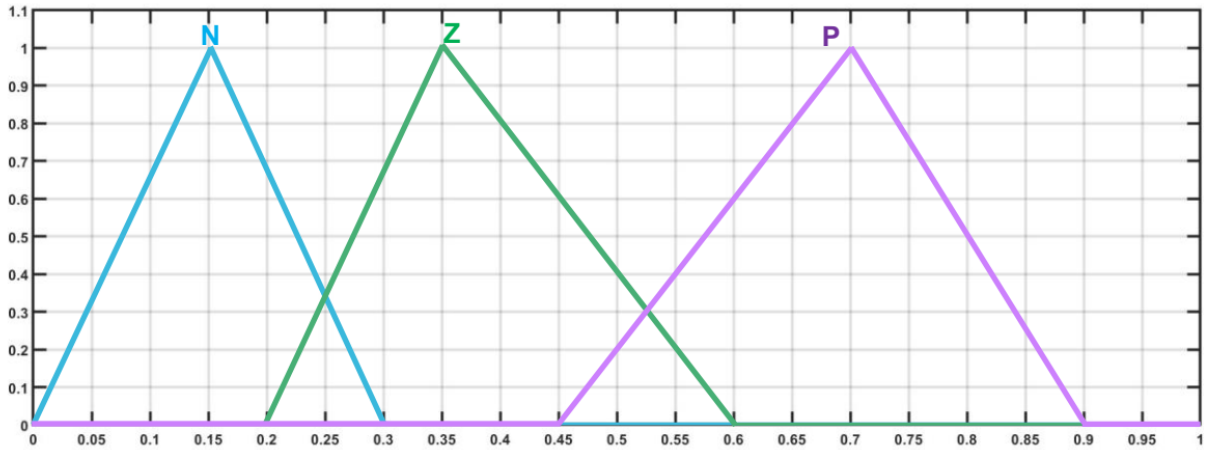

(b)

Figure C.6: Fuzzy controller input membership function (a) ΔV. (b) Delay.

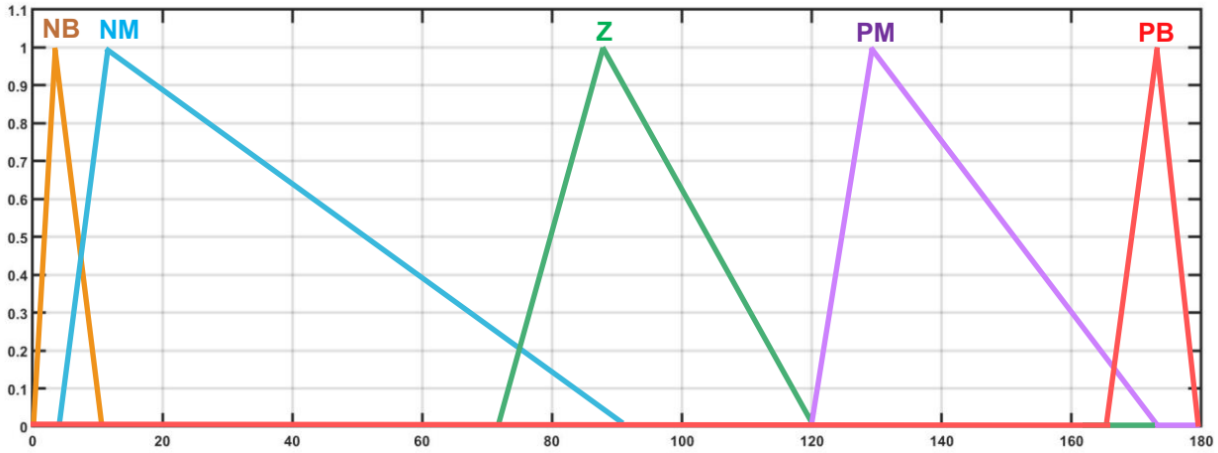

Figure C.7: Membership functions of fuzzy controller output Linear.

Table C.2 Membership functions of input and output

ΔV / D	NB	NM	Z	PM	PB
N	PB	PM	Z	NM	NB
Z	PB	PM	Z	NM	NB
P	PB	PM	Z	NM	NB

Formula (5) indicates the extent of conformance W_i of every fuzzy set using Mamdani's technique [41].

$$W_i = \mu_{Ai}(\Delta V) \times \mu_{Bi}(D) \tag{5}$$

Where $\mu_{Ai}(\Delta V)$ and $\mu_{Bi}(D)$ are membership grade values, in addition "i" is the provision of the section. The following middle area approach was used to compute the thyristor firing angle $\propto$.

$$\propto = \frac{W_i C_i}{W_i} \tag{6}$$

Where C_i is the fuzzy logic - based table's value for $\propto$.

C.4.2 Adapted Predictor Method

The signal in Figure C.8 was adjusted for transmission delay using the suggested improved predictor approach before being sent to the controller. Figure C.9 depicts the flow diagram for the updated predictor approach. Before sending the delayed signal into the controller, the prediction

method's algorithm can alter it to the original curve. The prediction approach is versatile in that it can adapt to any controller. If the time delay is t_d, the predicted ΔV could be determined given the level in comparison, previous recorded points, and estimation [43].

$$\Delta V_p = \Delta V_{previous} + t_d \Delta V c \tag{7}$$

$$\Delta V = \frac{\Delta V_k - \Delta V_{(k-1)}}{\Delta t} \tag{8}$$

With p indicating a predicted position, k represents the observed location position; c represents a steady value, and ΔV represents the rapidity at which the controller's signal changes. c was 0.25, as determined through trial and error.

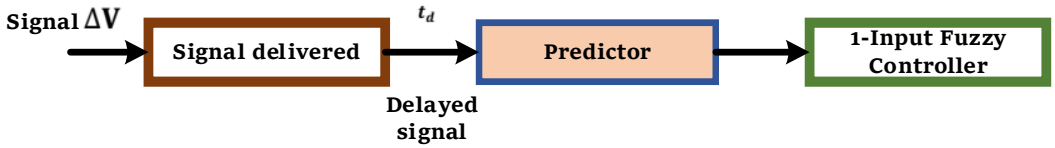

Figure C.8: Predictor model.

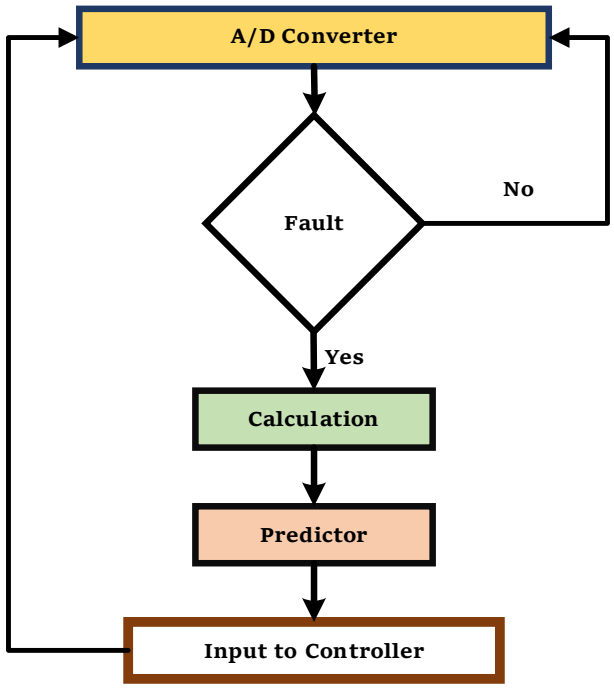

Figure C.9: The improved prediction method's diagram layout.

C.5 Simulation Results and Discussion

This study investigates the effect of latency issues on the effectiveness of a TSC-TCR device for increasing hybrid power system efficiency. The suggested method is simulated in this section using 64-bit MATLAB version 2020a.

C.5.1 PV Jali in Grid-Following mode, PQ control, and irradiance variation

As can be seen from the figure C.10 results, our grid has a Jali PV plant which is based on SS9 Mount Kigali. In its operation it is based on inputs conduction of temperature and irradiance, therefore the temperature has a range of 25-45 ℃ and the irradiance has a range of between 200-1000 W/m^2. Figure C.10 shows how V_{dc} and P_{dc} change depending on temperature and irradiance, and then the measured values at 10 second (On-Grid) show that active power and reactive power are required for Load 20 and Filter C before working with the grid on SS9 Mount Kigali. By going on the grid, it appears that there is a power drop but it is able to support Load 20, moreover when it is completely off you see that there is a disturbance in the measurements obtained from all the G1-G6 generators.

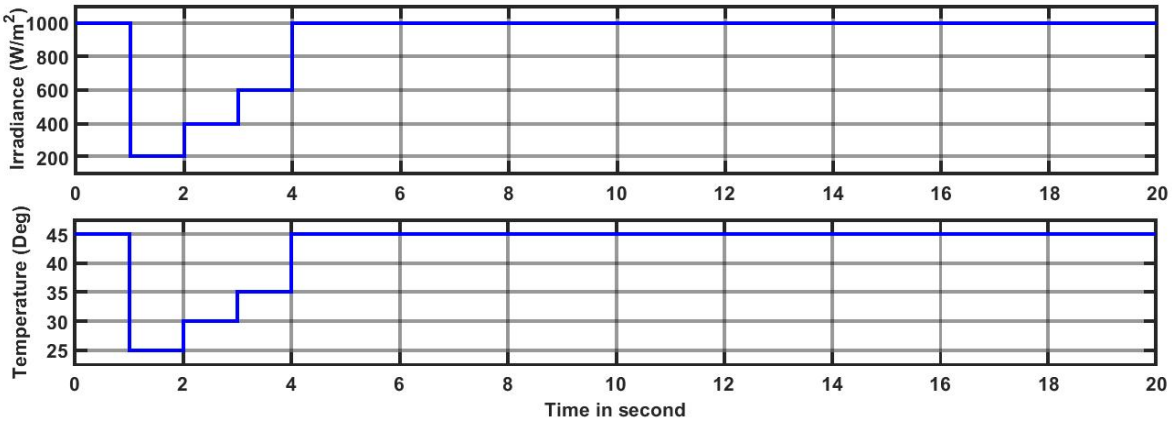

Figure C.10: Variations of Jali PV module parameters with irradiance and temperature.

Table C.3 shows the simulated power flow results for a solar panel connected to the electric network at various levels of solar irradiance with demand. As demonstrated in Table C.3, the power generated by a solar panel was related to its solar irradiation. There are several types of testing. The first alternative is that when the PV system's output power exceeds the power load, the excess electricity is consumed by the utility grid. The second option is that if the PV system's power generated equals the power demand, no power will be supplied to the grid. Once the energy generated from the PV plant is inadequate for self-sufficiency, in the third situation, the solar panel and the grid will be shared to provide the load. As we have shown, employing around 30℃ with 400 W/m^2 provides us with the optimum option to serve our utility grid based on Mount Kigali SS9.

Table C.3 Power flow simulation results for the planned system for various levels of solar irradiation.

N_0	Temperature (℃)	Irradiation (W/m^2)	V_{dc} (V)	P_{dc} (Kw)	Active Power (Kw)		Load capacity (Kw)
					PV	Grid	
4	45	1000	481.2	241.5	117.5	-132.5	250.8
3	35	600	493.4	148.6	730.6	-50.9	780.9
2	30	400	497.2	99.75	489.6	356	133.6
1	25	200	495.9	49.67	245.9	-245.9	300.4

Figures C.11 and C.12 show how the grid behaved at different times. For example in Figure C.11 and the PV was removed when there was an example r separated by the Grid and operating at 45 degrees and 1000 degrees of irradiance. These changes were observed from 0 to 18 seconds and affected the active power, reactive power, P_{dc} and V_{dc} grids.

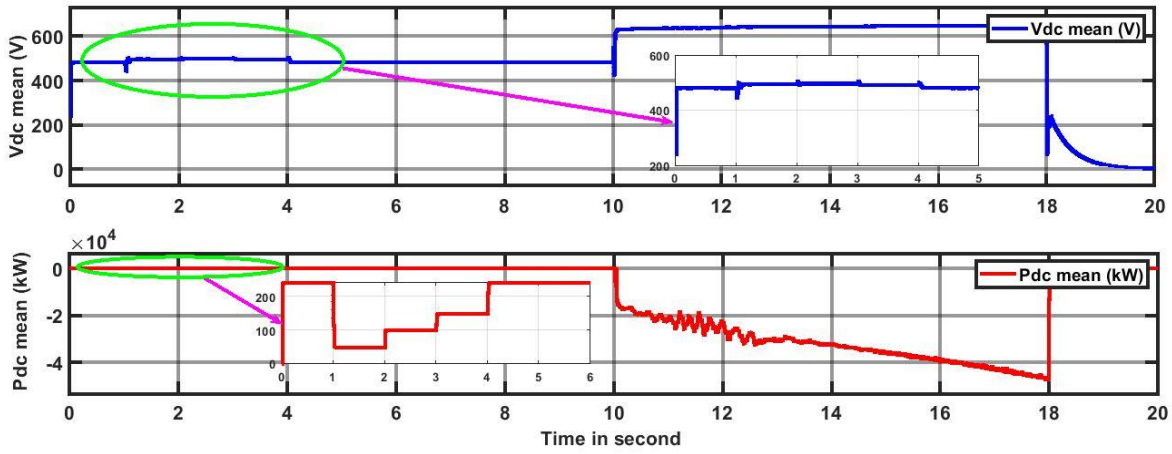

Figure C.11: P_{dc} and V_{dc} grid-connected PV inverter power conversion signal four step-irradiance.

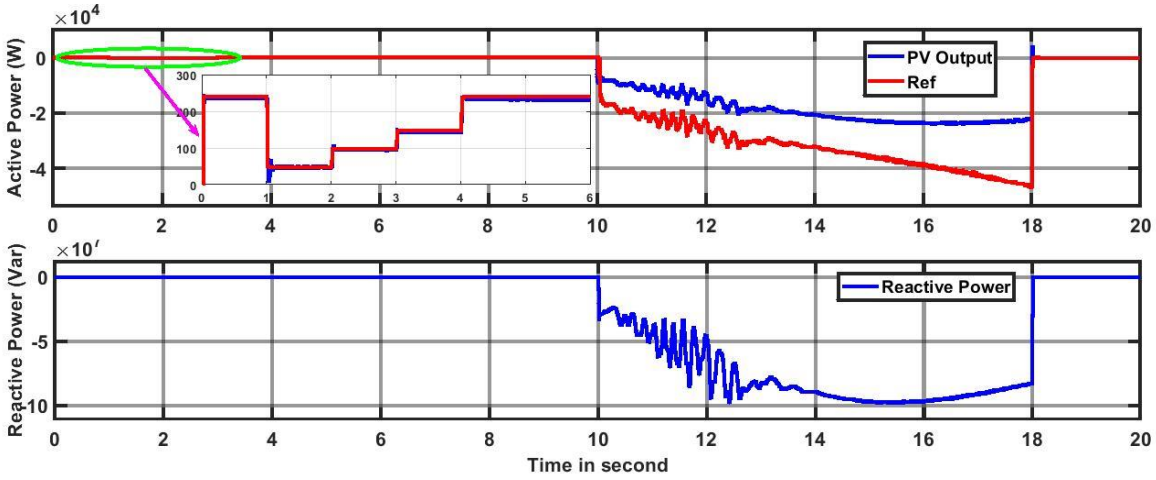

Figure C.12: PV active and reactive power outputs.

C.5.2 Effect of Time Delay without Minimization Methods

The modeling tests showed how much communication latency was accepted by the system in order to maintain the system stability. The impact of time delay was assessed from the following perspectives: without communication delay, as well as with the lowest and maximum communication delays that the system could tolerate in order to maintain acceptable performance. When there was a delay of 900 ms in the generator, the system responded to the failure scenario (G1–G6). As seen in the graph, due to the delay, it took the controller longer to detect the defect and respond to it. The controller could still provide a strong damping performance and efficiently compensate for the delay.

When there was a delay of 900 ms in the generator (G1–G6), it took longer for the controller to respond to the issue. The controller still provided sufficient damping performance. The entire Kigali National Grid (KNG) system, however, grew unstable. The simulation findings from the study implied that low latency communication was required to preserve the system's stability. The longer the communication latency, the slower the control operations, which could lead to power system instability and oscillation. The control system experienced increased system overshoots and longer settling times when network delays grew from 100 ms to 900 ms.

Figure C.13 of the active power and reactive power shows how different changes occurred on the grid when the shunt reactor and the two capacitance banks started to work from 10 s when there was a 7 s inundation of the PV system. At 18 s, there was an impact when the Jali PV plant was disconnected.

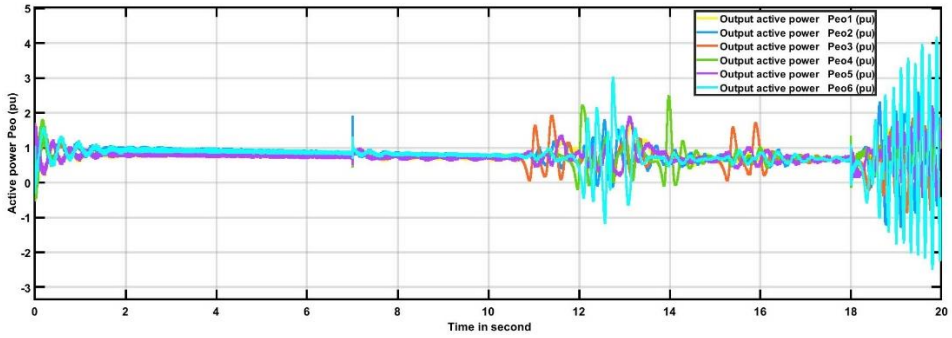

(a)

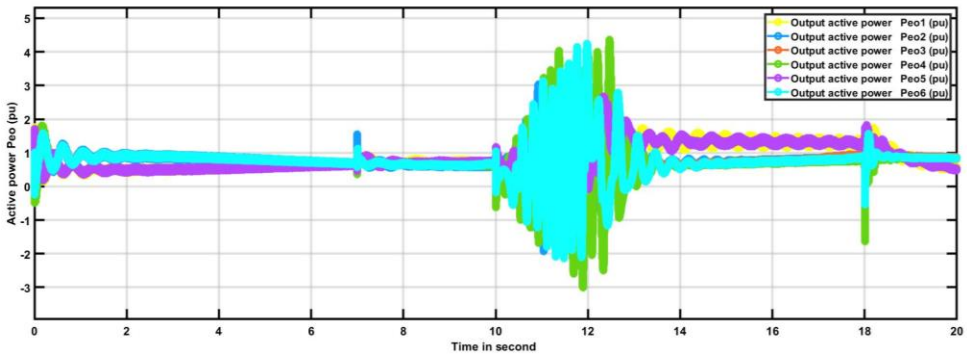

(b)

Figure C.13: System responses to fault scenario with constant time delay of 900 ms (a), 100 ms (b).

C.5.3 The proposed method's performance in terms of the voltage index

In this work, the influence of latency upon the performance of only one fuzzy regulated TSC-TCR was first explored. It was determined that raising the controller signal's significant delay decreased the controller's performance. The voltage responses at the PCC for both permanent and temporary three-line-to-ground (3LG) failures at location A without any controller, no latency, and a 900 ms delay are shown in Figures C.14 and C.15. Table C.4 displays the voltage indicators for such 3LG faults at sites A, B, and C. The indices in Table C.5 show that the delay time degraded the efficiency of the TSC-TCR controller.

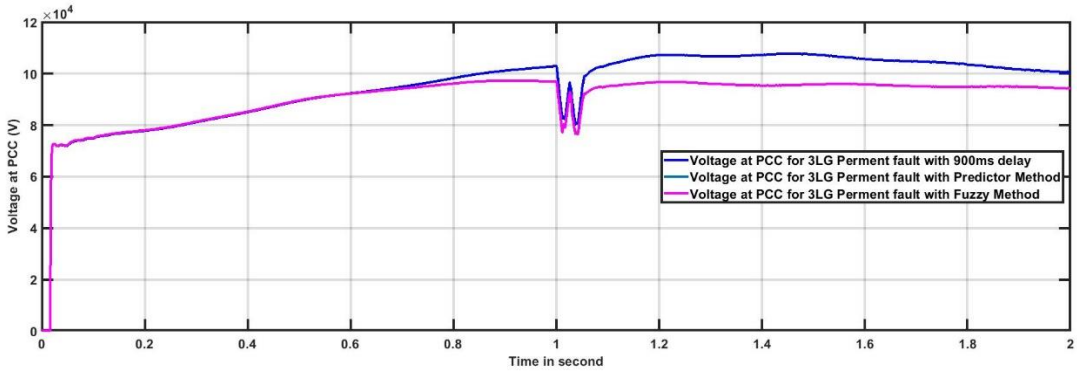

Figure C.14: 3LG permanent faulty PCC voltage at B.

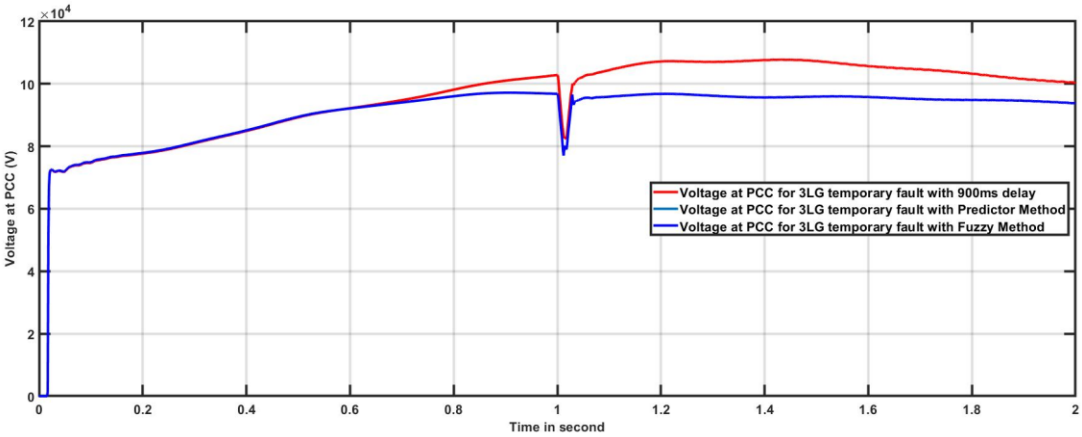

Figure C.15: 3LG temporary faulty PCC voltage at B.

Table C.4 Voltage's indices.

Fault type	Fault point	No Controller	Predictor Method	1-Input fuzzy	1-Input fuzzy +900 ms delay
3 LG Term	A	0.2201	0.1975	0.1797	0.1904
	B	0.2035	0.1932	0.1772	0.1892
	C	0.2201	0.1961	0.1798	0.1905

As previously stated, with the efficiency of a suggested delay reduction strategy, the voltage index V_{index}, presented below, was used, where ΔV represents the total voltage variation of the generators, and T represents the simulation period of 20.0 s. The smaller the index value, the higher the functionalized.

$$V_{index} = \int_0^T |\Delta V| dt \tag{9}$$

Table C.5 shows the voltage indices at the PCC during permanent and temporary 3LG faults with delays approaching 900, 700, 500, 300, and 100 ms at power system locations A, B, and C using the modified predictor-delayed minimization strategy, as well as the fuzzy-regulated delayed reduction technique. The result indicators clearly show that fuzzy controlled methodologies with updated predictor techniques were helpful in decreasing latency issues while improving the system voltage stability. Furthermore, the enhanced prediction approach was outperformed by the fuzzy-regulated strategy.

Table C.5 Voltages Indices at PCC.

Delay Value	Fault Type	Fault Point	Voltage Indices at PCC		
			No compensation	Predictor method	Fuzzy method
900 ms	3LG Temp	A	0.2201	0.1967	0.1797
		B	0.2035	0.1942	0.1772
		C	0.2201	0.1968	0.1798
	3LG Perm	A	0.1973	0.1897	0.1727
		B	0.0521	0.0189	0.0172
		C	0.2088	0.1897	0.1727
700 ms	3LG Temp	A	0.2265	0.1990	0.1823
		B	0.2079	0.1943	0.1773
		C	0.2265	0.1991	0.1741
	3LG Perm	A	0.1975	0.1911	0.1741
		B	0.0660	0.0169	0.0132
		C	0.1975	0.1911	0.1741
500 ms	3LG Temp	A	0.2085	0.1975	0.1805
		B	0.2072	0.1932	0.1762
		C	0.2213	0.1961	0.1791
	3LG Perm	A	0.1885	0.1881	0.1711
		B	0.0848	0.0218	0.0048
		C	0.1885	0.1463	0.1293
300 ms	3LG Temp	A	0.2105	0.1984	0.1804
		B	0.2060	0.1927	0.1747
		C	0.2168	0.1948	0.1768
	3LG Perm	A	0.1960	0.1897	0.1717
		B	0.0715	0.0482	0.3213
		C	0.1995	0.1866	0.1656
100 ms	3LG Temp	A	0.2030	0.1947	0.1767
		B	0.2019	0.1889	0.1720
		C	0.2140	0.1920	0.1742
	3LG Perm	A	0.1857	0.1766	0.1596
		B	0.1117	0.0566	0.0405
		C	0.1664	0.1489	0.1472

A three-phase failure occurred on the Ndera and Gasogi Lines (Line 3–8) for 0.009 s between $t_1 = 1\,sec$ and $t_2 = 0.009\,sec$. The usefulness of TSC-TCR with the fuzzy logic control was demonstrated in this model. Figures C.15 and C.16 depict fuzzy TSC-TCR modelled using

Simulink/MATLAB. When a fault occurred, the TSC-TCR attempted to sustain the voltage by injecting reactive power onto the line if the voltage fell below the reference voltage (1.009 pu). With the fuzzy (TSC-TCR) controller in the system, the PCC terminal voltage oscillated less and stabilized faster, as shown in Figures 14 and 15. When Lines 2–8 failed because of fault B, the terminal inter-area voltage V amounts of inter-areas 1–2, 2–3, 1–3, and 1–4 were also affected, as shown in Figures C.14 and C.15. Figure C.15 shows that the system was constructed with a fuzzy (TSC-TCR) controller. At $t_2 = 1.009$, 0.2 s after the fault was cleared, the controller stabilized the active power differential faster.

Table C.6 demonstrates the PV generator voltage indices for both temporary and permanent 3LG faults at power system locations A, B, and C with 900, 700, 500, 300, and 100 ms delay for the fuzzy-controlled delay reduction approach and the improved predictor delayed optimization methodology. According to indicators, fuzzy-controlled techniques with predictive methods could minimize the delay and improve the voltage profile in the hybrid grid. The improved predictor approach, on the other hand, outperformed the more-fuzzified, regulated strategy.

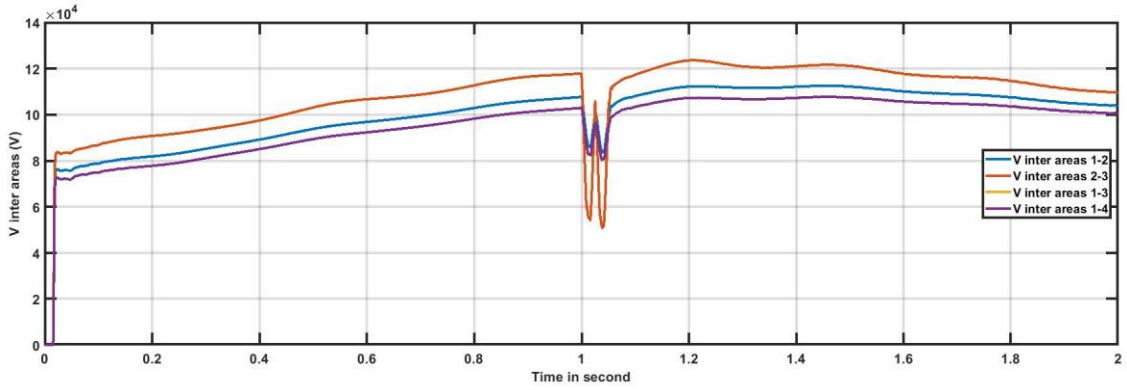

Figure C.16: Inter areas voltage for 3LG permanent fault at B.

Table C.6 Voltage indices of PV plant

Delay Value	Fault Type	Fault Point	Voltage Indices at PCC		
			No compensation	Predictor method	Fuzzy method
900 ms	3LG Temp	A	0.2128	0.1898	0.1698
		B	0.2055	0.1966	0.1776
		C	0.2128	0.1976	0.1776
	3LG Perm	A	0.1090	0.1060	0.0789
		B	0.1651	0.1551	0.1351
		C	0.1828	0.1091	0.0891
700 ms	3LG Temp	A	0.2126	0.2084	0.1894
		B	0.2043	0.1978	0.1778
		C	0.2265	0.1992	0.1802
	3LG Perm	A	0.1059	0.1093	0,0893
		B	0.1659	0.1560	0.1352
		C	0.1827	0.1093	0,0893
500 ms	3LG Temp	A	0.2128	0.2097	0.1897
		B	0.2044	0.2004	0.1814
		C	0.2128	0.2035	0.1845
	3LG Perm	A	0.1061	0.1095	0.0895
		B	0.1669	0.1406	0.1216
		C	0.1819	0.1095	0.0895
300 ms	3LG Temp	A	0.2032	0.2059	0.1876
		B	0.2042	0.2053	0.1844
		C	0.2085	0.2056	0.1846
	3LG Perm	A	0.1059	0.1091	0.0891
		B	0.1655	0.1594	0.1384
		C	0.1678	0.1095	0.0895
100 ms	3LG Temp	A	0.2089	0.2090	0.1872
		B	0.2110	0.2066	0.1756
		C	0.2135	0.2080	0.1915
	3LG Perm	A	0.1062	0.1094	0.0894
		B	0.1664	0.1597	0.1297
		C	0.0111	0.0109	0.0074

C.5.4 Plot Performance of Proposed Risk Mitigation Methods

Figures C.16 and C.17 represent voltage changes at the PCC as a result of both 3LG temporary and permanent failures at location A with a 900 ms delay. The responses show that delayed minimization techniques worked well and enhanced the power performance of the system. In terms of improving hybrid grid power quality, the results also suggest that the fuzzy-logic-controlled strategy beat the modified predictor method. The proposed approach's efficacy in limiting the negative impacts of delay and enhancing the system power quality was proved. Therefore, the fuzzy-logic-controlled technique beat the improved logic-controlled predictor method. Figure C.18 shows the fluctuation in the active power of the generator in the test system (G1–G6). When the three-phase failure occurred, at $t_1 = 1$ the two generators immediately dropped out of the synchronization process.

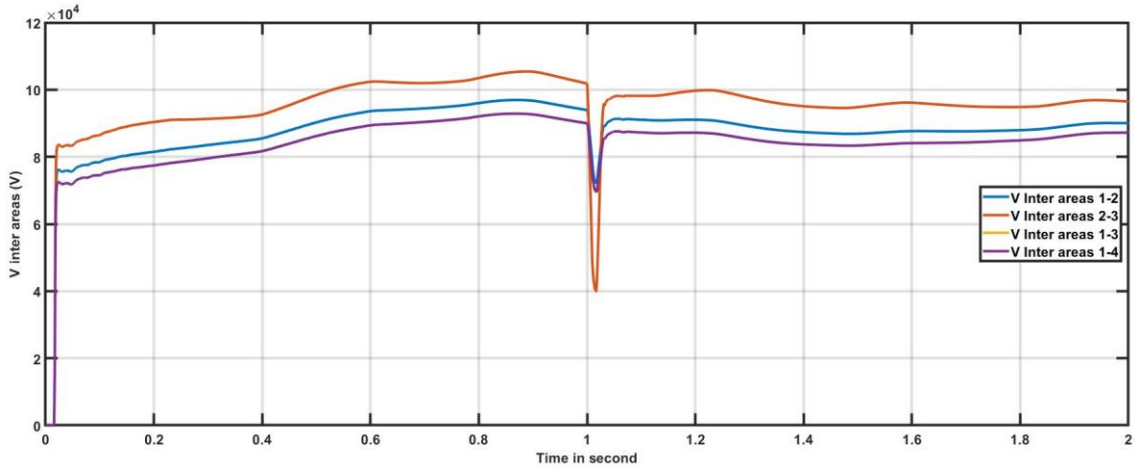

Figure C.17: Inter areas voltage for 3LG temporary fault at B.

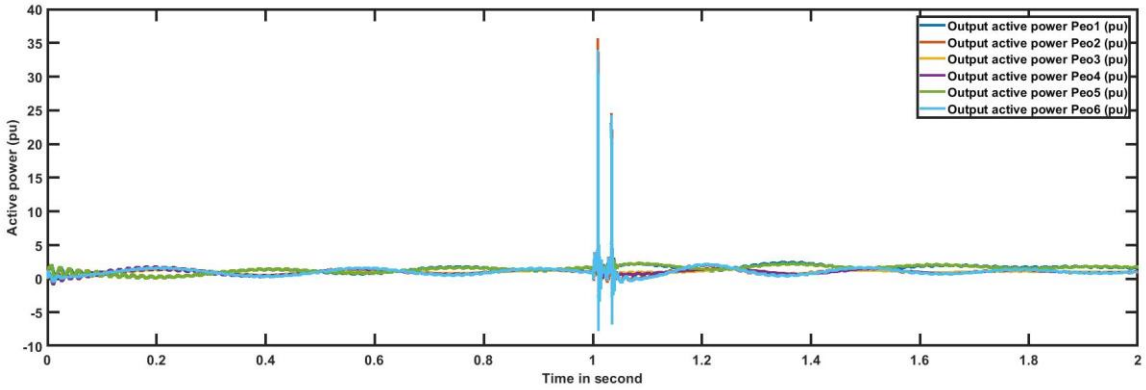

(a)

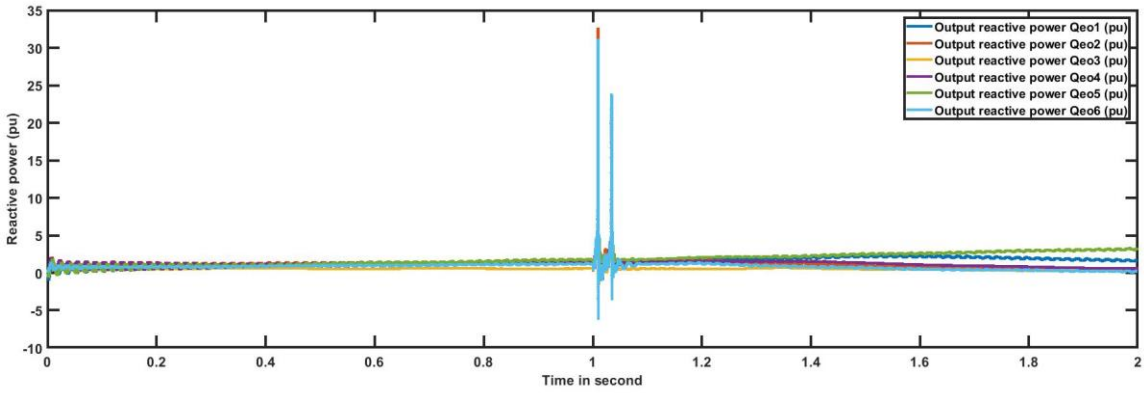

(b)

Figure C.18: Output active and reactive power for 3LG permanent fault at B with constant time delay of 900 ms (a), 100 ms (b).

C.5.5 Methods THD Performance of Suggested Minimization Methods

Equation (10) depicts the total harmonic distortion of the PCC voltage. The THD compares the harmonic currents to a basic element of the voltage or current signal [44], in which V1 is the fundamental voltage, while V2, V3, …, V_n represent cognitive harmonic parts of the PCC voltage [4]:

$$THDu = \frac{\sqrt{(V_2^2 + V_2^2 + V_2^2 + \cdots + V_2^2)}}{V_1} \times 100\% \qquad (10)$$

Table C.7 shows the THD values for both temporary and permanent 3LG faults with 900, 700, 500, 300, and 100 ms delays for the predictor latency reduction approach with the type- 2 fuzzy delay reduction method for power system sites A, B, and C. According to the THDu results, the fuzzy-regulated technique and the prediction method both efficiently minimized the delay effects and increased the system power reliability. In contrast, the enhanced predictor strategy outperformed the fuzzy logic steady electric approach. Furthermore, the oscillations presented a positive way to decrease harmonic currents in the voltage, at which the THDu in the PCC with had no control system with the modified predictor controller, although with type-2 fuzzy controller was proposed in the case of a 3LG temporary fault at location A for the 900 ms delay. The harmonics were shown to be reduced in the settings of the recommended controllers. Furthermore, the enhanced prediction approach was outperformed by the fuzzy-regulated strategy.

Table C.7 Total Harmonic Distortion at PCC.

Delay Value	Fault Type	Fault Point	Voltage Indices at PCC		
			No compensation	Predictor method	Fuzzy method
900 ms	3LG Temp	A	1.5086	1.2950	1.2587
		B	1.6314	1.6116	1.5076
		C	1.5012	1.2954	1.2591
	3LG Perm	A	3.0263	2.1098	1.8618
		B	1.6136	1.0170	1.0043
		C	3.0570	2.3504	2.1024
700 ms	3LG Temp	A	1.5991	1.3768	1.3405
		B	1.5934	1.2957	1.2594
		C	1.5856	1.2186	1.1823
	3LG Perm	A	5.9040	4.3510	3.6399
		B	4.8460	1.6722	1.5682
		C	5.9040	1.4579	1.3559
500 ms	3LG Temp	A	0.7082	0.2515	0.3256
		B	1.4309	0.2999	0.3412
		C	1.2684	0.2515	0.3256
	3LG Perm	A	8.4230	5.8590	5.3300
		B	3.3157	2.1337	1.8857
		C	8.7550	5.9864	5.4574
300 ms	3LG Temp	A	1.1173	0.2832	0.3489
		B	1.2487	0.6805	0.7429
		C	1.2663	0.2145	0.3045
	3LG Perm	A	6.3820	4.5632	4.3752
		B	3.9496	2.1593	1.9713
		C	5.5660	3.8029	3.1509
100 ms	3LG Temp	A	1.0109	0.3693	0.3861
		B	1.2750	0.3627	0.3854
		C	1.2105	0.2981	0.3124
	3LG Perm	A	5.3580	4.6171	4.1621
		B	3.5670	3.1431	2.4911
		C	3.3347	3.0456	2.9016

Each of these methods was useful in assessing the impact of antitraumatic activities caused by errors occurring in three different locations. Thus, Table C.8 outlines the pros and cons of each, indicating the advantages and disadvantages of certain approaches.

Table C.8: Advantages and disadvantages of FLC and MPM control techniques.

Approach's	Advantages	Disadvantages
Fuzzy Logic Control method	1. Uncertainties could be handled to a certain level 2. Good robustness (High precision THDu), strong anti-interference ability, no need for precise models	1. FLC is not useful for programs that are much smaller or larger than historical data 2. Poor ability to generalize outside the training range 3. For more accuracy, needs more fuzzy grades wich results to increase exponentialyy the rule
Modified Predictor Method	1. Provides good performance (THDu) in the especially when having very small changes ΔV at Point B. 2. Strong robustness, low requirements for model accuracy.	1. Heavy calculations, not suitable for fast time-varying systems

C.5.6 Nonlinear Load Harmonic Spectrum

The study's harmonic power flow types were employed for network distribution in three-phase balanced and unbalanced categories. At the specified time domain, the coordinating force was applied. Connectivity was also achieved in a number of other harmonic modes. The previous harmonic list employed in the research included seven spectra. Figure C.19 depicts the harmonic spectra in the form of the voltage, current, and nonlinear properties of the PCC employed in this investigation.

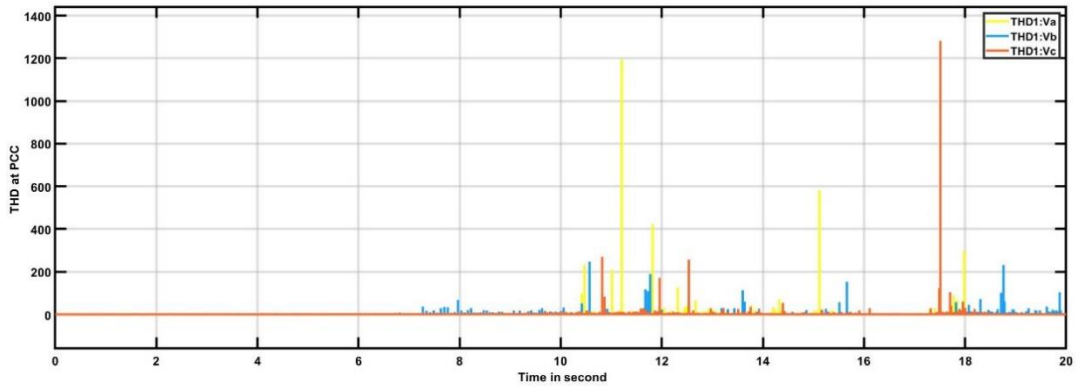

(a)

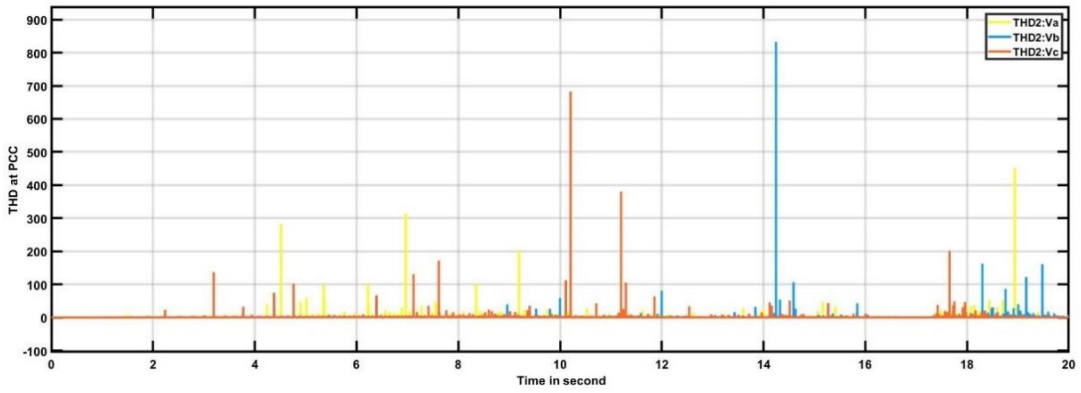

(b)

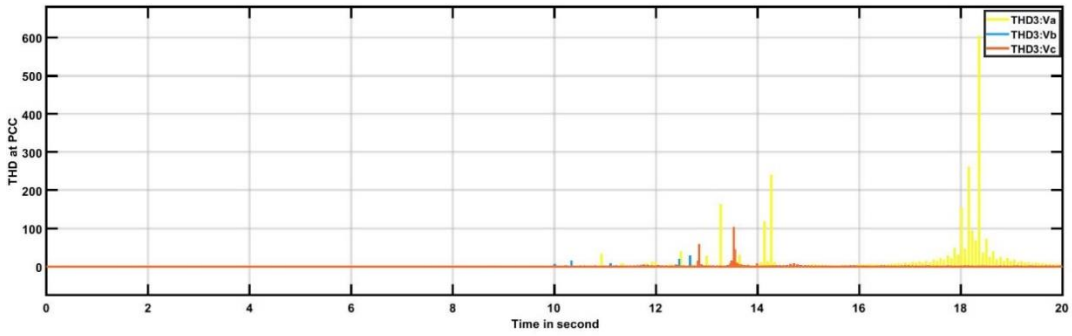

(c)

Figure C.19: Harmonic spectrum of voltage in PCC for (a) no control, (b) predictor controller, and (c) fuzzy controller methods.

C.5.7 TSC and TCR's cost-effectiveness

Surprisingly, TSC-TCR is an expensive tool that is becoming increasingly important in energy systems due to key features such as high speed, efficiency, and real-power management capabilities, among others [25–35]. Depending on their potential benefits and the environment, parts of the TSC-TCR system are expected to offer better storage and use to facilities in the future [36–40]. While the price of the TSC-TCR components may appear high at the moment, long-term research and development is expected to lower prices and improve grid security technology.

C.6 Conclusions

The impact of time delays on a mixed electric grid was investigated in this work, and two approaches for minimizing the bad consequences of latency affecting TSC-TCR electric improvements were proposed. Temporary and permanent faults, both balanced and unbalanced,

were considered at various locations throughout the power network. Based on the simulation results, the following conclusions and recommendations can be drawn:

1) The presented strategies were suitable in minimizing the negative impact of significant delays on the hybrid power system power quality improvement;
2) In most cases, fuzzy-controlled methods represented excellent alternatives to modified predictor methods;
3) It was possible that the burden could be controlled if the response was fast (less than 1 s), which could help in inertia response;
4) The plan to use SVCs and shunt reactors is not enough when using TSC-TCR (in the REG situation of resolving the Shango SS1 and Bugesera SS11 connection problems).

Other creative techniques, such as genetic algorithms and branch-and-bound methods, should be developed and evaluated in the future, allowing the application of fuzzy MPC methods to reduce the detrimental impact of random delays. In addition, delays caused by cyber-attacks should also be evaluated, as well as relevant mitigation strategies. Moreover, it would be fascinating to demonstrate the efficacy of the suggested approaches in a big power grid, such as the IEEE 118-bus test system and others, where THDu values can exceed 10%.

Author Contributions: Conceptualization, D.M., L.K.L. and B.B.M.; methodology, D.M., L.K.L. and B.B.M.; investigation, D.M., L.K.L. and B.B.M.; writing—original draft preparation, D.M.; writing—review and editing, D.M., L.K.L. and B.B.M.; supervision, L.K.L. and B.B.M.; funding acquisition, L.K.L. All authors have read and agreed to the published version of the manuscript.

Funding: This research was partially funded by the African Center of Excellence in Energy for Sustainable Development, University of Rwanda (research core funding no. ACE II-017).

Data Availability Statement: The data given in this study are available on request from the corresponding author.

Acknowledgments: The first author would like to thank the African Center of Excellence in Energy for Sustainable Development (ACEESD), University of Rwanda (UR), for their support in this investigation. The second author appreciates the opportunity presented to conduct more research and learn more by the Department of Electrical and Communications Engineering, Moi University. The third author recognizes the Department of Mechanical and Energy Engineering, University of Rwanda (UR), for their support in strengthening the role of successful systems of knowledge and technology in short-term analysis.

Conflicts of Interest: The authors declare no conflict of interest.

References

[1] Muyizere, D.; Letting, L.K.; Munyazikwiye, B.B. Effects of Communication Signal Delay

on the Power Grid: A Review. *Electronics* **2022**, *11*, 874. [CrossRef]
[2] Chompoobutrgool, Y.; Vanfretti, L.; Ghandhari, M. Survey on power system stabilizers control and their prospective applications for power system damping using Synchrophasor-based wide-area systems. *Eur. Trans. Electr. Power* **2011**, *21*, 2098–2111. [CrossRef]
[3] Li, M.; Chen, Y. A Wide-Area Dynamic Damping Controller Based on Robust H¥ Control for Wide-Area Power Systems with Random Delay and Packet Dropout. *IEEE Trans. Power Syst.* **2018**, *33*, 4026–4037. [CrossRef]
[4] Ghosh, S.; Ali, M.H. Minimization of Adverse Effects of Time Delay on Power Quality Enhancement in Hybrid Grid. *IEEE Syst. J.* **2019**, *13*, 3091–3101. [CrossRef]
[5] Khalili, M.; Ali Dashtaki, M.; Nasab, M.A.; Reza Hanif, H.; Padmanaban, S.; Khan, B. Optimal instantaneous prediction of voltage instability due to transient faults in power networks taking into account the dynamic effect of generators. *Cogent Eng.* **2022**, *9*, 2072568. [CrossRef]
[6] Salman, G.A.; Abood, H.G.; Ibrahim, M.S. Improvement the voltage stability margin of Iraqi power system using the optimal values of FACTS devices. *Int. J. Electr. Comput. Eng.* **2021**, *11*, 984–992. [CrossRef]
[7] Aikins, L.; Kwaku Amuzuvi, C. Power System Stability Improvement of Ghana's Generation and Transmission System Using FACTS Devices. *J. Electr. Electron. Eng.* **2020**, *8*, 47. [CrossRef]
[8] Hoseynpoor, M.; Najafi, M.; Ebrahimi, R.; Davoodi, M. Power system stability improvement using comprehensive FACTS devices. *Int. Rev. Model. Simul.* **2011**, *4*, 1660–1665.
[9] Stahlhut, J.W.; Browne, T.J.; Heydt, G.T.; Vittal, V. Latency viewed as a stochastic process and its impact on wide area power system control signals. *IEEE Trans. Power Syst.* **2008**, *23*, 84–91. [CrossRef]
[10] Mokhtari, M.; Zouggar, S.; M'sirdi, N.K.; Elhafyani, M.L. Voltage regulation of an asynchronous wind turbine using statcom and a control strategy based on a combination of single input fuzzy logic regulator and sliding mode controllers. *Int. J. Power Electron. Drive Syst.* **2020**, *11*, 1557–1569. [CrossRef]
[11] Liu, S.; Wang, X.; Liu, P.X. Impact of Communication Delays on Secondary Frequency Control in an Islanded Microgrid. *IEEE Trans. Ind. Electron.* **2015**, *62*, 2021–2031. [CrossRef]
[12] Amin, M.; Al-Durra, A.; Elmannai, W. Experimental Validation of High-Performance HIL Based Real-Time PMU Model for WAMS. *IEEE Trans. Ind. Appl.* **2020**, *56*, 2382–2392. [CrossRef]
[13] Fan, Z.; Kulkarni, P.; Gormus, S.; Efthymiou, C.; Kalogridis, G.; Sooriyabandara, M.; Zhu, Z.; Lambotharan, S.; Chin, W.H. Smart grid communications: Overview of research challenges, solutions, and standardization activities. *IEEE Commun. Surv. Tutor.* **2013**, *15*, 21–38. [CrossRef]
[14] Nan, J.; Yao, W.; Wen, J.; Peng, Y.; Fang, J.; Ai, X.; Wen, J. Wide-area power oscillation

damper for DFIG-based wind farm with communication delay and packet dropout compensation. *Int. J. Electr. Power Energy Syst.* **2021**, *124*, 106306. [CrossRef]
[15] Liu, M.; Dassios, I.; Milano, F. Delay margin comparisons for power systems with constant and time-varying delays. *Electr. Power Syst. Res.* **2021**, *190*, 106627. [CrossRef]
[16] Bimali, B.; Uprety, S.; Pandey, R.P. VAR Compensation on Load Side using Thyristor Switched Capacitor and Thyristor Controlled Reactor. *J. Inst. Eng.* **2021**, *16*, 111–119. [CrossRef]
[17] Ghaeb, J.A.; Alkayyali, M.; Tutunji, T.A. Wide Range Reactive Power Compensation for Voltage Unbalance Mitigation in Electrical Power Systems. *Electr. Power Compon. Syst.* **2022**, *49*, 715–728. [CrossRef]
[18] Li, Y.; Zhou, Y.; Liu, F.; Cao, Y.; Rehtanz, C. Design and Implementation of Delay Dependent Wide-Area Damping Control for Stability Enhancement of Power Systems. *IEEE Trans. Smart Grid* **2017**, *8*, 1831–1842. [CrossRef]
[19] Zappone, A.; Sanguinetti, L.; Debbah, M. Energy-Delay Efficient Power Control in Wireless Networks. *IEEE Trans. Commun.* **2018**, *66*, 418–431. [CrossRef]
[20] Sargolzaei, A.; Yen, K.K.; Abdelghani, M.N. Preventing Time-Delay Switch Attack on Load Frequency Control in Distributed Power Systems. *IEEE Trans. Smart Grid* **2016**, *7*, 1–10. [CrossRef]
[21] Molina-Cabrera, A.; Ríos, M.A.; Besanger, Y.; Hadjsaid, N.; Montoya, O.D. Latencies in power systems: A database-based time-delay compensation for memory controllers. *Electronics* **2021**, *10*, 208. [CrossRef]
[22] Musleh, A.S.; Muyeen, S.M.; Al-Durra, A.; Kamwa, I.; Masoum, M.A.S.; Islam, S. Time Delay Analysis of Wide-Area Voltage Control Considering Smart Grid Contingences in a Real-Time Environment. *IEEE Trans. Ind. Inform.* **2018**, *14*, 1242–1252. [CrossRef]
[23] Ullah, U.; Khan, A.; Altowaijri, S.M.; Ali, I.; Rahman, A.U.; Vijay Kumar, V.; Ali, M.; Mahmood, H. Cooperative and delay minimization routing schemes for dense under water wireless sensor networks. *Symmetry* **2019**, *11*, 195. [CrossRef]
[24] Hai-Long, Z.; Guo-Yi, Z. A time synchronization method of power grid based on TD LTE frame synchronization. In Proceedings of the IEEE Power and Energy Society General Meeting, Chicago, IL, USA, 1 February 2018; pp. 1–5. [CrossRef]
[25] Padhy, B.P. Adaptive latency compensator considering packet drop and packet disorder for wide area damping control design. *Int. J. Electr. Power Energy Syst.* **2019**, *106*, 477–487. [CrossRef]
[26] Zhang, F.; Cheng, L.; Li, X.; Sun, Y.Z. A Prediction-Based Hierarchical Delay Compensation (PHDC) Technique Enhanced by Increment Autoregression Prediction for Wide-Area Control Systems. *IEEE Trans. Smart Grid* **2020**, *11*, 1253–1263. [CrossRef]
[27] Park, J.; Jang, G.; Son, K.M. Modeling and control of VSI type FACTS controllers for power system dynamic stability using the current injection method. *Int. J. Control Autom. Syst.* **2008**, *6*, 495–505. [CrossRef]
[28] Zand, M.; Nasab, M.A.; Hatami, A.; Kargar, M.; Chamorro, H.R. Using adaptive fuzzy

logic for intelligent energy management in hybrid vehicles. In Proceedings of the 2020 28th Iranian Conference on Electrical Engineering, ICEE 2020, Tabriz, Iran, 4–6 August 2020. [CrossRef]

[29] Manikandan, S.; Kokil, P. Stability analysis of load frequency control system with constant communication delays. In Proceedings of the 6th Conference on Advances in Control and Optimization of Dynamical Systems ACODS 2020, Chennai, India, 16–19 February 2020. *Electronics* **2022**, *11*, 3114 21 of 21[CrossRef]

[30] Rwanda Energy Group. Rwanda: Least Cost Power Development Plan (LCPDP) 2020 2040. Nyarugenge City, Kigali-Rwanda. 2021. Available online: https://www.reg.rw/fileadmin/user_upload/Least_Cost_Power_Development_Plan_2020 2024.pdf (accessed on 17 May 2022). [CrossRef]

[31] Rwanda Energy Group. Rwanda Electricity Distribution Master Plan. June 2021 Revision. 2021. Available online: https: //www.reg.rw/fileadmin/user_upload/Rwanda_Electricity_Distribution_Master_Plan.PD (accessed on 17 May 2022). [CrossRef]

[32] Rwanda Energy Group Limited. Annual Report For Rwanda Energy Group, of the Year 2019–2020. District, Nyarugenge City, Kigali-Rwanda. 2020. Available online: https://www.reg.rw/fileadmin/REG_ANNUAL_REPORT_2020-2021_V3.pdf (accessed on 30 September 2021). [CrossRef]

[33] Rwanda Energy Group (REG). Transmission Master Plan for Rwanda Plan (2020–2028). No. June. 2019, pp. 1–57. Available online: https://www.reg.rw/fileadmin/user_upload/Rwanda_Transmission_Master_Plan_2020_-_2028.pdf (accessed on 30 June 2021). [CrossRef]

[34] Rwanda Energy Group (REG). Distribution. Available online: https://www.reg.rw/what we-do/distribution/ (accessed on 17 May 2022). [CrossRef]

[35] Shukla, S. Smart ANN Controller for TCR/TSC Devices used in Power System Applications. *Int. J. Emerg. Trends Eng. Res.* **2020**, *8*, 3534–3537. [CrossRef]

[36] Jing, W.; Chang, F.; Wang, G.; Chen, J. Research on TSC control strategy based on the average of TCR threephase trigger angles. *Zhongshan Daxue Xuebao/Acta Sci. Natralium Univ. Sunyatseni* **2021**, *60*, 54–61. [CrossRef]

[37] Awad, F.; Mansour, A.; Elzahab, E.A. Reduction of harmonics generated by thyristor controlled reactor for RL loads. In Proceedings of the ACCS/PEIT 2017–2017 International Conference on Advanced Control Circuits Systems and 2017 International Conference on New Paradigms in Electronics and Information Technology, Alexandria, Egypt, 5–8 November 2017. [CrossRef]

[38] Gamal, M.; Sadek, N.; Rizk, M.R.M.; Abou-Elsaoud, A.K. Delay compensation using Smith predictor for wireless network control system. *Alex. Eng. J.* **2016**, *55*, 1421–1428. [CrossRef]

[39] Mokhtari, M.; Aminifar, F.; Nazarpour, D.; Golshannavaz, S. Wide-area power oscillation damping with a fuzzy controller compensating the continuous communication delays. *IEEE*

Trans. Power Syst. **2013**, *28*, 1997–2005. [CrossRef]
[40] Tiep, D.K.; Lee, K.; Im, D.Y.; Kwak, B.; Ryoo, Y.J. Design of fuzzy-PID controller for path tracking of mobile robot with differential drive. *Int. J. Fuzzy Log. Intell. Syst.* **2018**, *18*, 220–228. [CrossRef]
[41] Hossain, M.K.; Ali, M.H. Transient Stability Augmentation of PV/DFIG/SG-Based Hybrid Power System by Nonlinear ControlBased Variable Resistive FCL. *IEEE Trans. Sustain. Energy* **2015**, *6*, 1638–1649. [CrossRef]
[42] Muyizere, D.; Letting, L.K.; Munyazikwiye, B.B. Under-frequency Load Shedding on the Performance Time Delay Relays of Transmission lines with difference Controllers. In Proceedings of the 2021 IEEE Southern Power Electronics Conference, SPEC 2021, Kigali, Rwanda, 6–9 December 2021. [CrossRef]
[43] Ghosh, S.; Ali, M.H. Minimization of adverse effects of time delay in smart power grid. In Proceedings of the 2014 IEEE PES Innovative Smart Grid Technologies Conference, ISGT 2014, Washington, DC, USA, 19–22 February 2014. [CrossRef]
[44] Nasini, P.R.; Narra, N.R.; Santosh, A. Modeling And Harmonic Analysis Of Domestic/Industrial Loads. *Int. J. Eng. Res. Appl.* **2012**, *2*, 485–491. [CrossRef]

Paper D

Title:	Effect on transient stability and analyses resulting from a cyber-attack on frequency relay device
Authors:	Darius Muyizere[1*], Lawrence K. Letting [1,2] and Bernard B. Munyazikwiye[1,3]
Affiliation:	[1] African Centre of Excellence in Energy and Sustainable Development, College of Science and Technology, University of Rwanda, KN 67 Street Nyarugenge, Kigali P.O. Box 3900, Rwanda [2] Department of Electrical & Communications Engineering, Moi University, Eldoret 30100, Kenya [3] Department of Mechanical and Energy Engineering, College of Science and Technology, University of Rwanda, KN 67 Street Nyarugenge, Kigali P.O. Box 3900, Rwanda
Article:	International Journal of Performability Engineering https://doi.org/10.23940/ijpe.23.01.p3.2032.
Layout:	The format of the paper has already been altered to match that of the thesis.

Paper D: **Effect on transient stability and analyses resulting from a cyber-attack on frequency relay device**

***Abstract* — Intelligent networks are the common form of cyber-physical networks, which provide a strong connection between cyber communications and physical networks. As smart grid applications and technologies are developed and put into use, cyber security is becoming a serious problem. Therefore, it is crucial to research how cyber-attacks effect on frequency relay device of the smart grids. The impact of cyber-attacks that cause information network latency and their effects on transient stability are covered in this research. The cyber-attacks were carried out using measurement results devices, such as an SVC or STATCOM linked to such grid. This study suggests two new approaches created on nonlinear controller (NL) and PI controller to mitigate the adverse special effects of cyber-attacks on the mentioned-on relay, and a new detection and mitigation method based on the voltage starting point for the FACTS. Case studies that examine the effects of fixed communication delays on transient stability of voltage and angle on the grid system are provided. Two methods of cyber-attack are reviewed and their impacts are demonstrated using the MATLAB Simulink-implemented Kigali national grid (KNG). According to simulation studies, a number of network delays brought on by cyber-attacks can cause the system to become unstable. Then, suggestions are made to improve electrical security in the event of cyber-attacks, damage and delay in the future power system grids against potential cyber-attacks.**

***Keywords*:** Smart grid, cyber-attacks, network delays, transient stability, SVC and STATCOM, Kigali national grid (KNG).

D.1 Introduction

Electrical utility systems are increasingly integrating technological devices with sophisticated surveillance and control applications to run into the needs of the future energy infrastructure. This encourages the creation of intelligent grids, which are intended to contain considerable amounts of distributed generation units, decrease carbon emissions, and manage electricity supply in a dependable and efficient manner [1].

To improve power system operations, several power network technologies, which including Advanced Metering Infrastructure (AMI), Flexible AC Transmission System (FACTS), Wide Area Metering System (WAMS), and Demand Response (DR), are widely used. The primary aspect of these apps is their dependence on enhanced two-way connectivity, which therefore unavoidably exposes them to cyber-attacks.[2][3]. In addition, the topographical thinning out of

smart grids also provides an opportunity for potential attackers to carry out a cyber-attack or a physical attack [4].

To investigate the consequences of cyber-attacks on electrical network, a variety of approaches have been implemented, including risk evaluation, framework design, test platform design, and computer hackers modeling. Power system cyber vulnerabilities have been found in [5], [6]. A methodology for analyzing the effects of cyber-attacks was put out in Reference [7], employing engaged diagrams to characterize both the cyber and physical units. Some academics have focused on the network latency brought on by Denial-of-Service (DoS) cyber-attacks in order to study the influence of cyber-attacks [8]. A logic-controlled brake resistor was subjected to a series of predetermined delays in Reference [9]. A significant delay might cause the test system to become unstable, according to simulation results in the research [10].

There are various test beds which utilize use of "co-simulation" technologies have been created recently in instruction to improved analyze the interplay in the middle of fake communications and physical control systems. In [11], researchers created a test environment in lieu of SCADA security study and executed a Distributed DoS attack at digital substations, subsequent in transmission line overload. Researchers created another test bed in [12], where a concerted DoS assault was launched against the control center of distributed energy resources (DERs). The network latency caused a line to become overloaded.

The authors have previously studied the effects of cyber-attacks conducted against a a static synchronous compensator (STATCOM) and a static var compensator (SVC) on the stability of the power system during transient periods [13]. In order to mitigate the effects of flicker and maintain the voltage level, static var compensators (SVC) are addressed concerns about computer hackers on electric arc furnaces (EAFs), that could lead to connectivity concerns in SVC measuring data or relevant information [14]. A variation attack occurred against an SVC in [15], and simulation results revealed that when strong positive biases were used, the generators might lose synchronization. It is demonstrated in [10] that a cyber-attack on an SVC may result in system angle and voltage instability, which is followed by physical failures. In [16] discusses a few cyber-attacks on FACT devices used in power systems. This study demonstrates that an SVC might be a possible target for a cyber-attack by an enemy looking to breach the EAF system.

To address this issue with cyber-attacks, this effort goes through one of the essential parts of a smart grid, voltage boost plans like SVC and STATCOM are utilized for VAR adjustment to enhance electrical energy transfer. There are many forms of cyber-attacks that can target the communication paths between the control center, measurement unit, and field operation[17]. Therefore, it is essential to research how unstable voltage support devices affect system stability.

The power grid behavior during faults and cyber-attacks could be significantly different and need in the direction of be considered while performing a risk assessment [18]. The preceding study assumes that network delays are exclusively caused by cyber-attacks, disregarding the regular network delays that are present throughout data transfer. In addition, it is in the past that the concentration is always assumed to be constant in the dynamic-flow analysis, which is not taken into account in the steady-static analysis. Moreover, the steady-state analysis cannot handle sequential switching events as well as post-disruption response. To address these gaps, this paper studies the dynamic effects of network latency analyses of a real interconnected power system during different types of cyber-attacks and network delay. However, the researchers have only examined the effects of one type of attack, which is the time delay switch, and the analysis of the effects of different types is not clear. Common switching attacks, data integrity attacks and DoS attacks are the most likely to cause false traffic-commands on relays.

As a result, this paper presents an experimental transient stability study based of the results during several cyber-attack study of frequency relay on the Kigali National Grid (KNG) bus system is presented. As an outcome, the hard work done in this research provide a new wide scope for investigating that creating new network delay induced by cyber-attacks detection and mitigation strategies that make use of nonlinear process reactions system features.

The remains of the paper is prearranged this way. Section D.2 focuses on cyber-attacks on network communication. Section D.3 reviews control of the voltage in the power system and stable transients. In section D.4, the description of a simulation results and discussion. In last Section D.5, this paper concludes the conclusion of this research and future directions.

D.2. Network communication cyber attacks

A collection of protective settings for a digital frequency relay—the primary target of cyber-attacks—that include built-in digital logic processing capacity are addressed in this section. Figure D.1 depicts a simplified schematic representation of the digital under and over frequency relay. Communication methods that allow operators and customers to obtain the information instantly are being incorporated into smart grids more often. This necessitates data transmission between the switch center and end consumers, considerably facilitating power network operation [10]. Meanwhile, new cyber vulnerabilities are always being developed. A cyber-attack like a denial-of-service attack, manipulation attack, Restart communication attack and Switching attack, etc. can be readily carried out by a possible threat who is acquainted with network topologies [5][16][17]. The emphasis of this research is network latency because it is the cyber-attack result that is most frequently highlighted. This part describes cyber-attacks on transceivers technologies that result in system delays.

D.2.1 Cyber-attacks delaying the network

Propagation, transmission, queuing, and processing delays are all types of network delays. Cyber-attacks that are successful can 1) lengthen the line to increase transmission and queuing delays, and 2) use compute resources to increase processing delays. Since many of the protocols used in the existing power system are not sufficiently safeguarded, attackers may launch a variety of cyber-attacks [20]. The following introduces common cyber-attacks that cause network lag.

D.2.1.1 DoS attack

In an attempt to destroy resources, denial-of-service attacks aim transport network and system programs. Two denial-of-service assaults are included in the data sets. The improper cyclic redundancy code (CRC) attack injects numerous network packets into a network with incorrect CRC values. The network master traffic jamming method applies a non-addressed slave address to send accidental information to random end point addresses indefinitely.

DOS assaults on the cyber system try to deactivate applications operating on system endpoints that operate the system, log data, and manage communications. DOS attacks on the physical system range from control device, switch opening and closing to the destruction of elements of the physical development that avoid action. This paper focuses on denial-of-service attacks on the communication system.

D.2.1.2 Switching attack

Switching attacks are often relay tripping attempts or assaults on the switching mechanism that alter the CB's mode of operation. Considered is a stochastic shifting vector input $S(x,t)\epsilon\mathbb{R}^{m\times 1}$, wherever $S(x,t)$ determines as soon as a specific breaker should be opened or closed for a certain switching attack.

$$S(x,t) = [S_1 S_2 \dots S_m]^T = [00 \dots 0]^T \quad (1)$$

Where m is the quantity of under attack CB, might be the attack vector. A numerical relay, which panels the tie-line CBs and may potentially have an influence on the protection of a generator substation, is vulnerable to a mischievous switching physical attack from an outside attacker [18]. Such assaults may separate the generating substation from the break of the grid and knock out a particular interconnector in the middle of two locations, which will impact the flow of power through tie lines.

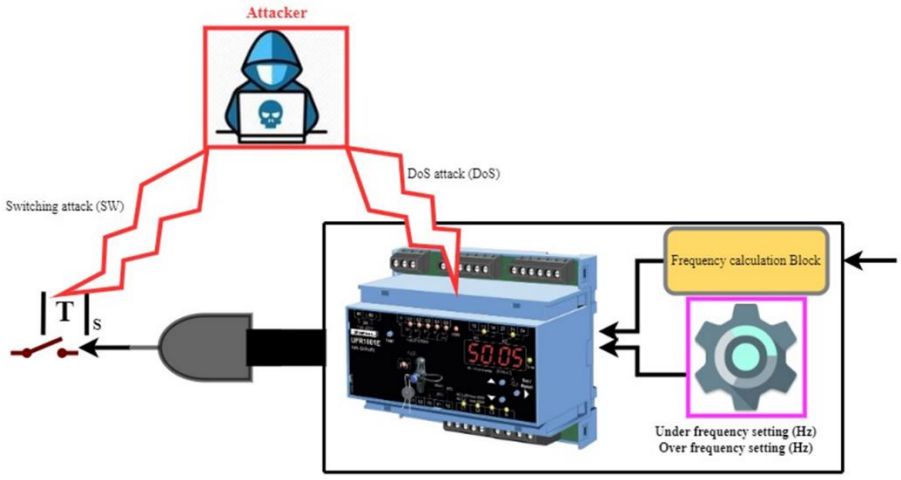

Figure D.1: Attacks on comparable distributed generator circuit with a frequency relay that operates synchronously with a utility.

D.2.2 Modeling for network delays

The latency throughout this study is simulated using one of the most extensively adopted delay models in sensor network examination: constant interruption [21][22]. By changing the communication link's constant values, it is simple to mimic fixed delay. A pseudo random seed can be used to produce an exponential distributed delay at random. Because it is created at random, we refer to it as "random delay." An exponential distributed delay's probability density function (pdf) [23] may be described as follows:

$$f(x;\beta) = \begin{cases} \frac{1}{\beta} e^{-x/\beta}, & x \geq 0 \\ 0, & x < 0 \end{cases} \tag{2}$$

When the exponential distribution's mean value is the scale parameter $\beta > 0$, which is a distributional constant. Larger delays may be seen when β is increased.

D.3 Control of the voltage in the power system and stable transients

D.3.1 Control of power system voltage

Power system security operation is very concerned with the stability of the contemporary, linked power system [24]. Bus voltages are crucial to the stability of the power system. System instability and even a voltage collapse might be brought on by poor voltage profiles. Therefore, maintaining bus voltage within a reasonable range is crucial for the proper operation of the power system and voltage regulation. An effective voltage control technique to increase the constancy of the power

system voltage is reactive power compensation. In addition to excitation switch in generating units, Power electronics have lately grown in favor because of their quick reactive power management [10][25].

D.3.2 Cyber-attacks on SVC and STATCOM

The typical components of an FCTS are an SVC and STATCOM controller, at least one activator, such as a thyristor switched capacitor (TSC) and a thyristor controlled reactor (TCR) [26]. Measurement signals are received by the SVC controller from a distributed wireless or wired network. This is a collection. Depending on the control technique used by the SVC controller, the signal may originate from nearby measuring tools in the similar substation or/and from a distant bus. Cyber-attacks, like those described in section II, can be launched by a prospective attacker to impede the transmission of data from sensing devices to a controller and then from the controller to the operator.

By communications resonance appeal packets with an SVC, STATCOM controller's IP address, for instance, a hacker can launch a switching or DoS attack using getting plenty of additional network components should respond with Network interface. A lot of information volumes lengthen processing and waiting times. By changing the time stamp of packets, a switching attack may also be used to impede communication between a sensor and a controller. The SVC and STATCOM control blocks are represented in Figure D.2 and Figure D.3. The voltage at Mount Kigali SSB 9 bus is linked to the situation value, and the difference is then transmitted via a PI or NL controller to calculate the shunt capacitance. By adding a cyber-attack bolted fault on frequency relay, two case studies were performed.

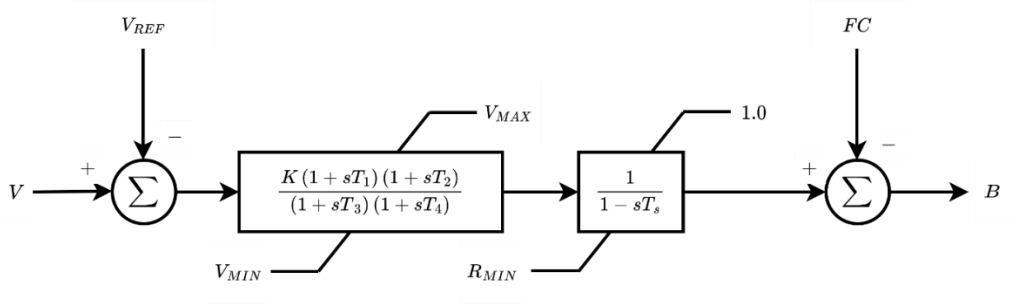

Figure D.2: Schematic of the SVC control loop

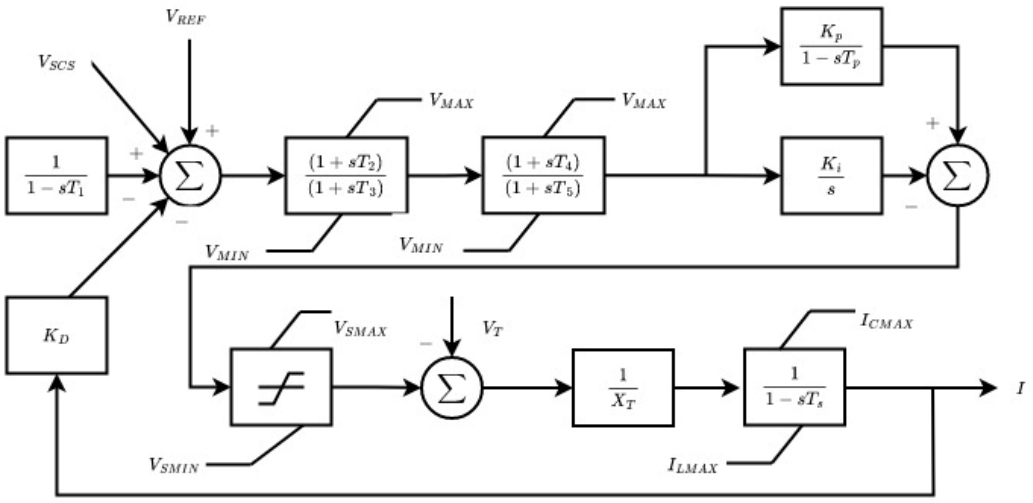

Figure D.3: Schematic of the STATCOM control loop.

D.3.3 Suggested Control Algorithms

Various types of electrical network flaws take a direct effect on PCC voltage. Therefore, restoring the PCC voltage as soon as possible to the necessary level following cyber-attacks is our main objective. To reduce the negative effects of cyber-attacks on the SVC and STATCOM system two types of controllers have been proposed in this work: a basic non-linear controller and a PI controller. The fundamental algorithm for the suggested detection and mitigation strategies is depicted in Figure D.4. The PCC voltage serves as the proposed controller's input. The voltage deviation (V_{pcc}) at the PCC is checked as the first step in the planned detection and moderation method. Any variation, if present, denotes one or the other a network issue or a cyber-attack.

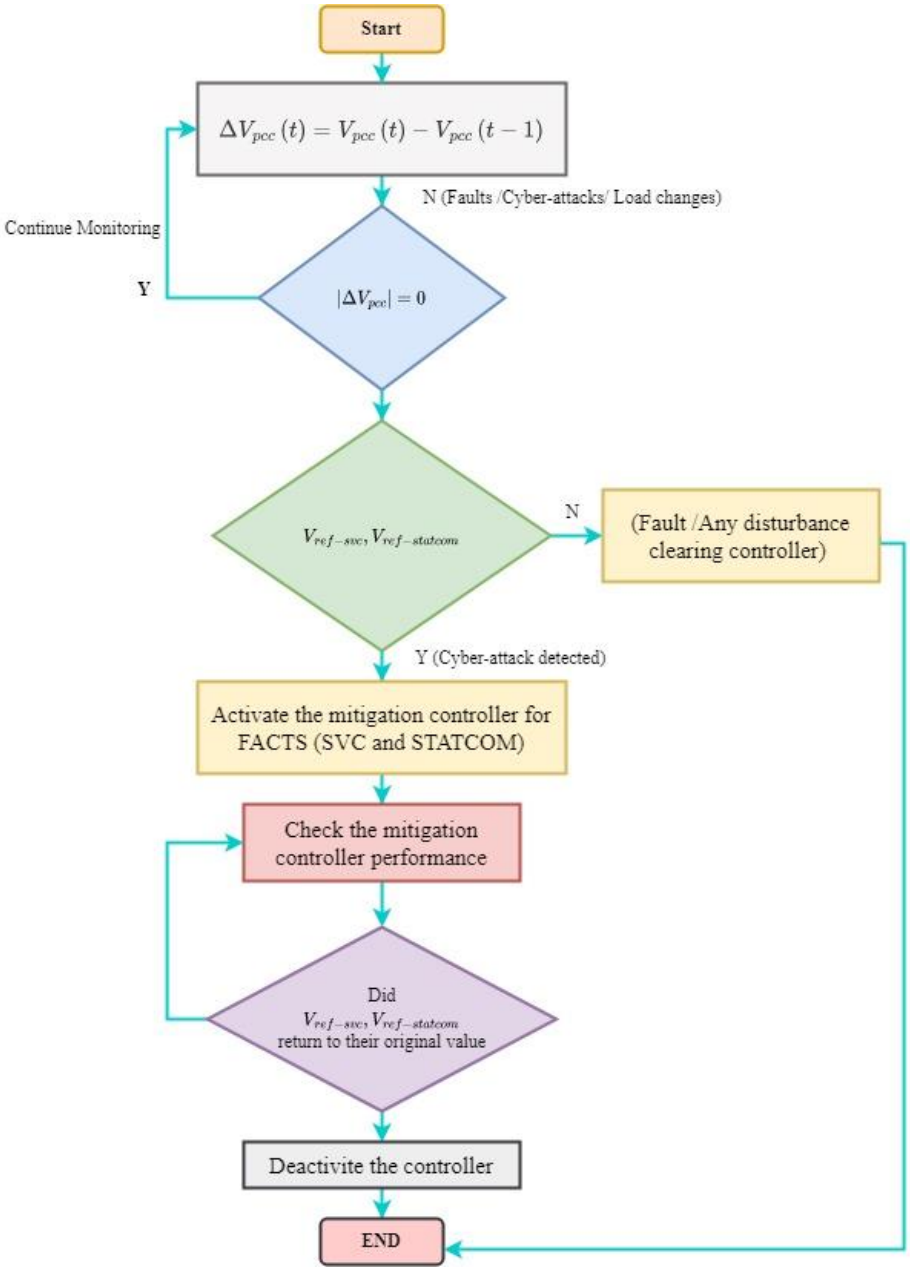

Figure D.4: Proposed control algorithm for SVC and STATCOM.

D.3.4 Proposed Mitigation Methods

D.3.4.1 Non-Linear Controller for SVC and STATCOM

Non-Linear Controller for SVC and STATCOM as the electricity grid remains extremely non-linear, grid technologies of non-linear controllers in network is widely favored. Any nonlinear differential equations or mathematical model can regulate this step response. A basic nonlinear formula has also been employed under this study, as illustrated below:

$$V_{vr_{ref(SVC)}} = \left(K_1 \times \left|\Delta V_{pcc}\right|^2\right) \quad (3)$$

$$V_{vr_{ref(STATCOM)}} = \left(K_2 \times \left|\Delta V_{pcc}\right|^2\right) \quad (4)$$

Where ΔV_{pcc} is the controller's input and K_1 and K_2 are constant values. The necessary values of the $V_{vr_{ref(SVC)}}$ and $V_{vr_{ref(STATCOM)}}$ are achieved by adjusting the values of K_1 and K_2. The parameters were chosen such that the controller could tolerate any voltage fluctuation, from extremely high to extremely low.

D.3.4.2 PI Controller for SVC and STATCOM

One of the most common controllers that is often utilized in automation and control is the PI controller. The following transfer function has been applied to the PI controller in the Laplace domain(s):

$$V_{vr_{ref(SVC)}} = \left|\Delta V_{pcc}\right| \left[K_{p1} + \frac{1}{s} K_{i1}\right] \quad (5)$$

$$V_{vr_{ref(STATCOM)}} = \left|\Delta V_{pcc}\right| \left[K_{p2} + \frac{1}{s} K_{i2}\right] \quad (6)$$

Where the proportional and integral gains of the PI controller are, correspondingly K_{p1}, K_{p2} and K_{i1}, K_{i2}. The controller's input is ΔV_{pcc}, and its output variables are $V_{vr_{ref(SVC)}}$, $V_{vr_{ref(STATCOM)}}$ respectively. These parameters were discovered by using trial and error, and they are capable of mitigating any sudden change in the input.

D.3.4.3 Mitigation Technique for FACTS

The IGBT gate signals and the power level of the energy storage are both monitored by the suggested mitigation method for the FACTS. Any alteration in the gate signal value activates the controller and supersedes the SCADA signal. The gate signal is reset to the necessary constant values, bringing the P_{pcc} value back to 2 MW.

D.3.5 Transient stability of power systems

The capacity of an connected synchronous coordination to reestablish synchrony as well as a state of operational balance following exposure to a practical disruption is known as power system transient stability [27]. Power system stability may be classified according to the factors measured,

like direction, amplitude, and oscillation. This study examines how cyber-attacks affect voltage stability and angle stability. Two stabilization criteria, the voltage quality index and the angle accurate parameter, were used to assess the impact of cyber-attacks on the power system's transient stability.

D.3.5.1 Angle stability and angular stabilization factor

Angle stability refers to a power system's ability to maintain synchronization in the face of a disturbance by keeping or recovering the balance across physical and magnetic force [28]. To analyze a movement of a mono synchronous machine, utilize the simplified swing equation (2) [10].

$$J\frac{d^2\theta}{dt^2} = T_m - T_e \tag{7}$$

Where θ is the rotor's angular position, J would be the combined inertia moment of both the paired compressor and rotor flux mass, while T_m and T_e denote the hydraulic and electromechanical rotational torque, respectively [13]. An angle stability index [28] is presented to measure the effect of cyber-attacks on point of view constancy or stability (3) [10].

$$\eta = \frac{360^0 - \delta_{max}}{360^0 + \delta_{max}} \times 100\%, -100 < \eta < 100 \tag{8}$$

Where the post-contingency system's maximum angle separation between any two generators is denoted by δ_{max}. Be aware that $\eta > 0$ and $\eta \leq 0$ signify stable and unstable states, respectively.

D.3.5.2 Voltage Stability and Voltage Stability Index

When a disturbance occurs, a power system's capacity to keep the voltage at all buses within a given range is referred to as voltage stability [24][29]. Protective relays may trip a circuit breaker as a result of a degraded voltage profile, or cascade failures may result.

D.3.6 Case study: Kigali National Grid

In this study, the Kigali national grid (KNG) bus test system is taken to study the impression of cyber-attacks purposes on fleeting stability (Figure D.3). Total 95 MW loads are connected to the system and six generators of 154 MVA, 110 kV and 50 MVA, 16.5 kV (generator 5) and one infinite bus are connected to support the power demand of the system. Infinite bus, generator 5 is

connected to Mount Kigali Sub Station 9 (Mount Kigali SS9) respectively. CBs and relays are used to connect and disconnect generators and transmission lines on a substation.

Smart meter instruments integrated in relay stations at various substations detect voltages and currents and generate CB tripping commands. Each separate bus in the model depicted in Figure D.3 represents a substation to which relays and breakers are linked. Mount Kigali Substation 5 is an example of a remotely situated switchgear that is susceptible to hacking. Hackers use the electronic protection coordination relay RG5 to launch various forms of cyber-attacks and to maliciously operate the CB BR 5. The total frequency of the system is 60 Hz [18]. The loads, generators and transmission lines data have been shown in REG reports [30][31].
The following two conditions must be met by load bus voltages in accordance with the Kigali national grid guidelines [32] following an incident or breakdown that results in the defeat of a particular component of the national grid: 1) The voltage dip/sag shouldn't be greater than 25%; and 2) The dip/sag in voltage cannot be greater than 20 percent for extra than 20 cycles (330 milliseconds in 60 Hz settings). The bus voltage stability index was demarcated as the longest period for a load bus system is lower than 0.8pu, out of all bus voltages, based on these parameters and the fact that all the contingencies examined in this research result in voltage dips.

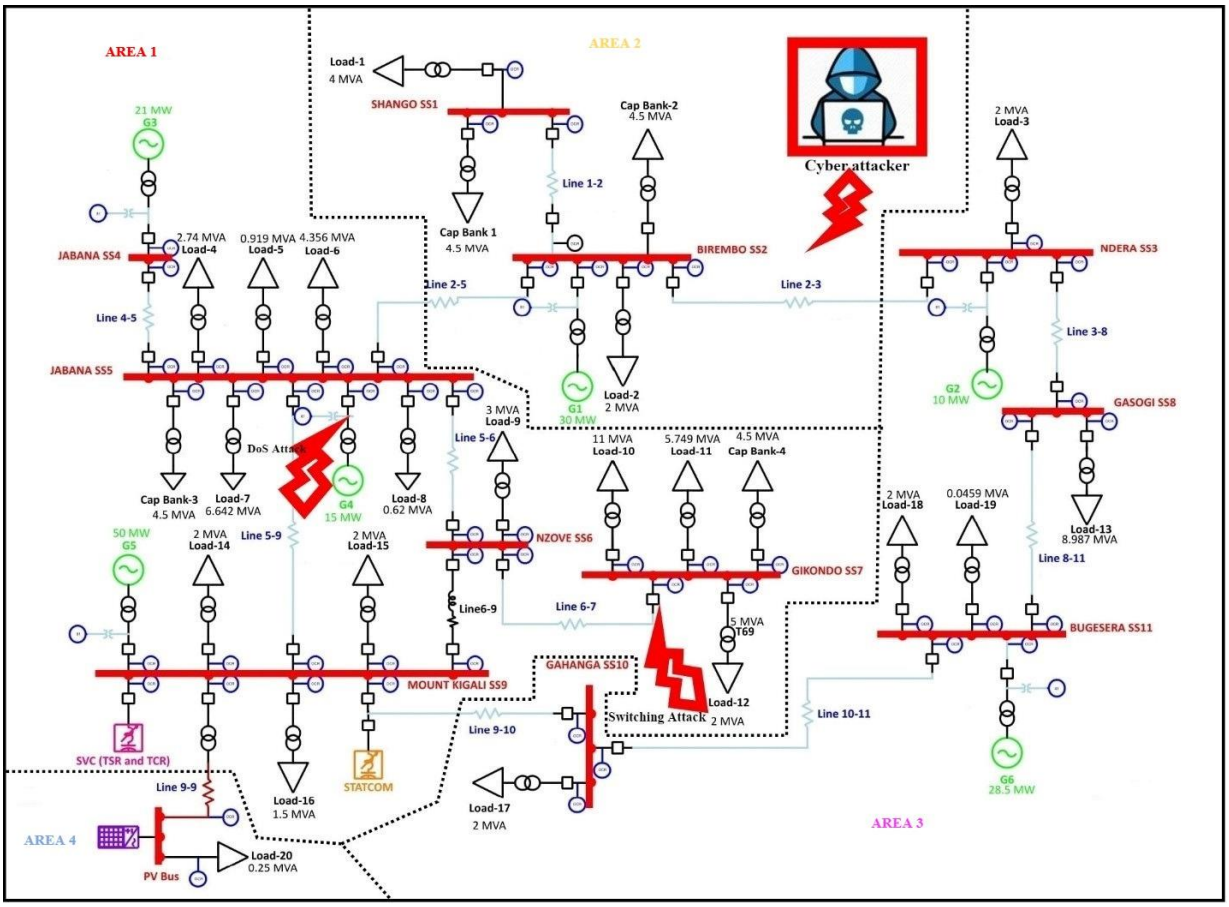

Figure D.5: Kigali national grid system.

D.3.7 System Modeling

Transient Security Assessment Tool (TSAT) of the DSAToolsTM platform type 13 was used to model this system [33]. TSAT is a time-domain modeling program created by analyzing the dynamics of power systems. Every one machine was represented as a synchronous round-rotor generator with a power system stabilizer and exciter (PSS). Constant PQ loads were used to mimic the system's loads. Transmission lines and transformers were modeled using Pi models. Utilizing blocks from the element library, UDM enables a user to construct a custom control function. We stored a number string with random delays in a lookup table. The string was created at random by MATLAB. In the simulation, TSAT applied the delay to the SVC, and STATCOM controller after progressively reading the number from the lookup table. Table D.1 displays the angle, frequency and voltage stability indices for these three scenarios of 3-phase bolted fault at Gikondo SS7 bus at 15s which became exonerated afterward 67ms by opening line 6-7. Although the system was angle stable in the absence of SVC, the voltage stability condition failed. Because the voltage stability index (8.48%) exceeded the maximum allowable level (7%) without controller. In the case of SVC and STATCOM, both the angle, frequency and voltage stability indices were improved. As we have been able to see from others who have tried to use the IEEE 39 bus, it is found that the national grid is very difficult to achieve, and the Stability Index Angle and Voltage are larger than what they see, as you can find in this paper written by Bo Chen [13].

According to the optimum allocation stated in [34], SVC and STATCOM are anticipated to be allocated at SS9 Mount Kigali. With a fixed capacitor of 10 MVar, the capacity varies between -50 MVAr to 50 MVAr. As a result, the customizable capacity ranges between -40 MVAr to 60 MVAr. With the assistance of SVC and STATCOM, the transient voltage profile can be assured to meet the standards in the event of a transmission line contingency. Figures D.6 and D.7 show the control blocks for the SVC and the STATCOM. Due to space constraints, the properties of SVC and STATCOM are not fully shown in Figures D.6 and D.7. According to their V-I characteristics, the SVC and STATCOM controllers will be disabled when the measured voltage falls below 0.7 pu [35]. They will then form a fixed capacitor. When the observed voltage falls below 0.3 pu, STATCOM will be isolated.

Table D.1 Transient response index for scenarios with and without SVC, STATCOM when faced to a DOS attack

Case No	Case Description	Transient Stability Indices		
		Angle	Frequency	Voltage
A	Without controllers	26.98%	02.77%	0.394%
B	With SVC	24.45%	01.62%	0.146%
C	With STATCOM	22.93%	06.61%	0.131%

D.3.7.1 Cyber Attack Scenarios

The attacker can perform cyber-attacks when the electric grid is in a regular, warning, crisis, severe, or rehabilitative state. As a result, different scenarios should be taken into account depending on when cyber-attacks are conducted. Due to a lack of available space, this research examines the possibility of simultaneous, backup cyber-attacks.

D.4. Simulation results and discussion

This division comprises the findings of 11 TSAT case studies. In cases 1–6, a system equipped with an SVC experienced a fixed delay caused by cyber-attacks. For example, Case 1 wen no network latency was taken into account for comparative reasons. For examples 2–6, fixed delays varied from 100 ms to 900 ms, with a 200 ms step. Designed for each case, the fixed delay of the lookup table was between 100 ms and 900 ms. All these 6 cases compared the time difference between the two cyber-attacks on the frequency relay of Generator 4 and Gikondo SS7, which was a 3-phase bolted fault on generator bus 6 at time 10.0 s for DoS attack and 6.0 s for Switching attack.

To demonstrate a DoS attack scenario, at 10.0 s, a three-phase on ground fault is smeared to line generator 4 to Jabana SS5 bus. Although the over frequency protection relay RG4 detects the over frequency instantly, the execution command has been delayed by 0.4 s due to the DoS attack, and the CB GR4 trips after 0.6 s. Such a delay violates the power system's standard and has a significant impact on its dynamic behavior. In power systems, a 0.2 s delay is reflected the processing and communication time to complete the tripping command. The system becomes more unstable than the typical cleaning time as the fault lingers longer than the normal performance time (0.2 s). All of this made it feel under the load break down to about 5s of simulation. After three steps to break the load, about 18 s, system. The frequency starts to recover because generator 5 is ready because it has to deal with load shedding, and it is a swing type machine while the others are PV type machines.

D.4.1 Effects of fixed network delay at SVC

Table A.2 displays the angles, frequency and voltage stability indices for cases 1–6. In case 1, the added facts controller was zero. In other words, this case did not model any fixed delay network on the SVC controller system. In contrast, most cases 2-6 (with Dos fixed delays) demonstrated lower angle stability index, frequency stability index and voltage stability index when compared to case 1 (no delay) [13][36]. Increases in delay length steadily (100 ms – 900 ms) lowered both indices in cases 2–6, but the system remained unstable ($\eta > 0$). In cases 1-6 of disturbance caused by switching attack, but the system remained stable ($\eta > 0$) and even a better reduction in the results of NL compared to PI. According to the results of SVC table 2 it is that the controller like PI would use 300 ms and 500 ms it causes a problem so that $pvcc$ appears to be unstable and while

in the results of STATCOM table 3 it is that when the controller PI uses shows the problem of unstable at 700 ms and 800 ms.

D.4.2 STATCOM's constant network delay effects

The angle, frequency, and voltage stability indices for cases 1-6 are exposed in Table D.3. Each example was fixed delay periods with various sets of random relays with the same β value. The system remained stable in all circumstances due to fixed delay ($\eta > 0$).

Figures D.6 and D.7 depict the generator frequency, angles, inter areas electrical energy. In that figures, the STATCOM controller received measurement values with a 900-ms delay. This created a delay in STATCOM output. As a result, the voltage at PCC bus changed more dramatically, causing relative generator frequency and angles to take longer to stabilize. In Figure D.7, STATCOM output in case 6 (Dos attack) increased Vpcc to 1.2 p.u. at 8 seconds while decreasing Vpcc to 0.4 p.u. at 10 seconds. In comparison to instance 1, STATCOM in situation 6 engrossed reactive power as soon as Pcc bus required the aforementioned the greatest. This represents the most catastrophic scenario. When the generator angles diverged, the system became unstable. From the results found in figures D.6 and D.7 and Table D.3, it is found that our controller works so well that the NL method is improved than PI in the case of switching attacks and in the event of a sudden attack such as DoS, PI is the best one as shown in Table D.3.

Cyber-attacks are becoming more and more capable of opening the power lines in the generator bus 5. After that, the frequency decreases or increases below the acceptable limits as shown in the above diagram. This causes the bottom of the load line to collapse which occurs within 30s of the simulation. Usually, switching frequency begins to restore after three phases of loading, which takes around 6 seconds. It finally settles to a frequency lower than the standard 60Hz. As a result, a cyber-attack results in a load of 90 MW, corresponding to something like a complete blackout. Finally, the network is showing up and it has been found that the effect of different attacks depends on the technique and the way to protect the network, DOS continues to show less effect compared to the switching attack though. Another result is that in this way it is possible to compare the load-shedding method to improve the efficiency of the Kigali national grid.

In summary, network delays persuaded by cyber-attacks might reduce the system's transient stability margin or make it unstable. Outsized fixed delays might cause the gird to become unstable like in DoS. In contrast, fixed delay has less of an impact on transient stability at switching attack. After that, according to the results in Tables D.2 and D.3, there is a critical value such that the voltage values are higher than 1 which makes our system work in a bad way, which means that the system is in unstable.

Table D.2 Angle and Voltage stability indices for SVC cases 1 to 6.

Case No.	Fixed Delay/ β	Cyber attack	Transient Stability Indices					
			SVC					
			PI			NL		
			Angle (%)	Freq (%)	Voltage (s)	Angle (%)	Freq (%)	Voltage (s)
1	0	DoS	27.93	0.823	0.5400	24.00	1.623	0.1594
2	100 ms	DoS	27.63	6.567	0.4900	24.00	1.623	0.1468
3	300 ms	DoS	27.38	4.838	1.9310	24.00	1.620	0.1172
4	500 ms	DoS	27.37	1.278	1.1430	24.00	1.624	0.1756
5	700 ms	DoS	28.59	12.81	0.4040	24.00	1.614	0.0864
6	900 ms	DoS	25.06	39.50	0.4180	24.00	1.622	0.1441
1	0	Switching	29.13	01.65	0.0004	5.594	0.202	0.0123
2	100 ms	Switching	28.87	01.74	0.1078	5.679	0.212	0.0979
3	300 ms	Switching	28.48	02.51	0.0881	6.338	0.531	0.0726
4	500 ms	Switching	27.97	03.55	0.0449	6.848	0.099	0.0334
5	700 ms	Switching	27.52	04.02	0.0211	6.825	0.171	0.0024
6	900 ms	Switching	27.21	04.20	0.0187	7.328	0.195	0.0008

Table D.3 Angle and Voltage stability indices for STATCOM cases 1 to 6.

Case No.	Delay/ β	Fixed Cyber attack	Transient Stability Indices					
			STATCOM					
			PI			NL		
			Angle (%)	Freq (%)	Voltage (s)	Angle (%)	Freq (%)	Voltage (%)
1	0	DoS	26.96	1.1280	0.6961	22.93	6.612	0.1318
2	100 ms	DoS	26.63	4.4470	0.6795	22.93	6.612	0.1315
3	300 ms	DoS	26.32	2.3630	0.1220	22.93	6.611	0.1384
4	500 ms	DoS	26.66	16.260	0.0566	22.93	6.611	0.1320
5	700 ms	DoS	23.95	18.320	3.6300	22.93	6.612	0.1311
6	900 ms	DoS	23.38	29.560	4.4782	22.93	6.612	0.1291
1	0	Switching	40.65	24.970	0.00150	6.204	0.141	0.00065
2	100 ms	Switching	40.56	24.590	0.00278	5.879	0.012	0.00214
3	300 ms	Switching	39.66	22.090	0.00239	5.766	0.048	0.00166
4	500 ms	Switching	38.49	19.090	0.00242	5.438	0.074	0.00060
5	700 ms	Switching	37.49	16.700	0.00095	5.324	0.147	0.00062
6	900 ms	Switching	36.84	15.120	0.00096	5.976	0.073	0.00273

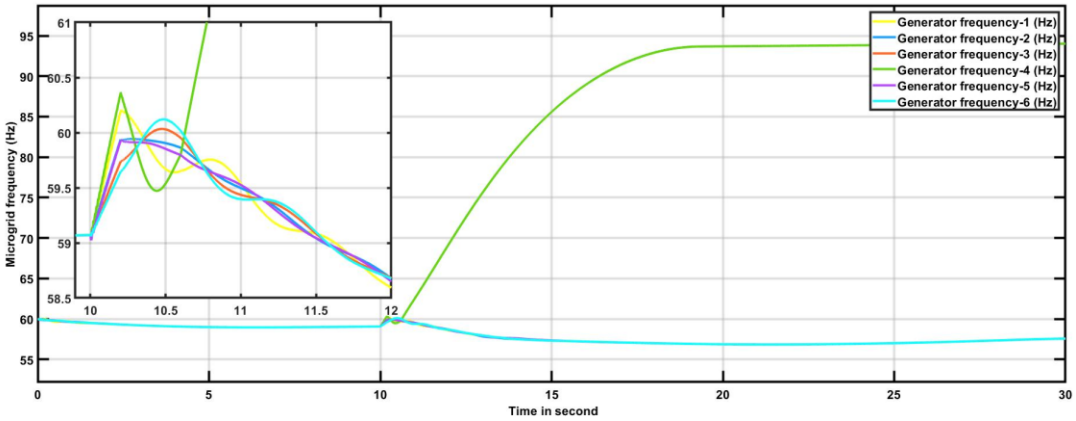

(a)

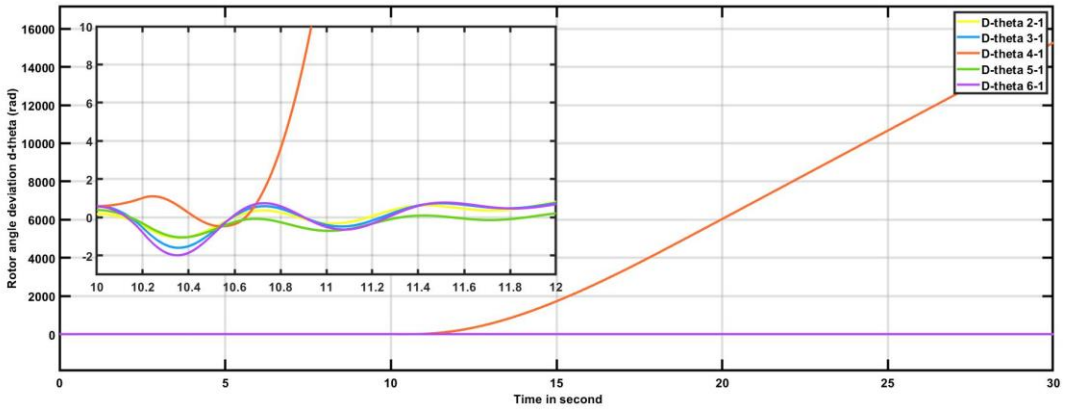

(b)

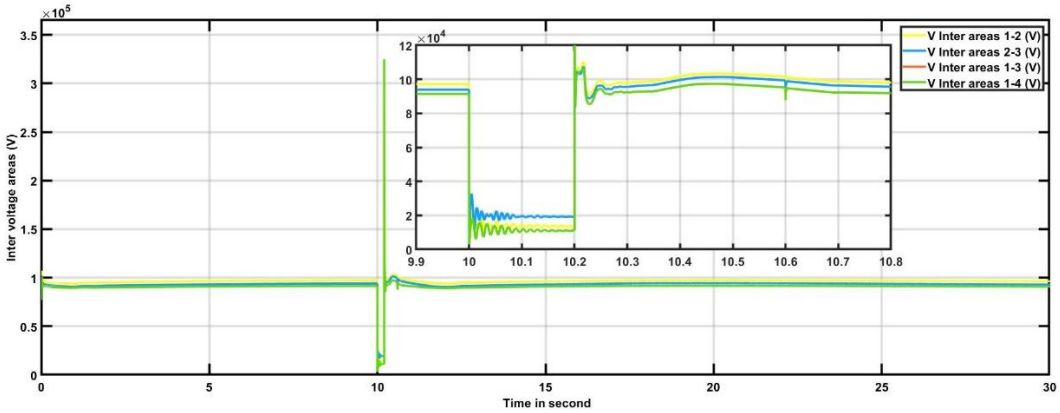

(c)

Figure D.6: Microgrid frequency, angles and voltages STATCOM output in event of DoS attack

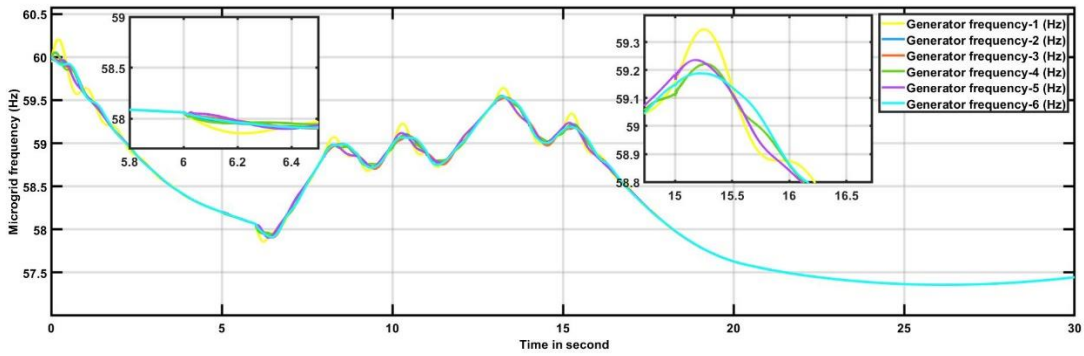

(a)

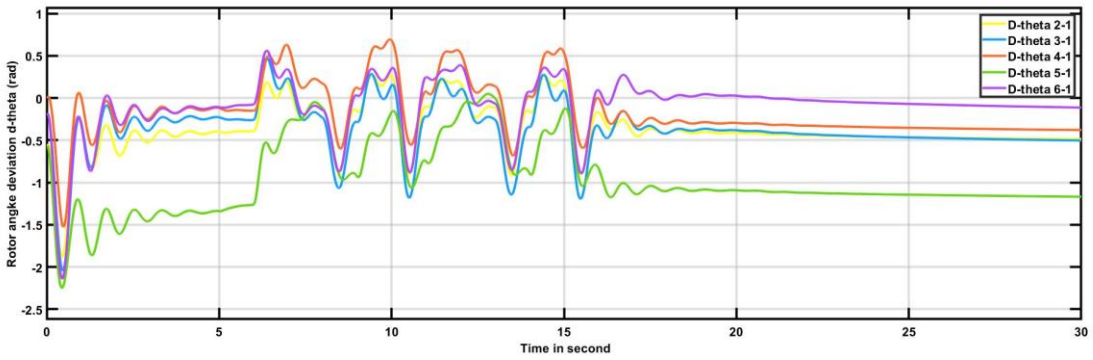

(b)

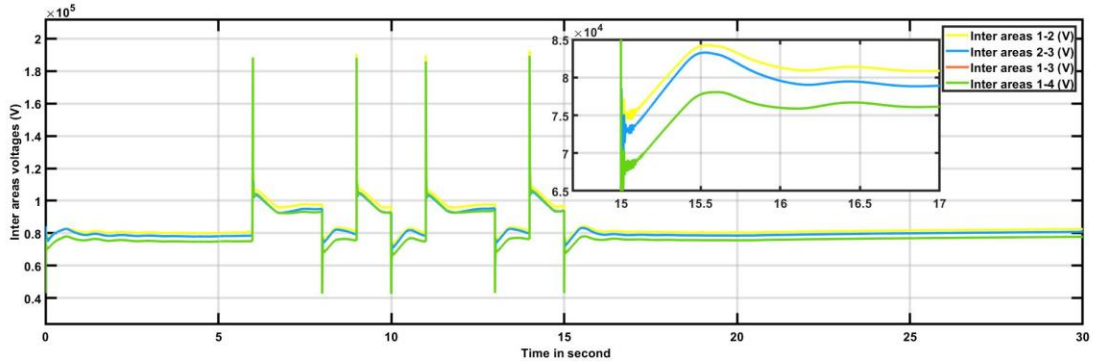

(c)

Figure D.7: Microgrid frequency, angles and voltages for STATCOM output in event of switching attack

D.4.3 Comparisons of facts controller

Based on the results of Figure D.8, it shows that the performance of STATCOM is much better than that of using SVC and STATCOM during the attack through frequency relay. Going to the modern or new function shows that STATCOM solve a lot even though it is an obstacle to fraud as shown in table D.4. In these instances, the potential cost of FACTS controllers must be considered. FACTS controllers are really costly when compared to ordinary devices. The

estimated cost is also determined by the quantity of the FACTS controller's set and adjustable parts [37].

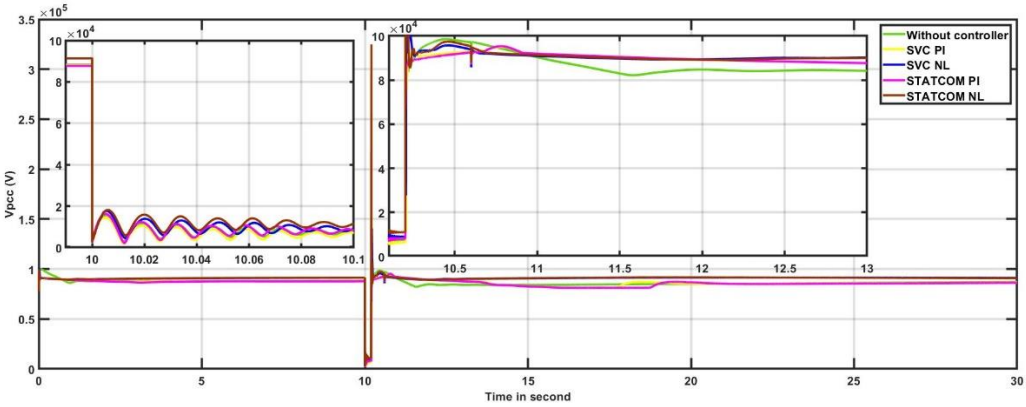

(a)

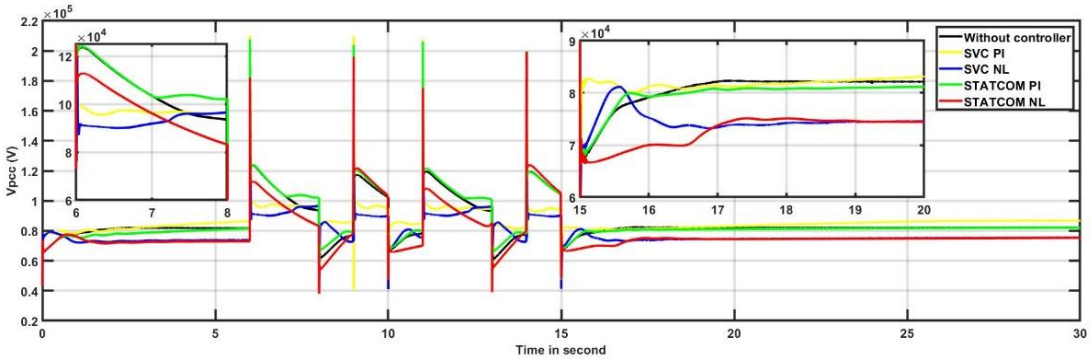

(b)

Figure D.8: Comparison of various controllers for the simulation results.

Table D.4 Comparisons of facts controller.

Facts devices	**Improved power system stability**	**Load flow**	**Voltage control**	**Transient stability**	**Dynamic stability**
STATCOM	Yes	Medium	High	Medium	Medium
SVC	Yes	Low	High	Low	Medium

D.5 Conclusions and Plans

This paper addressed cyber security concerns in the Kigali national grid. The findings of fixed delay tests of two cyber-attacks impact on transient stability of smart grids using voltage support devices, such as SVC or STATCOM, were then presented. In the investigations, the attacker got access to the communication link between the sensor and the frequency relay device's controller and manipulated it by inserting an unexpected signal into the measurement data. To assess the

impact of the assaults on network dynamic response, three stability indices for angle, frequency, & voltage profile have always been utilized. According to simulation studies, cyber-attacks on frequency relays could reduce the system's stability margin or potentially make it unstable. According to NL and PI results, NL is more effective during various attacks and is employed for STATCOM than SVC. The effectiveness of the attacks was found to be highly dependent on the type of attack magnitude and support device. Additional research would consist of a more complete assessment of the influence of cyber-attacks on other power grids, research into new prevention methods, or the development of mechanisms for identifying cyber physical security vulnerability.

References

[1] G. Dileep, "A survey on smart grid technologies and applications," *Renew. Energy*, vol. 146, pp. 2589–2625, 2020, doi: 10.1016/j.renene.2019.08.092. [CrossRef]

[2] D. Muyizere, L. K. Letting, and B. B. Munyazikwiye, "Effects of Communication Signal Delay on the Power Grid: A Review," *Electronics (Switzerland)*, vol. 11, no. 6. 2022. doi: 10.3390/electronics11060874. [CrossRef]

[3] M. Amin, F. F. M. El-Sousy, G. A. A. Aziz, K. Gaber, and O. A. Mohammed, "CPS Attacks Mitigation Approaches on Power Electronic Systems with Security Challenges for Smart Grid Applications: A Review," *IEEE Access*, vol. 9, pp. 38571–38601, 2021, doi: 10.1109/ACCESS.2021.3063229. [CrossRef]

[4] M. B. Mollah *et al.*, "Blockchain for Future Smart Grid: A Comprehensive Survey," *IEEE Internet of Things Journal*, vol. 8, no. 1. pp. 18–43, 2021. doi: 10.1109/JIOT.2020.2993601. [CrossRef]

[5] Y. Mo *et al.*, "Cyber-physical security of a smart grid infrastructure," *Proc. IEEE*, vol. 100, no. 1, pp. 195–209, 2012, doi: 10.1109/JPROC.2011.2161428. [CrossRef]

[6] S. Mavale, J. Katade, N. Dunbray, S. Nimje, and B. Patil, "Review of Cyber-Attacks on Smart Grid System," in *Lecture Notes in Electrical Engineering*, 2022, vol. 844, pp. 639–653. doi: 10.1007/978-981-16-8862-1_42. [CrossRef]

[7] A. Agrawal, D. M. Momin, D. Syndor, and S. Affijulla, "Impact Analysis of Cyber Attack under Stable State of Power System: Voltage Stability," 2020. doi: 10.1109/TENSYMP50017.2020.9230732. [CrossRef]

[8] H. Yang, S. Ju, Y. Xia, and J. Zhang, "Predictive Cloud Control for Networked Multiagent Systems with Quantized Signals under DoS Attacks," *IEEE Trans. Syst. Man, Cybern. Syst.*, vol. 51, no. 2, pp. 1345–1353, Feb. 2021, doi: 10.1109/TSMC.2019.2896087. [CrossRef]

[9] M. H. Ali, T. Murata, and J. Tamura, "Influence of communication delay on the performance of fuzzy logic-controlled braking resistor against transient stability," *IEEE Trans. Control Syst. Technol.*, vol. 16, no. 6, pp. 1232–1241, 2008, doi: 10.1109/TCST.2008.919443. [CrossRef]

[10] B. Chen, K. L. Butler-Purry, S. Nuthalapati, and D. Kundur, "Network delay caused by cyber attacks on SVC and its impact on transient stability of smart grids," in *IEEE Power*

and Energy Society General Meeting, 2014, vol. 2014-Octob, no. October. doi: 10.1109/PESGM.2014.6938963. [CrossRef]

[11] P. S. Sarker, V. Venkataramanan, D. S. Cardenas, A. Srivastava, A. Hahn, and B. Miller, "Cyber-physical security and resiliency analysis testbed for critical microgrids with IEEE 2030.5," Apr. 2020. doi: 10.1109/MSCPES49613.2020.9133689. [CrossRef]

[12] G. Ravikumar, A. Singh, J. R. Babu, A. Moataz A, and M. Govindarasu, "D-IDS for cyber-physical der modbus system - Architecture, modeling, testbed-based evaluation," in *2020 Resilience Week, RWS 2020*, Oct. 2020, pp. 153–159. doi: 10.1109/RWS50334.2020.9241259. [CrossRef]

[13] B. Chen, S. Mashayekh, K. L. Butler-Purry, and D. Kundur, "Impact of cyber attacks on transient stability of smart grids with voltage support devices," 2013. doi: 10.1109/PESMG.2013.6672740. [CrossRef]

[14] L. Zeng *et al.*, "A novel machine learning-based framework for optimal and secure operation of static var compensators in eafs," *Sustain.*, vol. 13, no. 11, Jun. 2021, doi: 10.3390/su13115777. [CrossRef]

[15] V. K. Singh, M. Govindarasu, and R. Nuqui, "Impact analysis of data integrity attacks on FACTS-based wide-area voltage control system," Feb. 2021. doi: 10.1109/ISGT49243.2021.9372232. [CrossRef]

[16] C. W. Ten, K. Yamashita, Z. Yang, A. V. Vasilakos, and A. Ginter, "Impact assessment of hypothesized cyberattacks on interconnected bulk power systems," *IEEE Trans. Smart Grid*, vol. 9, no. 5, 2018, doi: 10.1109/TSG.2017.2656068. [CrossRef]

[17] B. Chen, K. L. Butler-Purry, and D. Kundur, "Impact analysis of transient stability due to cyber attack on FACTS devices," 2013. doi: 10.1109/NAPS.2013.6666849. [CrossRef]

[18] B. M. R. Amin, S. Taghizadeh, M. S. Rahman, M. J. Hossain, V. Varadharajan, and Z. Chen, "Cyber attacks in smart grid - Dynamic impacts, analyses and recommendations," *IET Cyber-Physical Syst. Theory Appl.*, vol. 5, no. 4, 2020, doi: 10.1049/iet-cps.2019.0103.

[19] R. Moreno Chuquen and H. R. Chamorro, "Cyber Physical Systems Security for the Smart Grid," 2021. doi: 10.1007/978-3-030-57589-2_6. [CrossRef]

[20] V. S. Rajkumar, M. Tealane, A. Stefanov, and P. Palensky, "Cyber attacks on protective relays in digital substations and impact analysis," Apr. 2020. doi: 10.1109/MSCPES49613.2020.9133698. [CrossRef]

[21] D. Muyizere, L. K. Letting, and B. B. Munyazikwiye, "Under-frequency Load Shedding on the Performance Time Delay Relays of Transmission lines with difference Controllers," 2021. doi: 10.1109/SPEC52827.2021.9709464. [CrossRef]

[22] S. Aerts *et al.*, "Lessons Learned from a Distributed RF-EMF Sensor Network," *Sensors*, vol. 22, no. 5, Mar. 2022, doi: 10.3390/s22051715. [CrossRef]

[23] W. Sun, F. Brannstrom, and E. G. Strom, "On clock offset and skew estimation with exponentially distributed delays," in *IEEE International Conference on Communications*, 2013, pp. 1872–1877. doi: 10.1109/ICC.2013.6654794. [CrossRef]

[24] "Power System Stability Controls," in *Power System Stability and Control*, 2020, pp. 169–

188. doi: 10.1201/9781420009248-18. [CrossRef]
[25] "Power System Stability Controls," in *Power System Stability and Control*, CRC Press, 2020, pp. 169–188. doi: 10.1201/9781420009248-18. [CrossRef]
[26] G. Penchalaiah and R. Ramya, "Investigation on Power System Stability Improvement Using Facts Controllers," in *Lecture Notes in Electrical Engineering*, 2022, vol. 795, pp. 499–506. doi: 10.1007/978-981-16-4943-1_46. [CrossRef]
[27] J. Ansari, A. R. Abbasi, M. H. Heydari, and Z. Avazzadeh, "Simultaneous design of fuzzy PSS and fuzzy STATCOM controllers for power system stability enhancement," *Alexandria Eng. J.*, vol. 61, no. 4, 2022, doi: 10.1016/j.aej.2021.08.007. [CrossRef]
[28] P. Kundur *et al.*, "Definition and classification of power system stability," *IEEE Trans. Power Syst.*, vol. 19, no. 3, 2004, doi: 10.1109/TPWRS.2004.825981. [CrossRef]
[29] L. L. Grigsby, *Power system stability and control*. 2017. doi: 10.4324/b12113.
[30] Rwanda Energy Group Ltd, "Annual Report For Rwanda Energy Group 2019-2020," Kigali, Aug. 2020. Accessed: Aug. 09, 2022. [Online]. Available: https://www.reg.rw/fileadmin/user_upload/FINAL_REG_ANNUAL_REPORT_19-_2020.pdf[CrossRef]
[31] Rwanda Energy Group Ltd, "Annual Report For Rwanda Energy Group 2020-2021," no. Septembre. Kigali, p. 29, Sep. 2021. Accessed: Aug. 09, 2022. [Online]. Available: https://www.reg.rw/fileadmin/REG_ANNUAL_REPORT_2020-2021_V3.pdf[CrossRef]
[32] C. Battistelli and A. Monti, "Dynamics of modern power systems," in *Converter-Based Dynamics and Control of Modern Power Systems*, Elsevier, 2021, pp. 91–124. doi: 10.1016/b978-0-12-818491-2.00005-5. [CrossRef]
[33] H. Yuan and Y. Xu, "Trajectory sensitivity based preventive transient stability control of power systems against wind power variation," *Int. J. Electr. Power Energy Syst.*, vol. 117, May 2020, doi: 10.1016/j.ijepes.2019.105713. [CrossRef]
[34] M. Ćalasan, T. Konjić, K. Kecojević, and L. Nikitović, "Optimal allocation of static var compensators in electric power systems," *Energies*, vol. 13, no. 12, Jun. 2020, doi: 10.3390/en13123219. [CrossRef]
[35] W. H. Wellssow, M. Ostermann, H. Acker, W. Heckmann, and D. Cremer, "Advanced model of static var compensators for power flow calculations," Jul. 2016. doi: 10.1109/ISGTEurope.2016.7856336. [CrossRef]
[36] D. Muyizere, L. K. Letting, and B. B. Munyazikwiye, "Decreasing the Negative Impact of Time Delays on Electricity Due to Performance Improvement in the Rwanda National Grid," *Electron. 2022, Vol. 11, Page 3114*, vol. 11, no. 19, p. 3114, Sep. 2022, doi: 10.3390/ELECTRONICS11193114. [CrossRef]
[37] A. Jamali and I. Z. M. Darus, "Intelligent Evolutionary Controller for Flexible Robotic Arm," in *Journal of Physics: Conference Series*, May 2020, vol. 1500, no. 1. doi: 10.1088/1742-6596/1500/1/012020. [CrossRef]

PHD THESIS MUYIZERE DARIUS I

ORIGINALITY REPORT

13%	8%	9%	2%
SIMILARITY INDEX	INTERNET SOURCES	PUBLICATIONS	STUDENT PAPERS

PRIMARY SOURCES

1	encyclopedia.pub Internet Source	1%
2	ir.bdu.edu.et Internet Source	1%
3	Zhang, Y.. "Power injection model of STATCOM with control and operating limit for power flow and voltage stability analysis", Electric Power Systems Research, 200608 Publication	1%
4	Bo Chen, Karen L. Butler-Purry, Sruti Nuthalapati, Deepa Kundur. "Network delay caused by cyber attacks on SVC and its impact on transient stability of smart grids", 2014 IEEE PES General Meeting | Conference & Exposition, 2014 Publication	1%
5	Sagnika Ghosh, Mohd. Hasan Ali. "Minimization of Adverse Effects of Time Delay on Power Quality Enhancement in Hybrid Grid", IEEE Systems Journal, 2019 Publication	1%

6	eprints.qut.edu.au Internet Source	1 %
7	dokumen.pub Internet Source	<1 %
8	Joseph Benedict Bassey, Isaac F. Odesola. "Effect of Grid Instability on Power Generation System's Reliability", Journal of Engineering Research and Reports, 2020 Publication	<1 %
9	M. Talaat, A.Y. Hatata, Abdulaziz S. Alsayyari, Adel Alblawi. "A smart load management system based on the grasshopper optimization algorithm using the under-frequency load shedding approach", Energy, 2020 Publication	<1 %
10	Submitted to Oxford Brookes University Student Paper	<1 %
11	www.worldresearchlibrary.org Internet Source	<1 %
12	Bo Chen, Salman Mashayekh, Karen L. Butler-Purry, Deepa Kundur. "Impact of cyber attacks on transient stability of smart grids with voltage support devices", 2013 IEEE Power & Energy Society General Meeting, 2013 Publication	<1 %

13	unsworks.unsw.edu.au Internet Source	<1%
14	www.tandfonline.com Internet Source	<1%
15	vdocuments.site Internet Source	<1%
16	Mohamed Ramadan Younis, Reza Iravani. "Structure preserving energy function including the synchronous generator magnetic saturation and sub-transient models", IET Generation, Transmission & Distribution, 2017 Publication	<1%
17	Wei Yao, L. Jiang, Jinyu Wen, Q. H. Wu, Shijie Cheng. "Wide-Area Damping Controller of FACTS Devices for Inter-Area Oscillations Considering Communication Time Delays", IEEE Transactions on Power Systems, 2014 Publication	<1%
18	B.M. Ruhul Amin, Seyedfoad Taghizadeh, Md. Shihanur Rahman, Md. Jahangir Hossain, Vijay Varadharajan, Zhiyong Chen. "Cyber attacks in smart grid – dynamic impacts, analyses and recommendations", IET Cyber-Physical Systems: Theory & Applications, 2020 Publication	<1%
	publications.rifs-potsdam.de	

19	Internet Source	<1%
20	vdoc.pub Internet Source	<1%
21	Tharangika Bambaravanage, Asanka Rodrigo, Sisil Kumarawadu. "Modeling, Simulation, and Control of a Medium-Scale Power System", Springer Science and Business Media LLC, 2018 Publication	<1%
22	www.research.manchester.ac.uk Internet Source	<1%
23	Mohd. Hasan Ali, Dipankar Dasgupta. "Effects of communication delays in electric grid", 2011 Future of Instrumentation International Workshop (FIIW) Proceedings, 2011 Publication	<1%
24	Ola Ali, Tung-Lam Nguyen, Osama A. Mohammed. "Assessment of Cyber-Physical Inverter-Based Microgrid Control Performance under Communication Delay and Cyber-Attacks", Applied Sciences, 2024 Publication	<1%
25	Mohd. Hasan Ali, Sultana Razia Akhter. "Nonlinear Controller-Based Mitigation of Adverse Effects of Cyber-Attacks on the DC Microgrid System", Electronics, 2024	<1%

Publication

26	Yasir Zaki. "Future Mobile Communications", Springer Science and Business Media LLC, 2013 Publication	<1 %
27	Submitted to iGroup Student Paper	<1 %
28	Arindam Ghosh, Gerard Ledwich. "Power Quality Enhancement Using Custom Power Devices", Springer Science and Business Media LLC, 2002 Publication	<1 %
29	Sathit Chimplee, Sudarat Khwan-on. "Comparative Analysis of Fuzzy Controller Based on Input Current Slope and PI Controller for Two-Stage Cascaded Boost Converter", 2022 International Conference on Power, Energy and Innovations (ICPEI), 2022 Publication	<1 %
30	www.blog.iass-potsdam.de Internet Source	<1 %
31	Samuel Bimenyimana, Godwin N. O. Asemota, Lingling Li. "The State of the Power Sector in Rwanda: A Progressive Sector With Ambitious Targets", Frontiers in Energy Research, 2018 Publication	<1 %

32	"Proceedings of International Conference on Data Science and Applications", Springer Science and Business Media LLC, 2022 Publication	<1 %
33	Submitted to RDI Distance Learning Student Paper	<1 %
34	Yang Zhou, Sagnika Ghosh, Mohd. Hasan Ali, Thomas Edgar Wyatt. "Minimization of negative effects of time delay in smart grid system", 2013 Proceedings of IEEE Southeastcon, 2013 Publication	<1 %
35	ir.lib.uwo.ca Internet Source	<1 %
36	journaljenrr.com Internet Source	<1 %
37	researchrepository.ucd.ie Internet Source	<1 %
38	Imdadullah, Syed Muhammad Amrr, M. S. Jamil Asghar, Imtiaz Ashraf, Mohammad Meraj. "A Comprehensive Review of Power Flow Controllers in Interconnected Power System Networks", IEEE Access, 2020 Publication	<1 %
39	erepo.usm.my Internet Source	<1 %

40	www.ijrte.org Internet Source	<1%
41	Submitted to Heriot-Watt University Student Paper	<1%
42	Li, Jian, Zhaohui Chen, Dongsheng Cai, Wei Zhen, and Qi Huang. "Delay-Dependent Stability Control for Power System With Multiple Time-Delays", IEEE Transactions on Power Systems, 2015. Publication	<1%
43	orca.cardiff.ac.uk Internet Source	<1%
44	researchspace.ukzn.ac.za Internet Source	<1%
45	Lecture Notes in Electrical Engineering, 2015. Publication	<1%
46	d197for5662m48.cloudfront.net Internet Source	<1%
47	link.springer.com Internet Source	<1%
48	Submitted to Curtin University of Technology Student Paper	<1%
49	"Static Compensators (STATCOMs) in Power Systems", Springer Science and Business Media LLC, 2015	<1%

Publication

50	9pdf.net Internet Source	<1%
51	www.grafiati.com Internet Source	<1%
52	"Wide Area Power Systems Stability, Protection, and Security", Springer Science and Business Media LLC, 2021 Publication	<1%
53	Submitted to Higher Education Commission Pakistan Student Paper	<1%
54	soar.wichita.edu Internet Source	<1%
55	Hale Bakir, Ahmet Afsin Kulaksiz. "Modelling and Voltage Control of the Solar-Wind Hybrid Micro-Grid with Optimized STATCOM", 2019 23rd International Conference Electronics, 2019 Publication	<1%
56	IFIP Advances in Information and Communication Technology, 2012. Publication	<1%
57	Kiran Nathgosavi, Prasad Joshi. "Enhancement of power transfer capacity of transmission network using multilevel	<1%

multifunction inverter", Acta Polytechnica, 2023
Publication

58	Submitted to Universiti Teknologi Malaysia Student Paper	<1 %
59	digitallibrary.aau.ac.ae Internet Source	<1 %
60	fastercapital.com Internet Source	<1 %
61	"Intelligent Computing", Springer Science and Business Media LLC, 2023 Publication	<1 %
62	digital.lib.washington.edu Internet Source	<1 %
63	dspace.uii.ac.id Internet Source	<1 %
64	sciencedocbox.com Internet Source	<1 %
65	www.3ciencias.com Internet Source	<1 %
66	Oscar Danilo Montoya, Walter Gil-González, Alejandro Garcés, Gerardo Espinosa-Pérez. "Indirect IDA-PBC for active and reactive power support in distribution networks using SMES systems with PWM-CSC", Journal of Energy Storage, 2018	<1 %

Publication

67	cyberleninka.org Internet Source	<1 %
68	etheses.bham.ac.uk Internet Source	<1 %
69	ir.uitm.edu.my Internet Source	<1 %
70	mountainscholar.org Internet Source	<1 %
71	www.oer.unn.edu.ng Internet Source	<1 %
72	"Frontiers in Genetics Algorithm Theory and Applications", Springer Science and Business Media LLC, 2024 Publication	<1 %
73	Paul A. Adedeji, Stephen A. Akinlabi, Nkosinathi Madushele, Obafemi O. Olatunji. "Beyond site suitability: Investigating temporal variability for utility-scale solar-PV using soft computing techniques", Renewable Energy Focus, 2021 Publication	<1 %
74	Saffet Ayasun. "Computation of time delay margin for power system small-signal stability", European Transactions on Electrical Power, 2008 Publication	<1 %

75	Zhan, Peng, Chenghao Li, Jinyu Wen, Yu Hua, Meiqi Yao, and Naihu Li. "Research on hybrid multi-terminal high-voltage DC technology for offshore wind farm integration", Journal of Modern Power Systems and Clean Energy, 2013. Publication	<1 %
76	backend.orbit.dtu.dk Internet Source	<1 %
77	ebiltegia.mondragon.edu Internet Source	<1 %
78	garuda.kemdikbud.go.id Internet Source	<1 %
79	jcreview.com Internet Source	<1 %
80	pure.tudelft.nl Internet Source	<1 %
81	vbn.aau.dk Internet Source	<1 %
82	www.atlantis-press.com Internet Source	<1 %
83	www.ir.juit.ac.in:8080 Internet Source	<1 %
84	Ali M. Eltamaly, Mohamed A. Mohamed. "Optimal Sizing and Designing of Hybrid	<1 %

Renewable Energy Systems in Smart Grid Applications", Elsevier BV, 2018
Publication

---

85 Alvin Huseinovic, Sasa Mrdovic, Kemal Bicakci, Suleyman Uludag. "A Survey of Denial-of-Service Attacks and Solutions in the Smart Grid", IEEE Access, 2020 <1%
Publication

---

86 Guangdou Zhang, Jian Li, Olusola Bamisile, Yankai Xing, Dongsheng Cai, Qi Huang. "An H Load Frequency Control Scheme for Multi-Area Power System Under Cyber-Attacks and Time-Varying Delays", IEEE Transactions on Power Systems, 2022 <1%
Publication

---

87 Hamed Badrsimaei, Rahmat-Allah Hooshmand, Soghra Nobakhtian. "Observable placement of phasor measurement units for defense against data integrity attacks in real time power markets", Reliability Engineering & System Safety, 2023 <1%
Publication

---

88 Hengfei Yang, Bo Shen, Gaoyang Xu, Yonghua Chen. "Modeling Method and Correctness Verification of Power Grid Safety and Stability Control Strategy System", 2022 IEEE 22nd International Conference on Software Quality, <1%

Reliability, and Security Companion (QRS-C), 2022
Publication

89	Hossein Mahvash, Seyed Abbas Taher, Josep M. Guerrero. "Detecting and mitigating cyber-attacks in AC microgrid composed of marine current turbine DFIGs to improve energy management system", e-Prime - Advances in Electrical Engineering, Electronics and Energy, 2024 Publication	<1%
90	I.A. Hiskens. "Analysis tools for power systems-contending with nonlinearities", Proceedings of the IEEE, 1995 Publication	<1%
91	M.H. Ali, T. Murata, J. Tamura. "Effect of Coordination of Optimal Reclosing and Fuzzy Controlled Braking Resistor on Transient Stability During Unsuccessful Reclosing", IEEE Transactions on Power Systems, 2006 Publication	<1%
92	Markos Asprou, Elias Kyriakides. "The effect of time-delayed measurements on a PMU-based state estimator", 2015 IEEE Eindhoven PowerTech, 2015 Publication	<1%
93	Mohammad Kamrul Hasan, Rabiu Aliyu Abdulkadir, Shayla Islam, Thippa Reddy	<1%

Gadekallu, Nurhizam Safie. "A review on machine learning techniques for secured cyber-physical systems in smart grid networks", Energy Reports, 2024
Publication

---

94 Mohd. Hasan Ali. "Influence of Communication Delay on the Performance of Fuzzy Logic-Controlled Braking Resistor Against Transient Stability", IEEE Transactions on Control Systems Technology, 2008 <1%
Publication

---

95 Robert Smolenski. "Conducted EMI Issues in Smart Grids", Power Systems, 2012 <1%
Publication

---

96 Sagnika Ghosh, Mohd. Hasan Ali. "Augmentation of Power Quality of Grid-Connected Wind Generator by Fuzzy Logic Controlled TSC", 2018 IEEE/PES Transmission and Distribution Conference and Exposition (T&D), 2018 <1%
Publication

---

97 Seyed Hossein Rouhani, Ebrahim Abbaszadeh, Mohammadreza Askari Sepestanaki, Saleh Mobayen, Chun-Lien Su, Abbas Nemati. "Adaptive Finite-Time Tracking Control of Fractional Microgrids Against Time-Delay Attacks", IEEE Transactions on Industry Applications, 2024 <1%
Publication

98	Sushree Diptimayee Swain, Pravat Kumar Ray, Kanungo Barada Mohanty. "Improvement of Power Quality Using a Robust Hybrid Series Active Power Filter", IEEE Transactions on Power Electronics, 2017 Publication	<1 %
99	Zhang Chu, Peng Chen, Zhang Jin, Zhang Heng. "Communication and control of wide-area power systems: A survey", 2015 34th Chinese Control Conference (CCC), 2015 Publication	<1 %
100	commons.und.edu Internet Source	<1 %
101	cris.tuni.fi Internet Source	<1 %
102	digitalcommons.lib.uconn.edu Internet Source	<1 %
103	ds.amu.edu.et Internet Source	<1 %
104	era.ed.ac.uk Internet Source	<1 %
105	forskningskart-nve.nina.no Internet Source	<1 %
106	hal.archives-ouvertes.fr Internet Source	<1 %

107	my.ece.msstate.edu Internet Source	<1 %
108	oaji.net Internet Source	<1 %
109	palensky.org Internet Source	<1 %
110	repository.unn.edu.ng Internet Source	<1 %
111	sensorweb.engr.uga.edu Internet Source	<1 %
112	stax.strath.ac.uk Internet Source	<1 %
113	tepesjournal.org Internet Source	<1 %
114	theses.lib.polyu.edu.hk Internet Source	<1 %
115	vdocuments.mx Internet Source	<1 %
116	www.ycce.edu Internet Source	<1 %
117	"Innovations in Electrical and Electronic Engineering", Springer Science and Business Media LLC, 2021 Publication	<1 %

118	Amirreza Jafari, Hakan Ergun, Dirk Van Hertem. "Set-point Adjustment Attacks on Under Frequency Load Shedding Relays: A Risk Assessment Study", 2023 IEEE PES Innovative Smart Grid Technologies Europe (ISGT EUROPE), 2023 Publication	<1%
119	Hossain, Md. Kamal, and Mohd. Hasan Ali. "Transient stability augmentation of PV/DFIG/SG-based hybrid power system by parallel-resonance bridge fault current limiter", Electric Power Systems Research, 2016. Publication	<1%
120	Jafar Mohammadi, Firouz Badrkhani Ajaei. "Adaptive Voltage-Based Load Shedding Scheme for the DC Microgrid", IEEE Access, 2019 Publication	<1%
121	Yi Yu, Guo-Ping Liu, Hui Xiao, Wenshan Hu. "Design of Networked Secure and Real-Time Control Based on Blockchain Techniques", IEEE Transactions on Industrial Electronics, 2022 Publication	<1%
122	Amirhossein Dolatabadi, Behnam Mohammadi-Ivatloo. "Stochastic risk-constrained optimal sizing for hybrid power	<1%

system of merchant marine vessels", IEEE Transactions on Industrial Informatics, 2018
Publication

---

123 Janaka Ekanayake, Kithsiri Liyanage, Jianzhong Wu, Akihiko Yokoyama, Nick Jenkins. "Smart Grid", Wiley, 2012 <1%
Publication

---

124 Katundu Imasiku, Etienne Ntagwirumugara, Billy Coop. "Policies lost in translation: Combating the green house gas emission merry-go-round for increased utilization of renewable energy technologies", 2018 9th International Renewable Energy Congress (IREC), 2018 <1%
Publication

Exclude quotes On
Exclude bibliography On
Exclude matches Off